THESIS

Design and Validation of a Non-Invasive Intra-abdominal Pressure Measurement Device

Natasha Jacobson, P.Eng.

Department of Mechanical Engineering
McGill University
Montreal, Quebec, Canada

August 2021

A Thesis submitted to McGill University in partial fulfillment of the requirements of the Degree of Doctor of Philosophy (Ph.D.) in Mechanical Engineering.

Dedication

This thesis is dedicated to my family, namely my Mom and Dad, for inspiring a high level of excellence in all aspects of life, and supporting me regardless of how many provinces lie between us. Also, for my husband, Kris, this thesis serves as a reminder of what you have supported me through. Thank you for washing the dishes while I worked, listening to me practice presentations, and supplying endless board game nights in the meantime.

Contents

List of Figures

List of Tables

Glossary

ex vivo Experiment performed outside of organisms in a manufactured environment.

in silico Experiment performed using computer simulations.

in vivo Experiment performed on living organisms.

Abdominal Compartment Also known as the abdominopelvic cavity or abdominal cavity, this vessel is enclosed by the diaphragm (superior), pelvic floor (inferior), abdominal wall (anterior), and spine (posterior). The compartment is commonly assumed to be a closed volume of incompressible fluid such that a uniform pressure exists.

Abdominal Compartment Syndrome Clinical definition for a severe prolonged increase in baseline intra-abdominal pressure. Diagnosed by consistent intra-abdominal pressures greater than 20 mmHg collected over 4 to 6 hours.

Abdominal Compliance Measure of ease of abdominal expansion, or, the ratio of change in intra-abdominal volume to change in intra-abdominal pressure. Typically measured in mL/mmHg.

Abdominal Perimeter Circumference of the human abdomen measured at the navel. Synonymous with waist circumference. Typically measured in meters.

Abdominal Wall The tissues contained between the skin and the peritoneum of the abdominal cavity. This is a laminar-composite material whose layers vary with anatomical position.

Detrusor Pressure Bladder pressure due to bladder wall muscle contraction.

Head of Bed Height at which the head is raised from supine position. Typically measured at an angle with supine position.

Hyperelastic A non-linear elastic classifier for materials that exhibit large strain for relatively low stresses. Typically used to characterize rubber or rubber-like materials.

Incompressible Material A perfectly incompressible material is said to have a Poisson's ratio of 0.5. Incompressible materials do not change volume under deformation.

Intra-abdominal Hypertension Clinical definition for a prolonged increase in baseline intra-abdominal pressure. Diagnosed by consistent intra-abdominal pressures greater than 12 mmHg collected over 4 to 6 hours.

Intra-abdominal Pressure Pressure contained within the abdominal compartment. Typically measured in mmHg.

Intra-abdominal Volume Volume contained by the peritoneum in the abdominal compartment, including the volume of visceral contents. Typically measured in L.

Isotropic Describes a material that responds the same way to stress in all directions. In other words, isotropic materials have the same mechanical properties in all planes.

Lumbosacral Orthoses Waist support belt to support the spine or prevent herniation. Also known as hernia belts or abdominal binders.

Normal Intra-abdominal Pressure Intra-abdominal pressure taken at supine position, end-expiration, without abdominal activation, and by urinary bladder pressure. Bounds for normality are dependant on BMI, pregnancy, and age. Also known as baseline intra-abdominal pressure. See Table 1.2.1 for a compilation of published bounds for normal intra-abdominal pressure. Typically measured in mmHg.

Spinal Stability Ability of the spine to return to its (natural) original position.

Stiffness Resistance to deformation under an applied force. Typically measured in N/m.

Transversely Isotropic Describes a material that has the same material properties in one plane, and differing properties in the plane orthogonal to the previous plane. Many biological materials present as transversely isotropic, including wood and cortical bone.

Urinary Bladder Pressure Existing popularized method of intra-abdominal pressure measurement. Measurements require a known volume of saline (typically 25 mL) to be injected into the bladder by way of an indwelling catheter. The resulting pressure is then measured by pressure transducer or manometer and equated to the intra-abdominal pressure assumed to exist throughout the abdominal compartment.

Valsalva Maneuver Breathing technique in which the nose and mouth are closed, and pressure is built by pushing air into the nose. A commonly used means of equalizing ear pressure during flight or diagnosing herniation.

Viscoelasticity The property of a material to change its elasticity depending on the applied strain rate.

Xiphoid Process Lowest (most inferior) point of the sternum.

Young's Modulus Describes a material's resistance to strain, or, relative deformation, and found as the slope of a material's stress-strain curve. An increase in elasticity is synonymous with material stiffening. Also known as elasticity, or Modulus of Elasticity, E. Typically measured in kPa.

Acronyms

E Young's modulus, or, Modulus of Elasticity [kg/m· s^2 or kPa].

F Normal force [kg· m/s^2 or N].

G Shear modulus [kg/m·s^2 or kPa].

K Bulk modulus [kg/m· s^2 or kPa].

P Pressure [Pa].

$P-V$ Pressure-Volume.

S Stiffness [kg/s^2 or N/m]. Alternatively, refers to maximum stress [kPa] in Chapter 3.

V Volume [m^3].

Δ Change in.

δ Linear deformation [m].

ε Normal mechanical strain.

η Geometric ratio.

κ Coefficient dependent on membrane pre-tension used in Hencky's maximum deformation equation (Chapter 3).

ν Poisson's ratio.

ω Coefficient dependent on membrane pre-tension used in Hencky's maximum stress equation (Chapter 3).

$\phi(\eta)$ Function of geometry.

π Constant: pi.

ρ Density [kg/m^3].

ρ Pearson's correlation.

$\rho_{\mathbf{s}}$ Spearman's rho.

σ Normal mechanical stress [kg/m· s^2 or kPa].

σ-ε Stress-Strain.

$\vec{a}$ Acceleration [m/s^2].

a Novel device radius [m].

g Force due to gravity, typically 9.807 [m/s^2].

k Number of testers in a multi-rater study.

m Mass [kg].

n Sample size.

r Radius [m].

t Tissue thickness [m].

x Coefficient for sensitivity analyses.

ACS Abdominal Compartment Syndrome.

AVI Abdominal Volume Index.

AW Abdominal Wall.

AWT Abdominal Wall Tension.

AWTh Abdominal Wall Thickness.

BMI Body Mass Index.

C Abdominal Perimeter, or, Waist Circumference, taken at the navel.

$\mathbf{C_{ab}}$ Clinical Abdominal Compliance.

CT Computed Tomography.

DIC Digital Image Correlation.

ES Effect Size.

FEA Finite Element Analysis.

GRRAS Guidelines for Reporting Reliability and Agreement Studies.

H_0 Null hypothesis.

IAH Intra-abdominal Hypertension.

IAP Intra-abdominal Pressure.

IAV Intra-abdominal Volume.

ICC Intraclass Correlation Coefficient.

ICU Intensive Care Unit.

IPP Intra-peritoneal Pressure.

IVT Intra-vaginal Transducer.

LG Gastrocnemius Lateralis.

MDC Minimum Detectable Change.

MDC% Minimum Detectable Change Percent; ratio of MDC to the data mean.

MG Gastrocnemius Medialis.

MRI Magnetic Resonance Imaging.

NSERC Natural Sciences and Engineering Research Council of Canada.

P_{det} Detrusor Pressure.

PSH Parastomal Herniation.

RIP Respiratory Inductance Plethysmography.

SEM Standard Error of Measurement.

SRM Standardized Response Mean.

SWUE Shear Wave Ultrasound Elastography.

UBP Urinary Bladder Pressure.

UGT Ultrasound Guided Tonometry.

US Ultrasound.

WSACS World Society on Abdominal Compartment Syndrome; presently known as the Abdominal Compartment Society.

Acknowledgements

I would like to express my sincere gratitude to my research supervisor, Professor Mark Driscoll, for his continued support, encouragement, and direction throughout my thesis. Prof. Driscoll not only proposed the research project at its onset, but provided guidance throughout. Prof. Driscoll was a mentor, a supervisor, and a good friend, who jointly celebrated in professional and personal accomplishments, alike. In my opinion, he sets the standard for what it means to be a role model in this field.

In addition, I would like to acknowledge the financial support of the Les Vadasz Engineering Fellowship and Graduate Excellence Award.

Efforts by Mr. Trevor Cotter in clinical testing and design advising deserve tremendous credit. His time commitment to in-person studies, and expertise in manufacturing were instrumental to the success of this project.

Professor Emeritus Waldemar Lehn (Department of Electrical and Computer Engineering, University of Manitoba, and my Opa) merits special recognition for his contributions in editing and mathematical insight via long phone calls throughout the thesis. In particular, deriving the Hencky solution needed to evaluate intra-abdominal pressure given an applied suction, was a collaborative effort that I am honoured to say was done together with my Opa.

Finally, a warm thank you to friends and family cannot go unnoticed – particularly for insight and reviews by my Mom, Dad, Oma, and brothers, Kristjan and Stefan. Moreover, my wonderful husband, Kristopher Kogut, has, time and again, earned thanks, not only for his emotional and mental support throughout my time at McGill University, but also for his technical advice in circuitry design and soldering.

To those I have missed, but not forgotten, I am grateful for you. Research is built on community, and I feel blessed to have been a part of this one.

Abstract

Given the physiological and physical demands of the human abdomen, abdominal afflictions can be frequent and severe. Two physiological properties associated with said conditions are intra-abdominal pressure (IAP) and abdominal wall elasticity (E). Despite the prevalence of abdominal complications, and the known roles of IAP and abdominal wall E, accepted measurement methods for both properties remain invasive or unreliable. Therefore, it is the global objective of this research to **design, optimize and validate a novel, direct, non-invasive IAP measurement device for use in the analysis of spinal and abdominal conditions**.

The novel device (Patent Application No. 63/028,241, PCT, PCT/CA2021/050696) uses a localized known pressure (namely aspiration) to measure resulting tissue deformation, from which internal pressures can be inferred by considering the extended Hencky solution. Two male participants were tested with the device to confirm feasibility of the theoretical device function for IAP measurement. Participants' abdominal wall E were calculated with measured IAP values. Results were consistent with participant body mass indices and overall health.

Following on this feasibility study, and using existing popularized tools (MyotonPro, a myometer, and IndentoPro, an indenter) as benchmarks, the novel device was evaluated on 14 study participants to assess reliability and validity as an E measurement tool. Tests were conducted on both the abdomen and the superficial posterior calf muscle. At the abdomen, low correlation was found for intra- and inter-rater reliability, as well as convergent validity with the MyotonPro. However, at the calf, intra-rater reliability was excellent. Further, low to moderate correlation was found between the novel device and benchmark tools at the calf. That said, of the three devices, only the novel device demonstrated correct and consistent response to changes in anatomical position and presented E within range of published data.

Finally, in a cadaveric study (n = 13), the novel device was tested 5 cm subxiphoid, using urinary bladder pressure (UBP) as a benchmark to evaluate reliability and validity. Concurrently, 14 healthy, living participants were tested with the novel device, though without UBP. Intra- and inter-rater reliability were found to be excellent in both living and cadaveric specimen. Convergent validity was evaluated against published average IAP values and found to be excellent (in living participants) and moderate (in cadavers), while convergent validity against UBP was inconclusive.

In all, a novel device was designed, developed, and proposed for non-invasive IAP and E measurement, thus achieving the outset objective. Positive results indicate the feasibility of the novel device described herein, and suggest the need for comparative testing against UBP on living participants in the future.

Résumé

Compte tenu des exigences physiologiques et physiques de l'abdomen humain, les problèmes abdominales peuvent être fréquentes et sévères. Deux propriétés physiologiques associées aux problèmes abdominales sont la pression intra-abdominale (IAP) et l'élasticité (E) de la paroi abdominale. Malgré la prévalence des complications abdominales et les rôles connus de l'IAP et de l'E de la paroi abdominale, les méthodes de mesure acceptées pour les deux propriétés restent invasives ou peu fiables. Par conséquent, l'objectif global de cette recherche est **de concevoir, optimiser et valider un nouveau appareil de mesure IAP directe et non invasive destiné à être utilisé dans l'analyse des affections de la colonne vertébrale et de l'abdomen**.

Le nouveau appareil (Brevet No. 63/028,241, PCT, PCT/CA2021/050696) utilise une pression localisée connue (l'aspiration) pour mesurer la déformation tissulaire résultante, à partir de laquelle les pressions internes peuvent être divulguées en considérant la solution de Hencky étendue. Deux participants de sexe masculin ont été testés avec l'appareil pour confirmer la faisabilité de la fonction théorique pour la mesure de l'IAP. Les E de la paroi abdominale des participants ont été calculés avec des valeurs de l'IAP mesurées. Les résultats étaient cohérents avec les indices de masse corporelle des participants et l'état de santé général.

Suite à cette étude de faisabilité et en utilisant les outils existants (le MyotonPro et l'IndentoPro) comme référence, le nouveau appareil a été évalué sur 14 participants pour évaluer la fiabilité et la validité des mesures d'E. Des tests ont été réalisés à la fois sur l'abdomen et le muscle superficiel du mollet postérieur. Sur l'abdomen, une faible corrélation a été trouvée pour la fiabilité intra- et inter-évaluateurs, ainsi que la validité convergente avec le MyotonPro. Cependant, au mollet, la fiabilité intra-évaluateur était excellente. De plus, une corrélation faible à modérée a été trouvée entre le nouveau appareil et les outils de référence au mollet. Cela dit, sur les trois appareils, seul le nouveau appareil a démontré une réponse correcte et cohérente aux changements de position anatomique et a présenté des E dans les l'intervalle des données publiées.

Enfin, dans une étude cadavérique (n = 13), le nouveau appareil a été testé sous-xiphoïde de 5 cm, en utilisant la pression de la vessie (UBP) comme référence pour évaluer la fiabilité et la validité. Parallèlement, 14 participants vivants en bonne santé ont été testés avec le nouveau appareil, mais sans UBP. La fiabilité intra- et inter-évaluateurs était excellente dans les spécimens vivants et cadavériques. La validité convergente a été évaluée par rapport aux valeurs moyennes publiées de l'IAP et était excellente (chez les participants vivants) et modérée (chez les cadavres), tandis que la validité convergente par rapport à l'UBP n'était pas concluante.

Au total, un nouveau appareil a été conçu, développé et proposé pour la mesure non invasive de l'IAP et de l'E, atteignant ainsi l'objectif initial. Des résultats positifs indiquent la faisabilité

du nouveau appareil décrit ici, et suggèrent le besoin de tests comparatifs contre UBP sur des participants vivants à l'avenir.

Author's Contribution

I, Natasha Jacobson, certify that I am the primary author of all the material included within this dissertation. Under the supervision of Professor Mark Driscoll, I designed, prototyped and tested a non-invasive method of intra-abdominal pressure measurement. Following initial design synthesis and concept validation, I improved upon the existing design by adjusting data calculation for more robust and responsive systems. In addition, I planned and oversaw both clinical studies with living participants and cadavers. I conducted data and statistical analyses on each clinical study to confirm reliability, validity, agreement, and responsiveness of the comprehensive design. Finally, I synthesized all results into readable formats for use in manuscript preparation and conference presentation.

Original Contribution

The following contributions to knowledge were made through the completion of the presented thesis:

1. A novel application for the Hencky solution was proposed - namely, a circular membrane under uniform lateral loading, fixed at its bounds, and presenting large deflections. The physiological application for this set of equations was suggested for the abdomen, assumed to be an infinitely flat surface, undergoing locally applied suction by a cup of fixed radius, given a frictionless contact between the cup and skin;

2. Equations for the non-invasive evaluation of intra-abdominal pressure, given a locally applied suction to the abdomen, were developed;

3. A novel application for the elasticity equation via suction was proposed in which a macropipette (suction diameter of 60 mm) is used to divulge deep, composite, soft tissue elastic properties;

4. Minimum tensile requirements for lumbosacral orthoses were calculated to limit the occurrence of parastomal herniation following colostomies;

5. Reliability, validity, agreement, and responsiveness of a novel method for *in vivo* soft tissue elasticity measurement were evaluated in human testing at the abdomen and posterior calf muscles against two popularized stiffness measurement tools: MyotonPro and IndentoPro. Reported values supplement existing data on the soft tissue elasticity of these anatomical locations for a wider database of physiological measurements;

6. Immediate (within 30 seconds) and short-term (within 2 to 3 minutes) effects of flash cupping on soft tissue elasticity were evaluated in human testing at the abdomen and posterior calf muscles. Immediately improved elasticity, and short-term stiffening were identified;

7. Reliability, validity, agreement, and responsiveness of a novel method for *in vivo* intra-abdominal pressure measurement were evaluated in human and cadaveric testing against the popularized measurement method: urinary bladder pressure. Reported values supplement existing data on intra-abdominal pressure for a wider database of physiological measurements.

1 Literature Review

The human abdomen not only contains and protects organs vital to life, but is responsible for the structure and support of the spine [1]. Spinal support, or stability, is made possible by both the activation of abdominal muscles and increase in pressure contained in the abdominal compartment (or, Intra-abdominal Pressure (IAP)) [2], [3]. Given the demands of this anatomical region, abdominal conditions can be frequent and severe [4]–[6]. Two physiological properties associated with abdominal conditions are IAP and Clinical Abdominal Compliance (C_{ab}) [2], where C_{ab} is the measure of ease of abdominal expansion [7]. Both properties are directly affected by a subject's Intra-abdominal Volume (IAV), the volume of the abdominal compartment at a known time or position [2], and Abdominal Wall (AW) elasticity [8]. Despite the prevalence of abdominal complications, and the known roles of IAP and C_{ab}, accepted measurement methods for both properties remain invasive or unreliable [4], [9], [10]. As such, the need for a novel device is evident. To better understand the clinical and mechanical scope of this project, four concepts were identified for review in which the definitions, mechanics, and existing measurement methods of each were described: (1) IAV, (2) IAP, (3) AW elasticity, and (4) C_{ab}. Finally, the clinical relevance of the research, herein, and application of aspiration as a potential elasticity and IAP measurement tool were explored.

1.1 Intra-abdominal Volume

The abdominal compartment (also referred to as the abdominopelvic cavity [1] or the abdominal cavity [11], [12]) is assumed to contain a closed volume of incompressible fluid, such that a uniform pressure exists [13]–[15]. This compartment is not to be confused with the peritoneal cavity, or, the space enclosed by the peritoneum (innermost layer of the AW [11]), as the peritoneal cavity does not consider visceral contents to be part of the defined volume [16]. Bordering the abdominal compartment is the diaphragm (superior), pelvic floor (inferior), AW (anterior), and spine (posterior), as shown in Figure 1.1.1 [11]. Of these four boundaries, the spine and pelvic floor are rigid [2]. Due to the controlled flexibility of the AW and, to a lesser extent, the diaphragm, the volume contained in the abdominal compartment is variable [2], [10]. Given the irregular nature of this space, the volume of the abdominal compartment at a known time or position is the "intra-abdominal volume" [2].

1.1.1 Mechanics

Baseline IAV, the minimally stretched volume, is measured in patients in supine position, at end-expiration, without abdominal tightening [2], [6]. A study completed by the Digestive System Research Unit in Spain determined the average baseline IAV using a helical multislice

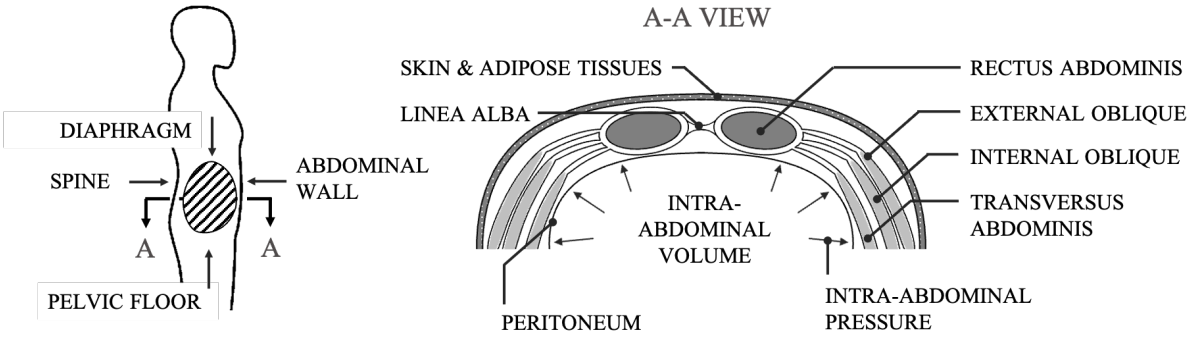

Figure 1.1.1: Side profile showing the location of the intra-abdominal volume, juxtaposed with a cross-sectional annotated view of the abdomen.

Computed Tomography (CT) scanner [17]. Results showed baseline IAV values of 12.5 ± 1.2 L for healthy subjects [17]. One year later, another research group measured baseline IAVs of 7.64 L in hernia patients, pre-operatively [18]. Discrepancies between studies can largely be attributed to test patient populations, and indicate a range of possible physiological IAVs. The maximally stretched volume (maximum IAV) is dependent on a patient's C_{ab} and diaphragmatic response [19], [20]. As such, defining a "normal" maximum IAV is not possible [10].

Passive IAV inflation can be discretized into 3 phases: (1) a linear reshaping phase, (2) a stretching phase, and (3) a pressurization phase [2], [20]. Phase 1 has been well established in literature for IAP up to 12 mmHg [21], [22] and 15 mmHg (though this study measured Intra-peritoneal Pressure (IPP) rather than IAP) [23]. In fact, Song *et al*. mapped AW motion during insufflation up to 12 mmHg and noted that, in addition to a linear relationship between IAV and IAP, the shape of the AW changed [24]. During inflation, the AW expanded in the cranial-caudal axis (anteroposterior diameter), and decreased in the transverse axis (lateral diameter), resulting in a profile change from elliptical to near-spherical [20], [24]. Mulier *et al*. corroborated these findings in 2008, presenting CT scans pre- and post-inflation that indicated a shape change in the peritoneum [25]. During the second phase of IAV inflation, above an IAP around 15 mmHg [2], [20], stretching of the rectus abdominis causes the AW to increase in surface area by around 15% [20], [24]. Finally, at the elastic limits of the AW (IAP of approximately 25 mmHg [2], [20]), with further insufflation, IAP increases exponentially, yielding the name: "pressurization phase" [20]. Figure 1.1.2 illustrates an approximated version of the Pressure-Volume ($P-V$) curve, with relative abdominal cross-sections identified.

In a 2011 case report by Pracca *et al*., data contrary to the 3-phase IAV inflation model was published [26]. In this study, four patients were tested with a novel IAP reduction device (the ABDOPRE) which applied an extra-abdominal negative pressure to the abdomen to forcibly

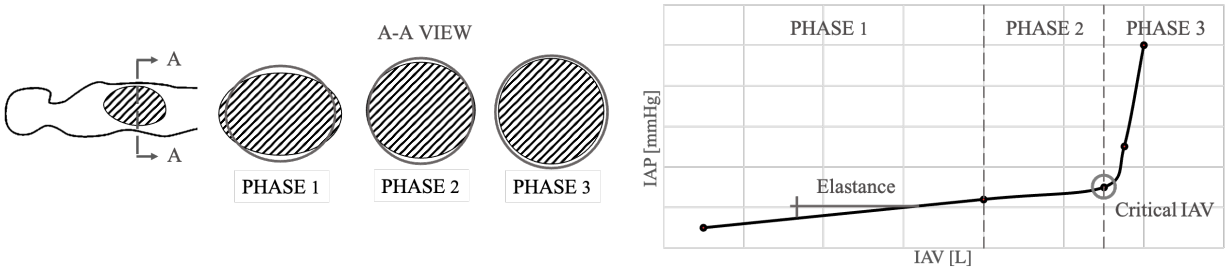

*Figure 1.1.2: Approximated pressure-volume (*P-V*) curve of the human abdomen. Relative changes in abdominal cross-section are illustrated for each phase of inflation.*

increase IAV with an expected IAP reduction to result [26], [27]. Of these four patients, one was an obese female (Body Mass Index (BMI) 34.9) whose IAP did not decrease, but increased by 38% when IAV was increased [26]. This paradox introduces the effect of body shape on IAV behaviour, though Pracca's research group attributed the error to the insufficient size of the ABDOPRE, itself [26]. For obese patients whose waist-to-hip ratio is greater than 1, there is excess visceral fat (also known as android obesity) [2], [20]. As such, the abdominal compartment does not follow the traditional phases of passive IAV inflation. Android obese patients present with a circular abdominal cross-section, as opposed to a healthy elliptical shape (also known as gynoid obesity) [4]. Therefore, only stretching and pressurization of the IAV is possible [2], [20]. Thus, the effect of body shape on IAV behaviour must be considered.

1.1.2 Existing Measurement Methods

Due to its variability with time and patient-to-patient differences, there is no standard measurement tool for IAV [2], [20]. In experimental studies, the IAV has been estimated using Respiratory Inductance Plethysmography (RIP), imaging techniques (helical multislice CT scans [17]–[19], Magnetic Resonance Imaging (MRI) [4], [28], Ultrasound (US) [4], [28]), and geometrically. Geometric identifiers have included the waist-to-hip ratio [29], abdominal perimeter (circumference taken at the navel) [30], BMI [29], Abdominal Volume Index (AVI) [31], and conicity index [32]. To note, the conicity index refers to the following relation [32]:

$$Conicity\ Index = \frac{abdominal\ girth}{0.109\sqrt{\frac{waist}{hip}}} \tag{1.1.1}$$

where abdominal girth is the widest abdominal circumference between the xiphoid process and hip bones (a potentially variable measure between clinicians), waist is the circumference taken at the navel, and hip is the widest circumference at the hips ($\frac{waist}{hip}$ more commonly known as waist-to-hip ratio). Alternatively, AVI approximates the volume of the entire abdominal compartment by

summation of a cone and a cylinder, given similar waist and hip dimensions [17], [18], [31]:

$$AVI = \frac{(2\ cm(waist)^2 + 0.7\ cm(waist - hip)^2)}{1000} \tag{1.1.2}$$

AVI is the preferential geometric IAV technique [4], however, it includes anterior AW musculature and adipose tissues, resulting in higher IAV values than measurements through imaging (such as 12.8 L with AVI, versus 12.3 L with imaging, using results from [17]) [31]. Therefore, though faster and simpler, AVI is not as accurate a measurement tool for IAV as its imaging counterparts. Of available imaging modalities, CT is most recommended for its high accuracy and availability in commercial hospitals [28]. RIP, however, combines geometry and electrical impedance tomography. In RIP, two bands of wire coils and known inductance are placed across the rib cage (resting at the armpit), and at the abdomen (placed along the navel) [33], [34]. As the volume of the thorax changes, from breathing or other motion, this volume is recorded by RIP using the equation

$$IAV = \kappa(\frac{\alpha}{\beta}\Delta L_{\text{rib cage}}\Delta L_{\text{abdomen}}) \tag{1.1.3}$$

where κ is a dimension conversion factor, α/β is a weighting coefficient, and ΔL is the change in length of the respective wire coil at the denoted anatomical location [34]. It is important to consider the fact that RIP measures the length change in the chest wall (with $\Delta L_{\text{rib cage}}$), which may be beyond the scope of the abdominal compartment. An ideal, indisputable change in IAV that can be measured is by the intake of measured fluid, such as drinking water. Though not a means of measuring total volume, this change in IAV may be of interest in future studies.

1.2 Intra-abdominal Pressure

Intra-abdominal pressure is the pressure contained in the abdominal compartment [2]. In 2007, an article endorsed by the World Society on Abdominal Compartment Syndrome; presently known as the Abdominal Compartment Society (WSACS) was published to standardize IAP definitions and measurement techniques [6]. The WSACS defined "normal" (or, baseline) IAP as between 5 and 7 mmHg in critically ill patients taken at supine position during end-expiration with a bladder catheter [6]. However, more recent IAP studies [35]–[41] expanded on this definition, and the WSACS published an updated version of the article redefining normal IAP as between 5 and 7 mmHg in healthy adults, and 10 mmHg in critically ill patients, taken at a supine position during end-expiration with a bladder catheter [2], [20]. Critically ill children have been shown to have lower normal IAP than adults with a range of 4 to 10 mmHg [42]–[44].

High levels of IAP are denoted by the terms Intra-abdominal Hypertension (IAH) or Abdominal Compartment Syndrome (ACS), depending on measured values [45]. Both conditions are prevalent in Intensive Care Unit (ICU), and are often caused by peritoneal inflammation and/or abdominal fluid build-up, typically as a result of acute abdominal injury or surgery [7]. Rates of IAH have been recorded in between 20 and 50% in ICU patients, with rates increasing in ventilated patients [46]. This increased IAP can reduce blood flow to vital organs, perpetuating further pressure build-up as organs become unable to drain excess fluids [7], [45]. These life-threatening complications are diagnosed by IAP measurements collected over 4 to 6 hours that are consistently greater than 20 mmHg and 12 mmHg for ACS and IAH, respectively [45] [47]. Though diagnosis of high IAP conditions is not a prerogative of this research, it is important to recognize the dangers associated with high IAP.

1.2.1 Mechanics

As mentioned previously, the WSACS defined normal IAP as between 5 and 7 mmHg in healthy adults taken at a supine position during end-expiration with a bladder catheter [2], [20]. This recommendation was later supported in a review conducted by Milanesi *et al*. [47]. Further research has indicated a wider range of normal IAP, dependent on position and BMI [36]. De Keulenaer *et al*. reviewed a range of researchers' work [29], [37], [38], [40], [41], [48], [49] aimed at measuring IAP and determining norms [36]. Tests by each researcher were conducted for different BMIs (from normal to obese), as well as different body positions (from supine to prone). It should be noted that IAP was not compared during activity, such as inhalation/exhalation or trunk movement. De Keulenaer *et al*. concluded that, with the acquired data of nearly 300 patients, normal IAP was between 5 and 7 mmHg, a range in agreement with the WSACS definition [20], [36]. However, this resting pressure increased with BMI, such that overweight (BMI 25 thru 29.9

kg/m^2), obese (BMI 30 thru 34.9 kg/m^2), and morbidly obese (BMI greater than 35 kg/m^2) patients saw IAPs between 6.3 and 11.2 mmHg [38], [39], [50], 7.4 and 13.7 mmHg [39], [49], and 8.4 and 16.2 mmHg [29], [48], respectively. As such, De Keulenaer's research group suggested a range of normal IAP for patients with BMIs greater than 25 between 7 and 14 mmHg [35], [36]. IAP's positive correlation with BMI has been hypothesized to be due to the direct relationship between pressure and visceral fat layer [36], a theory reinforced in 2016 [51]. This lends insight into the trend of health conditions in the obese population.

Other factors that have been shown to increase IAP include the inclination of the head of a patient's bed [36], [52], the use of an external support band, such as a brace or corset [53], [54], abdominal fitness [8], and inhalation/exhalation [55]. Therefore, though published definitions by WSACS are widely used, these values are only applicable to patients in a specific category, *i.e.* those with normal BMI, in a fully supine position at end-expiration without abdominal tightening, being measured with a bladder catheter [6]. It is also noteworthy that some factors have been shown to not affect IAP. These include sex [35], abdominal perimeter [30], [51], and waist-to-hip ratio [51]. Additionally, pregnancy has been shown to greatly alter "normal" IAP values. Al-Khan *et al*. studied 100 women at term and found "normal" IAP to be 22 (2.9) mmHg and 16.4 (2.6) mmHg pre- and post-operatively [56]. Though these values are in the "unhealthy" range of IAP, because of the increase in C_{ab} due to pregnancy, conditions of IAH or ACS are uncommon [56]. That said, patients with previous rectus muscle plications (surgical tightening of the AW) may be at risk, given the limited compliance of the AW [56].

Understanding normal IAP is not sufficient to extrapolate the mechanics of the abdomen. As such, changes in IAP are investigated. If a pressurized cylinder containing an incompressible fluid is considered, given basic mechanics, it follows that a change in cylinder volume, wall elasticity, or orientation would affect the internal pressure [57]. In 1982, Primiano proposed modeling the abdomen as a pressurized cylinder, and the model has been repeated since [14], [24], [35], [58]–[60]. As such, it is appropriate to state that IAP is affected by IAV, AW elasticity, and body orientation. Experimental studies have further validated the determining factors for IAP. The $P-V$ curve of the abdomen suggests that IAP increases linearly with IAV until a critical volume, at which point, IAP increases exponentially [20]. The "critical volume", though, is dependent on an individual's AW elasticity; a stiffer AW resists volumetric strain [7], [20]. In physiological conditions, such as breathing, IAP tends to increase upon inhalation, due to the caudal movement of the diaphragm, thereby decreasing IAV [55]. During exercise, when abdominal muscles contract, IAV is also reduced anteriorly [35]. Given this reduction, IAP increases, with peaks recorded up to 252 mmHg when jumping [35], and 360 mmHg during an Olympic level lift [58]. Finally, grav-

itational effects are evident when considering body position [35]. The sensitivity of IAP to body position was made clear in Cheatham *et al*.'s study, indicating that a 15° incline of a patient's head of bed (angle made at waist with the ground) increases IAP by around 1.5 mmHg [52]. Although general agreement has been seen between Primiano's abdominal model and experimental studies, pressure differences have been measured *in vivo*, concurrently, at different places in the abdominal compartment [61]. Thus, it is important to consider the possibility of the IAV not containing an ideal compressible fluid.

To summarize known values of IAP under a range of conditions, Table 1.2.1 is shown. To note, some IAP measurements may be greater than normal blood pressure (115/75 mmHg [62]), suggesting the impossibility of such peaks in IAP. That said, extreme IAP levels during exercise are impulse peaks to support the spine the moment before the abdominal muscles further distribute given loads [63]. It is when high IAP is prolonged, as in the cases of IAH and ACS, that dangerous conditions arise.

Table 1.2.1: Intra-abdominal pressures at various physiological states

Physiological State	IAP [mmHg]	IAP [kPa]	Ref.
Normal - Healthy and Normal BMI	5-7	0.7-0.9	[2], [20]
Normal - Critically Ill and Normal BMI	10	1.3	[2], [20]
Normal - Critically Ill Children	3-10	0.4-1.3	[42]–[44]
Normal - Overweight	6-11	0.8-1.5	[38], [39]
Normal - Obese	7-14	0.9-1.9	[39], [49]
Normal - Morbidly Obese	8-16	1.1-2.1	[29], [48]
Normal - Pregnant at term (post-op)	11-24	2.0-3.9	[56]
Normal - Pregnant at term (pre-op)	15-29	1.5-3.2	[56]
Critically Ill - Intra-abdominal Hypertension	$>$ 12 over 4-6 hours	$>$ 1.6 over 4-6 hours	[45], [47]
Critically Ill - Abdominal Compartment Syndrome	$>$ 20 over 4-6 hours	$>$ 2.7 over 4-6 hours	[45], [47]
Critically Ill - Intra-abdominal Hypertension (Children)	$>$ 10 over 4-6 hours	$>$ 1.5 over 4-6 hours	[44]
Critically Ill - Abdominal Compartment Syndrome (Children). Note: Must be in combination with associated new or deteriorating organ dysfunction	$>$ 10 over 4-6 hours	$>$ 1.5 over 4-6 hours	[44]
Inclined head of bed (15°)	Normal + 1.5	Normal + 0.2	[52]
Inclined head of bed (30°)	Normal + 3	Normal + 0.4	[10]
Inclined head of bed (45°)	Normal + 6	Normal + 0.8	[10]
Sitting	10-21	1.3-2.8	[35]
Standing	15-27	2.0-3.6	[35]
Voluntary Cough	102	13.6	[64]
Defecation/Valsalva	120	16.0	[58], [65]
Dynamic Loading	208	27.7	[58]
Jumping	252	33.6	[35]
Extreme Loading	360	48.0	[58]

1.2.2 Existing Measurement Methods

Currently, there is no "gold standard" for measuring IAP [9], [66]. "Direct" pressure readings use microtransducers embedded just under the AW to measure IPP, which has been shown to have no statistical difference with IAP [67]–[69]. That said, embedded microtransducers are not widely recommended measurement methods, given the invasive nature of the procedure [4], [9]. The WSACS recommend IAP measurement via the bladder (known as intra-vesical pressure,

urinary bladder pressure (UBP), or intra-bladder pressure), given that most patients requiring IAP monitoring already have a catheter implanted, making measurements minimally invasive [7], [70]. Further, patients have noted less discomfort in UBP measurement in comparison to other methods (gastric or rectal) [71]. However, some researchers disagree with UBP measurement, especially in dynamic testing, as the system is position dependent and prone to air bubbles that can skew readings [70]. Regardless, UBP measurement is currently the most common method of obtaining IAP, and has been used as a reference method against novel technologies [60], [72]. As an aside,

Though UBP represents the most popular measurement method for IAP, measurements at the bladder (intra-vesical pressure, P_{ves}) represent a summation of IAP and detrusor pressure (P_{det}), or the pressure within the bladder created by bladder wall muscle contraction [73], [74]:

$$P_{\text{ves}} = IAP + P_{\text{det}} \tag{1.2.1}$$

The consideration of P_{det} is relevant in the diagnosis of lower urinary tract dysfunctions, including incontinence, and is typically measured using cystometry [73], [74]. Cystometry is synonymous with UBP, though uses the rectum as a reference measure (for IAP), whereas UBP uses the mid-axillary line of the iliac crest for reference with patients in supine position [9], [75], [76]. During urodynamic testing, patients' bladders are infused with saline in 50 mL increments until a maximum capacity is reached (noted by patients' strong desire to void) to simulate urine storage [73]. Typically urodynamic testing is completed with patients in either a sitting or standing position and without anesthetic [73]. Following, patients are asked to void their bladders, at which point P_{det} (and, consequently, P_{ves}) should spike to prompt urine evacuation [73], [74]. In the case of urinary tract pathologies, P_{det} may spike inadvertently, causing unwanted bladder leakage, termed detrusor overactivity incontinence [73]. Conversely, urodynamic stress incontinence refers to unwanted bladder leakage due to increased IAP without P_{det} activation [73]. Normal P_{det} is around 0 mmHg with an empty to nearly empty bladder, while around 20 mmHg is needed to evacuate the bladder. If high P_{det} is accompanied by low urine flow rates during bladder emptying, this is indicative of potential pathologies of the urethra [73].

Despite the effect of detrusor muscle activation on IAP measurement via the bladder, UBP remains the recommended form of IAP measurement given that patients' bladders are evacuated prior to testing. However, patients with diagnosed detrusor overactivity may be undesirable study participants for novel IAP device testing in the future. In addition, should UBP measurements present higher than those at other anatomical positions (stomach, rectum, vagina, or other), detrusor effects may offer the explanation.

Most accepted forms of IAP measurement follow the same underlying principles: a known

volume of fluid (air, saline) is injected into a closed abdominal space (bladder [70], stomach [77], [78], rectum [79], uterus [80], or central venous system [71], [81]) via the corresponding tube (catheter, nasogastric) [9], [71]. The resulting pressure is then measured (via transducer, manometer, or strain gauge) and related to IAP for relevant diagnostics [9]. Though a common procedure, IAP measurement is sensitive to procedural discrepancies. This includes, but is not limited to, diaphragm position [55], patient position [36], [52], the amount of saline injected, or time before pressure reading [9]. As such, standards from the WSACS exist to limit said discrepancies, such as measuring at end-expiration, supine position, and with a saline instillation volume of 25 mL with an indwelling bladder catheter (as low as 3 mL is acceptable in children [44]) [20]. Alternatively, an Intra-vaginal Transducer (IVT) is invasive, but a highly accurate means of continuous IAP measurement, while offering wireless capabilities [82], [83]. However, IVTs are limited to the female population, and intra-rater reliability has not been evaluated. The following discusses more recent IAP measurement tools that offer non-invasive techniques.

1.2.2.1 Ultrasonography

Ultrasound Guided Tonometry (UGT) refers to the evaluation of pressure by measurement of applied force and displaced liquid volume [84]. UGT has only been studied in porcine models, but resulted in the ability to distinguish between three defined categories of IAP: normal, mid-range, and high [84]. Though non-invasive, this technology is not portable and does not offer fine IAP measurement resolution.

Similar is the use of an applied fluid force contained in a bottle held against the AW. As liquid is removed, the force decreases. If the response, or return, of the peritoneum to its neutral state is monitored by US, then it can be said that the fluid pressure that returns the peritoneum to its neutral position is equal to the pressure in the underlying cavity [34]. This procedure has had excellent correlation to UBP, though, is a slow, manual procedure that requires a fluid pressure to be orthogonal to the tissue of interest [34].

Two other forms of IAP measurement via US are Doppler US and Laser US. In both scenarios, IAP is correlated with another variable. That is, blood flow and wavelength of a transmitted pulse in Doppler and Laser, respectively [34]. Doppler US correlates blood flow at the femoral vein to IAP, though, results were inferior to those of UGT [34]. Laser US sends a signal across the entire cross-section of the thorax; sent at the AW and retrieved by the spine. If the attenuation of every tissue along the length of the body is known, changes in IAP can be determined by changes in the received pulse wavelength. However, this is a highly individualized procedure, and theoretical in its current state [34].

1.2.2.2 Correlation to Anatomic Geometries

The measurement of Abdominal Wall Tension (AWT), also known as tensiometry, and its correlation to IAP has also been investigated. Due to the direct relationship between AW stress and internal pressure in pressurized cylinders, van Ramshorst *et al*. assumed the measurement of AWT could provide insight into IAP [57], [85]. In further studies, the anatomical landmarks that offered the greatest reliability in AWT testing were 5 cm caudal to the xiphoid process and 5 cm cranial to the umbilicus [59]. Another group of researchers followed up on these findings by measuring AWT at 5 cm subxiphoid on 51 living patients [60]. AWT was then correlated to IAP measured via UBP [60]. The results from this study agreed with van Ramshorst *et al*.'s, proving AWT could be used to interpret IAP, however, correlation equations varied significantly [59], [60]. This discrepancy was largely attributed to patient population variation, but demonstrates the unreliability of IAP measurement with correlation equations.

Following up on the work of AWT correlation, David *et al*. considered the correlation of Abdominal Wall Thickness (AWTh) to IAP using bioimpedance and microwave reflectometry (termed AbdoRF) [86], [87]. Just as in the work of van Ramshorst *et al*., positive correlation was evident, but poor sensitivity and limited pressure ranges (up to 14 mmHg) were noted [86], [87].

Another means of IAP correlation to anatomic geometries is via RIP, as described in Section 1.1.2. If C_{ab} is known, and IAV is measured via RIP, IAP can be directly calculated by the equation [7]

$$IAP = C_{\text{ab}} IAV. \tag{1.2.2}$$

Alternatively, in the more likely scenario that C_{ab} is unknown, IAP can be correlated to measured IAV [7].

1.2.2.3 Other

Smart pills (or, wireless motility capsules) were studied in porcine models as potential IAP measurement systems [34]. When compared directly to UBP, however, the expensive smart pills underestimated IAP, a finding that could have severe clinical consequences [34].

Digital Image Correlation (DIC) has not been studied as a means of IAP measurement, although, its use in AW elasticity measurement by Song *et al*. suggests its potential in this area [24], [34]. DIC employs multiple cameras to produce an individualized 3D image that is then inputted into a Finite Element Analysis (FEA) software for deformation to be mapped given a known loading pattern. Despite the potential of DIC, procedural discrepancies make it a difficult means of measurement, and long set up times are inopportune for a clinical setting [34].

1.2.2.4 Summary

To summarize, existing clinically-accepted IAP measurement techniques are invasive and not inter-rater reliable. Non-invasive alternatives allow reasonable results to be obtained, but do not directly measure pressure; UGT, bioimpedance, microwave reflectometry, and AWT/AWTh measurements interpret results and correlate them to IAP. Furthermore, non-invasive alternatives require continued research before clinical usage. As such, direct, non-invasive IAP measurement devices are not currently available. Recommendations from Tayebi *et al*. suggest bioimpedance and microwave reflectometry offer the most promise in future IAP measurement [34]. However, in their review of non-invasive IAP measurement methods, only wireless motility capsules were able to directly measure IAP. All other methods of measurement evaluated correlated IAP to an existing measure (IAV, AWT, AWTh, blood flow, applied force) [34]. Table 1.2.2 is available as a quick reference text for existing measurement methods.

Table 1.2.2: Summary of IAP measurement methods. Continuous refers to dynamic, rather than discontinuous, or impulse, measurements. Accepted methods of measurement are those currently in use in clinics, today. Direct methods refer to those measurements able to determine IAP without correlation to another variable.

Method	Description	Non-Invasive	Continuous	Accepted	Portable	Direct	Advantages	Disadvantages	Ref.
Embedded micro-transducer	A cannula connected to Codman microsensor was tapped into the abdominal wall at the junction of the anterior rectus abdominis and line connecting iliac anterosuperior spines.		X	X		X	Potential for portability if wireless information transmission introduced. May be more feasible given technical advances.	Expensive. Risk of visceral perforation. Requires US guidance. More invasive than UBP. Fragile.	[67], [68]
Intra-vaginal transducer (IVT)	Pressure in the upper vagina is measured and compared to IAP measurements in a rectal balloon measurement system.		X		X		Wireless data transmission, high resolution.	Only viable in females.	[82], [83]
Bladder pressure, cystometry (UBP)	WSACS "gold standard" measurement system. With a transducer-tipped catheter, the pressure in a saline-filled bladder is measured and termed IAP.			X			WSACS standard, thus, widely studied and practiced.	Less reliable above IAP of 12 mmHg.	[70], [71]
Intra-gastric pressure	Catheter introduced through the nasogastric pathway to the stomach. Similar to UBP, the catheter is tipped with a transducer to measure IAP.			X			Preferred method should the bladder be inadvisable.	Highly uncomfortable for patients.	[61], [71], [77], [78]
Intra-uterine pressure	Introduction of a fluid-filled catheter into the uterus. An attached strain gauge provides insight into the intra-uterine pressure which is then correlated to IAP.			X			High accuracy and repeatability.	Only viable in females.	[80]
Intra-rectal pressure	Introduction of a fluid-filled balloon catheter into the rectum. An attached strain gauge provides insight into the intra-rectal pressure which is then correlated to IAP.			X			Alternative if the bladder and stomach are not viable.	Highly uncomfortable for patients.	[71], [79]

Continued on next page

Table 1.2.2: Continued from previous page

Method	Description	Non-Invasive	Continuous	Accepted	Portable	Direct	Advantages	Disadvantages	Ref.
Central venous pressure	Veins cannulated to correlate decrease in blood pressure to heightened IAP.		X	X			Alternative if digestive tracts compromised.	Indirect method; correlation technique. Only feasible in supine patients.	[71], [81], [84]
Indentation	AWT correlation with IAP	X			X		Small, simple, easily portable for on-site studies.	Discontinuous.	[59], [60]
US Tonometry	Probe held against AW, resulting AW push-back from increased IAP was measured and correlated to IAP.	X					Simple. US tends to be readily available in most clinics.	Can only distinguish between normal, high and very high IAP.	[84]
US and Peritoneal Rebound	Varying liquid forces are applied to the AW until the peritoneum rebounds to its neutral position, indicating a balanced system.	X					High correlation to UBP.	Can only be used with liquid orthogonal to tissue.	[34]
Doppler US	Correlation of IAP to blood flow.	X					Simple.	Poor inter-rater reliability and accuracy.	[34]
Laser US	Correlation of IAP to wavelength of a transmitted pulse.	X					Potential for wider applications, if all material properties are known.	Theoretical application in IAP.	[34]
Bioimpedence	The impedance of the AW is correlated to IAP.	X					High potential for future work [34].	Poor sensitivity.	[86], [87]
Microwave	The reflection coefficient between an antenna and AW was correlated to IAP. The antenna received the changes in abdominal wall wave impedance as varying frequencies.	X					High potential for future work [34].	Limited pressure range (up to 14 mmHg).	[86], [87]
Respiratory Inductance Plethysmography (RIP)	Correlation of IAP to IAV.	X	X		X		Simple and affordable.	Sensitive to motion. Only continuous monitoring in immobile patients.	[34]

Continued on next page

Table 1.2.2: Continued from previous page

Method	Description	Non-Invasive	Continuous	Accepted	Portable	Direct	Advantages	Disadvantages	Ref.
Digital Image Correlation (DIC)	With 2 cameras, a 3D image can be produced given a tissue with a defined pattern (such as fine, dark paint spray). Inputting images into FEA allows for deformation to be mapped given loading.	X					Individualized FEA may have wider applications.	Long set up time.	[24]
Wireless Motility Capsule	Smart pills that provide live measurements of IAP *in vivo*.	X	X		X	X	Simple.	Very expensive to produce and underestimated IAP when compared to UBP.	[34]

1.3 Abdominal Wall Elasticity

The AW is an anisotropic, dynamic, composite-laminar material, comprised of a number of soft tissue layers, as shown in Fig. 1.1.1 [10], [24], [88]. Due to the rigidity of the posterior muscle and fascia, only the anterolateral AW is of interest in the context of IAP, IAV, and C_{ab} [2], [15]. Further, only the AW from the xiphoid process to the pubic bone is considered, as semi-rigid connection points are made at these two anatomic junctions [1]. AW layers change across the abdomen, both longitudinally (cranial-caudal) and transversely (medial-lateral) [11]. Moving from the umbilical line, laterally, are three major AW regions: (1) at the umbilical line (or, linea alba), (2) at the rectus abdominis, and (3) at the oblique muscles [11]. The AW layers at each aforementioned region are approximately described from anterior to posterior: Region 1: skin, subcutaneous (also called superficial [1] or adipose) tissue, aponeuroses (creating the linea alba), transversalis fascia, extraperitoneal fascia, and the parietal peritoneum [11]; Region 2: skin, subcutaneous tissue, anterior rectus sheath, rectus abdominis, posterior rectus sheath, transversalis fascia, extraperitoneal fascia, and the parietal peritoneum [11]; Region 3: skin, subcutaneous tissue, oblique muscle aponeuroses, external oblique muscle, internal oblique muscle, transverse abdominis, transversalis fascia, extraperitoneal fascia, and the parietal peritoneum [11]. To note, ligaments, nerves, cardiovasculature and lymphatics are also present in the AW, but do not significantly contribute to the mechanical properties of the material [1]. A summary of average AW layer thicknesses is provided in Table 1.3.1.

Table 1.3.1: Abdominal wall anatomical layer thicknesses (SD: standard deviation). Where available, data ranges are provided.

Anatomy	Sample Size	Male/Female	Age Range (SD)	Thickness [mm] (SD) Male	Thickness [mm] (SD) Female	Notes	Ref.
Skin	449	141/308	18-80	2.35 (0.42)	2.28 (0.42)	Up to and including dermis	[89]
Subcutaneous Tissue	8	4/4	77-98	9.1 (4.4)		Thickness taken at IAP of 0 mmHg	[90]
Linea Alba	600	N/A	N/A	1.25		Dissections taken across the abdomen with up to 5 samples per donor	[14]
	8	6/2	78 (8.3) male 88.5 (5.5) female	1.97 (0.86)		Dissections taken above and below umbilicus	[91]
	84	N/A	>75	1.4 (0.7-2.7)		Formalin-fixed cadavers.	[92]
Anterior Rectus Sheath	12	7/5	45; 17-73	0.95 (0.37)		Dissected from left side of donors.	[93]
	8	4/4	77-98	0.73 (0.24)		Taken both above and below umbilicus and on either side of the linea alba.	[91]
	3	1/2	77.7	1.2 (0.3)			[94]
	12	0/12	46.08 (12.3)	1 (0.17)		Taken from right supraumbilical side.	[95]
Posterior Rectus Sheath	8	4/4	77-98	0.58 (0.18)		Taken entirely above arcuate line.	[91]
Transversalis Fascia	20 herniated, 4 control	19/1	N/A	0.6 (0.2) for hernia patients, and 0.9 (0.3) for healthy controls		Tissues removed during inguinal hernia repair surgery and the equivalent location for control specimen.	[96]
Rectus Abdominis	84	N/A	>75	3.1; 1.4-6.9		Formalin-fixed cadavers.	[92]
	8	4/4	77-98	5.4		Thickness taken at IAP of 0 mmHg	[90]
External Oblique	25	12/13	62.5; 44-86	0.472			[97]
Internal Oblique	25	12/13	62.5; 44-86	0.399			[97]
Transversus Abdominis	12	7/5	45; 17-73	2.79 (0.85)		Thickness averaged from all abdominal muscles (internal obliques, external obliques, rectus abdominis, transversus abdominis)	[93]
Peritoneum	25	12/13	62.5; 44-86	0.161		Pre- and subperitoneal tissue were kept together	[97]
Composite Abdominal Wall	18	9/9	51 (17.4) male; 61 (11.3) female	30.0		Thickness was measured with an US probe and averaged between 6 points across the abdominal surface.	[24]

Most authors who study the mechanical properties of the AW tend to simplify its anatomy. A number of studies argue that both skin and subcutaneous tissue can be ignored due to their comparably negligible elasticities [98], [99], or have negated these tissues without justification [2], [100]. Conversely, Tham *et al*. identified only three critical AW layers (skin, subcutaneous tissue, and muscle) to study the effects of localized negative pressure on the AW [101]. Contrary to both methods, Deeken *et al*. reviewed a number of studies on the AW and suggested the importance of the entire wall, from skin to peritoneum, given the anisotropic, mechanical effects of each layer [102]. As such, the composite properties of the entire wall of greatest interest in the present work. That said, to simplify, the AW is assumed to be a whole, isotropic material for relative, rather than absolute, measures.

1.3.1 Mechanics

The AW and its individual layers have been studied at length, both *ex vivo* (outside of the human body) [14], [90]–[97], [103]–[109] and *in vivo* [24], [89], [110]–[112]. Despite the volume of available information, results fluctuate between studies, largely due to experimental differences and patient sample variability. As the efforts of the present research focuses on the composite function of the AW, only human studies conducted on the AW as a whole [24], [100], [112], [113] are examined.

1.3.1.1 Research

Few research groups have studied the *in vivo* composite properties of the AW [24], [112]. Song *et al*., assuming the AW to be an isotropic, whole material, found an average Young's modulus (E) of 42.5±9 kPa and 22.5±2.6 kPa transversely and longitudinally, respectively [24]. Alternatively, Tran *et al*. published stiffness (S) values dependent on tissue thickness, muscle activation and AW position [112]. Though of use in verifying future studies, Tran *et al*.'s work cannot be directly compared to Song *et al*. due to the differences in test methods. However, the work of van Ramshorst *et al*. in 2011 resulted in E values comparable to Song *et al*. [59]. Average E was found to be 44.23 kPa by van Ramshorst *et al*., a value within 5% of Song *et al*.'s transverse E results [24], [59]. Though similar, van Ramshorst *et al*. assumed their measurements reflected effective modulus (E^*), contrary to Song *et al*. who identified the individual longitudinal (E_{long}) and transverse (E_{tra}) moduli. Converting Song *et al*.'s results to E^* (using $1/E^* = (1-\nu_{\text{long}}{}^2)/E_{\text{long}} + (1-\nu_{\text{tra}}{}^2)/E_{\text{tra}}$, and assuming Poisson's ratio, or ν = 0.49 [114]) gives a resultant of 19.6 kPa, in error with van Ramshorst *et al*. by nearly 50%. Given this discrepancy, it is critical to consider different orientations of E across the abdomen.

Due to the lack of published literature on the *in vivo* composite wall, Pachera *et al*. completed an *in silico* (simulation) study to determine if the combination of published layer properties

were within range of published composite properties [100]. Published mechanical properties were used for the linea alba [14], rectus sheath [94], and musculature [93]. A fiber-reinforced, nearly incompressible (Poisson's ratio (ν) near 0.5) hyperelastic constitutive model was employed, with the assumption of local transverse isotropy [100]. Though Pachera *et al*.'s results were in agreement with some *ex vivo* publications [98], [115], it was their similarity to Song *et al*. that indicated both the viability of individual layer usage, as well as Pachera *et al*.'s model; AW expansion (due to stretching) was calculated to be 14% by Pachera *et al*., a value in agreement with Song *et al*.'s measured growth of 15% [24], [100]. It is feasible that the addition of published fascial properties [91] could further improve the sensitivity of Pachera *et al*.'s model. In 2020, Todros *et al*. added the effects of IAP to the *in silico* model [113]. The addition improved AW characterization during muscular contraction and increased IAP [113]. As demonstrated in both Pachera *et al*. and Todros *et al*.'s studies, though patient-to-patient variation in abdominal mechanics prevents the strict definition of "normal" values, it is of interest to understand physiological ranges that exist.

1.3.1.2 Terminology

Tissue mechanical properties contrast between engineering definitions and their clinical counterparts. As such, distinctions must be made between the two. In engineering, constitutive material properties are divulged from a material's response to applied loading. The stress (σ) to strain (ε) curve (is a common graphical representation of this response. The slope of a material's Stress-Strain (σ-ε) curve is Young's modulus (also known as elasticity, or Modulus of Elasticity, E) and describes a material's resistance to strain, or, relative deformation. However, if the σ-ε slope changes under different loading rates (*i.e*. loaded faster or slower) then the material can be termed viscoelastic: presenting both viscous and elastic properties [116].

Clinicians may alternatively observe a physiological cavity's $P-V$ curve; the illustration of the enveloping tissue's resistance to expansion or contraction. In this case, the slope of the $P-V$ curve represents the tissue's elastance [16].

Another property of interest is Poisson's ratio (ν): the ratio of material strain in one axis against another axis. Poisson's ratio can range between -1 and 1, in which 0.5 represents a perfectly incompressible isotropic material [116]. Ideal isotropic, incompressible materials ($\nu = 0.5$) include air or water, such that the density of the material is not changed due to loading. Given the high water content of biological tissues, Poisson's ratio is often considered between 0.3 and 0.5 [117]–[120].

Given contradicting definitions, Table 1.3.2 is provided to distinguish between engineering terminology and the resulting clinical observation. In some instances, such as for elastance, there does not exist an associated mechanical definition.

Table 1.3.2: Engineering versus clinical mechanics terminology

Term	Symbol	Engineering Definition	Clinical Observation	Ref.
Bulk Modulus	K	Resistance to strain under hydrostatic conditions (uniform normal stress on entire material surface). For incompressible materials, K tends to infinity [kPa]	N/A	[114], [116]
Compliance	C	The inverse of stiffness [m/N]	Measure of tissue expansion (volumetric response) given a change in pressure. The inverse of elastance. [mL/mmHg]	[16], [116]
Elastance	N/A	N/A	Ability to maintain pressure given a change in volume. Measured by the slope of a tissue's pressure-volume curve. [mmHg/mL]	[16]
Elasticity	E	Resistance to strain under an applied stress. Measured by the slope of a material's stress-strain curve [kPa]	To be elastic/flexible/pliable. Antonym of stiffness.	[16], [116]
Poisson's Ratio	ν	Ratio of material strain in perpendicular directions. Incompressible, isotropic materials have a ν of 0.5	Material compensation; lengthening in one direction shortens in the perpendicular axis.	[116]
Shear Modulus	G	Resistance to strain under an applied shear stress (stress tangential to applied material surface) [kPa]	Slippage between tissue layers	[116]
Stiffness	S	Resistance to deformation under an applied force [N/m]	To be stiff/resist deformation.	[16], [116]
Strain	ε	Material length change per initial unit length [m/m]	Elongation, or shrinkage	[116]
Stress	σ	Load per unit area, normal to the applied material surface. Can be in tension (tensile stress) or compression (compressive stress) [kPa]	Pressure [kPa]	[16], [116]
Viscoelasticity	N/A	The property of a material to change its elasticity depending on applied strain rate.	Combination of viscous and elastic properties in a tissue.	[16], [121]

1.3.2 Existing Measurement Methods

Palpation is a qualitative method of *in vivo* (in living humans) soft tissue evaluation, with poor inter-rater reliability. The distinction between "unhealthy" and "normal" tissue or, at the other end of the spectrum, "normal" and "performant" has largely been a matter of perception. Regarding a static and dynamic touch, our fingers can sense very small differences in deformation and surface roughness. Further, it may be perceivable that clinicians inherently have, or gain over time, a more refined sense of touch; however, often one needs to make comparisons between before and after treatment, or gauge if a palpated tissue is deemed healthy [122]. Limited information on distinguishing metrics indicates the need for standardized, *in vivo* measurement devices. To provide a more objective evaluation of soft tissues, measurement devices have been developed which allow for quantitative measures to be acquired. Though no "gold standard" has been suggested, the use of such quantitative tissue tooling offers the potential of determining "normal", or, "healthy", stiffness values for select tissues, such as that of the AW. Thus, these tools offer a means for quantitative and objective comparisons to be made.

Ex vivo measurement methods for tissue characterization cannot accurately replicate a

physiological environment, as tests occur outside living organisms. Thus, *in vivo* alternatives are of greater interest, here. Table 1.3.3 lists said alternatives, detailing the advantages and disadvantages of each method.

Given the lack of a "gold standard" measurement technique, it has been suggested to use more than one measurement system for more comprehensive results [123]. As such, the following discusses several existing means of mechanically characterizing soft tissues. That said, consensus has been reached among experts that an all-inclusive, standardized, and portable device is still necessary to establish norms in tissue properties [123].

1.3.2.1 Static Deformation

Though manual palpation remains the simplest and cheapest form of *in vivo* soft tissue evaluation, it is a qualitative and practitioner-dependent method [124]. Robotic palpation has been proposed as an improvement to its human counterpart, though, the technology remains in its infancy [122]. Alternatively, static, quantitative measurement systems are wide ranging, and include indentation [125], myometry [126], aspiration [127], and durometry [128]. To measure the mechanical properties of fascia, only indentation, myometry (popularized by the MyotonPro [129]), and aspiration are discussed, as durometers report Shore hardness (resistance to indentation), as opposed to elasticity (a constitutive material property) [116]. Figure 1.3.1 illustrates each method of static deformation, with corresponding dimensions for mechanical characterization.

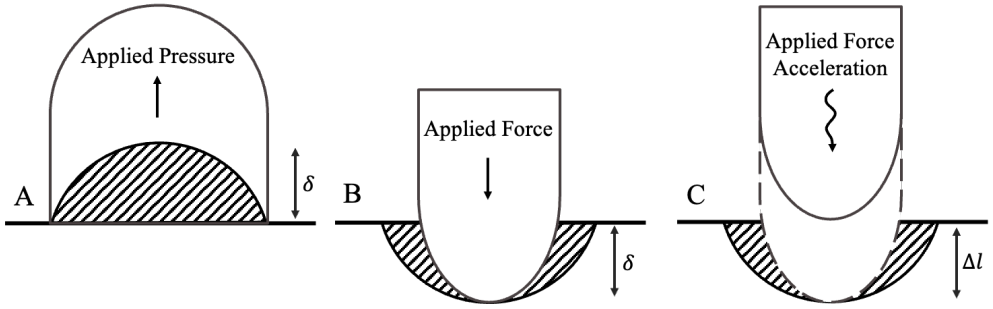

Figure 1.3.1: Methods for static deformation for tissue characterization. A: Suction, B: Indentation, C: Myometry. Tissue deformation distance indicated by double-headed arrow and associated symbol (δ for A and B, Δl for C).

Indentation, myometry, and aspiration devices use similar theories to determine stiffness (S); a known normal force (F) is applied to a local tissue, and the resulting linear displacement (δ) is measured [130], [131]. In its simplified form, this yields the equation $S = F/\delta$. That said, in the case of the MyotonPro, the popularized myometric method of measurement [126], an impulse,

rather than a single, continuous force, is applied to the tissue. As a result, stiffness is measured by

$$S = \frac{\vec{a_{\max}} m_{\text{probe}}}{\Delta l}, \tag{1.3.1}$$

where $\vec{a_{\max}}$ is the peak acceleration amplitude, m_{probe} is the preload due to the mass of the probe, and Δl is the peak displacement amplitude [129]. As Newton's Law states $F = ma$, stiffness measured by indentation, aspiration, and myometry are mathematically equivalent, though, device discrepancies may yield errors among the three techniques. These discrepancies include (1) strain rate, (2) indentation depth, and (3) tissue boundary conditions. Due to the viscoelasticity of biological tissues, strain rate variation may yield varying underlying material properties. Indenters typically do not use a set strain rate, thus depending on the speed at which a user arbitrarily deforms tissue. The MyotonPro (probe diameter 3 mm), however, consistently performs an impulse of 0.58 N within 15 ms for a rate around 0.04 N/ms [132]. Assuming a perfect force transmission across the face of the probe, this rate converts to around 5.7 mbar/ms. In popular aspiration devices, strain rate is again controlled, with a loading and unloading rate of 15 mbar/s (used in the Cutometer, probe diameter between 2 and 8 mm, and Nimble, probe diameter 10 mm, to name a few), or 0.015 mbar/ms [133].

Indentation depth also varies in devices. In indenters, such as the IndentoPro, indentation depth is preset (5 mm, 10 mm, and so on) to allow the device to register the applied force required to deform the tissue up to said depth [134]. Similarly, the Nimble deformation height is preset, with pressurization halting once the tissue has reached its predestined height [133]. Alternatively, the MyotonPro and Cutometer measure deformation based on the preset impulse force [132], [133]. Difference in indentation/deformation distance may affect results as deeper tissues begin to compound and stiffen the overall material.

Finally, particularly in the case of indentation and myometry, during localized deformation, soft tissue is stretched across a wider area than that of the probe, itself. Due to this absence in boundary conditions, indentation and myometry results may only speak to material properties in a particular loading scenario, rather than more generalized results. Aspiration devices, however, are presumed "fixed" at their perimeter, thus allowing for the entire deformed tissue volume to be described within the device's bounds.

In all, though outputting mathematically equivalent values for material stiffness, results for material properties using indentation, myometry, and aspiration should be critically anlayzed in future work.

Also of note in the discussion of static deformation tools is a second, dimensionless value outputted by the MyotonPro that the device producer has incorrectly termed "elasticity". This term

is defined as the logarithmic decrement of probe acceleration [129], in conflict with the engineering definition for elasticity (see Table 1.3.3) [135]. Thus, published values of "elasticity" from studies using the MyotonPro should be evaluated critically.

Though handheld, user-friendly systems are available (*ex*. MyotonPro [129], Cutometer [136], Nimble [133], Semi-Electronic Tissue Compliance Meter [125], IndentoPro [134]), none of the existing static deformation methods can distinguish between tissue layers, or provide insight into deeper fascia [123]. As such, said techniques are only recommended to evaluate superficial, and not deeper, tissues.

1.3.2.2 Bioimpedance

In all materials, there exists a unique impedance, or, resistance to electrical current. This also holds true in biological tissues, thus denoted as bioimpedance. Recent research has explored the possibility of exploiting this characteristic to correlate bioimpedance to mechanical properties, such as elasticity or thickness [86], [137]. Though simple, non-invasive, and potentially economical, further research must be pursued to provide inter- and intra-rater reliability studies against more conventional methods.

1.3.3 Virtual Imaging

Virtual imaging exploits computational power to build individualized models of anatomy for study [138]. This can be done either with cameras (DIC), or inversely (virtual fields method) using finite element models. Both a benefit and detriment to virtual imaging is its ability to uniquely define a patient's physiology. Virtual imaging offers great potential in the development of individualized medicine, but it only pertains to a single case, thus, cannot be generalized for diagnostics or treatment in a greater population. Therefore, though virtual imaging has far-reaching benefits in future applications, it remains impractical for clinical use.

1.3.3.1 Ultrasonography and Elastography

Modern technologies, such as US and elastography, offer greater detail and information about fascial layers, however, they are not handheld, portable, or widely economical [123], [131]. Sonography [139] and elastography [130], [140] methods have gained popularity owing to their ability to map deep viscera. Geometric distinctions between fascial layers in US provide benchmarks from which to measure thickness. As such, tissue thickness is typically measured with US [139].

Elastography is a medical imaging technique that maps stiffness in deep tissue by sending acoustic vibrations (in US) or harmonic vibrations (in MRI) through tissue layers. Both systems employ a shear wave such that the faster the shear wave, the stiffer the material [141]. Resulting

elasticities are then overlaid on MRI or US images to establish an anatomical map of tissue elasticity. All elastography methods determine local tissue properties (*i.e.* measuring along the length of the respective probe), not global, while assuming linear elastic, homogeneous, isotropic material properties (contrary to physiological properties: viscoelastic, multilayered, anisotropic) [142]. These limitations must be considered when comparing measurement methods. Further, adipose tissues cause shear waves to change at deeper tissue layers, therefore, this method is less reliable in overweight populations. This is particularly evident in fat deposit areas, such as the abdomen or upper legs. Finally, it should be noted that commercial shear wave elastography systems output measures of E. If shear modulus (also known as shear elasticity, G) is reported, linear elasticity can be calculated using $E = 2G(1+\nu)$ [133]. In this case, the material's ν is assumed to be 0.5 (*i.e.* incompressible), as suggested by recent studies [133].

Table 1.3.3: Summary of soft tissue measurement methods. (+, 0, -) refer to "improved", "equivalent", and "worse" than indentation. Tissue distinction refers to the ability of the technology to identify mechanical properties of individual tissue layers.

Method	Mech. Property	Description	Non-Invasive	Quantitative	Tissue Distinction	Portable	Reliable	Cost	Anatomy	Ref.
Manual Palpation	Relative stiffness	Qualitative evaluation of top layer tissue stiffness.	X			X	-	++	Superficial tissues	[143]
Robotic Palpation	Relative stiffness	Qualitative evaluation from machine learning to distinguish between stiff and flexible tissues for use in tumour identification.	X				0	N/A	Superficial tissues	[122], [144]
Myometry	Stiffness, "elasticity", "tone", "creep"	An impulse of known force is applied to a soft tissue, and the tissue response in acceleration vs. time and deformation vs. time are mapped.	X	X		X	0	-	Superficial tissues	[126], [130]
Indentometry	Stiffness	Measurement of resulting tissue deformation given an applied, known, point load (indent). Can also be inverse; measure tissue response force for given deformation.	X	X		X	0	0	Superficial tissues	[125], [145], [146]
Aspiration	Stiffness	The reverse of indentometry. A closed volume of soft tissue is resected using a locally applied negative pressure. Vertical tissue displacement and applied pressure are recorded to determine stiffness.	X	X		X	0	0	Superficial tissues	[127], [133], [147], [148]

Continued on next page

Table 1.3.3: Continued from previous page

Method		Mech. Property	Description	Non-Invasive	Quantitative	Tissue Distinction	Portable	Reliable	Cost	Anatomy	Ref.
Torsion/rotary shear		Shear modulus	Linear viscoelastic response of tissues under a vibrating torque. No axial force is applied, and the tissue's response vibrations are captured by electromagnetic transducers.	X	X			N/A	0	Superficial tissues	[149]
Durometry		Shore hardness	Measurement of resulting load impression in tissue given applied, known, point load (indent).		X		X	0	0	Skin or *ex vivo* tissues.	[128]
Bioimpedance	Electrode array	Geometry	An array of electrodes, placed across the tissue of interest, map tissue impedence given an applied frequency. Results can be mapped to produce a topographic image or correlated to a property of interest.	X				-	-	Superficial tissues.	[137]
	Piezoelectric ceramic material	Young's modulus	The impedance of a soft tissue is measured with a polymer film (PVDF), given a small applied voltage. This can be correlated to mechanical characteristics of the tissue.	X	X		X	N/A	0	Superficial tissues.	[150]
Ultrasonography (US)	B-Mode	Young's modulus, thickness	Standard US can be used to evaluate the thickness of tissues by direct measurement in produced images. If combined with indentometer, can also measure Young's modulus.	X	X	X		+	-	Superficial to deep tissues.	[139], [140]
	Strain US Imaging	Young's modulus	Use of an US to visualize tissue movement given varying normal stresses.	X	X	X		+	-	Superficial to deep tissues.	[140]

Continued on next page

Table 1.3.3: Continued from previous page

Method		Mech. Property	Description	Non-Invasive	Quantitative	Tissue Distinction	Portable	Reliable	Cost	Anatomy	Ref.
	Direct image correlation (DIC)	Bulk modulus	With 2 cameras, a 3D image can be produced given a tissue with a defined pattern (such as fine, dark paint spray). Inputting images into FEA allows for deformation to be mapped given loading.	X	X			N/A	N/A	Superficial tissues.	[138], [151]
Virtual Imaging	Virtual fields method	Shear modulus	Using an anatomically correct finite element model, the constitutive mechanical properties of soft tissues can be solved for given a known (experimental) applied force and resulting deformation. This is an inverse engineering problem, but only accurate for a given anatomical geometry and study participant.	X	X	X		N/A	N/A	Model-dependent.	[152]
Elastography	US Elastography (compression-based or shear wave)	Shear modulus/Young's modulus, thickness	Use of an US to visualize tissue shear strain given shear stress (by applied shear waves). Force or deformation mapping.	X	X	X		+	-	Deep viscera.	[130], [140], [153]
	MRI Elastography (compression-based or shear wave)	Shear modulus/Young's modulus, thickness	Use of MRI to visualize tissue shear strain given shear stress (by applied shear waves). Force or deformation mapping.	X	X	X		+	-	Deep viscera.	[130], [140], [153]
	Tomoelastography	Shear modulus/Young's modulus, thickness	Combination of an elastography method and an analysis system to reduce output noise.	X	X	X		+	-	Deep viscera.	[154]

1.4 Abdominal Compliance

Abdominal compliance, clinically, is the "measure of ease of abdominal expansion" [7]. Thus, high C_{ab} indicates that the abdomen can expand relatively freely, while low C_{ab} restricts abdominal expansion. According to the WSACS, C_{ab} can be determined given a change in abdominal volume and pressure [mL/mmHg] [2], [7]. This definition is not to be confused with its mechanical counterpart: the inverse of stiffness [155]. Given that stiffness describes a material's response to strain, mechanical compliance describes a material's response to stress [155]. Either stiffness or compliance, however, can be used to describe a material's overall behaviour [155]. More comparable to the clinical definition for compliance is bulk modulus (or, modulus of compressibility, K) [57]. Bulk modulus describes a material's resistance to strain under hydrostatic pressure [57]. Given discrepancies between mechanical and clinical definitions, the definition identified by WSACS [7] is used to describe C_{ab} for the purposes of the project put forth, herein, to remain clinically relevant and compare to a wider range of studies.

C_{ab} should not be confused with the similarly measured, bladder compliance ($C_{bladder}$). $C_{bladder}$ is evaluated given a change in bladder volume and detrusor pressure [mL/mmHg] [73]. Typically, $C_{bladder}$ is measured during bladder evacuation, such that discharge volume and detrusor pressure are measured concurrently [73]. That said, bladder volume should equal the volume of liquid present in the bladder, not just the volume induced.

1.4.1 Mechanics

C_{ab} is a variable mechanical property directly affected by the elasticity of the AW and, to a lesser extent, the diaphragm [2]. As IAV increases, AW elasticity increases (stiffens), resulting in a decrease in C_{ab} [2], [15]. C_{ab} is defined as the change in IAV per unit change in IAP, or, the inverse of elastance (slope of the *P-V* curve at a given point) [7]. C_{ab}, as opposed to elastance, is the preferred medical term due to clinicians' familiarity with a similar measure: respiratory compliance [15]. Given the linear to exponential shape of the *P-V* curve (see Section 1.1.1 for more information), it can be said that C_{ab} is constant until a critical IAV, at which time it begins to decrease (*i.e.* prevents abdominal expansion) [10], [20]. Animals do not exhibit the same *P-V* curve shape as humans [156]. In animals, non-linearity is evident from baseline IAV [156]. As such, animal studies are not a reliable source of information when discussing C_{ab}. "Normal" C_{ab} values have been published as between 250 and 450 mL/mmHg in supine position [20], and reduce to 48 mL/mmHg at sitting position [34]. Low C_{ab} prevents abdominal expansion, thus reducing the critical IAV at which IAP increases exponentially. As such, "improving" C_{ab} is synonymous with increasing it, and can be accomplished with an active lifestyle, or, more immediately, with pharmaceutical intervention (such as neuromuscular blockers) [2], [22]. Alternatively, women who

have given birth have demonstrated increased C_{ab} due to the fascial stretching that accompanies pregnancy [22].

1.4.2 Existing Measurement Methods

Existing measurement methods for C_{ab} have been described as a "crude estimate" of the property [10]. Some studies have calculated C_{ab} given a change in IAV and corresponding change in IAP (typically measured during either abdominal drainage or peritoneal dialysis procedures), however, this is not an accurate depiction of physiological conditions [15]. In Blaser *et al*.'s review of C_{ab}, a wide variation in study results was presented [15]. This inconsistency suggests the need for a standardized, reliable measurement method and protocol to better understand abdominal mechanics.

1.5 Clinical Relevance

As alluded to, unhealthy abdominal mechanics have negative clinical implications. Unhealthy levels of IAP are often caused by peritoneal inflammation and/or abdominal fluid build-up, typically as a result of acute abdominal injury or surgery [7]. As such, rates of IAH, have been recorded in between 20 and 50% of ICU patients, with rates increasing in ventilated patients [46]. This increased IAP can reduce blood flow to vital organs, perpetuating further pressure build-up as organs become unable to drain excess fluids [7]. If a patient has low C_{ab}, the abdomen is unable to accommodate these high pressures. Conversely, low levels of IAP are representative of poor spinal stability, a phenomenon linked to the onset of low back pain [3]. In fact, recent work has simulated a cross-section of the human trunk, based on work by Vleeming *et al*. [157], and found that increased IAP balanced the force profiles in back muscles and fascia [158]. This finding has emphasized the need for IAP and fascia inclusion in finite element models that evaluate spinal stability, which have, in turn, been developed by various groups [159], [160]. Thus, measuring and understanding a patient's *P-V* curve in conjunction with spinal stability may improve existing knowledge of diagnostics, monitoring, or treatment of unhealthy (high or low) levels of IAP. However, as mentioned previously (Section 1.1 and 1.2), non-invasive, comprehensive techniques to define individuals' *P-V* curves do not yet exist. One potential mechanism to elucidate the *P-V* curve is aspiration; introduced in Section 1.3, but with potential for expansion into IAP and IAV measurement. As such, this avenue is explored, further, in the following.

1.6 Aspiration Techniques for Tissue Mechanics

Aspiration techniques, also termed suction, myofascial decompression [161], dry or flash cupping therapy [162], endermology, vacuotherapy, depressomassage, or vacuum massage [163], use negative pressure against the skin to induce a desirable physical or physiological effect. A 2016 review of aspiration as a tool in biomechanics found a significant number of benefits in device use

(compiled in Table 1.6.1) leading to its recommendation as a standardized tool in musculoskeletal medicine [163], [164]. However, for the purposes of this thesis, only research evaluating the effects of suction on the biomechanics of underlying tissue is discussed.

Table 1.6.1: Physical and physiological benefits of aspiration on soft tissues

Type	Description	Ref.
Physical	Decrease in tissue hardness.	[163]
	Increase in tissue elasticity.	
	Decrease in skin fold thickness.	
	Increase in tissue elasticity.	
	Decrease in scar adhesions.	
	Decrease in tissue face volume.	
	Decrease in skin laxity.	
	Increase in epidermal thickness.	
	Decrease in skin roughness.	
Clinical	Improved pain management.	[163], [165]
	Increase in range of motion.	[161]
	Increase in flexibility.	[161]

During suction, tensile stresses are seen at the inner face of the suction device rim, while maximum compressive stresses are seen just under the suction device rim [101]. Normal stresses decrease with tissue depth, such that deep muscles undergo lower stresses than that of superficial tissues [101]. Despite the decrease in normal stress at deeper fascia, an increase in longitudinal collagen fibres has been seen in deeper tissues undergoing suction [163]. Both results, however, indicate the effect of suction on deep tissues, and suggest the efficacy of a suction tool on a range of fascia beyond the superficial.

One of the most popularized suction tools for biomechanical evaluation of skin is the Cutometer. The Cutometer induces a suction through a narrow probe (2 to 8 mm diameter), and resulting tissue deformation is measured via a light sensor [133]. The work of Müller *et al*. has suggested deficiencies in the Cutometer, however, which have been remedied in a replacement device titled the Nimble [133]. The Nimble (probe diameter of 6 mm) measures elasticity conversely to the Cutometer; that is, measuring pressure incline to a known tissue deformation, rather than tissue deformation to a known applied pressure [133]. Both devices, given narrow probe openings, are only able to measure elasticities of superficial tissues, such as the skin.

To the author's knowledge, there exists no biomechanical studies on the effects of suction on deeper tissue elasticity. Previous studies that objectively evaluated elasticity changes due to suction only used palpation or the Cutometer (a superficial tissue elasticity tool) to evaluate changes [166]. One study noted the separation of tissue layers via MRI during suction, though, elasticity was not mentioned [167]. DaPrato *et al*. noted that, after 2 min. of static suction, tissue layers began to stretch apart, however, this was a slow release, with tissue adherence evident at the immediate onset of suction [167]. Therefore, it may be of interest to exploit a novel tool in soft tissue

mechanics measurement to evaluate prolonged effects of suction on deeper fascia.

1.7 Conclusion

It is evident that there is a gap in existing measurement devices for both soft tissue mechanics and IAP. In fact, several authors recommend further research in such areas for the betterment of clinical practices [4], [7], [10], [20], [66]. Further, given the promise of aspiration techniques, using suction as a means of measurement is of interest. As such, it is hypothesized that a non-invasive, aspiration tool to measure a physiological cavity's internal pressure and elastic properties can be developed. Said tool may serve the unmet clinical need for both chronic condition diagnostics and surgical monitoring.

2 Research Rationale, Objectives, and Hypotheses

Given the lack of a non-invasive, reliable measurement mechanism for IAP and C_{ab}, the need for a novel device is evident. Thus, it is the effort of this thesis to **design, optimize and validate a novel, direct, non-invasive intra-abdominal pressure measurement device for use in the analysis of spinal and abdominal conditions**. To succeed in this global objective, a series of sub-tasks have been identified as necessary project milestones. To note, in appropriate instances, Intraclass Correlation Coefficient (ICC) and Pearson's correlation (ρ) were used to quantify reliability and validity, respectively, of the novel technology.

Objective 1: Develop a direct, non-invasive, handheld tool to measure internal pressures and material mechanical properties in pressurized vessels.

Hypothesis 1: A novel, non-invasive device can correctly detect changes in physiological pressures; that is, pressure increases around 0.2 and 0.4 kPa (1.5 and 3.0 mmHg) with increasing head inclination to 25°.

In the case of localized aspiration, a number of assumptions can be made: clamped edges, large deformation, elastic, thin membrane, circular resection area. Thus, the present problem agrees with the extended Hencky solution, allowing evaluation of the system for internal pressures given applied pressure and resulting deformation. As such, responsiveness of the device can be evaluated given a change in body position, from supine to inclined head of bed.

Objective 2: Demonstrate the novel tool's efficacy as an abdominal elasticity measurement tool.

Hypothesis 2: Isotropic Young's modulus measurements taken with the novel device have "good" (ICC > 0.75) intra- and inter-rater reliability, and "high" ($r > 0.7$) linear correlation against stiffness measurements taken 5 cm subxiphoid on the abdomen with existing popularized measurement methods (here, myometry with the MyotonPro and indentation with the IndentoPro) [125].

A measurement tool currently available for mechanical testing is the MyotonPro, a myometer developed for measuring soft tissue stiffness. The MyotonPro has been compared against similar measurement methods, including indentation, in which a quasi-static deformation state is evaluated. The ability of a developed preliminary device (the novel device) to measure soft tissue elasticity can be critically compared to the MyotonPro, as well as a standard indentation system in the IndentoPro.

Objective 3: Demonstrate the novel tool's efficacy as a muscle elasticity measurement tool.
Hypothesis 3: Isotropic Young's modulus measurements taken with the novel device have "good" (ICC > 0.75) intra-rater reliability, and "high" ($r > 0.7$) linear correlation against stiffness measurements taken at the gastrocnemius with existing popularized measurement methods (here, myometry with the MyotonPro and indentation with the IndentoPro) [125].

Concurrent to Objective 2, Objective 3 considers the novel tool at the gastrocnemius (posterior, superficial calf muscle). Again, the IndentoPro and MyotonPro serve as benchmarks from which the novel device's performance can be compared.

Objective 4: Demonstrate the novel tool's efficacy as an intra-abdominal pressure measurement tool.
Hypothesis 4: IAP can be measured directly to within 1 mmHg of existing gold standard methods (here, UBP) considering the force equilibrium between locally applied pressures, IAP, and AW tension.The reliability of a novel IAP measurement device has "good" (ICC > 0.75) intra- and inter-rater reliability, and "high" ($r > 0.7$) linear correlation against IAP measurements taken by UBP.

UBP measurement is currently the most common method of obtaining IAP, and has been used as a reference method against novel technologies [72]. Given this, in conjunction with the recommendations for novel device research as set by the WSACS, the ability of the novel device to measure IAP can be critically compared to UBP.

To illustrate the expected order of operations, Fig. 2.0.1 is shown. Objectives and hypotheses are outlined consecutively, such that the completion of one onsets the next. Associated manuscripts and chapters are noted.

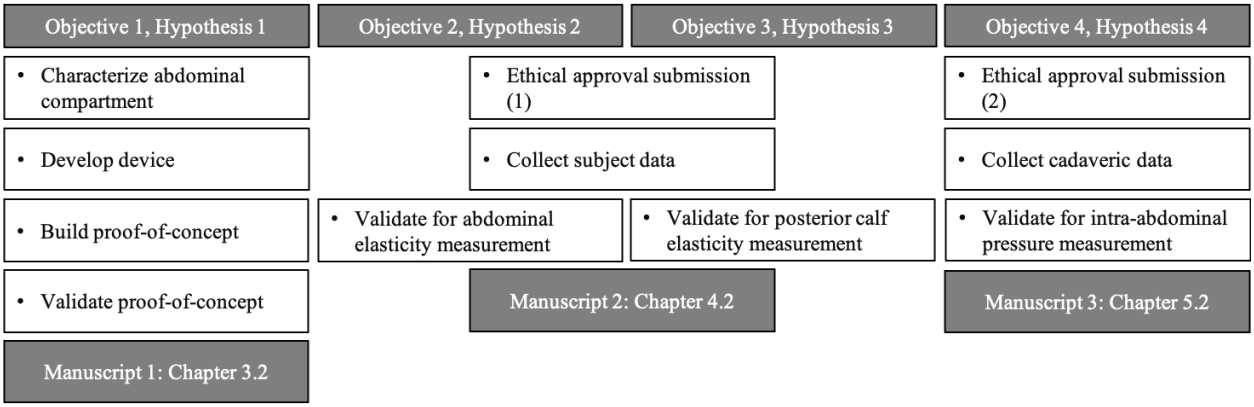

Figure 2.0.1: Objective and hypothesis flowchart

3 Design and development of a novel, non-invasive intra-abdominal pressure measurement device

3.1 Framework of Article 1

The study explored, herein, describes the theoretical design details of the final IAP measurement system. The extended Hencky solution in conjunction with the Lamé equation are used as the mathematical basis for pressure calculation. Preliminary proof-of-concept is validated with two ($n = 2$) study participants. As such, the following manuscript builds the foundation upon which the rest of the thesis is completed. The realization of Objective 1 and exploration of Hypothesis 4 are presented in the manuscript entitled, "Design synthesis and preliminary evaluation of a novel tool to non-invasively characterize pressurized, physiological vessels", for which the contribution of the first author is considered to be 85% including experimental method formulation, data analysis, and manuscript writing. The second author provided research direction and manuscript review, for which the contribution is considered to be 15%. The manuscript was published in the *Journal of Medical Devices* by ASME on November 11, 2020.

3.2 Article 1: Design synthesis and preliminary evaluation of a novel tool to non-invasively characterize pressurized, physiological vessels

Natasha Jacobson, EIT, Mark Driscoll, Ph.D., P. Eng.

Status: Published. DOI: 10.1115/1.4049088

McGill University, 845 Sherbrooke St. W, Montreal, Quebec, Canada, H3A 0G4

Address for notification, correspondence and reprints:

Mark Driscoll, Ph.D., P.Eng., Assistant Professor

Associate Member, Biomedical Engineering

Canada NSERC Chair Design Engineering for Interdisciplinary Innovation of Medical Tech.

Department of Mechanical Engineering

817 Sherbrooke St. West, Montreal, QC, H3A 0C3 Canada

T: +1 (514) 398 - 6299

F: +1 (514) 398 – 7365

E-Mail: mark.driscoll@mcgill.ca

3.2.1 Abstract

A prolonged increase in intra-abdominal pressure (IAP) is life-threatening, yet commonly seen in intensive care units. Despite this, existing clinically-accepted IAP measurement techniques are invasive and not inter-rater reliable. As such, it is the effort of this research to develop a direct, non-invasive, handheld tool to measure internal pressures in pressurized, physiological vessels. The novel device uses a localized known pressure (namely aspiration) to measure resulting tissue deformation, from which internal pressures can be divulged considering the extended Hencky solution. Two male participants were tested with the device to confirm feasibility of the theoretical device function for IAP measurement. Participants' Young's moduli of the abdominal wall were calculated with measured IAP values. Results were consistent with participant body mass indices and overall health. Average measured IAP was 0.42 kPa and 0.46 kPa at supine and inclined positions, respectively. Average measured abdominal wall elasticity was 14.91 kPa and 23.09 kPa at supine and inclined positions, respectively. These preliminary findings suggest the potential use of the device described herein as a measurement system for pressurized vessels, whereas the system will be tested on a larger sample size before recommending clinical use.

3.2.2 Introduction

The human body is comprised of a series of pressurized vessels, including muscles, organs, abdominal and thoracic compartments. One such vessel is the intra-abdominal volume (IAV),

or volume contained by the peritoneum, pressurized by intra-abdominal pressure (IAP) [1]. The World Society of Abdominal Compartment Syndrome (WSACS) defines "normal" (or, baseline) IAP as between 5 and 7 mmHg taken at a supine position during end-expiration with a bladder catheter [2]. High levels of IAP are denoted by the terms intra-abdominal hypertension or abdominal compartment syndrome, depending on measured values [3]. Both conditions are prevalent in Intensive Care Units (ICUs) and are often caused by peritoneal inflammation and/or abdominal fluid build-up, typically because of acute abdominal injury or surgery [4]. Rates of intra-abdominal hypertension have been recorded between 20 and 50% in ICU patients, with rates increasing further in ventilated patients [5]. This increased IAP can reduce blood flow to vital organs, perpetuating further pressure build-up as organs become unable to drain excess fluids [3], [4]. These life-threatening complications are diagnosed by IAP measurements collected over 4-6 hours that are consistently greater than 20 mmHg and 12 mmHg for abdominal compartment syndrome and intra-abdominal hypertension, respectively [3], [6]. Despite known risks associated with IAP, there remains no "gold standard" tool for measuring the property [7], [8]. As such, it is the effort of this research to develop a direct, non-invasive, handheld device to measure internal pressures and material mechanical properties in pressurized, physiological vessels.

3.2.2.1 Existing Technologies

Though no "gold standard" IAP measurement method exists, numerous methods of evaluating physiological pressures have been developed. "Direct" IAP readings use microtransducers embedded just under the abdominal wall [9], [10]. That said, embedded microtransducers are not widely recommended measurement methods, given the invasive nature of the procedure [1], [7], high cost [10], and fragility of the system [9]. The WSACS recommends IAP measurement via the bladder (known as urinary bladder pressure (UBP)), as most patients requiring IAP monitoring already have a catheter implanted, making measurements minimally invasive [4], [11]. Differences between microtransducers and pressure via a bladder catheter have been measured betweeen 0.286 $\pm$ 0.938 mmHg [10] and 0.1 $\pm$ 2.8 mmHg [9]. However, some researchers disagree with UBP measurement, especially in dynamic testing, as the system is position dependent and prone to air bubbles that can skew readings [11]. Further, UBP measurements above 20 mmHg have demonstrated less reliable results, with Cronbach's alpha of 0.98 and 0.79 for measurements below 12 mmHg and above 20 mmHg, respectively [11]. Regardless, UBP measurement is currently the most common method of obtaining IAP and has been used as a reference method against novel technologies [12].

More recent IAP measurement tools offer non-invasive techniques. Ultrasound guided

tonometry, or, the evaluation of pressure by measurement of applied force and displaced liquid volume, is one such method [13]. Ultrasound-guided tonometry has only been studied in porcine models but resulted in the ability to distinguish between three defined categories of IAP: normal (baseline to 15 mmHg), mid-range (between 15 and 25 mmHg) and high (above 25 mmHg) [13]. Though non-invasive, this technology is not portable and does not offer fine IAP measurement resolution. Alternatively, intravaginal transducers are invasive, but highly accurate means of continuous IAP measurement, while offering wireless capabilities [14], [15]. However, intravaginal transducers are limited to the female population, and intra-rater reliability has not been evaluated.

The measurement of abdominal wall tension (AWT) and its correlation to IAP has also been investigated. Due to the direct relationship between wall stress and internal pressure in pressurized cylinders, van Ramshorst *et al*. assumed the measurement of AWT could provide insight into IAP [16]. In further studies, the anatomical landmarks that offered the greatest reliability in AWT testing were 5 cm caudal to the xiphoid process and 5 cm cranial to the umbilicus [16]. This reliability was indicated by the greatest slope in regression lines between IAP and AWT; 0.079 N/mm/mmHg and 0.063 N/mm/mmHg for 5 cm subxiphoid and 5 cm supraumbilical, respectively [16]. Chen *et al*. followed up on these findings by measuring AWT 5 cm subxiphoid, as recommended, on 51 living patients [12]. AWT was then correlated to IAP measured via UBP [12]. The results from this study agreed with van Ramshorst *et al*.'s, proving AWT could be used to interpret IAP, however, linear correlation equations put forth by the authors varied significantly [12], [16]. Chen *et al*. published a linear correlation equation of IAP = 9.57(AWT) - 1.369, while van Ramshorst *et al*. contradicted with IAP = 12.66(AWT) - 20.38 for the same anatomical position [12], [16]. This discrepancy was largely attributed to variation in patient population but demonstrates the unreliability of IAP measurement by correlating against AWT. Following up on the work seeking pertinent AWT correlations to IAP, David *et al*. considered the relationship between abdominal wall thickness (AWTh) and IAP using bioimpedance and microwave reflectometry [17]. Similarly, positive correlation was evident, but poor sensitivity (maximum sensitivity at 4.25 GHz) and limited pressure ranges (up to 7 mmHg) were noted [17].

To summarize, existing clinically-accepted IAP measurement techniques are invasive and not inter-rater reliable. Non-invasive alternatives allow reasonable results to be obtained, but do not directly measure pressure; ultrasound-guided tonometry, bioimpedance, microwave reflectometry, and AWT/AWTh measurements interpret results and correlate them to IAP. This correlation technique is only successful when tested patients exist in the original sample. Variations in patient geometry and physiology may result in IAPs outside the original specifications. Furthermore, such non-invasive alternatives require additional research before suggesting its clinical usage. Thus, to

date, direct and non-invasive IAP measurement devices are not currently available, hence the purpose of the present innovative design research.

3.2.3 Methods

Research has suggested that the abdomen can be represented as a pressurized cylinder of incompressible fluid for the purpose of mathematical modeling [18]. Some successful IAP measurement tools exploit said model to evaluate the AWT and correlate this value with IAP [12], [16]. The current research looks to advance this theory, evaluating the system at a quasi-static equilibrium state to calculate, rather than correlate with, IAP. Correspondingly, a novel tool was designed. This tool induces a localized negative pressure (P_{app}) across a circle of tissue with radius, a, from which the resulting tissue deformation (w) is reported. Pressure is induced with a standard pressure bulb through an open end in the device. The device is 25 cm tall, 7.5 cm at its widest, and weighs approximately 250 g when fully assembled (Fig. 3.2.1). The device comprises a pressure sensor (BMP388), a distance sensor (VL6180), and luer-lock connections (Qosina) to improve air-tightness. The maximum lateral deformation reading of the VL6180 is 10 cm (100 mm), with noise of 2 mm (2%). The relative accuracy of the BMP388 is 8 Pa (0.06 mmHg). A microcontroller (ESP32) and rechargeable battery are also housed in the device for on-site analysis. Cup diameter (5 cm) and wall thickness (2 mm) matched similar commercial products to maintain frame rigidity and allow for deep tissue resection. Additionally, a biocompatible lubricant was used to improve device seal against skin.

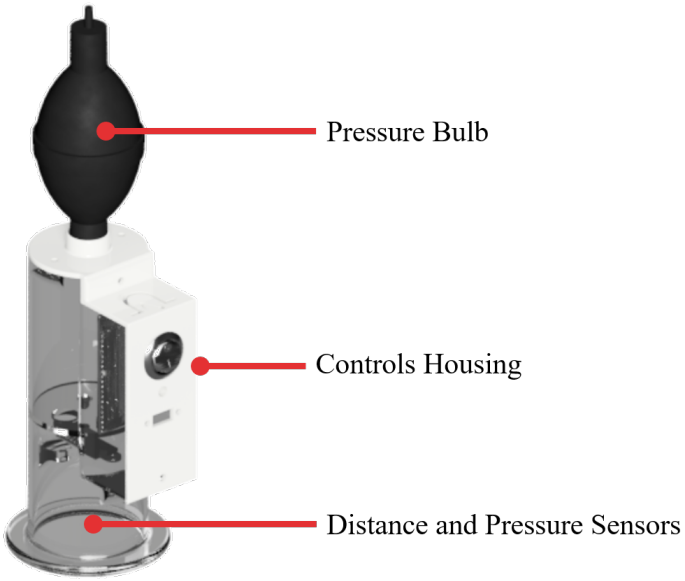

Figure 3.2.1: Device prototype with denoted components.

To correctly use the device, the system must be placed orthogonal to the abdominal wall, open end down, 5 cm subxiphoid along the linea alba. During use, enough pressure to achieve a complete seal against the skin is required. Upon patient end-exhalation, suction is induced by squeezing the pressure bulb. To release pressure, the pressure bulb can be removed. Sensors detect change in pressure and distance simultaneously and send the collected information to the microcontroller for analysis. The test is repeated three to five times for an average measure of IAP and abdominal wall elasticity.

For a circular membrane of radius, a, under uniform lateral loading (P_{net}), fixed at its bounds, and presenting large deflections (Fig. 3.2.2), the Hencky solution applies [19], [20].

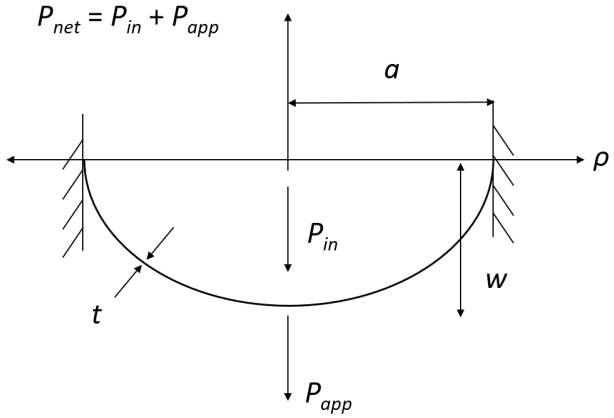

Figure 3.2.2: Free body diagram of theoretical design.

The Hencky solution states that the maximum lateral deflection (w) occurs at the center of such a pressurized, circular membrane, and can be defined by

$$w = \left(\frac{P_{\text{net}} a}{Et}\right)^{1/3} \kappa a \tag{3.2.1}$$

where κ is a constant dependent on pre-tension in the membrane and Poisson's ratio (ν) of the material, P_{net} is the net pressure, E is the material Young's modulus, and t is the material thickness [19]. In the classic Hencky problem, as that defined by Eq. 3.2.1, where no pre-tension exists in the membrane, κ reaches a maximum value of 0.5982 for ν of 0.49, or 0.5952 for ν of 0.499. With the introduction of pre-tension, the extended Hencky solution applies, such that [20]

$$w = \left(\frac{P_{\text{net}} a^4}{Et^4}\right)^{1/3} \kappa t \tag{3.2.2}$$

As pre-tension in the membrane increases, κ decreases.

Pre-tension (σ) may be calculated using the Lamé equation for hoop stress in thick-walled

cylinders. That is,

$$\sigma = P_{\text{in}} \frac{{r_1}^2 + {r_2}^2}{{r_2}^2 - {r_1}^2} \tag{3.2.3}$$

where r_1 and r_2 refer to inner and outer radii of the abdomen, respectively, and P_{in} is internal pressure [21]. Radii may be approximated by waist circumference taken at the navel. Published averages for waist circumference, abdominal wall thickness, Young's modulus and Poisson's ratio are compiled in Table 3.2.1.

Table 3.2.1: Published average physiological properties

	Male	Female	Reference
Waist Circumference [m]	0.9524	0.8129	[22]
Abdominal Wall Thickness [m]	0.03	0.03	[23]
***E* [kPa] at Linea Alba**	$0.957t$	$0.957t$	[24]
ν	0.499	0.499	[25]

In the context of IAP, published values of healthy and unhealthy pressure ranges are available. As such, these ranges may be applied to determine pre-tension, with results compiled as calculated pre-tensions in Table 3.2.2. Included is the Valsalva maneuver; a common testing method for herniation to evaluate the abdomen at peak pressures [26]. To compare, experimentally measured values for tension in the linea alba (central, vertical line of tissue in the abdomen), as determined by Konerding *et al*., are juxtaposed [27].

Table 3.2.2: Clinical states and associated pre-tensions

Clinical State	**IAP [mmHg]**	**Pre-tension calculated [kPa]**		**Pre-tension [kPa] [27]**	
		Male	**Female**	**Male**	**Female**
Normal – Normal BMI	5	3.04	2.56	–	–
Normal – High BMI	10	6.13	5.16	–	–
Intra-abdominal Hypertension	12	7.37	6.21	–	–
Abdominal Compartment Syndrome	20	12.26	10.32	8.89	8.33
Valsalva Maneuver	120	73.68	62.06	100.00	108.33

To illustrate the suggested theoretical concept, expected maximum lateral deformations were mapped against a series of pressures in Fig. 3.2.3. Calculations were made using Eq. 3.2.1 for a sample with no pre-tension, and 3.2.2 for samples with increasing pre-tension. Equations

used published values as compiled in Tables 3.2.1 and 3.2.2. Computations were made to a higher density for physiologically relevant points. Data was fit with second order exponentials to suggest trendlines.

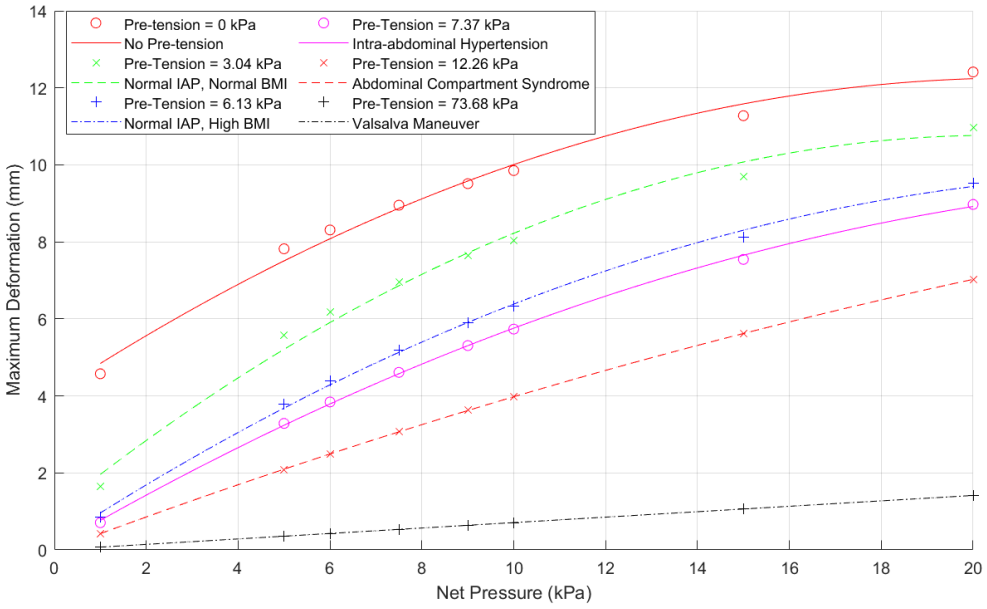

Figure 3.2.3: Theoretical maximum deformation versus pressure with increasing pre-tension.

Figure 3.2.3 shows three distinct regions of interest with respect to IAP: (1) below normal IAP, (2) normal IAP, and (3) above normal IAP (requiring monitoring). Region (1) is between curves for no pre-tension and normal body mass index (BMI), region (2) is between normal and high BMI, and region (3) is below the high BMI curve. It should be noted that these regions are relevant in a specific set of patient conditions; that is, measured with patients in supine position at end-expiration without any abdominal activation. Of greatest interest is the difference between "healthy" (normal, or below normal IAP) and "unhealthy" (high) IAP. This difference supports clinical decision making for patients in need of medical intervention.

To isolate a patient's IAP into "healthy" or "unhealthy" categories, a second set of equations describing maximum stress must be considered. The classic Hencky solution states that maximum stress (S) occurs at the center of a pressurized, circular membrane, and can be defined by

$$S = \left(\frac{P_{\text{net}} a}{Et}\right)^{2/3} \omega E t \tag{3.2.4}$$

where ω is a constant dependent on pre-tension in the membrane and Poisson's ratio (ν) of the material [19]. When pre-tension exists, the extended Hencky solution applies and the equation

adjusts to [20]

$$S = (\frac{P_{\text{net}} a^4}{Et^4})^{2/3} \omega \frac{Et^2}{a}. \tag{3.2.5}$$

As pre-tension in the membrane increases, ω increases.

To exemplify this concept in the context of IAP, a series of physiological pre-tensions were applied and graphed with respect to applied pressure and maximum stress. The results, as calculated with Eq. 3.2.4 and 3.2.4 and using published values for the abdomen, are shown in Fig. 3.2.4. Data were fit with first order polynomials to arrive at trendlines.

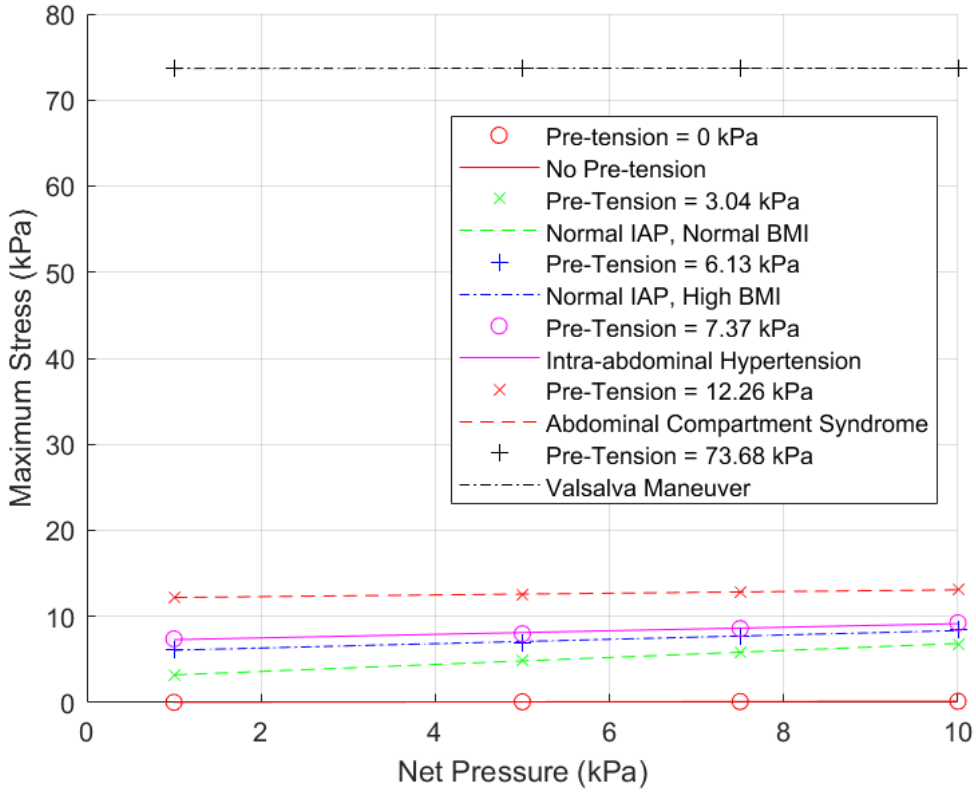

Figure 3.2.4: Theoretical maximum stress versus pressure with increasing pre-tension.

Of note in Fig. 3.2.4 is the relative consistency of maximum stress as applied pressure increases. At net pressures of 5 kPa, a maximum difference between maximum stress and pre-tension of 52% was seen at a pre-tension of 3.04 kPa. This difference decreases as pre-tension increases, and as net pressure decreases. As net pressures remain less than 5 kPa for supine patients at rest, an assumption is offered: the maximum stress may be approximated as the pre-tension in the abdomen ($S = \sigma$). In addition to low expected net pressures, it is anticipated that maximum stress is underestimated given original problem constraints. Rather than the uniform pressure that occurs

in reality, both the classic and extended Hencky solutions consider a membrane under uniform lateral loading, in which all force vectors are parallel. Conversely, uniform pressure results in an array of force vectors orthogonal to the membrane surface. Thus, maximum stress due to uniform pressures can be expected to increase, as radial stress increases, when compared to their uniform lateral loading counterparts [19]. That said, clinically, this results in an overestimation of IAP, yielding a fail-positive system. This is deemed acceptable as it is of greater significance to incorrectly test positive than miss a patient who is critically ill.

Given the unknown nature of variables ω and κ, another equation must be introduced. A force balance of the resected membrane is considered, resulting in

$$S = \frac{P_{\text{net}}(a^2 + w^2)}{4tw}. \tag{3.2.6}$$

If Eq. 3.2.3 and 3.2.6 are equated, using the proposed assumption, an equation for internal pressure is established:

$$P_{\text{in}} = \frac{P_{\text{app}}(a^2 + w^2)({r_2}^2 - {r_1}^2)}{4tw({r_1}^2 + {r_2}^2) - (a^2 + w^2)({r_2}^2 - {r_1}^2)}. \tag{3.2.7}$$

To evaluate the robustness of Eq. 3.2.7, a relation is proposed where $x = 1.00$ in $S = x\sigma$. If x increases to satisfy the theoretical relationship between S and σ, the question remains how calculated internal pressure is affected. Thus, P_{in} is varied depending on x to evaluate the sensitivity of the solution to the proposed assumption. Additionally, sensitivity of P_{in} to changes in waist circumference was considered. Assuming a circular waist, outer radii can be calculated by dividing waist circumference by 2π.

Using κ for no pre-tension as an approximation, an appraisal of Young's modulus can be found by adjusting Eq. 3.2.2 to

$$E = \frac{P_{\text{net}} a^4}{(t^4(\frac{w}{0.5952t})^3)}. \tag{3.2.8}$$

Sensitivity of Young's modulus to varying κ was also measured. Rather than using estimated κ for no pre-tension (0.5952), κ was approximated with known values for participants in supine position.

3.2.4 Results

Following ethical approval, a feasibility study proceeded. This resulted in two healthy males ($n = 2$) being tested with the novel device by one tester ($k = 1$). Physical details of the

participants are shown in Table 3.2.3, with waist circumference, abdominal wall thickness, E, and ν constrained to published averages.

Table 3.2.3: Participant physiological properties

	Male 1	**Male 2**
Age	26	28
Height [m]	1.85	1.78
Weight [kg]	82.8	75.7
Body Mass Index	24.2 (Normal)	23.9 (Normal)
Waist Circumference [m]	0.91	0.84

Each participant was tested five times 5 cm subxiphoid along the linea alba. Tests were conducted using WSACS recommendations, that is, in supine position at end expiration without abdominal activation [2]. Each peak pressure and deformation pair was mapped with time, as shown in Fig. 3.2.5, prior to data filtering.

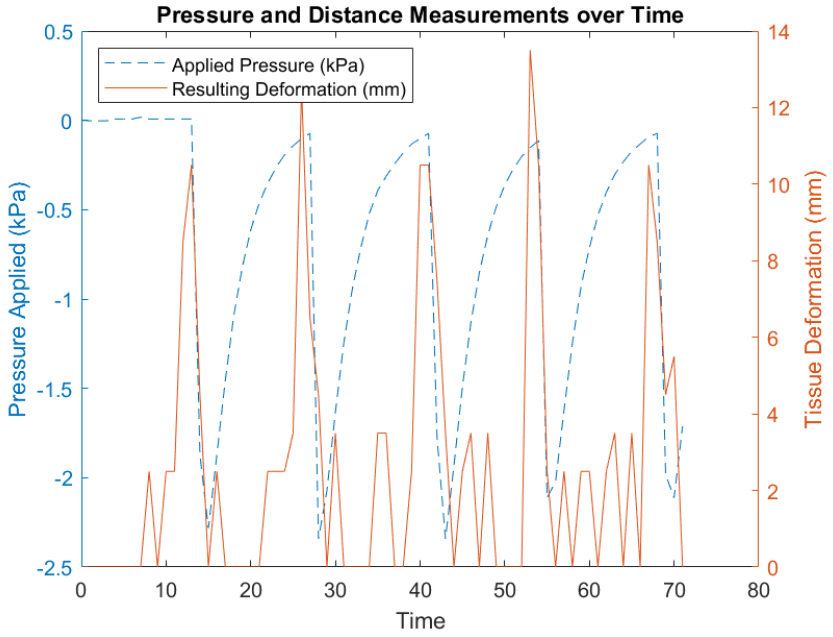

Figure 3.2.5: Raw functional data: applied pressure and resulting deformation over time.

Previous studies have indicated a direct relation between IAP and head position: 1.5 mmHg with 15° incline, and 3.7 mmHg with 30° incline [28]. This change is suggested to be due to the effect of gravity and visceral compression [28]. Therefore, to determine whether relative changes were evident, the participants were asked to lie with their head raised 30° from the sternum with respect to the ground, at which time measurements were retaken. Figure 3.2.6 shows averaged results from supine and inclined tests in comparison to theoretical results.

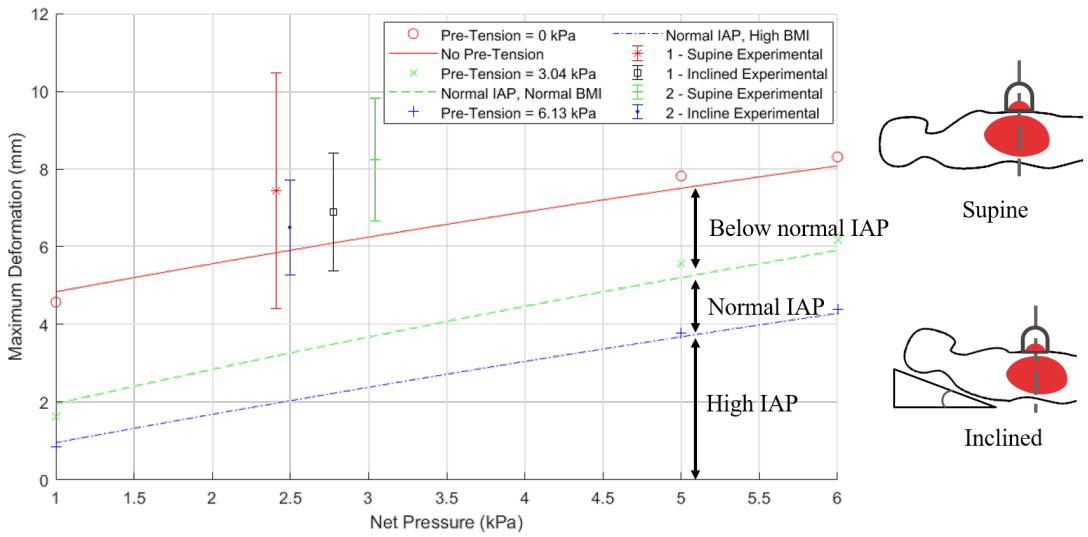

Figure 3.2.6: Functional versus theoretical results.

Participant IAPs were calculated with Eq. 3.2.7 and compiled in Table 3.2.4. For participant 1, calculated internal pressure was 0.38 kPa (2.9 mmHg) and 0.47 kPa (3.5 mmHg) for supine and inclined positions, respectively. Participant 2 presented a slight decrease in pressure, with calculated internal pressures of 0.45 kPa (3.4 mmHg) and 0.44 kPa (3.3 mmHg) for supine and inclined positions, respectively. Of note is the increase in IAP with an increase in head incline for participant 1.

Table 3.2.4: Experimentally determined intra-abdominal pressures for supine and inclined positions

	Body Pos.	**Male 1**	**Male 2**
Average peak app. pressure [kPa] (SD)	Supine	1.94 (0.3)	2.49 (0.3)
Average peak tissue deform [mm] (SD)	Supine	7.6 (3.0)	8.3 (1.6)
Average IAP [kPa] (SD)	Supine	0.38 (0.40)	0.45 (0.16)
Average E [kPa] (SD)	Supine	15.43 (53.8)	14.38 (13.7)
Average peak app. pressure [kPa] (SD)	Incline	2.20 (0.06)	1.95 (0.3)
Average peak tissue deform [mm] (SD)	Incline	6.90 (1.5)	6.50 (1.2)
Average IAP [kPa] (SD)	Incline	0.47 (0.16)	0.44 (0.20)
Average E [kPa] (SD)	Incline	22.28 (22.8)	23.9 (22.4)

Young's modulus for participant 1 and 2 was calculated with Eq. 3.2.8 to be 15.43 and 14.38 kPa, respectively, at supine position. This value increased at an inclined position with 22.28 and 23.90 kPa for participant 1 and 2, respectively. An increase in stiffness in both participants with increasing inclination indicates the activation of abdominal muscles, as supported by previous studies [24].

The strength of the proposed assumptions was evaluated in a brief sensitivity analysis, as summarized in Table 3.2.5. The results of the sensitivity of P_{in} to x are compiled in Table 3.2.5 for participant 1 and 2 supine results using Eq. 3.2.7. Also summarized is the sensitivity of actual participant waist circumferences to evaluate P_{in}. Finally, sensitivity of E to κ was evaluated. In each scenario, a control is set, and defined as the calculated variable using equations as set, that is, without variable adjustment. It is the effort of the sensitivity analysis to evaluate the robustness of equations, not device function.

Table 3.2.5: Sensitivity analyses: as noted

	Participant 1		**Participant 2**	
	Sensitivity of P_{in} to x			
P_{net} **[kPa]**	2.32	2.32	2.94	2.94
x	1.00	1.1726	1.00	1.2514
P_{in} **[kPa]**	0.38	0.32	0.45	0.34
% diff with control	N/A	16%	N/A	24%
	Sensitivity of P_{in} to waist circumference			
Waist circumf. [m]	0.952	0.91	0.952	0.84
P_{in} **[kPa]**	0.38	0.41	0.38	0.53
% diff with control	N/A	8%	N/A	18%
	Sensitivity of E to κ			
κ	0.5952	0.3282	0.5952	0.3603
E **[kPa]**	15.43	3.42	14.36	3.18
% diff with control	N/A	78%	N/A	78%

3.2.5 Discussion

A device to characterize pressurized, physiological vessels was developed and feasibility confirmed via preliminary analyses. The device uses a localized known pressure to measure resulting tissue deformation, from which the internal pressure range can be divulged. Changes in physiological pressures were correctly detected in one of two tested participants, while changes in abdominal wall elasticity were correctly detected in both tested participants.

Physically, errors in pressure and deformation sensors may have propagated through calculations. These errors include noise, as previously mentioned, of 8 Pa and 2 mm in the BMP388 and VL6180 sensors, respectively. As such, sensor error accounts for errors up to 0.08 kPa (0.6 mmHg) and 6 kPa for P_{in} and E, respectively. Air leakage in the device further constrained results to peak pressures, whereas maintained suction may have offered a relaxed state in tissue with greater IAP

and Young's modulus accuracies. Thus, improved sensors and system air-tightness may strengthen outcomes.

Theoretically, the assumptions presented in this study simplify the reality of the problem, leading to potential sources of error. These simplifications include (reality versus assumption): (1) uniform pressures versus uniform lateral loading, (2) differences between maximum stress and pre-tension versus consistency between the two, (3) non-linear Young's modulus versus constant Young's modulus. To improve on these areas, the extended Hencky solution in a uniform pressure setting must be considered. This future research may provide insight into the exact relation between maximum stress and pre-tension. In addition, following on the research of Hayes and Zhang who studied Young's modulus given tissue indentation, a theoretical study into the evaluation of Young's modulus given local uniform pressure is of value [29], [30].

Functionally, the greatest limitation in this study is limited sample size. With a larger study population, the wider impact of the novel device may be revealed. It is also of value to directly compare the novel device to existing technologies to evaluate the error between measurement systems. This comparison is necessary for both IAP and Young's modulus evaluation. Despite the lack of a "gold standard" measurement tool for either IAP or Young's modulus, it is recommended to compare IAP against UBP, and Young's modulus against the MyotonPro, given both devices' existing popularity. Nevertheless, the feasibility study showed promising results while the methods put forth may serve to assists others with similar design targets.

Results in Table 3.2.4 support physiological evidence that IAP increases, and, thus, pre-tension increases, with increased head inclination [28]. The decrease in pressure from supine to inclined position in participant 2 may be attributed to early inhalation or measurement error. In this scenario, measurement error refers to procedural inconsistencies, such as holding the device at an angle, rather than orthogonal to, the abdomen, or applying excessive pressure against the abdomen to seal the device to the skin. Additionally, deformations are seen to be greater than the theoretical maximum curve for no pre-tension in Hencky's solution. This error is likely due to differences in patient physiologies when compared to published averages.

The differences shown in Table 3.2.5 represent the greatest likely differences during testing. As noted from Fig. 3.2.6, the worst-case scenario is seen at high net pressures and low pre-tensions. In other words: patients at supine position with high applied pressures. To circumvent this error, a constant applied pressure of 2 kPa is suggested, at which time x is 1.13. This adjustment still yields a greater P_{in} than actual; however, it is deemed acceptable to support a false-positive device rather than a false-negative. In this case, false-positive refers to the incorrect diagnosis of high IAP. As intra-abdominal hypertension and abdominal compartment syndrome (high-IAP conditions) are

diagnosed by prolonged high IAP, a false-positive would require the monitoring of a patient's IAP over several hours before treatment is considered. The financial impact of false-positives is seen as minimal, when compared to the impact of a false-negative; a mistake that has life-threatening consequences.

Given the effect of waist circumference, it is recommended to use actual patient waist circumferences in final calculations. This is, in part, since smaller waist sizes demonstrate higher internal pressures. Therefore, if the correction is not made, results support false-negatives. As mentioned previously, this is financially and clinically inadvisable.

The sensitivity of E to κ indicates the lack of robustness in Eq. 3.2.8. Therefore, as suggested previously, a theoretical study into the evaluation of Young's modulus given local uniform pressure is of interest in determining a corrective factor that improves equation strength.

Contrary to existing methods of measurement, the innovative system, described herein, is handheld and non-invasive. Rather than correlating measures to IAP, the novel system directly measures IAP, as well as abdominal wall elasticity, simultaneously. Initial functional tests indicate the ability of the device to deduce the correct internal pressure range; all recorded pressures were within the healthy range of patients with normal BMI, complementing the participants tested. Further, changes in abdominal wall elasticity were correctly detected given a change in body inclination. That said, clinical studies are required to evaluate the novel device in a broader physiological setting. Future work includes the evaluation of the device as a physiological internal pressure measurement tool and abdominal wall elasticity measurement tool via reliability, validity, and agreement with existing methods of measurement prior to clinical use.

3.2.6 Acknowledgment

The authors have received grant funding (NSERC RGPIN-2017-04037) for the research, herein, as well as have the related patent 63/027,241 pending.

3.2.7 Funding Data

Natural Sciences and Engineering Research Council of Canada (NSERC) (Grant No. RGPIN-2017-04037; Funder ID: 10.13039/501100000038).

Bibliography

[1] M. Malbrain, D. Roberts, I. De Laet, J. De Waele, M. Sugrue, A. Schachtrupp, J. Duchesne, G. Van Ramshorst, B. De Keulenaer, A. Kirkpatrick, S. Ahmadi-Noorbakhsh, J. Mulier, R. Ivatury, F. Pracca, R. Wise, and P. Pelosi, "The role of abdominal compliance, the neglected parameter in critically ill patients — a consensus review of 16. Part 1: definitions and pathophysiology," *Anesthesiology Intensive Therapy*, vol. 46, no. 5, pp. 392–405, 2014.

[2] M. Malbrain, M. Cheatham, A. Kirkpatrick, M. Sugrue, M. Parr, J. De Waele, Z. Balogh, A. Leppaniemi, C. Olvera, R. Ivatury, S. D'Amours, J. Wendon, K. Hillman, and A. Wilmer, "Results from the international conference of experts on intra-abdominal hypertension and abdominal compartment syndrome. I. Definitions," in *Intensive Care Medicine*, vol. 32, 2006, pp. 1722–1732.

[3] T. Papavramidis, A. Marinis, I. Pliakos, I. Kesisoglou, and N. Papavramidou, "Abdominal compartment syndrome - Intra-abdominal hypertension: Defining, diagnosing, and managing.," *Journal of Emergencies, Trauma, and Shock*, vol. 4, no. 2, pp. 279–91, 2011.

[4] D. Roberts, J. De Waele, A. Kirkpatrick, and M. Malbrain, "Intra-abdominal hypertension and the abdominal compartment syndrome," *Surgical Intensive Care Medicine*, vol. 39, no. 7, pp. 621–644, 2016.

[5] A. Blaser, A. Regli, B. De Keulenaer, E. Kimball, L. Starkopf, W. Davis, P. Greiffenstein, and J. Starkopf, "Incidence, Risk Factors, and Outcomes of Intra-Abdominal Hypertension in Critically Ill Patients-A Prospective Multicenter Study (IROI Study)," *Critical Care Medicine*, vol. 47, no. 4, pp. 535–542, 2019.

[6] R. Milanesi and R. Caregnato, "Intra-abdominal pressure: An integrative review," *Einstein (Sao Paulo)*, vol. 14, no. 3, pp. 423–430, 2016.

[7] M. Malbrain, "Different techniques to measure intra-abdominal pressure (IAP): Time for a critical re-appraisal," *Intensive Care Med*, vol. 30, pp. 357–371, 2004.

[8] M. Cheatham, M. Malbrain, A. Kirkpatrick, M. Sugrue, M. Parr, J. De Waele, Z. Balogh, A. Leppaniemi, C. Olvera, R. Ivatury, S. D'Amours, J. Wendon, K. Hillman, and A. Wilmer, "Results from the international conference of experts on intra-abdominal hypertension and abdominal compartment syndrome. II. Recommendations," *Intensive Care Medicine*, vol. 33, pp. 951–962, 2007.

[9] J. Otto, D. Kaemmer, M. Binnebosel, M. Jansen, R. Dembinski, V. Schumpelick, and A. Schachtrupp, "Direct intra-abdominal pressure monitoring via piezoresistive pressure measurement: A technical note," *BMC Surgery*, vol. 9, no. 5, pp. 1–5, 2009.

[10] F. Pracca, A. Biestro, L. Moraes, C. Puppo, S. Calvo, J. Gorrasi, and M. Cancela, "Direct measurement of intra-abdominal pressure with a solid microtranducer," *Journal of Clinical Monitoring and Computing*, vol. 21, pp. 167–170, 2007.

[11] A. Al-Abassi, A. Al Saadi, and F. Ahmed, "Is intra-bladder pressure measurement a reliable indicator for raised intra-abdominal pressure? A prospective comparative study," *BMC Anesthesiology*, vol. 18, no. 69, pp. 1–9, 2018.

[12] Y. Chen, S. Yan, Y. Chen, Y. Zhuang, Z. Wei, S. Zhou, and H. Peng, "Noninvasive monitoring of intra-abdominal pressure by measuring abdominal wall tension," *World Journal of Emergency Medicine*, vol. 6, no. 2, pp. 137–141, 2015.

[13] A. Bloch, M. Glas, A. Kohler, U. Baumann, and S. Jakob, "Noninvasive assessment of intra-abdominal pressure using ultrasound-guided tonometry: A proof-of-concept study," *Shock (Augusta, Ga.)*, vol. 50, no. 6, pp. 684–688, 2018.

[14] T. Coleman, J. Thomsen, S. Maass, Y. Hsu, I. Nygaard, and R. Hitchcock, "Development of a wireless intra-vaginal transducer for monitoring intra-abdominal pressure in women," *Biomedical Microdevices*, vol. 14, no. 2, pp. 347–355, 2012.

[15] P. Johnson, E. Rosenbluth, I. Nygaard, M. Parikh, and R. Hitchcock, "Development of a novel intra-vaginal transducer with improved dynamic response," *Biomedical Microdevices*, vol. 11, no. 6, pp. 1213–1221, 2009.

[16] G. Van Ramshorst, J. Lange, R. Goossens, N. Agudelo, G. Kleinrensink, M. Verwaal, S. Flipsen, W. Hop, L. Wauben, and J. Jeekel, "Non-invasive measurement of intra-abdominal pressure: A preliminary study," *Physiological Measurement*, vol. 29, no. 8, 2008.

[17] M. David, A. Raviv, A. Peretz, U. Berkovich, and F. Pracca, "Towards a continuous non-invasive assessment of intra-abdominal pressure based on bioimpedance and microwave reflectometry: A pilot run on a porcine model," *Biomedical Signal Processing and Control*, vol. 44, pp. 96–100, 2018.

[18] F. Primiano, "Theoretical analysis of chest wall mechanics," *Journal of Biomechanics*, vol. 15, no. 12, pp. 919–931, 1982.

[19] W. Fichter, "Some Solutions for the Large Deflections of Uniformly Loaded Circular Membranes," *NASA Technical Paper*, vol. 3658, 1997.

[20] J. Sun, Y. Lian, Y. Li, X. He, and Z. Zheng, "Closed-form solution of elastic circular membrane with initial stress under uniformly-distributed loads: Extended Hencky solution," *ZAMM Zeitschrift fur Angewandte Mathematik und Mechanik*, vol. 95, no. 11, pp. 1335–1341, 2015.

[21] B. Muvdi and J. W. McNabb, "Selected Topics," in *Engineering Mechanics of Materials*, 3rd ed., Springer New York, 1991, ch. 13, pp. 590–646.

[22] A. Flint, K. Rexrode, F. Hu, R. Glynn, H. Caspard, J. Manson, W. Willett, and E. Rimm, "Body mass index, waist circumference, and risk of coronary heart disease: a prospective study among men and women," *Obesity Research and Clinical Practice*, vol. 4, no. 3, pp. 171–181, 2010.

[23] C. Song, A. Alijani, T. Frank, G. Hanna, and A. Cuschieri, "Mechanical properties of the human abdominal wall measured *in vivo* during insufflation for laparoscopic surgery," *Surgical Endoscopy and Other Interventional Techniques*, vol. 20, no. 6, pp. 987–990, 2006.

[24] D. Tran, F. Podwojewski, P. Beillas, M. Ottenio, D. Voirin, F. Turquier, and D. Mitton, "Abdominal wall muscle elasticity and abdomen local stiffness on healthy volunteers during various physiological activities," *Journal of the Mechanical Behavior of Biomedical Materials*, vol. 60, pp. 451–459, 2016.

[25] R. Miller, A. Kolipaka, M. Nash, and A. Young, "Relative identifiability of anisotropic properties from magnetic resonance elastography," *NMR in Biomedicine*, vol. 31, pp. 1–12, 2018.

[26] C. Aquina, J. Iannuzzi, C. Probst, K. Kelly, K. Noyes, F. Fleming, and J. Monson, "Parastomal hernia: A growing problem with new solutions," *Digestive Surgery*, vol. 31, pp. 366–376, 2014.

[27] M. Konerding, M. Bohn, T. Wolloscheck, B. Batke, J. Holste, S. Wohlert, J. Trzewik, T. Forstemann, and C. Hartung, "Maximum forces acting on the abdominal wall: Experimental validation of a theoretical modeling in a human cadaver study," *Medical Engineering and Physics*, vol. 33, no. 6, pp. 789–792, 2011.

[28] M. Cheatham, J. De Waele, I. De Laet, B. De Keulenaer, S. Widder, A. Kirkpatrick, A. Cresswell, M. Malbrain, Z. Bodnar, J. Mejia-Mantilla, R. Reis, M. Parr, R. Schulze, and S. Puig, "The impact of body position on intra-abdominal pressure measurement: A multicenter analysis," *Critical Care Medicine*, vol. 37, no. 7, pp. 2187–2190, 2009.

[29] W. Hayes, G. Herrmann, L. Mockros, and L. Keer, "Mathematical analysis for indentation tests of articular cartilage," *Journal of Biomechanics*, vol. 5, pp. 541–551, 1972.

[30] M. Zhang, Y. Zheng, and A. Mak, "Estimating the effective Young's modulus of soft tissues from indentation tests—nonlinear finite element analysis of effects of friction and large deformation," *Medical Engineering and Physics*, vol. 19, no. 6, pp. 512–517, 2006.

3.3 Additional related study: Minimum lumbosacral orthosis tension required to prevent parastomal herniation while supporting the spine

Complementing the work of Objective 1 was a study that used the set of equations developed in Section 3.2 in the context of a clinical application: defining minimum tensile requirements for lumbosacral orthoses (hernia belts). In collaboration with CDRM Inc.: Vêtements Compressifs et Thérapeutiques (Montreal, Canada), 5 hernia belt materials, developed in-house, were tested to determine the E of each. Following, a set of guidelines were developed using anthropometric measures and a thick-walled cylinder approximation for the abdomen. Results were presented in a technical report submitted to CDRM entitled "Minimum lumbosacral orthosis tension required to prevent parastomal herniation while supporting the spine". The technical report was presented in a poster format at the *International Society of Biomechanics* 2019 conference in Calgary, Canada on August 3, 2019.

3.3.1 Technical Report

Parastomal Herniation (PSH) is one of the most common complications in ostomy procedures (surgically created opening in an organ), with 10 to 70% of patients reporting the condition [54]. Though occasionally disputed [168], [169], most authors agree that the highest rates of PSH occur in end colostomies [54], [65], [168]. Further, risks tend to decrease if a colostomy is made through the rectus abdominis as opposed to lateral to the muscle [65]. For the purposes of this study, PSH is defined as a localized, visible protrusion upon a standing Valsalva maneuver in end colostomy patients [65]. The current recommended prevention method for PSH is the proactive implantation of a prophylactic mesh (termed prophylactic mesh augmentation) [170]. However, one other prevention method not well studied is the use of lumbosacral orthoses, or, waist support belts used to support the spine, or prevent herniation (also called hernia belts) [54]. CDRM specializes in custom hernia belts for patients. Both belts for standard herniation and PSH are available and come in five material options: 3D, Belgium, CDRM, NEK, and Regular. Though customizable, belts follow a standard sizing chart available through CDRM. Belt widths come in sizes between 4 and 12 inches, in 1 inch increments, while lengths depend on the patient's abdominal perimeter (C, measured at the navel). Belt lengths are small (C less than 114 cm), medium (C between 114 and 160 cm) and large (C greater than 160 cm). Due to the high frequency of PSH and disputes in literature regarding its prevention, the application of hernia belts was explored as a non-invasive alternative to other popular prevention methods. Specifically, the objective of the present work was to develop safe guidelines for tension required to prevent PSH using CDRM materials.

Five materials (3D, Belgium, CDRM, NEK, Regular), provided by CDRM, were tested axially at a constant rate of elongation using ASTM D76 standards for textiles. A Shimadzu EZ

test machine was employed and four strain rates (100, 150, 200 and 300 mm/min) were used to evaluate the mechanical behaviour and recovery of each material's elastic properties. To limit slippage at higher strains, 120 grit adhesive-backed sandpaper was used between the machine grips and belt material. The σ-ε curves of each material were obtained and compared to evaluate recovery of material properties. To note, material samples were stretched to extreme strains, thus, representing a worst-case scenario.

In this study, the average male and female with a standard end colostomy through the rectus abdominis were considered. The abdomen has repeatedly been modelled as a pressurized, thin-walled cylinder of incompressible fluid [171], [172], however, to use the thin-walled cylinder model, the internal and external radii of the cylinder must have a ratio no greater than 1.09 [173]. Given published data, ratios were found to be around 1.11 for males and 1.17 for females, thus, outside allowable parameters. Therefore, the thick-walled cylinder approximation (Lamé equation) was used as an alternative, assuming AW isotropy and rigidity:

$$\sigma = P(\frac{{r_1}^2}{{r_2}^2 - {r_1}^2})(\frac{1 - {r_2}^2}{{r_1}^2}), \tag{3.3.1}$$

where P is the IAP during a Valsalva maneuver, r_1 is the internal radius, and r_2 is the external radius [173]. To determine r_2, volume changes in the abdomen were considered at higher pressures from published relations [2]. Published data for each variable was used to determine AW stress (σ) and are summarized in Table 3.3.1.

Table 3.3.1: Reference data for calculations (IAP: intra-abdominal pressure; IAV: intra-abdominal volume; AWTh: abdominal wall thickness; C: abdominal perimeter)

	Male	**Female**	**Ref.**
IAP (Valsalva Maneuver) [mmHg]	120		[58], [65]
IAP (Dynamic Loading) [mmHg]	208		[58]
IAP (Normal, Healthy BMI) [mmHg]	7		[2], [20]
IAV (for IAP = 9 mmHg) [L]	4		[2]
IAV (for IAP = 34 mmHg) [L]	9		[2]
C [m]	0.95	0.81	[174]
Waist Width [m]	0.33	0.30	[175]
AWTh [m]	0.03	0.03	[24], [176]
r_1 (for IAV = 4 L) [m]	0.10	0.07	
r_2 (for IAV = 4 L) [m]	0.13	0.10	
r_1 (for IAV = 9 L) [m]	0.27	0.19	
r_2 (for IAV = 9 L) [m]	0.30	0.22	

In conjunction with measured belt material elasticities (E), and assuming a hernia belt bears

wall stress under applied IAP, the required belt strain (ε) was found with Hooke's law [173]. This equation assumed one-dimensional stress acting along the lengthwise axis of the belt, given limited deformation in the orthogonal planes, such as with a string in tension:

$$\sigma = E\varepsilon. \tag{3.3.2}$$

Tensile tests resulted in the average measured elasticities in each material, as shown in Table 3.3.2. Average percent loss refers to the percent difference in E between the first and last trials on the same material sample, while SD is the standard deviation of results.

Table 3.3.2: Elasticity results from tensile tests of CDRM materials (E: elasticity; SD: standard deviation; Avg. % Loss: average percent loss)

Material	**3D**	**Belgium**	**CDRM**	**NEK**	**Regular**
***E* [MPa]**	0.21	0.75	0.89	0.60	0.31
SD [MPa]	0.03	0.12	0.20	0.06	0.05
Avg. % Loss	21%	23%	31%	9%	23%

Materials demonstrated hyperelastic behaviours, with little variance in E between strain rates. In the interest of patient comfort, belt strains were limited to the average thoracic lumbar range of motion (between 35 and 50°) [177]. As such, linear elasticity could be approximated up to 60% strain in each material, with the exception of CDRM. The CDRM material demonstrated hyperelastic properties near 50% strain, and, thus, linear elasticity was approximated to this point. One property of note was the poor resilience of each material, as suggested by each material's average reduction in E after three cycles of loading (see average % loss in Table 3.3.2) and illustrated in Figure 3.3.1.

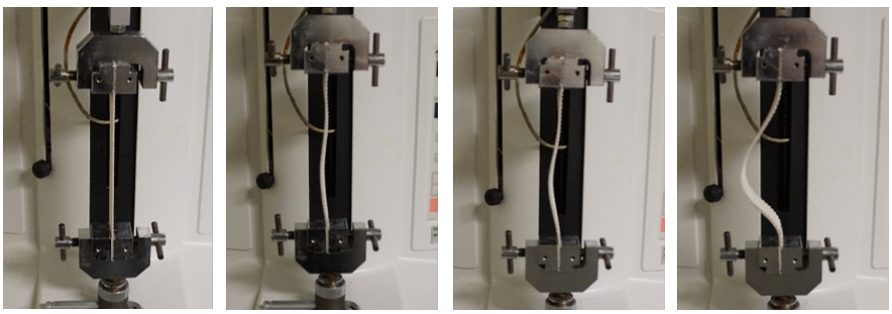

Figure 3.3.1: CDRM sample elongated at 100 mm/min. From left to right: initial, after 1 cycle, 2 cycles and 3 cycles. Similar patterns of plastic deformation were seen in all other material samples.

The objective of this study was to provide directives towards initial strain values such that, when equilibrium is reached, an appropriate IAP is achieved. Thus, to withstand the AW stress

resulting from a Valsalva maneuver (approximately 120 mmHg [58]), required belt strains for single material bands to realize said strains were evaluated. Table 3.3.3 summarizes required belt strains for males and females, separately. Two intensity levels were outlined for adjustments during varying activities: high intensity (dynamic loading) and regular [58]. For supine positions (at rest), strains were insignificant to warrant wear at all.

Table 3.3.3: Recommended baseline strains for belt materials during varying activity intensities

	Intensity	Stress [kPa]	3D	Belgium	CDRM	NEK	Regular
Male	**High Intensity**	114.0	53%	15%	8%	19%	37%
	Regular	65.8	31%	9%	5%	11%	21%
Female	**High Intensity**	72.7	34%	10%	5%	12%	23%
	Regular	41.9	20%	6%	3%	7%	13%

As a means of validation, results were compared to *in vivo* trials conducted by Konerding's research group [115]. Konerding *et al*. measured the tensile force required on a 6 cm long incision along the linea alba during insufflation up to 150 mmHg in 7 cadavers, both male and female [115]. Insufflation was performed using a balloon inserted into the peritoneal cavity (IAV) filled with water at a rate of 2 L/min [115]. The results from this study were converted from stress to force (F), given the relation [173],

$$\sigma = \frac{F}{A} \tag{3.3.3}$$

in which A refers to the cross-sectional area of the AW along the 6 cm long measurement line. In order to compare the present study to Konerding's research group, anatomical parameters, namely r_1 and r_2, had to be adjusted for inflated abdomens. To do so, the abdomen was assumed to be an elliptical cylinder of major and minor radii a and b, respectively, and height, h. If a is considered half the waist width, b can be determined given published data for abdominal perimeter (C), considering:

$$C = 2\pi\sqrt{(\frac{a^2+b^2}{2})}. \tag{3.3.4}$$

To determine b for the expanded volume (IAV, 9 L at an inflation pressure of 34 mmHg [2]), the geometric relation

$$IAV = \pi abh \tag{3.3.5}$$

was used. To note, IAV reaches a critical volume around 9 L of inflation beyond which minimal expansion results. Finally, r_2 is equated to b, and r_1 is determined by subtracting AWTh from r_2. Geometric assumptions are illustrated in Fig. 3.3.2.

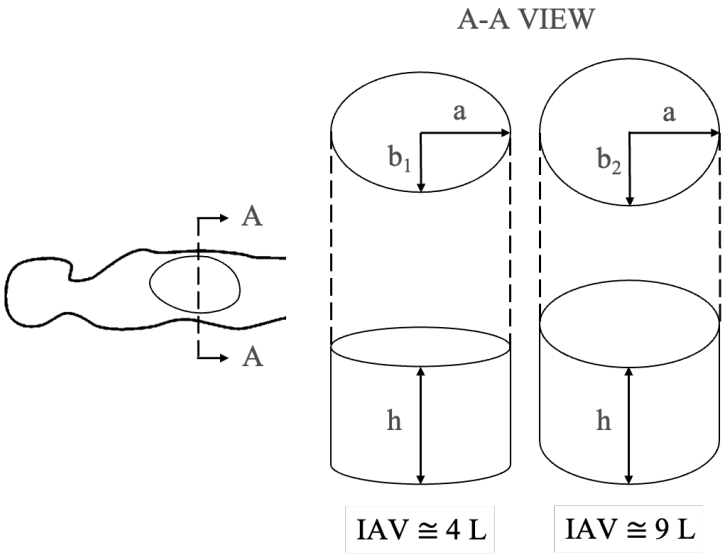

Figure 3.3.2: Theoretical model assumed in abdominal calculations. Geometries adjust upon forced inflation, i.e. as intra-abdominal volume (IAV) is increased.

Errors between Konerding *et al*.'s results were considered against the present study's values, and were found to be within 13% and 37% using the thick-walled cylinder approximation for females and males, respectively. As such, assumptions and approximations were validated for the purposes of this study at an inflated volume of 9 L. Results are summarized in Figure 3.3.3 alongside published values. Error bars for published values indicate values found for the 25th and 75th percentiles of Konerding's results [115]. It should be noted that results in Table 3.3.3 employed geometries at an IAV of 4 L, given that those calculated for 9 L only exist in IAVs undergoing forced inflation (*i.e*. without abdominal muscle activation). During everyday activity, the IAV does not expand as dramatically due to the tightening response of the AW muscles.

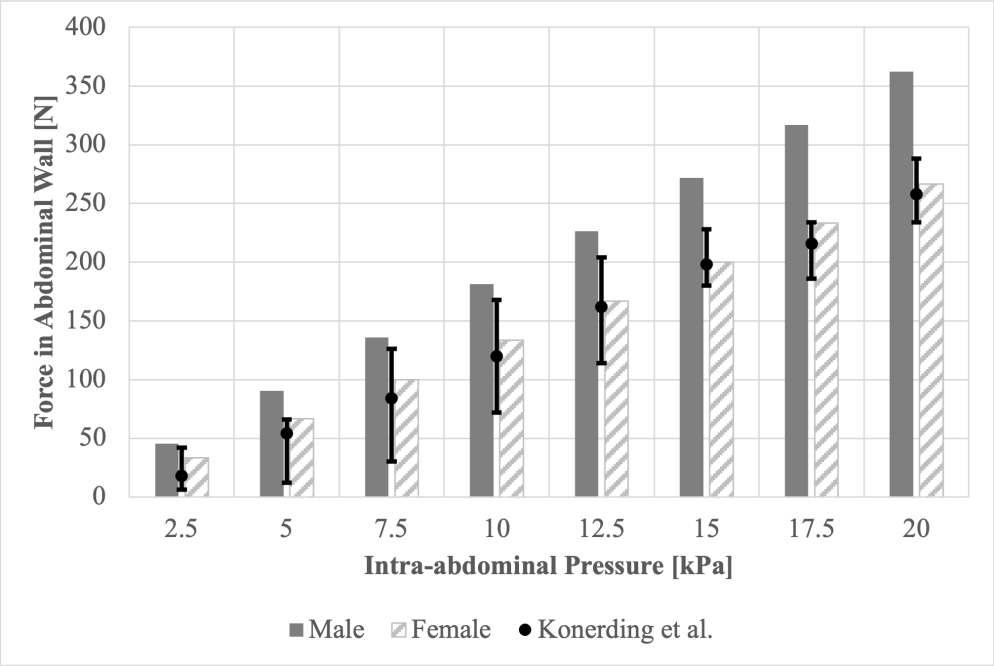

Figure 3.3.3: IAP versus response force in the abdominal wall for males and females at an assumed inflation volume of 9 L (here, equated to intra-abdominal volume, IAV), in comparison to published data from Konerding et al *[115].*

Five hernia belt materials were tested axially to quantify mechanical behaviour under varying strain rates. In conjunction, the AW stresses under a series of IAPs were calculated using a thick-walled cylinder model approximation of the abdomen. Calculated stresses were found to be within 13 and 37% of published data for women and men, respectively. As such, calculated values were treated as a reliable benchmark from which to determine the recommended amount of belt strain. Recommended belt strains ranged from 12 to 73% for men and 8 to 47% for women, depending on the material used. From a clinical standpoint, this data highlights minimum tensile requirements for hernia belts under standard loading, such as insufflation due to defecation or coughing. Consequently, patient-specific belt adjustments can be made given abdominal perimeter, physical activity level, and belt material to provide individualized support.

The present work assumes AW rigidity and homogeneity, which may have impacted results. In addition, average AWTh was taken at the rectus abdominis rather than at the linea alba, as in the case of Konderding *et al*.'s experiments, which may have altered validation [115]. It should also be noted that research was only conducted on the AW surface area supported by a hernia belt. Herniation may occur outside the space of the belt, such as at the groin or upper abdomen, and was out of the scope of this application. Regardless, this information stands as a relative guideline for patient and clinical use of hernia belts.

When considering the results of Table 3.3.3, most belts were within ergonomic limits, with the exception of the 3D material at high intensity activity in males. That said, it is recommended to manufacture belts with the CDRM, Belgium, or NEK materials, given their low minimum strain for males and females at high intensities, as well as their limited integrity loss in comparison to other materials. Should an alternative material be preferred, material bands may need to be doubled to reduce minimum tensions by 2. It is advisable to consult patients in terms of preferred material for comfort and thickness, as fabrics may cause irritation, while layering materials may obstruct clothing.

All belts suffered from some loss in elasticity upon repeated testing. This property must be evaluated, further, in long-term studies, to determine whether elasticity reduction affects the minimum tensile guidelines set at the onset of treatment. At this time, patient recommendations must be made to either replace their hernia belt after extended use, or modify the minimum line of tension to accommodate weaker materials (*i.e.* allow for further belt extension by moving Velcro straps).

In conclusion, this data highlights minimum tensile requirements for hernia belts used in PSH prevention. Patient-specific adjustments can be made based on individual C, physical activity level, and belt material. Long-term, *in vivo* studies are a necessary next step to confirm a decrease in PSH rates, while maintaining abdominal muscle health, as suggested by some authors [178], [179].

3.4 Additional study related to device design

Further physical tests indicated the need for optimization of both elasticity and IAP equations. As such, the following discusses said optimization, and the final equations used in future studies.

3.4.1 Elasticity Optimization

As mentioned in Section 3.2, the sensitivity of elasticity (E) to κ indicated the lack of robustness in Eq. 3.2.8. Therefore, an alternative equation for E was considered.

The tested elasticity (E) equations included:

$$E = \alpha(\zeta, \nu)\frac{3\phi(\eta)P_{\text{app}}a}{2\pi w} \tag{3.4.1}$$

where $\phi(\eta)$ is a function dependant on pipette radii [180], here, η being 0.1 results in $\phi(0.1)$ of 2.3. The coefficient $\alpha(\zeta, \nu)$ refers to a function dependant on the thickness (t) of the tissue being tested (average of 0.03 m at the abdomen [24], or 0.01 m at the calf [181]) [182]. P_{app} is the absolute pressure applied. This is a typical equation for micropipettes, though was used for the tested macropipette [131]. For the tissues of interest, here, assuming ν of 0.499 and adjoined tissue layers, α simplified to [182]

$$\alpha = 0.9965\frac{(\frac{t}{a})^{2.63}}{1.113 + (\frac{t}{a})^{2.63}}, \tag{3.4.2}$$

or, 0.47 for $t = a = 0.03$ m at the abdomen. At the calf this equates to 0.033 for $t = 0.01$ m, $a = 0.03$ m.

Finally, as suggested in Section 3.2 (Eq. **??**), another possible equation for E is

$$E = \frac{P_{\text{net}}a^4}{(t^4(\frac{w}{0.5952t})^3)} \tag{3.4.3}$$

where P_{net} refers to the summation of P_{app} and IAP.

Using the same patient data as in Section 3.2, average E was calculated with each equation. The results are shown in Table 3.4.1.

A couple points of interest in this data include: (1) increased accuracy with corrected t, (2) reduced standard deviation with Eq. 3.4.1, and (3) correct stiffening trends in each data set from supine to inclined. Though increased accuracy is seen with corrected t, this indicated a sensitivity to t that must be considered. That said, for its sensitivity to measurable, rather than estimated values (*i.e* t versus κ), its reduced standard deviation, and ability to correctly detect trends in stiffening, Eq. 3.4.1 performed best. As such, this equation was used for all future elasticity measurements in

Table 3.4.1: Elasticity equation comparison

E **Method**	**Body Pos.**	**Male 1**	**Male 2**
Eq. 3.4.1	Supine	196.11 (126.92)	178.57 (41.98)
Eq. 3.4.1 corrected t	Supine	39.22 (25.38)	13.095 (3.078)
Eq. 3.4.3	Supine	15.43 (53.80)	14.38 (13.70)
Eq. 3.4.1	Incline	215.44 (59.68)	229.27 (51.06)
Eq. 3.4.1 corrected t	Incline	43.09 (11.94)	16.813 (3.75)
Eq. 3.4.3	Incline	22.28 (22.80)	23.90 (22.40)

proceeding studies. To note, in future work, average t from tested participants (0.0145) was used to calculate α, rather than average t from literature (0.03 m) [24]. This resulted in a change of α from 0.472 (for t = 0.03 m) to 0.117 (for t = 0.0145).

The major assumptions associated with Eq. 3.4.1 are:

- The AW is a homogeneous, incompressible, isotropic, linear elastic material.
  - This assumption has been made in previous work analyzing the elastic response of the AW [24], though, only provides information for the tested strain rate. Due to the viscoelasticity of biological tissues in reality, elasticity may vary with changing strain rates such that a range of strain rates must be tested to provide a more representative series of elasticities for different levels of activation.
  - Due to the anisotropy of soft tissues, the effective modulus divulged from Eq. 3.4.1 only applies to the material properties in the loading direction; the axis orthogonal to the surface of skin.
  - Given the non-linear elastic material properties of human tissues, assuming linear elasticity typically overestimates stresses for a select strain. This yields stiffer absolute elastic moduli resultants than what may exist in reality.
- A frictionless, smooth contact with rim of suction device exists.
  - The proposed boundary conditions of the given problem suggest that there is no tissue slippage at the rim of the suction device. Thus, the tissue within the suction device perimeter is the only material considered. However, in reality, the tissue may slide under the rim due to the applied loading, thereby changing the volume of tissue deformed.

3.4.2 Intra-abdominal Pressure Optimization

Poor responsiveness in IAP measurement in Section 3.2 suggested the need for an optimized equation at varying body positions. This brought upon the consideration of fluid pressure. Fluid pressure (P_{fl}) considers the pressure due to gravity (9.807 m/s^2, g) at a certain depth (h) within a fluid of known density (ρ):

$$P_{\text{fl}} = \rho g h. \tag{3.4.4}$$

In the context of the human abdomen, h is the height of the centroid of the abdomen [183]. As the human body is largely comprised of water, particularly in the abdomen with rates ranging from 60% (reported in connective tissues) to 96% (at the bladder), the density (ρ) of the abdomen was approximated as 997 kg/m^3 [120]. Three major body positions were considered with the addition of fluid pressure: inclined, sitting and standing. Anthropometric data was exploited to standardize the equation across bodies, such that only the height of the body needed to be known.

At an incline of angle α (in rad) at the back, pelvis, and floor, h becomes

$$h_{\text{incline}} = 0.095 H sin(\alpha) \tag{3.4.5}$$

where H is body height (in m) and 0.095 is the height of centroid of the abdomen from the hips [183]. At a sitting position, h becomes

$$h_{\text{sit}} = 0.095 H. \tag{3.4.6}$$

At a standing position, h becomes

$$h_{\text{stand}} = 0.145 H \tag{3.4.7}$$

where 0.145 is the height of the centroid of the abdomen from the symphysis pubis [183]. Combining all equations gives a modified solution for IAP:

$$\begin{aligned} IAP &= P_{\text{in}} + P_{\text{fl}}; \\ IAP &= \frac{P_{\text{app}}(a^2+w^2)({r_2}^2-{r_1}^2)}{4tw({r_1}^2+{r_2}^2)-(a^2+w^2)({r_2}^2-{r_1}^2)} + \rho g h. \end{aligned} \tag{3.4.8}$$

This equation was employed in all future work, noting individual body heights and positions. The major assumptions associated with Eq. 3.4.8 are:

- The AW is a homogeneous, incompressible, isotropic material. The effect of this assumption is briefly discussed in Section 3.4.1.
- A frictionless, smooth contact with rim of suction device exists. The effect of this assumption is briefly discussed in Section 3.4.1.
- Suction yields uniform, lateral loading.
  - Eluded to in Section 3, rather than using the correct loading scenario of uniform pressure, uniform, lateral loading is assumed to simplify equations. As such, results for IAP may be slightly larger than that of the more realistic loading method. Due to the high risk associated with increased IAP, however, it is preferable to test with a greater false positive rate than a negative one.
- The maximum wall stress due to localized suction is equal to the pre-tension in the AW due to IAP.
  - It is imperative to consider this assumption in more dynamic scenarios. Moving from activated to unactivated AW muscles, or even from supine to sitting position, changes the tension in the AW. Thus, the equation must recalibrate for the new loading scenario.
- AWTh is constant when deformed.
  - Though AWTh is important to consider when measuring IAP between individuals, the difference in AWTh created under loading due to the tissue's compressibility is small enough to not have a significant impact on IAP results.
- Pressure in the abdomen is constant throughout, that is, IAP is constant throughout the IAV.
  - As shown in [61], IAP is not a constant value through the IAV. Therefore, though measurement location is recommended to stay consistent (5 cm subxiphoid), clinicians should be aware of the potential IAP range across the IAV, and consider measuring at multiple locations if a patient is borderline hypertensive.

The overall design, as described in Section 3, and underlying algorithm, as optimized in Eq. 3.4.8 and 3.4.1, were documented and submitted in a provisional patent application (No. 63/028,241) as of May 21, 2020. The proceeding PCT, PCT/CA2021/050696, was filed May 21, 2021.

4 Validity and reliability of a non-invasive tool and method to measure soft tissue elasticity *in vivo*

4.1 Framework of Article 2

Following up on the work of Objective 1 (Section 3), the present study explored the reliability, validity, accuracy and responsiveness of the novel system, specifically as an elasticity measurement tool. As such, using existing popularized tools as benchmarks, namely the MyotonPro (a myometer) and IndentoPro (an indenter), the novel tool was tested on 14 (n = 14) living participants to validate its use. Tests were conducted on the abdomen, alongside the posterior superficial calf muscle to exemplify the broader scope to which the novel device applied. The realization of Objective 2 and 3, as well as the investigation of Hypotheses 2 and 3 are presented in the manuscript entitled, "Validity, reliability, and responsiveness of a non-invasive tool and method to measure abdominal and calf muscle elasticity *in vivo*", for which the contribution of the first author is considered to be 85% including ethical approval application, experimental method formulation, data analysis, and manuscript writing. The second author provided research direction and manuscript review, for which the contribution is considered to be 10%. The third author supplied benchmark tooling, initial tool training, and manuscript review, for which the contribution is considered to be 5%. The manuscript was submitted to the *Computers in Biology and Medicine* on September 24, 2021. The work presented, herein, was also presented at the Canadian Society of Biomechanics Conference on May 25, 2021, entitled, "*In vivo* soft tissue elasticity - Measurement reliability and validity via novel suction methodology".

4.2 Article 2: Validity, reliability, and responsiveness of a non-invasive tool and method to measure abdominal and calf muscle elasticity *in vivo*

Natasha Jacobson, P.Eng.[1], Mark Driscoll, Ph.D., P. Eng.[1], Robert Schleip, Ph.D.[2]

Status: Submitted.

1: McGill University, 845 Sherbrooke St. W, Montreal, Quebec, Canada, H3A 0G4

2: Technical University of Munich, Munich 80333, Germany

Address for notification, correspondence and reprints:

Mark Driscoll, Ph.D., P.Eng., Assistant Professor

Associate Member, Biomedical Engineering

Canada NSERC Chair Design Engineering for Interdisciplinary Innovation of Medical Tech.

Department of Mechanical Engineering

817 Sherbrooke St. West, Montreal, QC, H3A 0C3 Canada

T: +1 (514) 398 - 6299

F: +1 (514) 398 – 7365

E-Mail: mark.driscoll@mcgill.ca

4.2.1 Abstract

Though manual palpation remains the simplest and cheapest form of *in vivo* soft tissue evaluation, it is a qualitative and practitioner-dependent method. Thus, quantitative soft tissue elasticity measurement tools are needed. It is the effort of this research to demonstrate the efficacy of a novel aspiration device for *in vivo* soft tissue elasticity measurement at the abdominal wall and posterior calf muscle by confirming reliability, convergent validity, and responsiveness. Using a myometer and indenter as benchmarks, a novel device was evaluated on 14 study participants. On the abdominal wall, low to moderate intra- and inter-rater reliability were found, while excellent intra-rater reliability resulted at the calf. Poor correlation was found between the myometer and novel device at the abdomen, with moderate correlation resulted between novel device against both the myometer and indenter. All results were statistically significant. Of the three devices, only the novel device demonstrated correct responsiveness to changes in anatomical position and elasticities within range of published data. While the novel device shows promising results as a measurement tool for soft tissue elasticity, findings emphasize the need for further research.

4.2.2 Introduction

The measurement of soft tissue elasticity *in vivo* may lead to the improved understanding of physiological biomechanics. That said, existing methods of measurement, such as elastography, ultrasonography, or bioimpedance, are either expensive or unable to measure deep tissue elasticities

[1]. Experts agree that the need for a comprehensive, standardized testing system is necessary to establish benchmarks in tissue mechanics [2]. Among many possible applications for soft tissue elasticity measurement, plausible areas of interest are the abdominal wall (AW) and calf muscles. These muscle groups are often targeted in rehabilitation for treatment and prevention of conditions including low back pain, shin splints, or sprained ankles. For this reason, as well as accessibility for clinical testing, the AW and calf muscles remain the anatomical focal points of the present study.

The AW is an anisotropic, dynamic, composite-laminar material, comprised of a number of soft tissue layers [3]–[6]. Few research groups have studied the *in vivo* (physiological) composite properties of the AW [5], [6]. Song *et al*. found an average (standard deviation, SD) Young's modulus (E) of 42.5 (9) kPa and 22.5 (2.6) kPa transversely and longitudinally, respectively, using motion analysis of the inflated abdomen [5]. Alternatively, Tran *et al*. published stiffness values dependent on tissue thickness, muscle activation and AW position using a combination of ultrasound and motion tracking [6]. Though of use in verifying future studies, Tran *et al*.'s work cannot be directly compared to Song *et al*. due to differences in test methods. However, the work of van Ramshorst *et al*. in 2011 resulted in elasticity values comparable to Song *et al*. [7]. Average E was found to be 44.23 kPa by van Ramshorst *et al*. with an indentometer, a value within 5% of Song *et al*.'s transverse E results [5], [7]. Though similar, van Ramshorst *et al*. assumed their measurements reflected effective modulus, contrary to Song *et al*. who identified the individual longitudinal and transverse elasticities. Given limited studies and inconsistency in test methods, a standardized, *in vivo* soft tissue elasticity measurement system for use on the abdomen is of interest.

The calf muscles, namely the gastrocnemius, are anisotropic, near the skin, with very little fatty tissue surrounding it. This muscle group has been studied at length in varying anatomical positions and physiologies. Of greatest interest in the present research is the elasticity of healthy Gastrocnemius Medialis (MG) and Gastrocnemius Lateralis (LG) in a neutral state, that is, without muscle activation and in a relaxed position (0° flexion). Under these conditions, shear moduli (G) was reported in a series of studies, summarized in Table . It should be noted that G can be converted to Young's moduli by $E = G(2(1+\nu))$ for isotropic materials where ν is Poisson's ratio, typically 0.499 for soft tissues [8]. Despite the anisotropy of the gastrocnemius, the mentioned conversion provides an estimate of Young's modulus to allow for direct comparisons to literature. This conversion gives a historical published range for Young's modulus of 18.59 to 53.42 kPa for the MG and LG; a similar range to that of the AW.

Table 4.2.1: Reported shear moduli (G) of the medial and lateral gastrocnemius. All measurements were taken with shear wave ultrasound elastography with standard deviations reported in brackets, where available.

Medial Gastrocnemius [kPa]	Lateral Gastrocnemius [kPa]	Sample Size	Ref.
12.1 (2.7)	8.5 (1.7)	10 (10 male)	[9]
9.0 (6.0)	6.2 (3.8)	20 (20 male)	[10]
10-15	185	52 (26 male)	[11]
17.82 (2.92)	14.19 (3.28)	20 (14 male)	[12]
13.12 (2.8)	11.45 (2.18)	20 (10 male)	[13]

4.2.2.1 Existing Technologies

Though manual palpation remains the simplest and cheapest form of *in vivo* soft tissue evaluation, it is a qualitative and practitioner-dependent method [14]. Alternatively, static, quantitative measurement systems are wide ranging, and include indentation [15], myometry [3], aspiration [16], and durometry [17]. To measure the mechanical properties of the AW, only indentation, myometry (popularized by the MyotonPro [18]) and aspiration are discussed, as durometers report Shore hardness (resistance to indentation), as opposed to elasticity (a constitutive material property) [19].

Indentation, myometry and aspiration devices use similar theories to determine stiffness (S): a known normal force (F) is applied to a local tissue, and the resulting linear displacement (δ) is measured [20], [21]. In its simplified form, this yields the equation $S = F/\delta$. That said, in the case of the MyotonPro, the popularized myometric method of measurement [22], an impulse, rather than a single, continuous force, is applied to the tissue. As a result, stiffness is measured by $S = (a_{\max} m_{\text{probe}})/\Delta l$, where $a_{\max}$ is the peak acceleration amplitude, m_{probe} is the preload due to the mass of the probe, and Δl is the peak displacement amplitude [18]. However, the MyotonPro outputs a second, dimensionless value: elasticity. This term is defined as the logarithmic decrement of probe acceleration [18], in conflict with the engineering definition for elasticity: resistance to deformation under an applied load [1]. Thus, published values of "elasticity" from studies using the MyotonPro should be evaluated critically.

Though handheld, user-friendly systems are available (ex: MyotonPro [18], IndentoPro [23], Cutometer [24], Nimble [25], Semi-Electronic Tissue Compliance Meter [15]), none of the existing deformation methods can distinguish between tissue layers, or provide insight into deeper fascia [2]. As such, said techniques are only recommended to evaluate superficial, and not deeper, tissues. One of the only non-invasive technologies that proposes direct measurement of deep soft tissue elasticity is that discussed by Jacobson and Driscoll [1], [26]. This system, of radius a, uses suction to induce a displacement in abdominal tissue from which E is calculated. When compared to alternative suction methods for elasticity measurement, a few significant differences emerge: device radii, deformation measurement system, and outputted parameters. With a radius of 3 cm, the Jacobson and Driscoll device is much larger than the 1 to 4 mm radius of the Cutometer or 3 mm radius of the Nimble, thus, permitting an increased suction distance. Further, in the Jacobson and Driscoll device, peak deformation of suctioned tissue is measured with a lidar sensor centered above the tissue. Alternatively, the Cutometer measures suctioned tissue height by measuring light transmission across the pipette, wherein no light transmission indicates the tissue is obstructing the signal. Finally, the Nimble is displacement-controlled, in which tissue is displaced to 0.5 mm with the applied pressure recorded. The last major distinguishing feature of the Jacobson and Driscoll device is its outputted parameter: the constitutive material property, E. Instead, the Cutometer and Nimble output S, a structural property dependant geometry and E. Despite the novelty of the Jacobson and Driscoll device, due to the pilot study's small sample size and lack of direct comparison to benchmark elasticity tools, further research on this method is required.

Given the lack of a "gold standard" measurement technique, it has been suggested to use more than one measurement system for more exhaustive results [2]. That said, consensus has been reached among experts that a comprehensive, standardized, and portable device is still necessary to establish norms in tissue properties [2]. Of interest is the potential of the non-invasive aspiration device developed by Jacobson and Driscoll to fill the market need. Therefore, it is the effort of this research to demonstrate the efficacy of this previously developed novel device for *in vivo* soft tissue elasticity measurement at the AW and posterior calf muscle [26].

4.2.3 Methods

4.2.3.1 Materials

A novel device of radius, a, as proposed in [26], was evaluated for reliability, validity and responsiveness using the following proposed methods. It was compared against the MyotonPro (Myoton AS, Estonia) and a standard indentometer: IndentoPro (Fascia Research Group, Ulm University, Germany). All 3 tested devices are shown in Fig. 4.2.1.

The novel device induces a suction (P_{app}) against the skin from which the resulting tissue

Figure 4.2.1: From left to right: IndentoPro (standard indentometer), MyotonPro (popularized myometer), and novel device.

deformation (w) is measured. Utrasound jelly is used between the device and skin to improve air-tightness and resulting suction. Three suction pulses are applied, from which the average elasticity is calculated. Contrary to the authors' previous work [26], E was determined using the equation for suction [21] to improve responsiveness of the system:

$$E = \frac{\alpha(\zeta,\nu)3\phi(\eta)(P_{\text{atm}} - P_{\text{app}})a}{2\pi w}, \tag{4.2.1}$$

where P_{atm} is atmospheric pressure and $\phi(\eta)$ is a function dependant on pipette radii [27], here, η being 0.1 results in $\phi(0.1)$ of 2.3. The coefficient $\alpha(\zeta,\nu)$ refers to a function dependant on the thickness (t) of the tissue being tested (average of 0.03 m at the abdomen [5], or 0.01 m at the calf [28]) [29]. This is a typical equation for micropipettes, though was used, here, for the tested macropipette [21]. For the tissues of interest, here, assuming ν of 0.499, and adjoined tissue layers, α simplifies to [29]

$$\alpha = 0.9965\frac{(\frac{t}{a})^{2.63}}{1.113 + (\frac{t}{a})^{2.63}}, \tag{4.2.2}$$

or, 0.47 for $t = a = 0.03$ m. At the calf this equates to 0.033 for $t = 0.01$ m, $a = 0.03$ m. Based on a thorough review of available non-invasive soft tissue elasticity measurement devices [1] and prior device study [26], novelty of the present device exists in its new application for Eq. 4.2.1.

The MyotonPro and IndentoPro output stiffness values ($S = F/\delta$) deduced by a probe pushing into the tissue of interest by a given force (F) to a measured distance (δ). To critically com-

pare measurements, stiffnesses collected from the MyotonPro and IndentoPro were converted to Young's modulus (E) using [21]

$$E = \frac{(1-\nu^2)F}{2d\delta}, \tag{4.2.3}$$

where ν is again assumed to be 0.499 [8] and d is the radius of the respective indenter (2 mm for the MyotonPro [18] and 5.5 mm for the IndentoPro [30]).

4.2.3.2 Participants

Fourteen young, healthy participants (n = 14) were recruited, all of whom provided informed consent during the study. Intraclass correlation coefficient (ICC) values ranged from 0.56 to 0.87 for previous soft tissue elasticity studies [15]. Therefore, sample size calculation was determined using Walter *et al*.'s suggested model for ICC values between 0.56 and 0.87 (alpha = 0.05, beta = 0.2), yielding 14 required participants [31].

Inclusion criteria were a body mass index (BMI) less than 25 to reduce abdominal wall thickness (AWTh), and age greater than 18 years old. A reduced AWTh ensured measurements with the novel device deformed deeper tissues including muscle, rather than superficial tissues like adipose layers. Sex was not an exclusion criterion, however, women who were or had previously been pregnant were ineligible. Additional exclusion criteria include a history of abdominal surgery, use of muscle relaxants, acute peritonitis, abdominal mass, acute injury to the urinary bladder, acute cystitis, neurogenic bladder, pelvic hematoma, and pelvic fracture, to match previous studies that measured elasticity at the AW [7].

Ethical approval for this study was received from a university's International Review Board prior to participant recruitment (study number A12-M63-19A).

4.2.3.3 Procedure (Abdominal Wall)

Prior to to elasticity analysis, participant anthropometrics were recorded, including abdominal and hip circumference, taken at the navel and widest part of the hips, respectively. AWTh was also measured 5 cm subxiphoid by two raters using a linear ultrasound probe and averaged. These geometric markers allowed correlation to elasticity to be divulged.

All devices were used 5 cm subxiphoid, as suggested by van Ramshorst *et al*. [7]. (1) Reliability (intra-, inter-) and (2) validity studies were completed based on GRRAS (Guidelines for Reporting Reliability and Agreement Studies) and work by Wilke *et al*. [15], [32]. An (3) external responsiveness study was further completed as suggested by Husted *et al*. [33].

(1) Two measurements (M1a and M2a) for elasticity were taken with the novel device on study participants in the supine position, at end-expiration, and without abdominal activation

(intra-rater reliability). A second researcher repeated the measurement (M3a) immediately after M2a (inter-rater reliability). Test locations were noted with an indelible marker for repeatability.

(2) After a 10-minute washout period, a final two measurements were taken using the MyotonPro (M4a), and the IndentoPro (M5a). The order of device trials was randomly determined.

(3) Following the same order of events, the entire procedure was immediately repeated with patients at (b) a head tilt of 25°, (c) sitting, and (d) standing, resulting in 15 additional measurements denoted as M1b-d through M5b-d.

4.2.3.4 Procedure (Calf Muscle)

Juxtaposing AW tests, the calf muscle was tested to evaluate the function of the devices in a different muscle group. All devices were used at the widest portion of the posterior calf muscle. Participants were asked to lie prone, with feet hanging off the edge of the bed in a relaxed state. No muscle activation occurred. (1) Reliability (intra-) and (2) validity studies were completed based on GRRAS and work by Wilke *et al*. [15], [32].

(1) Two measurements (CM1 and CM2) for elasticity were taken with the novel device on study participants, with one on each leg (intra-rater reliability). Test locations were noted with an indelible marker for repeatability.

(2) A final four measurements (two on each leg) were taken using the MyotonPro (CM3, CM4) and the IndentoPro (CM5, CM6). The order of device trials was randomly determined.

Figure 4.2.2 illustrates the procedure of Part 1 and Part 2.

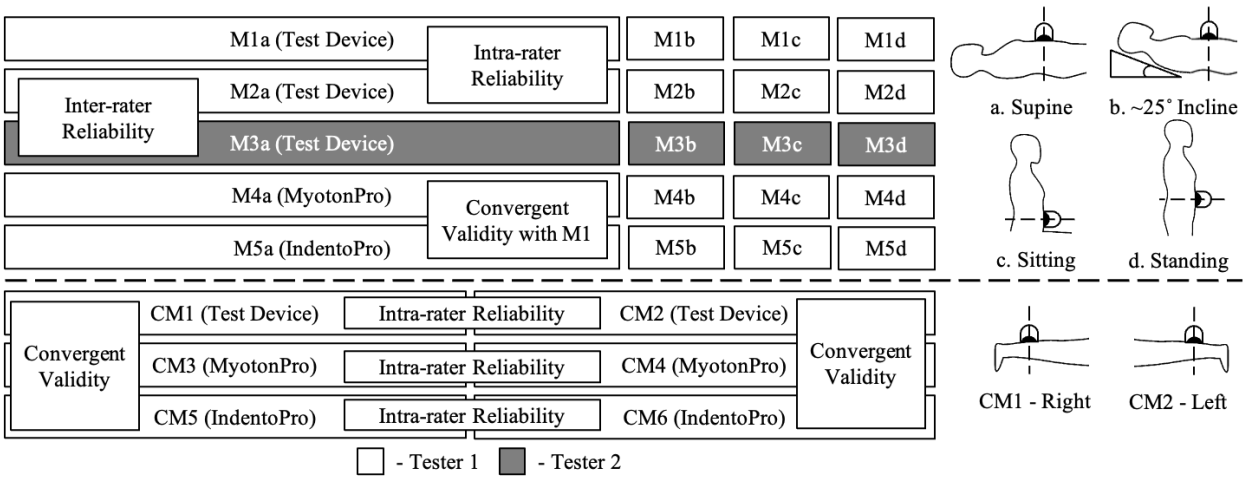

Figure 4.2.2: Illustrated procedure for Part 1 and 2 of the present study. Tested anatomical position are pictured, left: a. Supine, b. Inclined, c. Sitting, d. Standing, CM1 Right Leg, CM2 Left Leg.

4.2.3.5 Statistical Analyses

The study followed a crossover design of devices with a Bland-Altman analysis. Given this, the carryover effect or effect of one device against the other, was of concern. That said, washout periods like those previously reported existed to reduce error [15]. Normality was evaluated with a Shapiro-Wilk test and indicated normal distributions for MyotonPro (M4, CM3, CM5) and IndentoPro (M5, CM4, CM6) results, as well as calf measurements (CM1, CM2), however, novel device results at the abdomen (M1, M2, M3) presented with non-normal distributions.

As the objective was to determine whether the intra- and inter-rater reliability (M1, M2, M3) of the device exceeds a Spearman's rho (ρ_s) of 0.7 (rule of thumb for "high" correlation [34]), the Null hypothesis (H_0) was defined as r_s less than 0.7. As r_s only describes the degree of linear correlation between two variables, Bland-Altman was also considered to evaluate the absolute agreement (or, bias). H_0 greater than 1 mmHg was defined for said bias. Together, r_s and bias may confirm device reliability. Convergent validity was evaluated, similarly, between devices (M1, M4, M5), using r_s, where r_s greater than 0.7 is deemed "high" correlation [34]. Just as with reliability, Bland-Altman plots are also used to confirm agreement, or bias, between devices.

For normally distributed data (CM1 through CM6), intra-rater reliability was evaluated using ICC, for which H_0 was defined as an ICC less than 0.75 (rule of thumb for "good" correlation) [35]. ICC estimates were based on a 95% confidence interval and were calculated based on a single rating (1), absolute agreement, two-way mixed effects model (model 2, 1) [35]. Also evaluated were the Minimum Detectable Change (MDC) and Standard Error of Measurement (SEM) based on r_s for intra-rater reliability. MDC% refers to the ratio of MDC to the data mean [36]. Convergent validity for Part 2 was evaluated, similarly, between devices (CM1, CM3, CM5), using Pearson correlation (r), where r greater than 0.7 is deemed "high" correlation [34]. Just as with reliability, Bland-Altman plots were also used to confirm agreement, or bias, between devices.

Internal responsiveness of the system was evaluated at varying body positions to gauge the ability of all three device to detect change. Responsiveness was calculated using Effect Size (ES) and Standardized Response Mean (SRM), as suggested in previous studies [33], [37]. ES values of 0.2, 0.5 and 0.8 attribute to small, moderate, and high responsiveness, respectively [33].

4.2.4 Results

Fourteen participants (n = 14) were recruited, with physiological details outlined in Table 4.2.2. Despite increased BMIs in five participants, recruitment proceeded to determine whether said participants presented as outliers in the data or defended the use of the novel device in wider BMI ranges than originally hypothesized. Results were within acceptable ranges, therefore, data remained. During prolonged use, the device microcontroller (ESP32, SparkFun, USA) stopped

relaying data, unexpectedly. Due to these technical difficulties, measurements for the superficial posterior calf muscle (the final measurement set during in-person studies) were only collected in 10 of the 14 participants.

Table 4.2.2: Summary of participant descriptions (C: circumference; AWTh: abdominal wall thickness)

ID	Age [years]	Height [cm]	Weight [kg]	BMI [kg/m^2]	Gender	Abd. C [cm]	Hip C [cm]	AWTh [cm]	Left Calf C [cm]	Right Calf C [cm]
01	26	184	83.46	24.7	M	91	105	2.2	36	37
02	31	167.5	66.50	23.7	F	90	107	1.75	N/A	N/A
03	30	185	81.30	23.8	M	85.5	102.5	1.375	37	36
04	33	179	85.37	26.6	M	98	108	1.8	37	37
05	25	166.5	71.57	25.8	M	87.5	103	1.575	37	37
06	24	161.5	48.50	18.6	F	66.5	88	0.75	N/A	N/A
07	25	172	66.20	22.4	F	80	103	1.525	37	37.5
08	27	184.5	90.00	26.4	M	98	108	1.8	40.5	40.5
09	24	193	104.20	28.0	M	103.5	115	1.125	41	41.5
10	30	169	58.50	20.5	F	75.5	83	0.95	33.5	34
11	28	182.5	89.80	27.0	M	99.5	109.5	2.5	38	38.5
12	29	166.5	65.20	23.5	F	76	100.5	0.675	N/A	N/A
13	28	175	59.00	19.3	F	75	93	1.25	33.5	33
14	27	164.5	60.42	22.3	F	74	92.5	1.05	34	34.5

Measurement details for E of the AW and posterior calf are compiled in Tables 4.2.3 and 4.2.4, respectively. To note, elasticities of the novel device were calculated using Eq. 4.2.1, while elasticities of the MyotonPro and IndentoPro were calculated using Eq. 4.2.3. All elasticities represent the effective modulus of the corresponding material. Historically published ranges are appended to tables as a benchmark from which measured data can be compared.

Table 4.2.3: Summary of average effective modulus 5 cm subxiphoid on participants (n = 14). Published ranges are indicated as benchmarks. (SD: standard deviation)

Device	Supine [kPa] (SD)	Incline [kPa] (SD)	Sit [kPa] (SD)	Stand [kPa] (SD)
Novel Device	25.34 (10.68)	25.53 (11.00)	27.20 (6.55)	29.42 (7.28)
MyotonPro	49.67 (8.38)	46.34 (7.31)	45.63 (11.54)	48.38 (11.90)
IndentoPro	81.00 (16.13)	71.32 (23.68)	59.03 (20.03)	66.89 (17.88)
Historical Data	Supine: 5-22.5 kPa longitudinally; 15-42.5 kPa transversely [24, 26]			

Table 4.2.4: Summary of average effective modulus of the superficial posterior calf muscle on participants (n = 10). Historically published ranges are indicated as benchmarks. (SD: standard deviation)

Device	Left Leg [kPa] (SD)	Right Leg [kPa] (SD)
Novel Device	16.98 (7.77)	20.40 (11.12)
MyotonPro	53.76 (13.07)	52.99 (12.55)
IndentoPro	73.95 (16.98)	76.08 (20.66)
Historical Data	18.59 to 53.42 kPa for the gastrocnemius [5, 17, 22, 32-33]	

4.2.4.1 Reliability

Intra-rater reliability was considered between M1 and M2, while inter-rater reliability was considered between M2 and M3. Intra-rater r_s was 0.317 ($p < 0.05$) (n = 52), indicating low positive correlation. Bias (mean and standard deviation, SD) between M1 and M2 was 1.4 (10.8) kPa. Similarly, inter-rater r_s was 0.558 ($p < 0.05$) (n = 49), indicating low positive correlation. Bias between M2 and M3 was 0.9 (11.1) kPa.

At the calf muscle, intra-rater reliability was considered between the left and right leg (CM1 and CM2). Intra-rater ICC (mean and 95% confidence interval bounds: upper, lower, respectively) was 0.80 (0.344, 0.941) (n = 12), indicating good reliability [35]. Comparatively, the intra-rater ICC of the MyotonPro (CM3 and CM4) and IndentoPro (CM5 and CM6) was 0.896 (0.655, 0.968) (n = 13) and 0.894 (0.657, 0.968) (n = 13), respectively, both of which indicate excellent positive correlation.

Reliability results from the AW and calf muscle are summarized in Table 4.2.5.

Table 4.2.5: Reliability results summary by Spearman's rho (r_s) and Bland-Altman bias [kPa] for the abdomen 5 cm subxiphoid, and intraclass correlation (ICC) for the superficial posterior calf. 95% confidence interval bounds denoted in brackets (upper, lower) for ICC. Minimum detectable change (MDC) and Standard Error of the Mean (SEM) are also reported.

	Abdomen – Novel (r_s, Bias [kPa])	Calf – Novel (ICC)	Calf – MyotonPro (ICC)	Calf - IndentoPro (ICC)
Intra-rater	0.317, 1.4	0.80 (0.344, 0.941)	0.896 (0.655, 0.968)	0.894 (0.657, 0.968)
Inter-rater	0.558, 0.9	N/A	N/A	N/A
SEM [kPa]	6.69	4.24	4.05	6.04
MDC [kPa]	18.54	11.76	11.23	16.75
MDC %	73%	63%	21%	22%

4.2.4.2 Validity

Spearman rho between M1 and M4 (MyotonPro) was 0.338 ($p < 0.05$) indicating low positive correlation. Results for correlation against M5 (IndentoPro) were inconclusive and require additional test subjects to evaluate critically. Similarly, the MyotonPro and IndentoPro demonstrated low positive correlation, as suggested by an r_s value of 0.412 ($p < 0.05$).

At the calf muscle, Pearson correlation between CM1 and the control devices was 0.481 ($p < 0.2$) and 0.623 ($p < 0.05$) for the MyotonPro (CM3) and IndentoPro (CM5), respectively (n = 12). Said r values indicated low to moderate positive correlation for the MyotonPro and IndentoPro, respectively. Conversely, the MyotonPro and IndentoPro demonstrated high positive correlation, as suggested by an r value of 0.850 ($p < 0.001$) (n = 13).

Validity results from the AW and calf muscle are summarized in Table 4.2.6. Validity is illustrated in Bland-Altman plots for the MyotonPro and IndentoPro against the novel device at the abdomen in Fig. 4.2.3.

Table 4.2.6: Convergent validity results summary by Spearman's rho (r_s) for the abdomen and Pearson correlation (r) for the superficial posterior calf.

r	**MyotonPro**	**IndentoPro**
Novel Device – Abdomen (r_s)	0.338 ($p < 0.05$)	N/A
Novel Device – Calf (r)	0.481 ($p < 0.2$)	0.623 ($p < 0.05$)
MyotonPro – Abdomen (r_s)	N/A	0.412 ($p < 0.05$)
MyotonPro – Calf (r)	N/A	0.850 ($p < 0.001$)

4.2.4.3 Responsiveness

ES and SRM of each device at the varying body transitions are listed in Table 4.2.7. Of note are the negative trends in each device (shaded cells), as well as the peak ES/SRM from supine to standing by the novel device. Negative trends indicated the opposite expected change, that is, a decrease in elasticity with increasing body erectness. Alternatively, peak ES/SRM indicates the most significant positive difference in elasticity with increasing body erectness, suggesting the preferred body transition to test responsiveness of the system in the future.

Of the three devices, only the novel device exhibited consistent trends of stiffening (increasing E) with increasing head position with respect to the hips. This trend is illustrated in Fig. 4.2.4.

4.2.5 Discussion

A novel device was tested to evaluate its reliability, validity and responsiveness against existing popularized measurement methods with respect to soft tissue elasticity, specifically at the

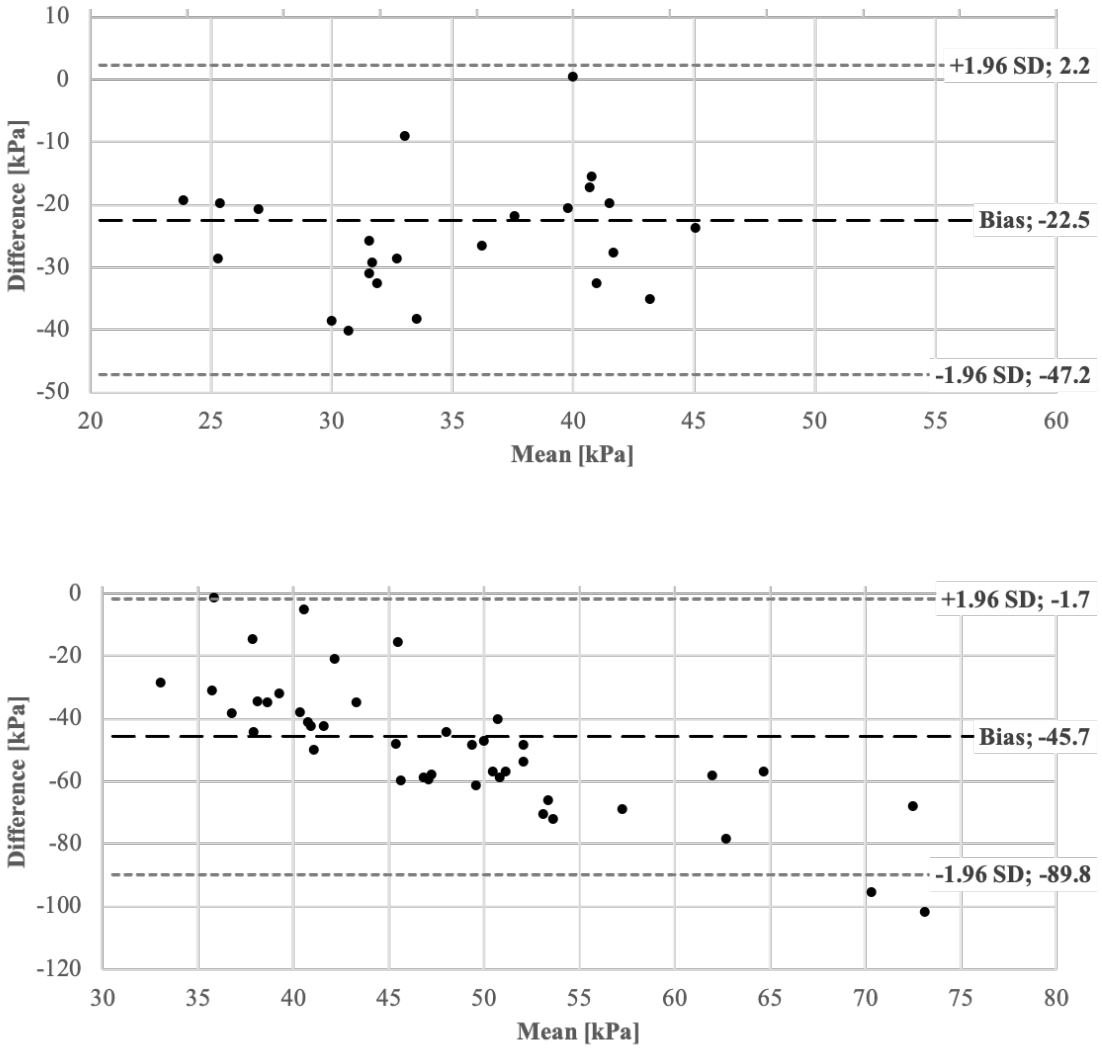

Figure 4.2.3: Bland-Altman plots for the novel device versus the MyotonPro (above) and IndentoPro (below) at the abdomen. Upper and lower dotted bounds at +1.96 SD, -1.96 SD, respectively. Center dashed line denotes the mean difference, or bias.

abdomen and posterior calf. Results indicated low and high intra-rater reliability at the abdomen and calf, respectively, and low and moderate convergent validity of the novel device at the abdomen and calf, respectively. However, accuracy and responsiveness of the novel device surpass that of the MyotonPro and IndentoPro, suggesting device improvement over existing tools.

The results of this study describe only the two testers, herein, and a small sample of homogeneous participants. This limitation narrows the focus of this paper and only permits restricted conclusions to be reached. Nevertheless, given the inherent positivity of results, it is recommended to pursue a multi-center study to widen the scope of the novel device's use and application.

Table 4.2.7: Effect size (ES) and standardized response mean (SRM) of the novel device, MyotonPro, and IndentoPro at each body transition. Shaded areas highlight negative effects.

Body Transition	Novel Device		MyotonPro		IndentoPro	
	ES	SRM	ES	SRM	ES	SRM
Supine – Incline	0.884	0.266	-0.398	-0.588	-0.600	-0.660
Supine – Sit	0.543	0.249	-0.187	-0.206	-0.952	-0.793
Supine – Stand	0.857	0.491	0.142	0.125	-0.464	-0.411
Incline – Sit	-0.102	-0.102	0.217	0.250	-0.291	-0.277
Incline – Stand	-0.008	-0.007	0.593	0.517	0.041	0.045
Sit – Stand	0.234	0.167	0.238	0.579	0.388	0.364

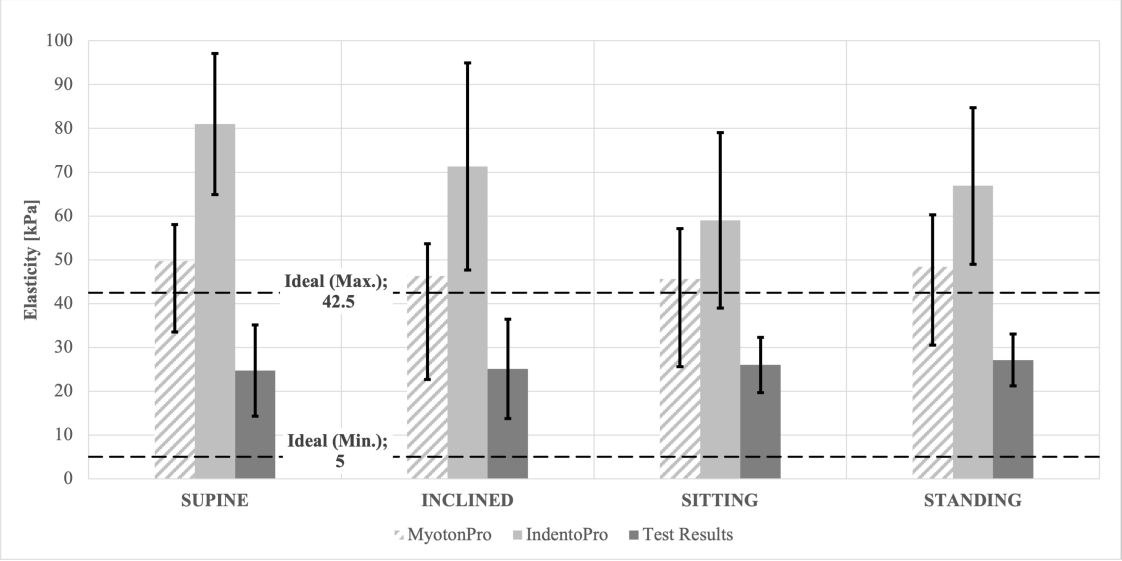

Figure 4.2.4: Average abdominal elasticity changes given change in body position, from supine, 25° incline, sitting, to standing. All three tested devices are denoted: Novel device, MyotonPro and IndentoPro. Bounds from published data are shown by dashed lines for the ideal minimum and maximum elasticities.

Though statistical conclusions suggest an unreliable and invalid novel system, the question remains whether it is a "bad" alternative to existing popularized methods. The abdomen is not conducive to repeatable elasticity testing as intrinsic sources of error exist, including passive or active abdominal activation and irregular breathing patterns. Both sources of error were reduced by asking participants to perform long exhales, and relax their abdomens, however, measurements may have been taken at early inhalation rather than late exhalation, or during a reflex abdominal activation by the participant. Further, tissue has been shown to stiffen with applied suction, that is, not relax to its original elasticity immediately after pressure release. This trend was evident across M1 to M3; measurements that were taken immediately after one another. That said, the MyotonPro has been tested on the abdomen, in in a 2020 study by Gilbert's research group, and demonstrated

high to excellent inter- and intra-rater reliabilities [38]. However, this previous test occurred on the lower abdomen, and may not speak to the reliability of the MyotonPro 5 cm subxiphoid along the linea alba, as done in the present study. When tested on the calf muscle, intra-rater reliability of the novel device increased to 0.80 (0.344, 0.941) ($n = 12$), indicating moderate reliability [35]. This improvement indicates the feasibility of the device in alternative muscle groups. Advancements in device training and circuitry may increase reliability, further.

It has been shown that core muscles activate significantly when moving from a supine to standing body position [39]. As muscles activate, they stiffen, thus leading to the conclusion that the AW should exhibit increased stiffness given increased body erectness. However, only the novel device supported this theory. The MyotonPro and IndentoPro did not exhibit correct and consistent responsiveness to changes in body position. In fact, the novel device exhibited the peak ES/SRM from supine to standing position with 0.857/0.491, contrary to the MyotonPro and IndentoPro that demonstrated 0.142/0.125 and -0.464/-0.411, respectively. One possible reason for the limited responsiveness of the MyotonPro and IndentoPro is the limited depth of indentation. The MyotonPro indents tissue to around 0.5 mm, while the IndentoPro indented to 5 mm at the calf muscle, and 10 mm at the AW [18], [30]. With indentation only reaching superficial tissues, particularly skin, little change in elasticity with changing body position is an expected result. Regardless, this theory emphasizes the limited scope of tissue elasticity measurement with the MyotonPro and IndentoPro, strengthening the argument for future research on the novel device. In subsequent investigations, however, what should be noted is the limited time delay between novel device measurement sets. In the present study, delays were between 1 and 2 minutes, which may have resulted in inherently higher stiffnesses due to the effect of suction [21]. During a measurement, three suction pulses were taken and averaged. If each pulse was compared, in nearly every measurement set, it was noted that stiffnesses increased between each average pulse. This trend may have continued between M1, M2, etc. resulting in the higher ES/SRM values noted, here. Regardless, recommendations for future research include longer delays between measurement sets, along with sustained suctions to evaluate elasticity over longer periods of time.

Published values for the AW have shown passive abdominal elasticity to be on the order of 5-10 kPa and 22.5 kPa longitudinally and 15-25 kPa and 42.5 kPa transversely [5], [6]. In the present study, at supine position, averaged results were 25.71 kPa, 49.67 kPa, and 81.0 kPa for the novel device, MyotonPro and IndentoPro, respectively. At the calf, published Young's moduli range from 18.59 to 53.42 kPa for the MG and LG [9]–[13]. In this scenario, the novel device and MyotonPro exhibited average elasticities at the bounds of historic data, with averages of 18.69 kPa and 53.37 kPa, respectively, between the two legs. The IndentoPro averaged results beyond the

given bounds, averaging 75.57 kPa. Therefore, of the three tested devices, only the novel device measured elasticities closest to published results at both anatomical positions. This demonstrates a higher reproduceability of the novel device when compared to existing methods of measurement. Additionally, participant 13 noted an anterior cruciate ligament repair surgery had been completed within the last 12 months on the right leg. Given recovery time, gastrocnemius atrophy in the recovering leg was a proposed hypothesis in this participant, yielding a lower elasticity in the right leg than the left. Of the three devices, only the novel device noted a significant difference in E between the left and right leg of this participant, measuring 15.20 kPa and 10.73 kPa in each, respectively. The MyotonPro measured 48.19 kPa and 46.31 kPa in the left and right, respectively, while the IndentoPro measured the opposite trend, with 52.58 kPa and 61.34 kPa in the left and right leg, respectively. This evidence supports the responsiveness of the novel device and the need for additional research at varying anatomical locations. However, as previously noted, due to their limited indentation depth, the MyotonPro and IndentoPro may have only yielded elasticities of the most superficial tissues, namely, skin. Despite this distinction, skin elasticity of the AW and calf have historically been recorded around 9 kPa, a value smaller than that of the composite wall tissues [40]. As such, the same conclusion stands, suggesting an improvement in elasticity repeatability with the novel device over benchmark tools.

Finally, correlation of elasticities to AWTh and AVI were considered. Insignificant r_s was found in both instances, leading to the conclusion that AW elasticity cannot be extrapolated from geometric data.

In summary, a novel device was tested for reliability and convergent validity against the MyotonPro and IndentoPro for abdominal and muscle (gastrocnemius) elasticity measurement. The MyotonPro and IndentoPro demonstrated better reliability when compared to the novel device, however, were unresponsive to changes in body position for abdominal elasticity, and were unable to reproduce values within the bounds of published data. The ability of the novel device to detect changes in body position and relative reading reproduceability suggest a promising tool for the measurement of deep, soft tissue elasticity.

4.2.6 Acknowledgment

The authors would like to acknowledge Mr. Trevor Cotter for his time and commitment to developing the prototype and conducting clinical studies, and Mr. Lorne Beckman for his contributions in study development.

This study was funded by grant RGPIN-2017-04037 from the Natural Sciences and Engineering Research Council of Canada (NSERC).

Bibliography

[1] N. Jacobson and M. Driscoll, "Mechanical deformation-based assessment methods," in *Fascia: The Tensional Network of the Human Body*, 2nd ed., ISBN: 978-070-207-1836-0 In Press, Elsevier, 2021, ch. 6.4, pp. 1–10.

[2] M. Zugel, C. Maganaris, J. Wilke, K. Jurkat-Rott, W. Klingler, S. Wearing, T. Findley, M. Barbe, J. Steinacker, A. Vleeming, W. Bloch, R. Schleip, and P. Hodges, "Fascial tissue research in sports medicine: From molecules to tissue adaptation, injury and diagnostics: Consensus statement," *British Journal of Sports Medicine*, vol. 52, pp. 1–9, 2018.

[3] S. Brown, "Mechanically relevant consequences of the composite laminate-like design of the abdominal wall muscles and connective tissues," *Medical Engineering and Physics*, vol. 34, pp. 521–523, 2012.

[4] D. Ott, "Abdominal compliance and laparoscopy: A review," *Journal of the Society of Laparoendoscopic Surgeons*, vol. 23, no. 1, pp. 1–5, 2019.

[5] C. Song, A. Alijani, T. Frank, G. Hanna, and A. Cuschieri, "Mechanical properties of the human abdominal wall measured *in vivo* during insufflation for laparoscopic surgery," *Surgical Endoscopy and Other Interventional Techniques*, vol. 20, no. 6, pp. 987–990, 2006.

[6] D. Tran, F. Podwojewski, P. Beillas, M. Ottenio, D. Voirin, F. Turquier, and D. Mitton, "Abdominal wall muscle elasticity and abdomen local stiffness on healthy volunteers during various physiological activities," *Journal of the Mechanical Behavior of Biomedical Materials*, vol. 60, pp. 451–459, 2016.

[7] G. Van Ramshorst, M. Salih, W. Hop, O. Van Waes, G. Kleinrensink, R. Goossens, and J. Lange, "Noninvasive assessment of intra-abdominal pressure by measurement of abdominal wall tension," *Journal of Surgical Research*, vol. 171, no. 1, pp. 240–244, 2011.

[8] R. Miller, A. Kolipaka, M. Nash, and A. Young, "Relative identifiability of anisotropic properties from magnetic resonance elastography," *NMR in Biomedicine*, vol. 31, pp. 1–12, 2018.

[9] J. Saeki, M. Nakamura, S. Nakao, K. Fujita, K. Yanase, and N. Ichihashi, "Muscle stiffness of posterior lower leg in runners with a history of medial tibial stress syndrome," *Scandinavian Journal of Medical Science in Sport*, vol. 28, no. 1, pp. 246–251, 2018.

[10] S. Ohya, M. Nakamura, T. Aoki, D. Suzuki, T. Kikumoto, E. Nakamura, W. Ito, R. Hirabayashi, T. Takabayashi, and M. Edama, "The effect of a running task on muscle shear elastic modulus of posterior lower leg," *Journal of Foot and Ankle Research*, vol. 10, no. 56, pp. 246–251, 2017.

[11] K. Chino and H. Takahashi, "Measurement of gastrocnemius muscle elasticity by shear wave elastography: association with passive ankle joint stiffness and sex differences," *European Journal of Physiology*, vol. 116, no. 4, pp. 823–830, 2016.

[12] J. Zhou, J. Yu, C. Liu, C. Tang, and Z. Zhang, "Regional elastic properties of the Achilles tendon is heterogeneously influenced by individual muscle of the gastrocnemius," *Applied Bionics and Biomechanics*, vol. 2019, pp. 1–10, 2019.

[13] J. Zhou, J. Yu, Y. Feng, C. Liu, P. Su, S. Shen, and Z. Zhang, "Modulation in the elastic properties of gastrocnemius muscle heads in individuals with plantar fasciitis and its relationship with pain," *Nature Scientific Reports*, vol. 10, no. 2770, pp. 1–8, 2020.

[14] L. Chaitow, P. Coughlin, T. Findley, and T. Myers, "Fascial palpation," in *Fascia: The Tensional Network of the Human Body*, R. Schleip, T. Findley, and P. Huijing, Eds., 1st ed., Elsevier, 2012, ch. 6.2, pp. 269–277.

[15] J. Wilke, L. Vogt, T. Pfarr, and W. Banzer, "Reliability and validity of a semi-electronic tissue compliance meter to assess muscle stiffness," *Journal of Back and Musculoskeletal Rehabilitation*, vol. 31, no. 5, pp. 991–997, 2018.

[16] G. Tarsi, R. Gould, J. Chung, A. Xu, A. Bozkurt, and J. Butcher, "Method for non-optical quantification of in situ local soft tissue biomechanics," *Journal of Biomechanics*, vol. 46, no. 11, pp. 1938–1942, 2013.

[17] P. Sahoo, "Tribology Measurements," in *Mechanical Engineers Handbook: Materials and Engineering Mechanics*, M. Kutz, Ed., John Wiley and Sons, 2015, pp. 837–860.

[18] A. Peipsi, R. Kerpe, H. Jager, S. Soeder, C. Gordon, and R. Schleip, "Myoton Pro: A novel tool for the assessment of mechanical properties of fascial tissues," *Journal of Bodywork and Movement Therapies*, vol. 16, no. 4, p. 527, 2012.

[19] K. Ramalingam, *Handbook of Mechanical Engineering Terms*. New Age International Ltd., 2009.

[20] Y. Feng, Y. Li, C. Liu, and Z. Zhang, "Assessing the elastic properties of skeletal muscle and tendon using shearwave ultrasound elastography and MyotonPRO," *Nature: Scientific Reports*, vol. 8, pp. 1–9, 2018.

[21] Y. Zheng and Y. Huang, *Measurement of Soft Tissue Elasticity in Vivo: Techniques and Applications*. Taylor and Francis Group, 2016.

[22] S. Agyapong-Badu, M. Warner, D. Samuel, and M. Stokes, "Practical considerations for standardized recording of muscle mechanical properties using a myometric device: Recording site, muscle length, state of contraction and prior activity," *Journal of Musculoskeletal Research*, vol. 21, no. 2, pp. 1–13, 2018.

[23] G. Wernicke, R. Rosenblatt, M. Rasca, P. Parhar, P. Christos, A. Fischer, B. Parashar, and D. Nori, "Quantitative assessment of radiation-induced fibrosis of the breast with tissue compliance meter, palpation, and radiological imaging: Preliminary results," *Breast Journal*, vol. 15, no. 6, pp. 583–592, 2009.

[24] L. Draaijers, Y. Botman, F. Tempelman, R. Kreis, E. Middelkoop, and P. Van Zuijlen, "Skin elasticity meter or subjective evaluation in scars: A reliability assessment," *Burns*, vol. 30, pp. 109–114, 2004.

[25] B. Muller, J. Elrod, M. Pensalfini, R. Hopf, O. Distler, C. Schiestl, and E. Mazza, "A novel ultra-light suction device for mechanical characterization of skin," *PLOS ONE1*, vol. 13, no. 8, pp. 1–22, 2018.

[26] N. Jacobson and M. Driscoll, "Design Synthesis and Preliminary Evaluation of a Novel Tool to Non-Invasively Characterize Pressurized, Physiological Vessels," *Journal of Medical Devices*, vol. 15, no. 2, pp. 1–7, 2020.

[27] D. Theret, M. Levesque, M. Sato, R. Nerem, and L. Wheeler, "The application of a homogeneous half-space model in the analysis of endothelial cell micropipette measurements," *Journal of Biomechanical Engineering*, vol. 110, no. 3, pp. 190–199, 1988.

[28] M. Kuyumcu, M. Halil, O. Kara, B. Cunib, G. Caglayan, S. Guven, Y. Yesil, G. Arik, B. Yavuz, M. Cankurtaran, and L. Ozcakar, "Ultrasonographic evaluation of the calf muscle mass and architecture in elderly patients with and without sarcopenia," *Archives of Gerentology and Geriatrics*, vol. 65, pp. 218–224, 2016.

[29] T. Boudou, J. Ohayon, Y. Arntz, G. Finet, C. Picart, and P. Tracqui, "An extended modeling of the micropipette aspiration experiment for the characterization of the Young's modulus and Poisson's ratio of adherent thin biological samples: Numerical and experimental studies," *Journal of Biomechanical Engineering*, vol. 39, no. 9, pp. 1677–1685, 2006.

[30] A. Kett and F. Sichting, "Sedentary behaviour at work increases muscle stiffness of the back: Why roller massage has potential as an active break intervention," *Applied Ergonomics*, vol. 82, pp. 1–6, 2020.

[31] S. Walter, M. Eliasziw, and A. Donner, "Sample size and optimal designs for reliability studies," *Statistics in Medicine*, vol. 17, pp. 101–110, 1998.

[32] J. Kottner, S. Brorson, A. Donner, and B. Gajewski, "Guidelines for reporting reliability and agreement studies (GRRAS) were proposed," *Journal of Clinical Epidemiology*, vol. 64, no. 1, pp. 96–106, 2011.

[33] J. Husted, R. Cook, V. Farewell, and D. Gladman, "Methods for assessing responsiveness: a critical review and recommendations," *Journal of Clinical Epidemiology*, vol. 53, no. 5, pp. 459–468, 2000.

[34] M. Mukaka, "Statistics corner: A guide to appropriate use of correlation coefficient in medical research," *Malawi Medical Journal*, vol. 24, no. 3, pp. 69–71, 2012.

[35] T. Koo and M. Li, "A guideline of selecting and reporting intraclass correlation coefficients for reliability research," *Journal of Chiropractic Medicine*, vol. 15, no. 2, pp. 155–163, 2016.

[36] P. Lee, C. Liu, C. Fan, C. Lu, W. Lu, and C. Hsieh, "The test-retest reliability and the minimal detectable change of the Purdue pegboard test in schizophrenia," *Journal of the Formosan Medical Association*, vol. 112, no. 6, pp. 332–337, 2013.

[37] F. Angst, M. Verra, S. Lehmann, and A. Aeschlimann, "Responsiveness of five condition-specific and generic outcome assessment instruments for chronic pain," *BMC Medical Research Methodology*, vol. 8, no. 26, pp. 1–8, 2008.

[38] I. Gilbert, N. Gaudreault, and I. Gaboury, "Intra- and inter-evaluator reliability of the MyotonPRO for the assessment of the viscoelastic properties of caesarean section scar and unscarred skin," *Skin Research and Technology*, 2020.

[39] D. Chmielewska, M. Stania, G. Sobota, K. Kwasna, E. Blaszczak, J. Taradaj, and G. Juras, "Impact of different body positions on bioelectrical activity of the pelvic floor muscles in nulliparous continent women," *Biomedical Research International*, vol. 2015, pp. 1–9, 2015.

[40] Y. Yang, L. Wang, F. Yan, X. Xiang, Y. Tang, L. Zhang, J. Liu, and L. Qiu, "Determination of normal skin elasticity by using real-time shear wave elastography," *Journal of Ultrasound in Medicine*, vol. 37, no. 11, pp. 2507–2516, 2018.

4.3 Additional Related Study: Flash cupping and its effect on soft tissue elasticity

Following up on the work of Objective 1 and 2 (Section 3 and 4, respectively), the present study exploited the novel system specifically as an elasticity measurement tool. Both immediate (within 30 s) and short-term (within 1 and 3 min.) effects of suction were analyzed. Tests were conducted on the abdomen, alongside the posterior superficial calf muscle. Results are presented in the manuscript entitled, "Flash cupping and its effect on soft tissue elasticity", for which the contribution of the first author is considered to be 85%. The extended conference paper was submitted to the *Canadian Medical and Biological Engineering Society* 2021 Conference on January 29, 2021 and presented May 12, 2021.

4.3.1 Conference Paper

Cupping therapy is a growing treatment option for myofascial pain, however, the effects of suction on deeper tissues' elasticity has not been well documented. As such, elasticity was derived using a novel device that employs a flash cupping technique to resect deeper fascia. Fourteen participants were recruited and tested with the device 5 cm subxiphoid on the abdomen and posterior calf muscle. Of results at the abdomen, 88% indicated immediate (within 30 s) increase in tissue compliance. At the calf, 64% of results indicated immediate increase in elasticity. In the short-term (1-3 min.), stiffening occurred in 64% of results at the abdomen. Given results, it is of interest to consider the long-term effects of dry cupping on soft tissue elasticity to determine potential mechanical benefits of localized suction. The presented evidence of dynamic changes in elasticity may lend insight into the causes and treatment effects of myofascial pain.

To the author's knowledge, there exists no biomechanical studies on the effects of suction on deeper tissue elasticity. Previous studies that objectively evaluated elasticity changes due to suction only used palpation or the Cutometer (a superficial tissue elasticity tool) to evaluate changes [166]. One study noted the separation of deep tissue layers via MRI during suction, though, elasticity was not mentioned [167]. Therefore, it is the effort of the present research to exploit a novel tool in soft tissue mechanics measurement for the evaluation of the effect of suction on deeper fascia.

A novel device of radius, a, was used as a flash cupping method to evaluate elasticity changes in soft tissue. Flash cupping refers to pulsating applied suction (pressure held less than 30 s), on healthy skin to induce a tissue deformation (w). Typical applied suction is light; between 10 and 30 kPa (100-300 mbar). In the present study, suction (P_{app}) was applied and immediately released, at pressures between 2 and 4 kPa per impulse. E was determined by Eq. 3.4.1:

$$E = \frac{\alpha(\zeta,\nu)3\phi(\eta)(P_{\text{atm}} - P_{\text{app}})a}{2\pi w}. \tag{4.3.1}$$

The same participants as tested in Section 4 were evaluated. Three sets of 3 suction pulses were applied 5 cm subxiphoid on the abdomen with 1-2 min. of relaxation between tests. Participants were in supine position with no abdominal activation, and measurements were taken at end expiration. Elasticity at each suction pulse was reported. One tester completed the first two sets of 3 suction pulses, and a different tester completed the final set.

Secondly, one set of 3 suction pulses was applied at the widest portion of the posterior calf with 1-2 min. of relaxation between tests. Participants were asked to lie prone, with feet hanging off the edge of the bed in a relaxed state. Each calf (left and right) was tested and no muscle activation occurred. Elasticity at each suction pulse was reported. The same tester completed tests on both legs.

Finally, suction in 5 consecutive pulses was applied, then with delays increased to 30 s over 3 pulses, and 1 min. over 3 pulses at 5 cm subxiphoid on the abdomen. Timing was approximated to allow for measurements to take place at end expiration. Elasticity at each suction pulse was reported. The same tester completed all test sets in this phase.

Fourteen participants (7 male, 7 female) were recruited for Parts 1 and 2, with physiological details (including body mass index, BMI) outlined in Table 4.2.2. Only participants 01 and 03 participated in Part 3.

In 88% of abdominal impulse sets, a decrease in Young's modulus (E) was seen, indicating increased tissue compliance. The mean (standard deviation, SD) reduction in E was 3.45 (10.10) kPa. However, when pulses were averaged, an increase in E between sets was identified in 64% of results. The mean (SD) increase in E was 3.17 (18.70) kPa.

At the posterior calf, only 64% of impulse sets saw a decrease in E. The mean (SD) reduction in E was 2.69 (31.78) kPa. Results for the abdomen and calf are compiled in Table 4.3.1.

Table 4.3.1: Changes in Young's modulus (E) at varying anatomical locations.

Anatomy	Average Reduction in E [kPa] (SD)	Reduction Frequency
Abdomen	3.45 (10.10)	88%
Calf	2.69 (31.78)	64%

The elasticity results at each pulse including those with increased delays are shown in Fig. 4.3.1. Delay increases are denoted by vertical lines. No correlation between delay and elasticity could be derived with the given data.

Cupping therapy is a growing treatment option for myofascial pain, however, the effects of suction on deeper tissues' elasticity has not been well documented. As such, elasticity was derived using a novel device that employs a flash cupping technique to resect deeper fascia. Results

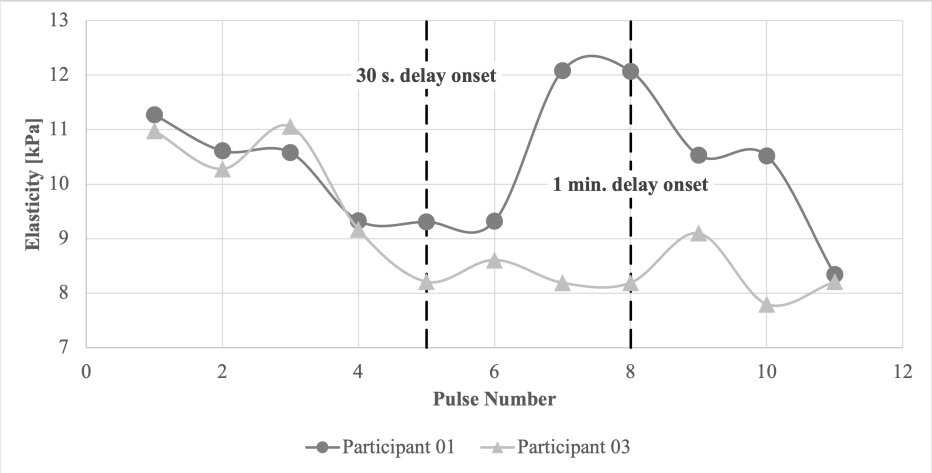

Figure 4.3.1: Changes in Young's modulus (E) given varying pulse delays.

indicated immediate increase in tissue compliance, and short-term stiffening.

The results of this study describe only a small sample of homogeneous participants. This limitation narrows the focus of this paper and restricts possible conclusions. Further, the novel device used to test elasticity has not yet been validated for use as an absolute measurement tool, thus, results should be analyzed as relative measures.

At both the abdomen and the calf, an increase in tissue compliance (decrease in E) was identified given consecutive, immediate suction pulses (flash cupping), a finding in agreement with previous studies [163], [166]. Less common, however, is the increase in E between test sets. It is known that suction causes increased blood flow to an area, therefore, this short-term stiffening may be credited to blood recession following perfusion during consecutive applied suction. However, further research is needed to critically identify the cause.

Work by Adcock *et al*. has shown that, more significant than the suction force, itself, is the effect of force from massage during cupping therapy [184]. In the present study, two testers were studied, and both saw increases in elasticity given consecutive suction pulses. That said, the initial force applied by each tester to achieve device seal against the body was not measured. This initial force may have had an effect on progressive short-term stiffening of the tissue. To standardize future studies, it is recommended to train testers to apply a consistent amount of initial pressure. This allows conclusions on the effect of suction pressure to be reached, rather than the greater effect of massage force.

After 5 subsequent pulses, elasticity continued to increase. Soft tissues, or fascia, are known to be viscoelastic materials [161], such that their presenting elasticity changes given changes in loading patterns. An increase in elasticity, however, suggests an asymptote must exist, though whether this is a universal or individual asymptote is of interest. Regardless, there may be an

effect of reaching said asymptote in therapy and its conjunction with myofascial pain relief. It is recommended to study the limits of elasticity in soft tissue given applied suction pulses, and determine whether reaching said limit has clinical benefits.

In summary, the immediate and short-term effects of flash cupping therapy on soft tissue elasticity were evaluated. Immediate (within 30 s) increase in tissue compliance was noted, with short term (1-3 min.) stiffening to follow. It is recommended to consider a wider range of cupping techniques, particularly by varying time durations and number of treatments in dry cupping. This may lend insight into the long term, rather than immediate effects of localized suction on deeper tissues' mechanical properties.

5 Validity and reliability of a novel, non-invasive tool and method to measure intra-abdominal pressure *in vivo*

5.1 Framework of Article 3

Concurrent to the work of Objectives 2 and 3 (Section 4), the present study explored the reliability, validity, accuracy and responsiveness of the novel system, specifically as an IAP measurement tool. As such, using UBP as a comparative system, the novel tool was tested on 13 (n = 13) cadaveric specimen to validate its use. Tests were conducted on the abdomen, and repeated on the same 14 (n = 14) participants recruited for Objectives 2 and 3. Living participants were tested to gauge responsiveness of the system to varying body positions, but were not evaluated for convergent validity with UBP. The realization of Objective 4 and investigation of Hypothesis 4 are presented in the manuscript entitled, "Validity and reliability of a novel, non-invasive tool and method to measure intra-abdominal pressure *in vivo*", for which the contribution of the first author is considered to be 85% including ethical approval application, experimental method formulation, data analysis, and manuscript writing. The second author provided research direction and manuscript review, for which the contribution is considered to be 15%. The manuscript was submitted to the *Journal of Biomechanics* on September 23, 2021. Some findings also contributed to poster presentations at the European Society of Biomechanics Conference on July 12, 2021, and the International Society of Biomechanics Conference on July 28, 2021.

5.2 Article 3: Validity and reliability of a novel, non-invasive tool and method to measure intra-abdominal pressure *in vivo*

Natasha Jacobson, P.Eng., Mark Driscoll, Ph.D., P. Eng.

Status: Submitted.

McGill University, 845 Sherbrooke St. W, Montreal, Quebec, Canada, H3A 0G4

Address for notification, correspondence and reprints:

Mark Driscoll, Ph.D., P.Eng., Assistant Professor

Associate Member, Biomedical Engineering

Canada NSERC Chair Design Engineering for Interdisciplinary Innovation of Medical Tech.

Department of Mechanical Engineering

817 Sherbrooke St. West, Montreal, QC, H3A 0C3 Canada

T: +1 (514) 398 - 6299

F: +1 (514) 398 – 7365

E-Mail: mark.driscoll@mcgill.ca

5.2.1 Abstract

Intra-abdominal hypertension has been recorded in between 20 and 50% of intensive care unit patients, with rates increasing in ventilated patients. This increased intra-abdominal pressure (IAP) can reduce blood flow to vital organs, perpetuating further pressure build-up as organs become unable to drain excess fluids. Measurement of IAP for the diagnosis of intra-abdominal hypertension remains highly invasive, thus, a non-invasive alternative to traditional IAP measurement was developed and validated, herein. Fourteen living participants and 13 cadaveric specimen were tested with this novel device for IAP measurement. Living participant results were compared to published IAP averages, while cadavers were tested against the existing gold standard: urinary bladder pressure (UBP). Intra- and inter-rater reliability in both living and cadaveric tests presented excellent results. Convergent validity against published IAP values was also excellent (in living participants) and moderate (in cadavers), while convergent validity against UBP was inconclusive. These promising results support the interest in further research, particularly with UBP comparisons in living participants.

5.2.2 Introduction

Intra-abdominal pressure (IAP) is the pressure contained in the abdominal compartment [1]. Normal IAP has been defined as between 5 and 7 mmHg in healthy adults, and 10 mmHg in critically ill patients, taken at a supine position during end-expiration with a urinary bladder catheter (UBP) [1], [2]. High levels of IAP are denoted by the terms intra-abdominal hypertension (IAH) or abdominal compartment syndrome (ACS), depending on measured values [3]. Both

conditions are prevalent in intensive care units, and are often caused by peritoneal inflammation and/or abdominal fluid build-up, typically as a result of acute abdominal injury or surgery [4]. Rates of IAH have been recorded in between 20 and 50% in intensive care unit patients, with rates increasing in ventilated patients [5]. This increased IAP can reduce blood flow to vital organs, perpetuating further pressure build-up as organs become unable to drain excess fluids [3], [4]. These life-threatening complications are diagnosed by IAP measurements collected over 4 to 6 hours that are consistently greater than 20 mmHg and 12 mmHg for ACS and IAH, respectively [3], [6]. Conversely, low levels of IAP are representative of poor spinal stability, a phenomenon linked to the onset of low back pain [7]. In fact, recent work has simulated a cross-section of the human trunk, based on work by Vleeming *et al*. [8], and found that increased IAP balanced the force profiles in back muscles and fascia [9]. This finding has emphasized the need for IAP and fascia inclusion in finite element models that evaluate spinal stability, which have, in turn, been developed by various groups [10], [11]. That said, currently, there is no "gold standard" for measuring IAP [12], [13]. The World Society of Abdominal Compartment Syndrome (WSACS) recommend IAP measurement via the bladder (known as intra-vesical pressure, urinary bladder pressure (UBP), or intra-bladder pressure), given that most patients requiring IAP monitoring already have a catheter implanted, making measurements minimally invasive [4], [14]. However, some researchers disagree with UBP measurement, especially in dynamic testing, as the system is position dependent and prone to air bubbles that can skew readings [14]. Further, the invasive nature of UBP measurement makes it unappealing as a research tool for healthy participants or IAP measure sought outside such clinical context.

Non-invasive alternatives to traditional bladder pressure measurement have been investigated, though, yielded inconclusive or unreliable results. Ultrasound guided tonometry (UGT), or, the evaluation of pressure by measurement of applied force and displaced liquid volume, is one such method [15]. UGT has only been studied in porcine models which resulted in the ability to distinguish between three defined categories of IAP. These were normal, mid-range and high, while this relative range indicates UGT's inability to offer fine IAP measurement resolution [15]. Further, though non-invasive, this technology is not portable, thus, limiting its use in clinics [15].

Similar is the use of an applied fluid force contained in a bottle held against the abdominal wall. As liquid is removed, the force decreases. If the response, described as the return of the peritoneum to its neutral state, is monitored by ultrasound (US), then it can be said that the causative fluid pressure that returns the peritoneum to its neutral position is equal to the pressure in the underlying cavity [16]. This procedure has had excellent correlation to UBP, though, is a slow, manual procedure that requires a fluid pressure to be orthogonal to the tissue of interest. Thus,

this technology is largely limited to conducive static body positions, namely those in which the abdomen is accessible.

Two other forms of IAP measurement via US are Doppler US and Laser US. In both scenarios, IAP is correlated with another variable: that is, blood flow and wavelength of a transmitted pulse in Doppler and Laser, respectively [16]. Doppler US correlates blood flow at the femoral vein to IAP, though, results were inferior to those of UGT [16]. Laser US sends a signal across the entire cross section of the thorax; sent at the abdominal wall and retrieved by the spine. If the attenuation of every tissue along the length of the body is known, changes in IAP can be determined by changes in the received pulse wavelength. However, this is a highly individualized procedure, and theoretical in its current state; that is, was only proposed as a technique, and has not yet been tested as a device [16].

The measurement of abdominal wall tension (AWT), also known as tensiometry, and its correlation to IAP has also been investigated. Due to the direct relationship between wall stress and internal pressure, in pressurized cylinders, van Ramshorst *et al*. assumed the measurement of AWT could provide insight into IAP [17], [18]. In further studies, the anatomical landmarks that offered the greatest reliability in AWT testing were 5 cm caudal to the xiphoid process and 5 cm cranial to the umbilicus [19]. Another group of researchers followed up on these findings by measuring AWT at the recommended anatomic position on 51 living patients [20]. AWT was then correlated to IAP measured via UBP [20]. The results from this study agreed with van Ramshorst *et al*.'s, proving AWT could be used to interpret IAP, however, correlation equations varied significantly [19], [20]. This discrepancy was largely attributed to patient population variation, but demonstrates the unreliability of IAP measurement with correlation equations. Following up on the work of AWT correlation, David *et al*. considered the correlation of abdominal wall thickness (AWTh) to IAP using bioimpedance and microwave reflectometry [21]. Similarly, positive correlation was evident, but poor sensitivity and limited pressure ranges (up to 7 mmHg) were noted [21].

Another means of IAP correlation to anatomic geometries is via respiratory inductance plethysmography (RIP). If abdominal compliance (C_{ab}) is known, and intra-abdominal volume (IAV) is measured via RIP, IAP can be directly calculated by the equation:

$$IAP = C_{ab} IAV. \tag{5.2.1}$$

That said, in the more likely scenario that C_{ab} is unknown, IAP can be correlated to measured IAV [4].

Smart pills (or, wireless motility capsules) have also been studied in porcine models as potential IAP measurement systems [16]. That said, when compared directly to UBP, the expensive

smart pills underestimated IAP, a finding that could have severe consequences clinically [16].

Digital image correlation (DIC) has not been studied as a means of IAP measurement, however, its use in abdominal wall elasticity measurement by Song *et al*. suggests its possible use in this area [16], [22]. Despite the potential of DIC, procedural difficulties make it a difficult means of measurement, and long set up times are inopportune for a clinical setting [16].

One of the only novel, non-invasive technologies that proposes direct measurement of IAP is that discussed by Jacobson and Driscoll [23]. This system, of radius a, uses suction (P_{app}) to induce a displacement in abdominal tissue (w), from which IAP (or, P_{in}) is calculated using the equation

$$IAP = P_{\text{in}} = \frac{P_{\text{app}}(a^2 + w^2)({r_2}^2 - {r_1}^2)}{4tw({r_1}^2 + {r_2}^2) - (a^2 + w^2)({r_2}^2 - {r_1}^2)} \tag{5.2.2}$$

where r_1 and r_2 are the inner and outer radii of the abdomen, respectively, and t is the AWTh [23]. Due to limited tests on only two study participants, and the lack of direct comparison to the existing gold standard, further research on this method is required.

To summarize, existing clinically-accepted IAP measurement techniques are invasive and prone to procedural discrepancies. Non-invasive alternatives allow reasonable results to be obtained, but do not directly measure pressure; UGT, bioimpedance, microwave reflectometry, and AWT/AWTh measurements interpret results and correlate them to IAP. Furthermore, non-invasive alternatives require continued research before clinical usage. As such, direct, non-invasive IAP measurement devices are not currently available. Recommendations from Tayebi *et al*. suggest bioimpedance and microwave reflectometry to possess to he most promise in future IAP measurement [16]. However, in their review of non-invasive IAP measurement methods, only wireless motility capsules were able to directly measure IAP. All other methods of measurement evaluated correlated IAP to an existing measure (IAV, AWT, AWTh, blood flow, applied force) [16]. Not included in Tayebi *et al*.'s review was the direct, non-invasive suction device by Jacobson and Driscoll. Given the promise of the Jacobson and Driscoll system, and need for comparative testing, it is the effort of this research to build on previous work by validating this novel, non-invasive tool for IAP measurement.

5.2.3 Methods

Ethical approval for this study was received from a university's International Review Board prior to participant recruitment (study number A09-M59-20B). All living participants provided informed consent during the study.

5.2.3.1 Materials

A novel device as described in [23] and shown in Fig. 5.2.1, was tested against the existing "gold standard" IAP measurement method: UBP.

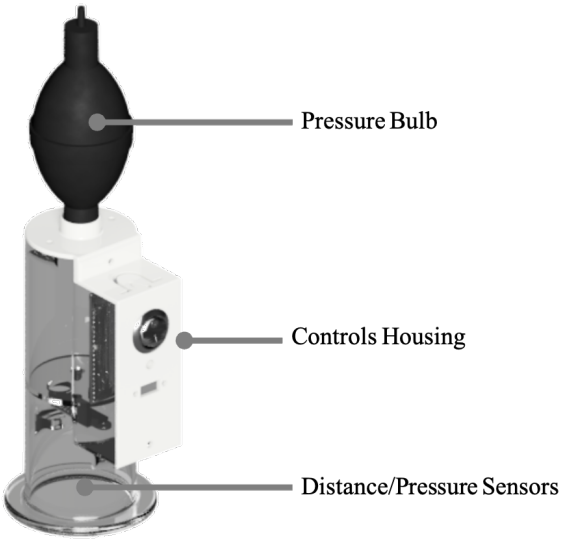

Figure 5.2.1: Prototype novel device, as described in [23].

The novel device induces a suction (P_{app}) against the skin from which the resulting tissue deformation (w) is measured. US jelly is used between the device and skin to improve airtightness and resulting suction. Three suction pulses are applied, from which the average IAP is calculated. Contrary to the authors' previous work [23], IAP was determined using the adjusted equation:

$$IAP = P_{\text{in}} + \rho gh \tag{5.2.3}$$

where P_{in} is the pressure calculated using suggestions from [23] (see Eq. 5.2.2), and $\rho\ gh$ is a modifier dependant on body position. As the human body is largely comprised of water, particularly in the abdomen with rates ranging from 60% (reported in connective tissues) to 96% (at the bladder), the density (ρ) of the abdomen was approximated as 997 kg/m^3 [24]. The force of gravity, g, was 9.807 m/s^2, while height (h) calculations were based on anthropometric relations [25], yielding:

$$h = 0.095Hsin(\alpha) \tag{5.2.4}$$

for inclined and sitting positions, where H is body height, and α is the angle of inclination (in rad). For standing positions,

$$h = 0.145H. \tag{5.2.5}$$

UBP outputs a fluid height that is directly translated to IAP in mmHg. In each cadaver, 25 mL was directly injected into the bladder via a urinary catheter, and the resulting pressure was measured by a physical manometer setup. The manometer was zeroed at the mid-axillary level of the line of the iliac crest. Setup was based on a summary by Lee in *Critical Care Nurse* for the manometer technique, and recommendations from the WSACS [26], [27].

5.2.3.2 Cadavers

All cadavers were fresh/frozen (up to 8 days post-mortem) and older than 18 years old. Sex was not an exclusion criterion. Due to the limited availability of cadavers, the only exclusion criterion was visible abdominal scarring at the testing site (5 cm subxiphoid), indicating surgical intervention.

Pearson correlation (r) values ranged from 0.86 to 0.98 for previous IAP studies [17]. Therefore, sample size calculation was determined using Bonett and Wright's suggested model for mean r values of 0.92 with a conservative confidence interval of 0.2 (alpha = 0.05, beta = 0.2), yielding 12 required participants [28].

Abdominal volume index (AVI [L]) was also recorded to evaluate potential correlation against test measurements. AVI was calculated by [29]:

$$AVI = \frac{(2\ cm(waist)^2 + 0.7\ cm(waist - hip)^2)}{1000}. \tag{5.2.6}$$

5.2.3.3 Participants

All living participants were older than 18 years old. Sex was not an exclusion criterion, however, women who were or had previously been pregnant were ineligible. Additional exclusion criteria included a history of abdominal surgery, use of muscle relaxants, acute peritonitis, abdominal mass, acute injury to the urinary bladder, acute cystitis, neurogenic bladder, pelvic hematoma, and pelvic fracture.

Intraclass correlation coefficient (ICC) values ranged from 0.56 to 0.87 for previous soft tissue elasticity studies [30]. Therefore, sample size calculation was determined using Walter *et al*.'s suggested model for ICC values between 0.56 and 0.87 (alpha = 0.05, beta = 0.2), yielding 14 required participants [31].

AVI was recorded to evaluate potential correlation against test measurements. AWTh was also measured 5 cm subxiphoid by two raters using a linear ultrasound probe and averaged.

5.2.3.4 Procedure

5.2.3.4.1 Part 1: Cadavers

Cadavers were in supine position with an inline catheter available. The novel device was used 5 cm subxiphoid, as suggested by [19]. UBP was measured concurrently. A (1) reliability (intra-, inter-) and (2) validity study were completed, along with an (3) external responsiveness study, as suggested by Husted *et al*. [32].

(1) Two measurements (M1a and M2a, Fig. **??**) for IAP were taken with the novel device with 2- to 5-minute washout periods (time interval between tests) between (intra-rater reliability). A second researcher repeated the measurement (M3a) immediately after M2a (inter-rater reliability).

(2) Both the novel device and UBP were tested simultaneously as the devices did not affect one another. UBP readings (UBP1a and UBP2a) were taken at the same time as the novel device measurement was read.

(3) The entire procedure was immediately repeated at a head tilt of 25° resulting in 3 additional measurements per test method, denoted as M1b through M3b and UBP1b through UBP2b.

5.2.3.4.2 Part 2: Living Participants

Living participants were in supine position, with tests conducted at end-expiration and without any abdominal activation. The novel device was used 5 cm subxiphoid. A (1) reliability (intra-, inter-) and (2) validity study, along with an (3) external responsiveness study were completed.

(1) Two measurements (ML1a and ML2a) for IAP were taken with the novel device with 2- to 5-minute washout periods (time interval between tests) between (intra-rater reliability). A second researcher repeated the measurement (ML3a) immediately after ML2a (inter-rater reliability).

(2) As no control device was used, novel device measurements were compared to published average values for IAP.

(3) The entire procedure was immediately repeated at (b) a head tilt of 25°, (c) sitting and (d) standing positions, resulting in 9 additional measurements, denoted as ML1b through ML3d.

Figure 5.2.2 illustrates the procedure for Part 1 and Part 2.

5.2.3.5 Statistical Analysis

As the objective was to determine whether the intra- (M1 and M2; ML1 and ML2) and inter-rater (M2 and M3; ML2 and ML3) reliability of the device exceeded an ICC of 0.75 (rule of thumb for "good" correlation), the null hypothesis (H_0) was defined as an ICC less than 0.75 [33]. This yields a range of "good" to "excellent" correlation, thus confirming device reliability. ICC estimates and their 95% confidence intervals were calculated using a single rating (1), absolute

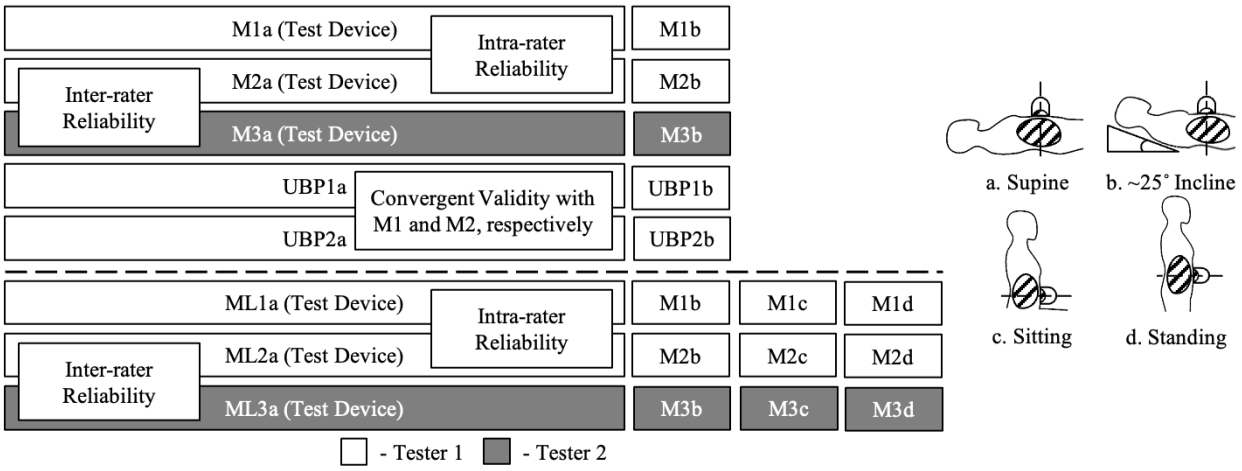

Figure 5.2.2: Illustrated procedure for Part 1 (cadavers) and Part 2 (living participants) of the present study. Tested anatomical positions are pictured, right: a. Supine, b. Inclined, c. Sitting, d. Standing where c. and d. only applied to living participants. Urinary bladder pressure (UBP) was only measured in cadaveric specimen.

agreement, two-way mixed effects model. Also evaluated were the minimum detectable change (MDC), MDC% and standard error of measurement (SEM) based on intra-rater reliability. MDC% refers to the ratio of MDC to the data mean [34].

Convergent validity was evaluated, similarly, between M1, UBP1, ML1, and published IAP values for Pearson's correlation r, where r greater than 0.7 was deemed "high" correlation [35]. Convergent validity for living participants was evaluated only against published average IAP values for varying body positions, as no reference measurement was taken during testing. This was a randomly generated, normally distributed set of numbers with a standard deviation (SD) and mean matching published data. In all scenarios, Bland-Altman analysis was conducted to evaluate the bias and limits of agreement for each comparison. Precision (standard deviation of the bias), coefficient of variation (precision divided by mean IAP), and percentage error (limits of agreement divided by mean IAP) were also evaluated [27].

Internal responsiveness of the system was determined at varying body positions to gauge the ability of the novel device to detect change. Responsiveness was calculated using effect size (ES) and standardized response mean (SRM). ES values of 0.2, 0.5 and 0.8 attribute to small, moderate, and high responsiveness, respectively [32].

5.2.4 Results

Fifteen cadavers were tested (5 male, 10 female), with physiological details outlined in Table 5.2.1. Due to technical difficulties, measurements were only collected in 13 of the cadavers (n = 13).

Table 5.2.1: Summary of cadaver descriptions (C: circumference; AVI: abdominal volume index)

ID	Age [years]	Gender	Abd. C [cm]	Hip C [cm]	AVI [L]	Days Post-mortem
01	72	M	74	78	11.0	3
02	77	F	77	82	11.9	5
03	88	F	89.5	97.8	16.1	8
04	80	M	85	93	14.5	3
05	83	F	89	95	15.9	3
06	73	F	91.5	100	16.8	6
07	92	F	84	87	14.1	4
08	100	F	N/A	N/A	N/A	6
09	89	M	107	106	22.9	2
10	93	M	88.5	95.5	15.7	4
11	87	F	76	82	11.6	3
12	95	F	71	83	10.2	4
13	85	F	76	86	11.6	6
14	78	F	80	90	12.9	4
15	79	M	71.5	79.5	10.3	2

Fourteen (n = 14) living participants (7 male, 7 female) were recruited, with physiological details outlined in Table 5.2.2.

Table 5.2.2: Summary of living participant descriptions (C: circumference; AWTh: abdominal wall thickness; AVI: abdominal volume index)

ID	Age [years]	BMI	Gender	Abd. C [cm]	Hip C [cm]	AVI [L]	AWTh [cm]
01	26	24.7	M	91	105	16.7	2.2
02	31	23.7	F	90	107	16.4	1.75
03	30	23.8	M	85.5	102.5	14.8	1.375
04	33	26.6	M	98	108	19.3	1.8
05	25	25.8	M	87.5	103	15.5	1.575
06	24	18.6	F	66.5	88	9.2	0.75
07	25	22.4	F	80	103	13.2	1.525
08	27	26.4	M	98	108	19.3	1.8
09	24	28.0	M	103.5	115	21.5	1.125
10	30	20.5	F	75.5	83	11.4	0.95
11	28	27.0	M	99.5	109.5	19.9	2.5
12	29	23.5	F	76	100.5	12.0	0.675
13	28	19.3	F	75	93	11.5	1.25
14	27	22.3	F	74	92.5	11.2	1.05

Average IAP for each body position are summarized in Table 5.2.3. Averages and SD

were taken by combining all data points (M1 through 3) for each body position. Juxtaposed are published IAP averages taken from literature [2], [36], [37].

Table 5.2.3: Summary of average IAP 5 cm subxiphoid on participants (n = 14) and cadavers (n = 13). Published ranges are indicated as benchmarks [2], [36], [37]. (SD: standard deviation)

Data Type	Supine [mmHg] (SD)	Incline [mmHg] (SD)	Sit [mmHg] (SD)	Stand [mmHg] (SD)
Cadaveric – Novel Device	3.66 (1.77)	8.62 (2.25)	N/A	N/A
Cadaveric – UBP	7.19 (2.84)	7.93 (2.45)	N/A	N/A
Living – Novel Device	5.10 (0.98)	10.2 (0.98)	16.88 (1.13)	23.7 (1.05)
Published Averages	6.0 (1.0)	9.0 (1.0)	16.73 (2.93)	20.25 (3.83)

5.2.4.1 Reliability Results

5.2.4.1.1 Part 1: Cadavers

Comparing M1 and M2, an ICC (mean and 95% confidence interval bounds: upper, lower, respectively) of 0.975 (0.943, 0.989) (n = 25) ($p < 0.001$) was found, indicating excellent intra-rater reliability. Comparing M2 and M3, an ICC of 0.917 (0.719, 0.970) (n = 21) ($p < 0.001$) was found, also indicating excellent inter-rater reliability. UBP1 and UBP2 were also compared and found to have an ICC 0.985 (0.954, 0.994) (n = 25) ($p < 0.001$) for excellent intra-rater reliability. SEM, MDC, and MDC% were all smaller for the novel device at 0.47 mmHg, 1.31 mmHg, and 23%, respectively, than for UBP measurements at 0.77 mmHg, 2.13 mmHg, and 28%, respectively.

5.2.4.1.2 Part 2: Living Participants

Comparing ML1 and ML2, an ICC of 0.996 (0.992, 0.997) (n = 52) ($p < 0.001$) was found, indicating excellent intra-rater reliability. Comparing ML2 and ML3, an ICC of 0.979 (0.852, 0.993) (n = 48) ($p < 0.001$) was found, also indicating excellent inter-rater reliability. SEM, MDC, and MDC% were 0.45 mmHg, 1.25 mmHg, and 9%, respectively.

Reliability results from Part 1 and 2 are summarized in Table 5.2.4.

5.2.4.2 Validity Results

5.2.4.2.1 Part 1: Cadavers

Comparing M1 against UBP did not give statistically significant results. The bias between M1 and UBP1 was 2.14 mmHg, while the precision was 4.23 mmHg. The coefficient of variation and percent errors were 63% and 124%, respectively. When comparing M1 against published IAP data gave r of 0.622 (n = 38) ($p < 0.001$) indicating moderate to good correlation. The bias between M1 and published IAP data was 2.02 mmHg, while the precision was 2.32 mmHg. The coefficient

Table 5.2.4: Reliability results summary by intraclass correlation (ICC). 95% confidence interval bounds denoted in brackets (upper, lower). Minimum detectable change (MDC), Standard Error of the Mean (SEM), and MDC% are also reported. (UBP: urinary bladder pressure)

	Cadaveric – Novel Device	Cadaveric - UBP	Living – Novel Device
Intra-rater Reliability	0.941 (0.813, 0.982)	0.985 (0.954, 0.994)	0.996 (0.992, 0.997)
Inter-rater Reliability	0.917 (0.719, 0.970)	N/A	0.979 (0.852, 0.993)
SEM [mmHg]	0.47	0.77	0.45
MDC [mmHg]	1.31	2.13	1.25
MDC %	23%	28%	9%

of variation and percent errors were 35% and 69%, respectively. Finally, as a benchmark, UBP1 was compared to published IAP data, and, again, gave statistically insignificant results ($p = 0.3$). However, the bias between UBP1 and published values was 0.11 mmHg, while the precision was 2.83 mmHg. The coefficient of variation and percent errors were 36% and 71%, respectively.

5.2.4.2.2 Part 2: Living Participants

Comparing ML1 against published IAP data gave r of 0.889 ($n = 56$) ($p < 0.001$) indicating excellent correlation. The bias between ML1 and published IAP data was 0.32 mmHg while the precision was 3.34 mmHg. The coefficient of variation was 50% and, finally, the percentage error was 98%.

Validity results from Part 1 and 2 are summarized in Table 5.2.5. Figure 5.2.3 shows the Bland-Altman plot for the novel device (M1) and UBP (UBP1) measurements in cadaveric specimen.

Table 5.2.5: Validity results summary by Pearson correlation (r). Bias, precision, coefficient of variation (C of V), and percentage error (% Error) are also reported. "Average" refers to published values. Limits as recommended by experts are appended for reference [27]. (UBP: urinary bladder pressure)

Data Type	r	Bias [mmHg]	Precision [mmHg]	C of V	% Error
Cadaveric – UBP	N/A	2.14	4.23	63%	124%
Cadaveric – Average	0.622	2.02	2.32	35%	69%
UBP – Average	N/A	0.11	2.83	36%	71%
Living – Average	0.889	0.32	3.34	50%	98%
Limits [27]	N/A	$\leq$1	$\leq$2	$\leq$15-20%	$\leq$20%

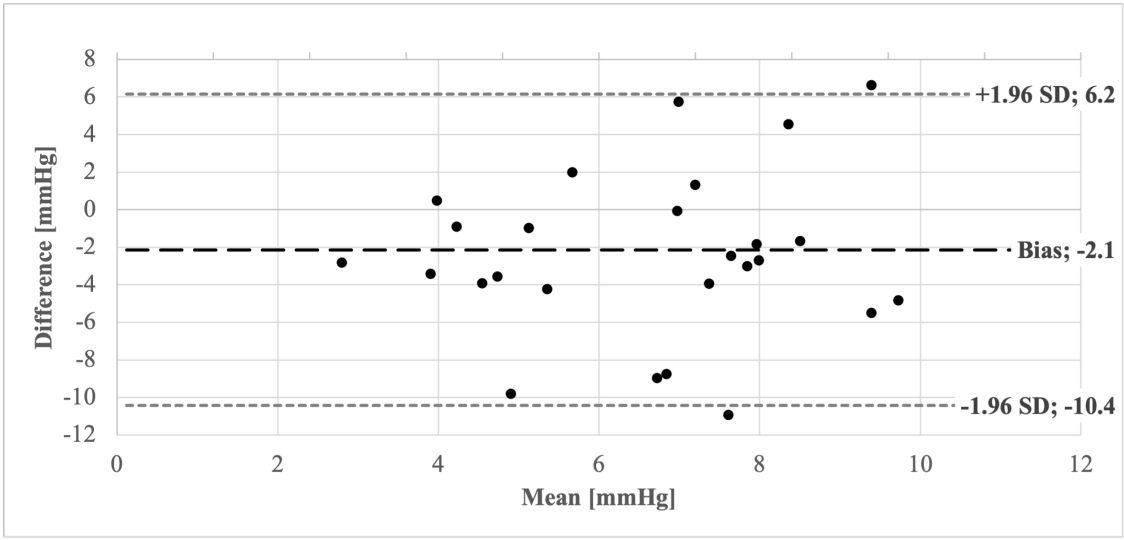

Figure 5.2.3: Bland-Altman plot comparing novel device and urinary bladder pressure (UBP) measurements for Part 1 (cadavers) of the present study. Upper and lower dotted bounds at +1.96 SD, -1.96 SD, respectively. Center dashed line denotes the mean difference, or bias.

5.2.4.3 Responsiveness Results

When moving cadaveric specimen from supine to inclined position, the novel device had large response, while UBP presented negligible response. Only the novel device presented with ES greater than published values. In living participants, from supine to standing, excellent response was seen with the novel device. The peak responsiveness was seen at the transition from supine to standing positions, with an ES of 25.38 and SRM of 18.13. Conversely, the least responsive transition was from an inclined to sitting positions, with an ES of 4.67, and SRM of 6.86. All ES of the novel device were greater than published values, with the exception of the transitions between inclined and sitting, and inclined and standing positions.

All responsiveness results are shown in Table 5.2.6.

5.2.5 Discussion

Experts recommend the development of a comprehensive, non-invasive soft tissue IAP measurement device [2], [4], [13], [38], [39]. Thus, a novel device was tested to evaluate its reliability, validity, and responsiveness against the existing popularized measurement method of UBP. Both cadaveric specimen (n = 13) and living participants (n = 14) were recruited. Tests indicated excellent intra- and inter-rater reliability in cadavers and living participants. No conclusive remarks can be made to correlation with UBP in cadavers, however, moderate correlation to published IAP values was seen in cadavers, which improved to excellent correlation in living participants. Finally large responsiveness was found for cadavers and living participants, and negligible to small responsiveness was found with UBP in cadavers. No significant correlations were found between

Table 5.2.6: Effect size (ES) and standardized response mean (SRM) of the novel device in cadavers and living participants, urinary bladder pressure (UBP) in cadavers, and published values for each body transition. Shaded areas highlight results less than published averages.

Body Transition	Cadaver				Living		Published Averages	
	Novel Device		UBP		Novel Device			
	ES	SRM	ES	SRM	ES	SRM	ES	SRM
Supine – Incline	3.40	2.63	0.17	0.34	7.65	3.85	2.47	1.14
Supine – Sit	N/A	N/A	N/A	N/A	16.28	14.29	12.60	3.57
Supine – Stand	N/A	N/A	N/A	N/A	25.38	18.13	17.29	3.04
Incline – Sit	N/A	N/A	N/A	N/A	4.21	4.67	6.86	2.74
Incline - Stand	N/A	N/A	N/A	N/A	8.65	9.66	10.04	2.68
Sit – Stand	N/A	N/A	N/A	N/A	5.80	10.22	1.53	1.07

novel device measurements and physiological parameters in living or cadaveric specimen, except for age: cadaveric IAP had moderate negative correlation with age (r = -0.572, $p < 0.05$), though this trend has not been reported in previous literature.

The results of this study describe only the two testers, herein, a small sample of homogeneous (that is: young, healthy, low BMI) participants, and a small sample of homogeneous (that is: above 72 years old) cadavers. This limits the scope of conclusions to a narrow audience. That said, age groups tested in cadaveric and living participants demonstrated effectiveness of the device in both the young (age 24 to 31) and old (age 72 to 100), suggesting its efficacy is independent of age. However, despite tester and participant limitations, as an IAP measurement tool, the novel device proved to be reliable and valid, particularly when compared to published IAP values. Further the device showed large responsiveness to change in body position. All these factors combine to suggest a possible replacement mechanism to UBP. That said, as suggested by the WSACS, a wider berth of baseline IAP (IAP at end-expiration in supine position) must be measured correctly, in a large sample of heterogeneous, living patients before measurement equity is considered. That is, a minimum of 20 study participants of whom 50% present with IAP measurements above 12 mmHg or more, and 5% of measurements are above 21 mmHg or more [27]. Therefore, it is recommended to test the present device against UBP in a large, multi-center study of varying patient BMI and baseline IAP to remark on its effect to correctly detect IAP, unanimously.

In 2009, a committee of experts on IAP, including clinicians and researchers, united to establish a set of guidelines for the development of future IAP measurement tools [27]. Quantitative targets were indicated for a device to be deemed successful or not; namely, a bias against UBP less than 1 mmHg, a precision less than 2 mmHg, a coefficient of variation less than 15-20%, and a percentage error less than 25% [27]. Cadaveric results for the present study were inconclusive

with respect to correlation against the novel device, however, suggested a bias around 2 mmHg, and precision of 4 mmHg, both of which exceed WSACS requirements. Errors may be attributed to saline leakage observed from the bladder in select cadavers, or the presence of air bubbles in bladder catheters. However, results from living participants and cadaveric specimen when compared to published IAP values demonstrated select values within bounds, such as bias in living participants (0.32 mmHg) and approximate precision in cadavers (2.32 mmHg). These preliminary results represent a significant step towards a non-invasive method of IAP measurement, though, indicate areas for improvement in the system design. Such improvement areas include air-tightness of the system, usability enhancement, and output refinement. That said, testing against concurrent UBP measurements in living participants must be taken to confirm this theory.

The present device, as it stands, may be used as a relative measure, or static guide for patient IAP. That said, the dynamic measurement of IAP may have broader clinical consequence. If the novel device is considered in a dynamic setting, perhaps by continuous negative pressure pulses or by sustained suction over short exercises, the point of peak IAP may be determined. This understanding could have significant consequences, clinically, as rehabilitation practices become better informed for an individual's needs. One potential example is in the context of engaged paraspinals during lifting patterns, where improved IAP control has been shown to impart important forces on vertebra believed to improve spine stability [8], [9]. Alternatively, IAP monitoring may identify unhealthy compensation methods adopted by patients with irregular mechanical properties of their underlying tissues, such as the thoracolumbar fascia [11]. In any case, the dynamic feasibility of the device requires further study prior to clinical adoption.

Another possible use for the novel device, given its efficacy as a relative measure, is as a C_{ab} indicator. C_{ab}, clinically, is the "measure of ease of abdominal expansion" [4]. Thus, high C_{ab} indicates that the abdomen can expand relatively freely, while low C_{ab} restricts abdominal expansion. According to the WSACS, C_{ab} can be determined given a change in abdominal volume and IAP [mL/mmHg], as noted in Eq. 5.2.1 [4]. Currently, there exists no tool to measure C_{ab} *in vivo*, however, with the novel device, relative IAP can be found before and after the ingestion of a known volume of fluid, such as water, thus providing a change in abdominal volume. Perhaps an individual's C_{ab} relation can be revealed from this relation. Knowing this value can help clinicians adjust for surgical interventions at the abdomen that require peritoneal dialysis, or laparoscopic inflation.

In summary, a novel device was proposed and validated for reliability, validity and responsiveness in non-invasive IAP measurement. The device was compared to UBP in cadaveric specimen, and against published IAP values in living participants. The inherent optimism of re-

sults supports the need for further research in multi-centre studies and more varied test subjects. Potential in dynamic testing, and C_{ab} measurement exist as future avenues for the technology.

5.2.6 Acknowledgements

The authors would like to acknowledge Mr. Trevor Cotter for his time and commitment to developing the prototype and conducting clinical studies. Thanks are also given to Prof. Gabriel Venne and his team for their efforts in study preparation. The authors have received grant funding (NSERC RGPIN-2017-04037) for the research, herein.

Bibliography

[1] M. Malbrain, D. Roberts, I. De Laet, J. De Waele, M. Sugrue, A. Schachtrupp, J. Duchesne, G. Van Ramshorst, B. De Keulenaer, A. Kirkpatrick, S. Ahmadi-Noorbakhsh, J. Mulier, R. Ivatury, F. Pracca, R. Wise, and P. Pelosi, "The role of abdominal compliance, the neglected parameter in critically ill patients — a consensus review of 16. Part 1: definitions and pathophysiology," *Anesthesiology Intensive Therapy*, vol. 46, no. 5, pp. 392–405, 2014.

[2] M. Malbrain, Y. Peeters, and R. Wise, "The neglected role of abdominal compliance in organ-organ interactions," *Critical Care*, vol. 20, no. 67, pp. 1–10, 2016.

[3] T. Papavramidis, A. Marinis, I. Pliakos, I. Kesisoglou, and N. Papavramidou, "Abdominal compartment syndrome - Intra-abdominal hypertension: Defining, diagnosing, and managing.," *Journal of Emergencies, Trauma, and Shock*, vol. 4, no. 2, pp. 279–91, 2011.

[4] D. Roberts, J. De Waele, A. Kirkpatrick, and M. Malbrain, "Intra-abdominal hypertension and the abdominal compartment syndrome," *Surgical Intensive Care Medicine*, vol. 39, no. 7, pp. 621–644, 2016.

[5] A. Blaser, A. Regli, B. De Keulenaer, E. Kimball, L. Starkopf, W. Davis, P. Greiffenstein, and J. Starkopf, "Incidence, Risk Factors, and Outcomes of Intra-Abdominal Hypertension in Critically Ill Patients-A Prospective Multicenter Study (IROI Study)," *Critical Care Medicine*, vol. 47, no. 4, pp. 535–542, 2019.

[6] R. Milanesi and R. Caregnato, "Intra-abdominal pressure: An integrative review," *Einstein (Sao Paulo)*, vol. 14, no. 3, pp. 423–430, 2016.

[7] I. Stokes, M. Gardner-Morse, and S. Henry, "Abdominal muscle activation increases lumbar spinal stability: Analysis of contributions of different muscle groups," *Clinical Biomechanics*, vol. 26, pp. 797–803, 2011.

[8] A. Vleeming, M. Schuenke, L. Danneels, and F. Willard, "The functional coupling of the deep abdominal and paraspinal muscles: the effects of simulated paraspinal muscle contraction on force transfer to the middle and posterior layer of the thoracolumbar fascia," *Journal of Anatomy*, vol. 225, pp. 447–462, 2014.

[9] K. El-Monajjed and M. Driscoll, "A finite element analysis of the intra-abdominal pressure and paraspinal muscle compartment pressure interaction through the thoracolumbar fascia," *Computer Methods in Biomechanics and Biomedical Engineering*, vol. 23, no. 10, pp. 585–596, 2020.

[10] I. El Bojairami, K. El-Monajjed, and M. Driscoll, "Development and validation of a timely and representative finite element human spine model for biomechanical simulations," *Scientific Reports*, vol. 10, no. 21519, pp. 1–15, 2020.

[11] E. Newell and M. Driscoll, "Investigation of physiological stress shielding within lumbar spinal tissue as a contributor to unilateral low back pain: A finite element study," *Computer in Biology and Medicine*, vol. 133, pp. 1–8, 2021.

[12] M. Malbrain, "Different techniques to measure intra-abdominal pressure (IAP): Time for a critical re-appraisal," *Intensive Care Med*, vol. 30, pp. 357–371, 2004.

[13] M. Cheatham, M. Malbrain, A. Kirkpatrick, M. Sugrue, M. Parr, J. De Waele, Z. Balogh, A. Leppaniemi, C. Olvera, R. Ivatury, S. D'Amours, J. Wendon, K. Hillman, and A. Wilmer, "Results from the international conference of experts on intra-abdominal hypertension and abdominal compartment syndrome. II. Recommendations," *Intensive Care Medicine*, vol. 33, pp. 951–962, 2007.

[14] A. Al-Abassi, A. Al Saadi, and F. Ahmed, "Is intra-bladder pressure measurement a reliable indicator for raised intra-abdominal pressure? A prospective comparative study," *BMC Anesthesiology*, vol. 18, no. 69, pp. 1–9, 2018.

[15] A. Bloch, M. Glas, A. Kohler, U. Baumann, and S. Jakob, "Noninvasive assessment of intra-abdominal pressure using ultrasound-guided tonometry: A proof-of-concept study," *Shock (Augusta, Ga.)*, vol. 50, no. 6, pp. 684–688, 2018.

[16] S. Tayebi, A. Gutierrez, I. Mohout, E. Smets, R. Wise, J. Steins, and M. Malbrain, "A concise overview of non-invasive intra-abdominal pressure measurement techniques: from bench to bedside.," *Journal of Clinical Monitoring and Computing*, 2020.

[17] G. Van Ramshorst, J. Lange, R. Goossens, N. Agudelo, G. Kleinrensink, M. Verwaal, S. Flipsen, W. Hop, L. Wauben, and J. Jeekel, "Non-invasive measurement of intra-abdominal pressure: A preliminary study," *Physiological Measurement*, vol. 29, no. 8, 2008.

[18] F. Beer, E. Johnston, J. DeWolf, and D. Mazurek, "Columns: Eccentric loading; the secant formula," in *Mechanics of Materials*, M. Lange, Ed., 6th ed., McGraw-Hill, 2012, ch. 10.5, pp. 649–654.

[19] G. Van Ramshorst, M. Salih, W. Hop, O. Van Waes, G. Kleinrensink, R. Goossens, and J. Lange, "Noninvasive assessment of intra-abdominal pressure by measurement of abdominal wall tension," *Journal of Surgical Research*, vol. 171, no. 1, pp. 240–244, 2011.

[20] Y. Chen, S. Yan, Y. Chen, Y. Zhuang, Z. Wei, S. Zhou, and H. Peng, "Noninvasive monitoring of intra-abdominal pressure by measuring abdominal wall tension," *World Journal of Emergency Medicine*, vol. 6, no. 2, pp. 137–141, 2015.

[21] M. David, A. Raviv, A. Peretz, U. Berkovich, and F. Pracca, "Towards a continuous non-invasive assessment of intra-abdominal pressure based on bioimpedance and microwave reflectometry: A pilot run on a porcine model," *Biomedical Signal Processing and Control*, vol. 44, pp. 96–100, 2018.

[22] C. Song, A. Alijani, T. Frank, G. Hanna, and A. Cuschieri, "Mechanical properties of the human abdominal wall measured *in vivo* during insufflation for laparoscopic surgery," *Surgical Endoscopy and Other Interventional Techniques*, vol. 20, no. 6, pp. 987–990, 2006.

[23] N. Jacobson and M. Driscoll, "Design Synthesis and Preliminary Evaluation of a Novel Tool to Non-Invasively Characterize Pressurized, Physiological Vessels," *Journal of Medical Devices*, vol. 15, no. 2, pp. 1–7, 2020.

[24] H. Woodard and D. White, "The composition of body tissues," *The British Journal of Radiology*, vol. 59, no. 708, pp. 1209–1219, 1986.

[25] R. Drillis and R. Contini, "Body Segment Parameters," Office of Vocational Rehabilitation, New York, Tech. Rep., 1966, Report 1166–03.

[26] R. Lee, "Intra-abdominal hypertension and abdominal compartment syndrome: A comprehensive overview," *Critical Care Nurse*, vol. 32, pp. 19–31, 2012.

[27] J. De Waele, M. Cheatham, M. Malbrain, A. Kirkpatrick, M. Sugrue, B. Z., R. Ivatury, B. De Keulenaer, and E. Kimball, "Recommendations for research from the international conference of experts on intra-abdominal hypertension and abdominal compartment syndrome," *Acta Clinica Belgica*, vol. 64, no. 3, pp. 203–209, 2009.

[28] D. Bonett and T. Wright, "Sample size requirements for estimating Pearson, Spearman and Kendall correlations," *Psychometrika*, vol. 65, no. 1, pp. 23–28, 2000.

[29] A. Accarino, F. Perez, F. Azpiroz, S. Quiroga, and J. Malagelada, "Abdominal distention results from caudo-ventral redistribution of contents," *Gastroenterology*, vol. 136, pp. 1544–1551, 2009.

[30] J. Wilke, L. Vogt, T. Pfarr, and W. Banzer, "Reliability and validity of a semi-electronic tissue compliance meter to assess muscle stiffness," *Journal of Back and Musculoskeletal Rehabilitation*, vol. 31, no. 5, pp. 991–997, 2018.

[31] S. Walter, M. Eliasziw, and A. Donner, "Sample size and optimal designs for reliability studies," *Statistics in Medicine*, vol. 17, pp. 101–110, 1998.

[32] J. Husted, R. Cook, V. Farewell, and D. Gladman, "Methods for assessing responsiveness: a critical review and recommendations," *Journal of Clinical Epidemiology*, vol. 53, no. 5, pp. 459–468, 2000.

[33] T. Koo and M. Li, "A guideline of selecting and reporting intraclass correlation coefficients for reliability research," *Journal of Chiropractic Medicine*, vol. 15, no. 2, pp. 155–163, 2016.

[34] P. Lee, C. Liu, C. Fan, C. Lu, W. Lu, and C. Hsieh, "The test-retest reliability and the minimal detectable change of the Purdue pegboard test in schizophrenia," *Journal of the Formosan Medical Association*, vol. 112, no. 6, pp. 332–337, 2013.

[35] M. Mukaka, "Statistics corner: A guide to appropriate use of correlation coefficient in medical research," *Malawi Medical Journal*, vol. 24, no. 3, pp. 69–71, 2012.

[36] W. Cobb, J. Burns, K. Kercher, B. Matthews, H. Norton, and T. Heniford, "Normal intraabdominal pressure in healthy adults," *Journal of Surgical Research*, vol. 129, no. 2, pp. 231–235, 2005.

[37] M. Cheatham, J. De Waele, I. De Laet, B. De Keulenaer, S. Widder, A. Kirkpatrick, A. Cresswell, M. Malbrain, Z. Bodnar, J. Mejia-Mantilla, R. Reis, M. Parr, R. Schulze, and S. Puig, "The impact of body position on intra-abdominal pressure measurement: A multicenter analysis," *Critical Care Medicine*, vol. 37, no. 7, pp. 2187–2190, 2009.

[38] M. Malbrain, I. De Laet, J. De Waele, M. Sugrue, A. Schachtrupp, J. Duchesne, G. Van Ramshorst, B. De Keulenaer, A. Kirkpatrick, S. Ahmadi-Noorbakhsh, J. Mulier, P. Pelosi, R. Ivatury, F. Pracca, M. David, and D. Roberts, "The role of abdominal compliance, the neglected parameter in critically ill patients — a consensus review of 16. Part 2: measurement techniques and management recommendations," *Anesthesiology Intensive Therapy*, vol. 46, no. 5, pp. 406–432, 2014.

[39] D. Ott, "Abdominal compliance and laparoscopy: A review," *Journal of the Society of Laparoendoscopic Surgeons*, vol. 23, no. 1, pp. 1–5, 2019.

6 General Discussion

Direct, non-invasive IAP measurement devices do not exist at this time. Further, existing handheld soft tissue elasticity devices are only able to measure properties of superficial tissues. As such, the present research worked to combine both needs and culminated in the design, development, and preliminary validation of a non-invasive IAP and soft tissue elasticity device (Patent Application No. 63/028,241, PCT/CA2021/050696). Using suction, abdominal tissue is resected and the resulting deformation is measured. With measured parameters, namely tissue deformation and applied pressure, IAP and elasticity are calculated. In a cohort of 14 participants, elasticity was compared to the MyotonPro and IndentoPro, and demonstrated greater accuracy and responsiveness than the latter two devices. Further testing compared the novel device's ability to measure IAP when compared to UBP and published values in 13 cadaveric specimen. All results supported device feasibility and preliminary validity.

Limitations on conclusions must be noted given the homogeneous, small sample size of participants tested. This included cadaveric specimen and living participants. All cadaveric specimen were above the age of 70 and presented with relatively small waist circumferences, whereas living participants were all young, fit (low BMIs), and healthy. Further, the same two testers were used in all clinical studies, thus, results are unique to these two rather than a broader testing base. The mathematical assumptions for this work are also limitations of the design. That is, it was assumed that the abdomen contains an incompressible fluid, of $\nu = 0.499$, despite the fact that literature argues the opposite [61]. Noise in sensors (BMP388, VL6180) may have attributed to errors up to 0.08 kPa (0.6 mmHg) and 6 kPa in IAP and E, respectively, which would have propagated throughout studies. Finally, physical errors in testing, such as inconsistent user force to hold the novel device against the body, or the presence of air bubbles in catheters during UBP testing in cadavers, may have led to discrepancies in measurements.

To improve mathematical formulae, it is of interest to consider the work of Hayes and Zhang who studied Young's modulus given tissue indentation [119], [185]. The combination of this work and the extended Hencky solution in a uniform pressure setting may be explored. The objective of this work is to more directly calculate internal pressures and boundary elasticities given the context of the novel device, described, herein.

Results in Section 4 suggested improved accuracy and responsiveness in elasticity measurement when compared to the MyotonPro and IndentoPro. The correction factor, ρgh, introduced in Section 3.4.2 and used throughout the thesis offered a means of improving system responsiveness given a change in anatomical position. This factor considered fluid pressure, such that IAP

increased as a participant's head was raised. With ρgh included in the final IAP equation, responsiveness of the novel system proved excellent, with ES greater than 0.8 in all body position transitions from supine through to standing (Section 5). In addition, results were within published bounds for IAP at varying body positions, showing a level of accuracy unmatched in existing non-invasive IAP measurement tools. Of interest is confirming this device improvement with SWUE as a benchmark. SWUE has the added benefit of visualizing deeper fascia by mapping applied forces on an US machine. This composite effect may demonstrate improved convergent validity with the novel device.

Cadaveric results were inconclusive, and suggested the inability of the present technology to correctly correlate with existing gold standard devices (namely, UBP). However, negative results in IAP testing may be attributed to measurement errors in UBP. Researchers were self-taught in UBP measurement, and, thus, inherently increased the possibility of error in readings. In addition, all tested cadavers were more than 8 hours post-mortem. Beyond this timeframe, fluids in the cadaver tend to settle at the lowest point in the body due to gravity and the lack of blood circulation [186]. In the case of supine bodies, this fluid buildup occurs along the back, thus resulting in post-mortem staining, or the reddish-blue discolouration of the body [186]. Therefore, fluid settling may have impacted IAP results with UBP measures, given the position of the bladder in relation to where the novel device was being tested (skin surface), yielding a secondary major source of error.

With evidence supporting the use of the novel device for IAP measurement, its use in abdominal compliance (C_{ab}) measurement may also be explored. As alluded to in Section 1.1, an ideal, indisputable change in IAV that can be measured is by the intake of a measured fluid, such as drinking water. With this change in IAV, and the associated changes in IAP, as measured with the novel device, C_{ab} may be divulged.

As alluded to in Section 4.3, there is value in considering the prolonged effects of suction on deep tissues and fascia. The lift and movement of fascia layers may lend insight into the effects of rehabilitation and treatments using suction. The use of imaging techniques, along with the novel device, may suggest how varying pressure and application duration affect macrostructures under the skin.

Clinically significant differences in elasticity and IAP must be discussed when interpreting results for clinical viability. Healthy IAP is between 5 and 7 mmHg, whereas IAP greater than 12 mmHg is considered unhealthy (IAH) in adults [20]. As such, the minimum possible difference in IAP between healthy and unhealthy (discounting considerations for BMI) is 5 mmHg. However, in children this difference decreases, with normal IAP in critically ill children between 3 and 10 mmHg, and IAH defined as IAP greater than 10 mmHg [44]. In this instance, physiological cues

other than just IAP measurement are also considered, including organ dysfunction or failure [44]. As such, a conservative clinically significant difference of 1 mmHg is estimated for use in ICUs.

Alternatively, research has been conducted on pain thresholds in the pelvic girdle due to raised IAP [179]. Mens *et al*. suggested an equation to determine the critical IAP at which pain occurs due to pelvic floor activation (through hip adduction, $F_{\text{adduction}}$) [179]:

$$IAP = \frac{F_{\text{adduction}}}{a - \frac{Ahcos\alpha}{C}} \tag{6.0.1}$$

where a is the cross-sectional area in the mid-sagittal plane of the pelvic cavity (defined as below the superior point of the iliac crest to the pelvic floor), A is the cross-sectional area in the mid-sagittal plane of the abdominopelvic cavity (defined as between the diaphragm and pelvic floor), C is the circumference of the pelvic cavity at the superior point of the iliac crest, h is the height from the pelvic floor to superior point of the iliac crest, and α is the angle between the frontal plane and AW [179]. Anatomic measurements by Mens's research group were taken using MRI scans. In two women, the average force created in the pelvic cavity during isometric hip adduction was found to be 90 N, resulting in critical IAPs of 65 mmHg and 53 mmHg in a nulliparous and pregnant (28 weeks) woman, respectively [179]. Thus, it may be proposed that an increase in IAP between 48 mmHg and 58 mmHg suggests the development of pelvic girdle pain (difference against low end of normal IAP).

The IAP MDC of the novel device was found to be 1.25 and 2.13 mmHg for living and cadaveric results, respectively (Section 5). Though of insufficient precision to warrant use in ICUs, the device may be used to support client education and monitoring during rehabilitation therapies; a setting currently devoid of IAP measurement tools due to the invasive nature of existing systems. Physiotherapists and other rehabilitation specialists design training programs to focus stress on their clients' bodies. With the aid of the novel device, IAP measurements may be taken during static hip adduction with and without treatment techniques (including timing of breath, support muscle activation). This provides both clinicians and patients, alike, a quantitative benchmark to better support and guide health programs. The device may be used as a client education tool, or to map progress through a regimen. However, it should be highlighted that Eq. 6.0.1 is highly dependant on individual anatomies and their capacity of the hip adductor. What is more, pain thresholds are highly personalized, meaning a sample size of $n = 2$, as in Mens *et al*.'s study is insufficient to make broad claims on critical IAPs for pelvic girdle pain reduction. Nonetheless, the novel device allows users to take static measurements in natural and corrected positions, with or without pain, to gauge personal bounds for IAP. This marks a significant advancement in available non-invasive technologies for IAP measurement outside of a hospital setting.

Recently, healthy and unhealthy AW elasticity was been measured in those with and without diastasis rectus abdominis, respectively [187]. AW elasticity in healthy (n = 24) and unhealthy (n = 36) participants was evaluated by SWUE. Tests were conducted at the rectus abdominis and oblique muscles, not at the linea alba as tested in Section 4. Due to its closest proximity to the linea alba, however, rectus abdominis elasticity results were considered. Thus, the minimum percent difference between healthy and unhealthy AW elasticity was found to be 1% corresponding to a difference of 0.1 kPa. The max. diff was 29% corresponding to a difference of 2.8 kPa. The MDC of the novel device was found to be 18.54 kPa at the abdomen, suggesting its inefficacy for clinical diagnostics. However, studies on muscle activation suggest a larger clinically significant difference, though for a rehabilitation audience. Using SWUE, the elasticity of the AW muscles in 11 participants (n = 11) was determined at rest, during a Valsalva maneuver, and during activation [112]. The maximum percent difference between active (Valsalva) and passive (at rest) elasticity was found to be 116%, or 43.8 kPa, at the rectus abdominis, whereas the minimum was 73%, or 75.8 kPa, at the external obliques [112]. That said, between the Valsalva maneuver and activation a difference of only 17%, or 9.3 kPa, was seen [112]. Therefore, the novel device may be used to compare muscle activation to passive elasticity, though, when distinguishing between various levels of activation, precision remains insufficient. As with IAP measurement, clinical value of the novel device persists, as it allows clinicians to gauge personal bounds for AW elasticity.

Considering the clinically significant differences in elasticity and IAP highlights the advantages of the novel device, as well as opportunities for growth. With technological improvements, such as improved suction, standardized testing methods, or more advanced sensors, meeting MDCs required for critical care (1 mmHg in IAP, 0.1 kPa in elasticity) may be realized.

In summary, a novel device for non-invasive *in vivo* assessment of IAP and soft tissue elasticity was designed, developed, and validated. Preliminary tests indicate the potential of the technology, and support the need for further research.

7 Conclusions and Recommendations

In conclusion, a novel, non-invasive device was designed and validated for soft tissue elasticity and IAP measurement (Patent Application No. 63/028,241, PCT/CA2021/050696). This is the first device to directly measure IAP non-invasively and directly by considering a novel use for the Hencky solution (Section 3). During validation, new data on AW elasticity 5 cm subxiphoid, along with elasticity for the superficial posterior calf were supplied (Section 4). Further, findings suggested an immediate (within 30 s.) decrease in stiffness, and short-term (within 1-3 min.) increase in stiffness given locally applied suction pulses. In addition, new data on IAP in cadaveric specimen was also provided for future comparisons (Section 5). Finally, no correlation was found between AW elasticity or IAP and AVI or AWTh. This leads to the conclusion that these geometric factors (AVI and AWTh) cannot be used to correlate for mechanical properties of the abdomen, though a larger sample size is advised to confirm this theory. All original contributions improve understanding of the abdomen and its mechanics, particularly when considering IAP. Conclusions for each of the outset hypotheses are denoted in the following.

Objective 1: Develop a direct, non-invasive, handheld tool to measure internal pressures and material mechanical properties in pressurized vessels.

Hypothesis 1: A novel, non-invasive device can correctly detect changes in physiological pressures; that is, pressure increases around 0.2 and 0.4 kPa (1.5 and 3.0 mmHg) with increasing head inclination to 25°.

High responsiveness was found in IAP measurement with the novel device in Section 5 using the final suggested equation:

$$\begin{aligned} IAP &= P_{\text{in}} + P_{\text{fl}}; \\ IAP &= \frac{P_{\text{app}}(a^2+w^2)({r_2}^2-{r_1}^2)}{4tw({r_1}^2+{r_2}^2)-(a^2+w^2)({r_2}^2-{r_1}^2)} + \rho g h, \end{aligned} \tag{7.0.1}$$

thus, proving Hypothesis 1. IAP measures correctly increased with increasing head position (inclined through to standing positions) with a bias of 0.3 mmHg and 2.0 mmHg in living and cadaveric studies, respectively, when compared to published "ideal" data. The overall design and underlying algorithm (Eq. 3.4.8) are included in the patent application number 63/028,241 (PCT/CA2021/050696).

Objective 2: Demonstrate the novel tool's efficacy as an abdominal elasticity measurement tool.

Hypothesis 2: Isotropic Young's modulus measurements taken with the novel device have "good" (ICC > 0.75) intra- and inter-rater reliability, and "high" ($r > 0.7$) linear correlation against stiffness measurements taken 5 cm subxiphoid on the abdomen with existing popularized measurement methods (here, myometry with the MyotonPro and indentation with the IndentoPro) [125].

Young's modulus using the novel device was calculated by the final suggested equation in Section 3.4:

$$E = \alpha(\zeta, \nu)\frac{3\phi(\eta)P_{\text{app}}a}{2\pi w}. \tag{7.0.2}$$

Due to data presenting with a non-normal distribution, Spearman's rho was used to evaluate intra- and inter-rater reliability, as well as convergent validity of the novel device. Hypothesis 2 was disproved with reliabilities presenting with moderate correlation. Further, only moderate correlation was found between the novel device and the MyotonPro. No statistically significant conclusions could be made against the IndentoPro. Though Hypothesis 2 was invalidated, it did not account for responsiveness and accuracy measurements taken in Section 4. With correct and consistent responsiveness to changes in anatomical position, and elasticities presenting within the existing range of published data, there may be inherent errors that exist in the benchmark tools.

Objective 3: Demonstrate the novel tool's efficacy as a muscle elasticity measurement tool.

Hypothesis 3: Isotropic Young's modulus measurements taken with the novel device have "good" (ICC > 0.75) intra-rater reliability, and "high" ($r > 0.7$) linear correlation against stiffness measurements taken at the gastrocnemius with existing popularized measurement methods (here, myometry with the MyotonPro and indentation with the IndentoPro) [125].

Contrary to Young's modulus measurements at the abdomen, those at the calf muscle (gastrocnemius) presented with normal distributions. As such, an ICC of 0.8 was found for intra-rater reliability, supporting Hypothesis 3. However, convergent validity disproved Hypothesis 3, with Pearson correlations of 0.481 ($p < 0.2$) and 0.623 ($p < 0.05$) against the MyotonPro and IndentoPro, respectively. Neither Pearson correlation indicated "high" linear correlation, yet, similar to Hypothesis 2, responsiveness and accuracy were most promising in the novel device. As such, potential inherent errors in benchmark tools require further exploration.

Objective 4: Demonstrate the novel tool's efficacy as an intra-abdominal pressure measurement tool.

Hypothesis 4: IAP can be measured directly to within 1 mmHg of existing gold standard methods (here, UBP) considering the force equilibrium between locally applied pressures, IAP, and AW tension.The reliability of a novel IAP measurement device has "good" (ICC > 0.75) intra- and inter-rater reliability, and "high" ($r > 0.7$) linear correlation against IAP measurements taken by

UBP.

Hypothesis 4 was correct with respect to reliability results, such that living and cadaveric results indicated "excellent" reliability (both intra- and inter-). However, conclusive remarks could not be made in regards to linear correlation against UBP. Despite errors in UBP methodology, Pearson correlation between the novel device and published data did support the current hypothesis in living studies. Bias was also within hypothesized values (1 mmHg) in living studies when compared, again, to published data rather than UBP measures.

Given results, recommendations for future research can be made. It is first recommended to redesign the novel device similarly to the Nimble [133]. That is, rather than measure the tissue deformation for a given pressure, measure the pressure for a known tissue deformation. This change has been shown to provide better accuracy and reliability than its counterpart [133].

Secondly, it is of interest to consider a wider testing sample. In other words, does the device work on higher BMI patients, or larger age brackets? Similar methodology can be used to approach testing, however, the sample must be more heterogeneous than previously studied participants. This study expansion also pertains to testers. In the present work, only two testers were evaluated to gauge inter-rater reliability. Increasing this number to include multi-center clinicians, and perhaps untrained individuals, may indicate more globally conclusive results.

The third major recommendation for future research is to use SWUE as a gold standard benchmark for elasticity measurements. SWUE has shown high sensitivities and specificities in previous studies, though, its precise accuracy is difficult to comment on given its dependancy on anatomic location and individual tissue properties [140]. Thus, a complementary measurement for all analysis is individual AWTh at the testing site (5 cm. subxiphoid). Knowing individual AWTh will adjust Eq. 3.4.8 and Eq. 3.4.1 for improved measurement precision. Benchmark devices used in Objectives 2 and 3, namely the MyotonPro and IndentoPro, did not exhibit consistent and correct responsiveness or accuracy when compared to published data. As such, comparing to SWUE may provide greater insight into the accuracy and precision of the novel device in soft tissue elasticity measurement. Similarly with IAP, it is recommended that UBP measurements be performed by a trained professional in a clinical setting as a means of gold standard reference testing. Both changes reduce user error, and provide greater evidence for the efficacy of the novel system.

The consideration of individual layer elasticity in soft tissue composites, such as the AW, is of interest, both clinically and academically. In order to use the novel device as a tool for elasticity measurement of individual layers, it is recommended to test the device using varying cup radii, such that new layers are resected with widening suction areas. This may lend insight into the effect of introduced layers, and individual layer elasticities may be determined. Existing

equations would not change, though, additional analysis would be required to consider individual tissue thickness as a ratio of the composite tissue thickness. Bioimpedance as a complimentary method of elasticity measurement for individual layers is also of interest, here. As suggested by Tayebi *et al*., bioimpedance offers the greatest potential in physiological measurement, and may be of benefit in future iterations of the present device, perhaps in tissue elasticity or thickness measurement [34].

Finally, a long-term interest for this technology is its conversion to a dynamic setting. If the novel device can be remodelled to become a wearable patch or band that provides live feedback of pressures and elasticities, the research potential for the technology expands significantly. During abdominal activation, an IAP increase occurs [2], [3], [188]. With continuous feedback, both property changes may be analyzed. This design expansion may be coupled with the lumbosacral orthoses materials tested in Section 3.3, though, *in vivo* evaluation of the belt materials must be considered, first, in long-term wear. Coupled with long-term material analysis is the consideration of mathematical assumptions made in orthoses tension requirements; that is, a homogeneous, rigid, constant AW. In addition, other variables must be considered in the pivot to dynamic measurement, including how fluid pressure (ρgh) changes with changing body position. Perhaps fluid pressure at a standing position should be considered as a baseline for exercise, and changes in measured IAP by suction seek to determine peaks in pressure.

In conclusion, a non-invasive alternative to UBP measurement was developed and preliminary validation occurred. Though numerous recommendations exist, they speak to the potential of the technology. This thesis, thus, serves as a reference guide for the future development of IAP and soft tissue elasticity measurement devices.

Bibliography

[1] S. Strandring, "Abdomen and pelvis: Overview and surface anatomy," in *Gray's Anatomy*, 41st ed., Elsevier Ltd., 2016, ch. 59, pp. 1029–1047.

[2] M. Malbrain, D. Roberts, I. De Laet, J. De Waele, M. Sugrue, A. Schachtrupp, J. Duchesne, G. Van Ramshorst, B. De Keulenaer, A. Kirkpatrick, S. Ahmadi-Noorbakhsh, J. Mulier, R. Ivatury, F. Pracca, R. Wise, and P. Pelosi, "The role of abdominal compliance, the neglected parameter in critically ill patients — a consensus review of 16. Part 1: definitions and pathophysiology," *Anesthesiology Intensive Therapy*, vol. 46, no. 5, pp. 392–405, 2014.

[3] I. Stokes, M. Gardner-Morse, and S. Henry, "Abdominal muscle activation increases lumbar spinal stability: Analysis of contributions of different muscle groups," *Clinical Biomechanics*, vol. 26, pp. 797–803, 2011.

[4] M. Malbrain, I. De Laet, J. De Waele, M. Sugrue, A. Schachtrupp, J. Duchesne, G. Van Ramshorst, B. De Keulenaer, A. Kirkpatrick, S. Ahmadi-Noorbakhsh, J. Mulier, P. Pelosi, R. Ivatury, F. Pracca, M. David, and D. Roberts, "The role of abdominal compliance, the neglected parameter in critically ill patients — a consensus review of 16. Part 2: measurement techniques and management recommendations," *Anesthesiology Intensive Therapy*, vol. 46, no. 5, pp. 406–432, 2014.

[5] P. Hodges, A. Eriksson, D. Shirley, and S. Gandevia, "Intra-abdominal pressure increases stiffness of the lumbar spine," *Journal of Biomechanics*, vol. 38, no. 9, pp. 1873–1880, 2005.

[6] M. Malbrain, M. Cheatham, A. Kirkpatrick, M. Sugrue, M. Parr, J. De Waele, Z. Balogh, A. Leppaniemi, C. Olvera, R. Ivatury, S. D'Amours, J. Wendon, K. Hillman, and A. Wilmer, "Results from the international conference of experts on intra-abdominal hypertension and abdominal compartment syndrome. I. Definitions," in *Intensive Care Medicine*, vol. 32, 2006, pp. 1722–1732.

[7] D. Roberts, J. De Waele, A. Kirkpatrick, and M. Malbrain, "Intra-abdominal hypertension and the abdominal compartment syndrome," *Surgical Intensive Care Medicine*, vol. 39, no. 7, pp. 621–644, 2016.

[8] K. Tayashiki, S. Maeo, S. Usui, N. Miyamoto, and H. Kanehisa, "Effect of abdominal bracing training on strength and power of trunk and lower limb muscles," *European Journal of Applied Physiology*, vol. 116, no. 9, pp. 1703–1713, 2016.

[9] M. Malbrain, "Different techniques to measure intra-abdominal pressure (IAP): Time for a critical re-appraisal," *Intensive Care Med*, vol. 30, pp. 357–371, 2004.

[10] D. Ott, "Abdominal compliance and laparoscopy: A review," *Journal of the Society of Laparoendoscopic Surgeons*, vol. 23, no. 1, pp. 1–5, 2019.

[11] R. Drake, W. Vogl, and A. Mitchell, "Abdomen," in *Gray's Basic Anatomy*, 2nd ed., Elsevier, Inc., 2018, ch. 4, pp. 133–206.

[12] J. Gosling, P. Harris, J. Humpherson, I. Whitmore, and P. Willan, "Abdomen," in *Human Anatomy, Color Atlas and Textbook*, 7th ed., Elsevier Ltd., 2017, ch. 4, pp. 135–212.

[13] V. Tuktamyshev, E. Kasatova, E. Truhacheva, and A. Kasatov, "The study of compressibility of abdominal contents.," *Russian Journal of Biomechanics*, vol. 20, no. 4, pp. 261–265, 2016.

[14] T. Forstemann, J. Trzewik, J. Holste, B. Batke, M. Konerding, T. Wolloscheck, and C. Hartung, "Forces and deformations of the abdominal wall - A mechanical and geometrical approach to the linea alba," *Journal of Biomechanics*, vol. 44, pp. 600–606, 2011.

[15] A. Blaser, M. Bjorck, B. De Keulenaer, and A. Regli, "Abdominal compliance: A bench-to-bedside review.," *The Journal of Trauma and Acute Care Surgery*, vol. 78, no. 5, pp. 1044–53, 2015.

[16] T. Stedman, *Stedman's Medical Dictionary*, 28th ed. Lippincott Williams and Wilkins, 2006, pp. 1274, 1465.

[17] A. Accarino, F. Perez, F. Azpiroz, S. Quiroga, and J. Malagelada, "Abdominal distention results from caudo-ventral redistribution of contents," *Gastroenterology*, vol. 136, pp. 1544–1551, 2009.

[18] S. Agnew, W. Small, E. Wang, L. Smith, I. Hadad, and G. Dumanian, "Prospective measurements of intra-abdominal volume and pulmonary function after repair of massive ventral hernias with the components separation technique," *Annals of Surgery*, vol. 251, no. 5, pp. 981–988, 2010.

[19] A. Villoria, F. Azpiroz, A. Soldevilla, F. Perez, and J. Malagelada, "Abdominal accomodation: A coordinated adaptation of the abdominal wall to its content," *American Journal of Gastroenterology*, vol. 103, pp. 2807–2815, 2008.

[20] M. Malbrain, Y. Peeters, and R. Wise, "The neglected role of abdominal compliance in organ-organ interactions," *Critical Care*, vol. 20, no. 67, pp. 1–10, 2016.

[21] T. Papavramidis, N. Michalopoulos, G. Mistriotis, I. Pliakos, I. Kesisoglou, and S. Papavramidis, "Abdominal compliance, linearity between abdominal pressure and ascitic fluid volume.," *Journal of Emergencies, Trauma, and Shock*, vol. 4, no. 2, pp. 194–197, 2011.

[22] J. Mulier, B. Dillemans, M. Crombach, C. Missant, and A. Sels, "On the abdominal pressure volume relationship," *The Internet Journal of Anesthesiology*, vol. 21, no. 1, pp. 1–7, 2008.

[23] B. Abu-Rafea, G. Vilos, A. Vilos, J. Hollett-Caines, and M. Al-Omran, "Effect of body habitus and parity on insufflated CO_2 volume at various intraabdominal pressures during laparoscopic access in women," *Journal of Minimally Invasive Gynecology*, vol. 13, pp. 205–210, 2006.

[24] C. Song, A. Alijani, T. Frank, G. Hanna, and A. Cuschieri, "Mechanical properties of the human abdominal wall measured *in vivo* during insufflation for laparoscopic surgery," *Surgical Endoscopy and Other Interventional Techniques*, vol. 20, no. 6, pp. 987–990, 2006.

[25] J. Mulier, K. Coenegrachts, and K. Van de Moortele, "Ct analysis of the elastic deformation and elongation of the abdominal wall during colon inflation for virtual coloscopy," *European Journal of Anaesthesiology*, vol. 25, no. 44, p. 42, 2008.

[26] F. Pracca, A. Biestro, J. Gorrassi, M. David, F. Simini, and M. Cancela, "ABDOPRE: An external device for the reduction of intra-abdominal pressure. Preliminary clinical experience," *Revista Brasileira de Terapia Intensiva*, vol. 23, no. 2, pp. 238–241, 2011.

[27] M. David, F. Pracca, and F. Simini, "Non-invasive negative pressure system to treat abdominal hypertension," *IFMBE Proceedings*, vol. 37, pp. 211–214, 2011.

[28] P. Severgnini, G. Inzigneri, C. Olvera, C. Fugazzola, M. Mangini, P. Padalino, and P. Pelosi, "New and old tools for abdominal imaging in critically ill patients," *Acta Clinica Belgica*, vol. 62, no. Suppl. 1, pp. 173–182, 2007.

[29] H. Sugerman, A. Windsor, M. Bessos, and L. Wolfe, "Intra-abdominal pressure, sagittal abdominal diameter and obesity comorbidity," *Journal of Internal Medicine*, vol. 241, pp. 71–79, 1997.

[30] M. Malbrain, I. De Laet, N. Van Regenmortel, K. Schoonheydt, and H. Dits, "Can the abdominal perimeter be used as an accurate estimation of intra-abdominal pressure?" *Critical Care Medicine*, vol. 37, no. 1, pp. 316–319, 2009.

[31] F. Guerrero-Romero and M. Rodriguez-Moran, "Abdominal volume index. An anthropometry-based index for estimation of obesity is strongly related to impaired glucose tolerance and type 2 diabetes mellitus," *Archives of Medical Research*, vol. 34, no. 5, pp. 428–432, 2003.

[32] R. Valdez, J. Seidell, Y. Ahn, and K. Weiss, "A new index for abdominal adiposity as an indicator of risk for cardiovascular disease. A cross-population study," *International Journal of Obesity*, vol. 17, pp. 77–82, 1993.

[33] K. Cohen, D. Panescu, J. Booske, J. Webster, and W. Tompkins, "Design of an inductive plethysmograph for ventilation measurement," *Physiological Measurement*, vol. 15, pp. 217–229, 1994.

[34] S. Tayebi, A. Gutierrez, I. Mohout, E. Smets, R. Wise, J. Steins, and M. Malbrain, "A concise overview of non-invasive intra-abdominal pressure measurement techniques: from bench to bedside.," *Journal of Clinical Monitoring and Computing*, 2020.

[35] W. Cobb, J. Burns, K. Kercher, B. Matthews, H. Norton, and T. Heniford, "Normal intraabdominal pressure in healthy adults," *Journal of Surgical Research*, vol. 129, no. 2, pp. 231–235, 2005.

[36] B. De Keulenaer, J. De Waele, B. Powell, and M. Malbrain, "What is normal intra-abdominal pressure and how is it affected by positioning, body mass and positive end-expiratory pressure?" *Applied Physiology in Intensive Care Medicine*, vol. 35, no. 6, pp. 219–226, 2012.

[37] J. Chionh, B. Wei, J. Martin, and H. Opdam, "Determining normal values for intra-abdominal pressure," *ANZ Journal of Surgery*, vol. 76, pp. 1106–1109, 2006.

[38] N. Sanchez, P. Tenofsky, J. Dort, L. Shen, S. Helmer, and R. Smith, "What is normal intra-abdominal pressure?" *American Journal of Surgery*, vol. 67, pp. 243–248, 2001.

[39] D. Vasquez, G. Berg-Copas, and R. Wetta-Hall, "Influence of semi-recumbent position on intra-abdominal pressure as measured by bladder pressure," *Journal of Surgical Research*, vol. 139, pp. 280–285, 2007.

[40] D. Lambert, S. Marceau, and R. Forse, "Intra-abdominal pressure in the morbidly obese," *Obesity Surgery*, vol. 15, pp. 1225–1232, 2005.

[41] B. Arfvidsson, B. Eklof, and J. Balfour, "Iliofemoral venous pressure correlates with intraabdominal pressure in morbidly obese patients," *Vascular and Endovascular Surgery*, vol. 39, pp. 505–509, 2005.

[42] P. Davis, S. Koottayi, A. Taylor, and W. Butt, "Comparison of indirect methods of measuring intra-abdominal pressure in children," *Intensive Care Medicine*, vol. 31, pp. 471–475, 2005.

[43] J. Ejike, K. Bahjri, and M. Mathur, "What is the normal intra-abdominal pressure in critically ill children and how should we measure it?" *Critical Care Medicine*, vol. 36, no. 7, pp. 2157–2162, 2008.

[44] F. Thabet and J. Ejike, "Intra-abdominal hypertension and abdominal compartment syndrome in pediatrics. A review," *Journal of Critical Care*, vol. 41, pp. 275–282, 2017.

[45] T. Papavramidis, A. Marinis, I. Pliakos, I. Kesisoglou, and N. Papavramidou, "Abdominal compartment syndrome - Intra-abdominal hypertension: Defining, diagnosing, and managing.," *Journal of Emergencies, Trauma, and Shock*, vol. 4, no. 2, pp. 279–91, 2011.

[46] A. Blaser, A. Regli, B. De Keulenaer, E. Kimball, L. Starkopf, W. Davis, P. Greiffenstein, and J. Starkopf, "Incidence, Risk Factors, and Outcomes of Intra-Abdominal Hypertension in Critically Ill Patients-A Prospective Multicenter Study (IROI Study)," *Critical Care Medicine*, vol. 47, no. 4, pp. 535–542, 2019.

[47] R. Milanesi and R. Caregnato, "Intra-abdominal pressure: An integrative review," *Einstein (Sao Paulo)*, vol. 14, no. 3, pp. 423–430, 2016.

[48] H. Sugerman, E. DeMaria, W. Felton, M. Nakatsuka, and A. Sismanis, "Increased intra-abdominal pressure and cardiac filling pressures in obesity associated pseudotumor cerebri," *Neurology*, vol. 49, no. 2, pp. 507–511, 1997.

[49] H. Sugerman, A. Windsor, M. Bessos, J. Kellum, H. Reines, and E. DeMaria, "Effects of surgically induced weight loss on urinary bladder pressure, sagittal abdominal diameter and obesity co-morbidity," *International Journal of Obesity*, vol. 22, pp. 230–235, 1997.

[50] A. Dejardin, A. Robert, and E. Goffin, "Intraperitoneal pressure in PD patients: Relationship to intraperitoneal volume, body size and PD-related complications," *Nephrology Dialysis Transplantation*, vol. 22, no. 5, pp. 1437–1444, 2007.

[51] M. Smit, M. Werner, O. Lansink-Hartgring, W. Dieperink, J. Zijlstra, and M. Van Meurs, "How central obesity influences intra-abdominal pressure: A prospective, observational study in cardiothoracic surgical patients," *Annals of Intensive Care*, vol. 6, no. 99, pp. 1–10, 2016.

[52] M. Cheatham, J. De Waele, I. De Laet, B. De Keulenaer, S. Widder, A. Kirkpatrick, A. Cresswell, M. Malbrain, Z. Bodnar, J. Mejia-Mantilla, R. Reis, M. Parr, R. Schulze, and S. Puig, "The impact of body position on intra-abdominal pressure measurement: A multi-center analysis," *Critical Care Medicine*, vol. 37, no. 7, pp. 2187–2190, 2009.

[53] J. Morris, D. Lucas, and B. Bresler, "Role of the trunk in stability of the spine," *The Journal of Bone and Joint Surgery*, vol. 43A, no. 3, pp. 327–351, 1961.

[54] A. Montgomery, "Parastomal Hernia," in *Textbook of Hernia*, W. Hope, W. Cobb, and G. Adrales, Eds., Switzerland: Springer International Publishing Switzerland, 2017, ch. 44, pp. 345–351. DOI: 10.1007/978-3-319-43045-4_44.

[55] H. Talasz, M. Kofler, and M. Lechleitner, "Misconception of the Valsalva maneuver," *International Urogynecological Journal*, vol. 22, pp. 1197–1198, 2011.

[56] A. Al-Khan, M. Shah, M. Altabban, S. Kaul, K. Dyer, M. Alvarez, and S. Saber, "Measurement of intraabdominal pressure in pregnant women at term," *Journal of Reproductive Medicine for the Obstetrician and Gynecologist*, vol. 56, no. 1-2, pp. 53–57, 2011.

[57] F. Beer, E. Johnston, J. DeWolf, and D. Mazurek, "Columns: Eccentric loading; the secant formula," in *Mechanics of Materials*, M. Lange, Ed., 6th ed., McGraw-Hill, 2012, ch. 10.5, pp. 649–654.

[58] P. Davis, "Intratruncal pressure mechanisms," *Ergonomics*, vol. 28, no. 1, pp. 293–297, 1985.

[59] G. Van Ramshorst, M. Salih, W. Hop, O. Van Waes, G. Kleinrensink, R. Goossens, and J. Lange, "Noninvasive assessment of intra-abdominal pressure by measurement of abdominal wall tension," *Journal of Surgical Research*, vol. 171, no. 1, pp. 240–244, 2011.

[60] Y. Chen, S. Yan, Y. Chen, Y. Zhuang, Z. Wei, S. Zhou, and H. Peng, "Noninvasive monitoring of intra-abdominal pressure by measuring abdominal wall tension," *World Journal of Emergency Medicine*, vol. 6, no. 2, pp. 137–141, 2015.

[61] M. Malbrain, I. De Laet, A. Willems, N. Van Regenmortel, K. Schoonheydt, and H. Dits, "Localised abdominal compartment syndrome: Bladder-over-gastric pressure ratio (B/G ratio) as a clue to diagnosis," *Acta Clinica Belgica*, vol. 65, no. 2, pp. 98–106, 2010.

[62] M. Freitag and V. Ramachandran, "What is normal blood pressure?" *Current Opinion in Nephrology and Hypertension*, vol. 12, no. 3, pp. 285–292, 2003.

[63] D. Hackett and C. Chow, "The Valsalva maneuver: Its effect on intra-abdominal pressure and safety issues during resistance exercise," *Journal of Strength and Conditioning Research*, vol. 27, no. 8, pp. 2338–2345, 2013.

[64] W. Addington, R. Stephens, M. Phelipa, J. Widdicombe, and R. Ockey, "Intra-abdominal pressures during voluntary and reflex cough," *Cough*, vol. 4, no. 1, pp. 1–9, 2008.

[65] C. Aquina, J. Iannuzzi, C. Probst, K. Kelly, K. Noyes, F. Fleming, and J. Monson, "Parastomal hernia: A growing problem with new solutions," *Digestive Surgery*, vol. 31, pp. 366–376, 2014.

[66] M. Cheatham, M. Malbrain, A. Kirkpatrick, M. Sugrue, M. Parr, J. De Waele, Z. Balogh, A. Leppaniemi, C. Olvera, R. Ivatury, S. D'Amours, J. Wendon, K. Hillman, and A. Wilmer, "Results from the international conference of experts on intra-abdominal hypertension and abdominal compartment syndrome. II. Recommendations," *Intensive Care Medicine*, vol. 33, pp. 951–962, 2007.

[67] J. Otto, D. Kaemmer, M. Binnebosel, M. Jansen, R. Dembinski, V. Schumpelick, and A. Schachtrupp, "Direct intra-abdominal pressure monitoring via piezoresistive pressure measurement: A technical note," *BMC Surgery*, vol. 9, no. 5, pp. 1–5, 2009.

[68] F. Pracca, A. Biestro, L. Moraes, C. Puppo, S. Calvo, J. Gorrasi, and M. Cancela, "Direct measurement of intra-abdominal pressure with a solid microtranducer," *Journal of Clinical Monitoring and Computing*, vol. 21, pp. 167–170, 2007.

[69] A. Al-Hwiesh, S. Al-Mueilo, I. Saeed, and F. Al-Muhanna, "Intraperitoneal pressure and intra-abdominal pressure: Are they the same?" *Peritoneal Dialysis International*, vol. 31, pp. 315–319, 2011.

[70] A. Al-Abassi, A. Al Saadi, and F. Ahmed, "Is intra-bladder pressure measurement a reliable indicator for raised intra-abdominal pressure? A prospective comparative study," *BMC Anesthesiology*, vol. 18, no. 69, pp. 1–9, 2018.

[71] L. Aguilera, L. Gallart, J. Alvarez, J. Valles, and J. Gea, "Rectal, central venous, gastric and bladder pressures versus esophageal pressure for the measurement of cough strength: A prospective clinical comparison," *Respiratory Research*, vol. 19, no. 191, pp. 1–7, 2018.

[72] J. De Waele, M. Cheatham, M. Malbrain, A. Kirkpatrick, M. Sugrue, B. Z., R. Ivatury, B. De Keulenaer, and E. Kimball, "Recommendations for research from the international conference of experts on intra-abdominal hypertension and abdominal compartment syndrome," *Acta Clinica Belgica*, vol. 64, no. 3, pp. 203–209, 2009.

[73] Y. Homma, J. Batista, S. Bauer, D. Griffiths, P. Hilton, G. Kramer, G. Lose, and P. Rosier, "Urodynamics," in *Incontinence*, Health Publication, Ltd., 2002, ch. 7, pp. 317–372.

[74] L. Leitner, M. Walter, U. Sammer, S. Knupfer, U. Mehnert, and T. Kessler, "Urodynamic investigation: A valid tool to define normal lower urinary tract function?" *PLOS One*, vol. 11, no. 10, pp. 1–15, 2016.

[75] National Kidney and Urologic Diseases Information Clearinghouse, "Urodynamic Testing," National Institutes of Health, Tech. Rep., 2014, NIH No. 12–5106.

[76] R. Lee, "Intra-abdominal hypertension and abdominal compartment syndrome: A comprehensive overview," *Critical Care Nurse*, vol. 32, pp. 19–31, 2012.

[77] J. Wauters, L. Spincemaille, A. Dieudonne, K. Van Zwam, A. Wilmer, and M. Malbrain, "A novel method (CiMON) for continuous intra-abdominal pressure monitoring: Pilot test in a pig model," *Critical Care Research and Practice*, vol. 2012, pp. 1–7, 2012.

[78] M. Sugrue, M. Buist, A. Lee, D. Sanchez, and K. Hillman, "Intra-abdominal pressure measurement using a modified nasogastric tube: Description and validation of a new technique," *Intensive Care Medicine*, vol. 20, pp. 588–590, 1994.

[79] A. Shafik, A. El-Sharkawy, and W. Sharaf, "Direct measurement of intra-abdominal pressure in various conditions," *European Journal of Surgery*, vol. 163, no. 12, pp. 883–887, 1997.

[80] M. Dowdle, "Evaluating a new intrauterine pressure catheter," *Journal of Reproductive Medicine for the Obstetrician and Gynecologist*, vol. 42, no. 8, pp. 506–513, 1997.

[81] S. Lacey, J. Bruce, S. Brooks, J. Griswald, W. Ferguson, J. Allen, T. Jewett, M. Karp, and D. Cooney, "The relative merits of various methods of indirect measurement of intraabdominal pressure as a guide to closure of abdominal wall defects," *Journal of Pediatric Surgery*, vol. 22, no. 12, pp. 1207–1211, 1987.

[82] P. Johnson, E. Rosenbluth, I. Nygaard, M. Parikh, and R. Hitchcock, "Development of a novel intra-vaginal transducer with improved dynamic response," *Biomedical Microdevices*, vol. 11, no. 6, pp. 1213–1221, 2009.

[83] T. Coleman, J. Thomsen, S. Maass, Y. Hsu, I. Nygaard, and R. Hitchcock, "Development of a wireless intra-vaginal transducer for monitoring intra-abdominal pressure in women," *Biomedical Microdevices*, vol. 14, no. 2, pp. 347–355, 2012.

[84] A. Bloch, M. Glas, A. Kohler, U. Baumann, and S. Jakob, "Noninvasive assessment of intra-abdominal pressure using ultrasound-guided tonometry: A proof-of-concept study," *Shock (Augusta, Ga.)*, vol. 50, no. 6, pp. 684–688, 2018.

[85] G. Van Ramshorst, J. Lange, R. Goossens, N. Agudelo, G. Kleinrensink, M. Verwaal, S. Flipsen, W. Hop, L. Wauben, and J. Jeekel, "Non-invasive measurement of intra-abdominal pressure: A preliminary study," *Physiological Measurement*, vol. 29, no. 8, 2008.

[86] M. David, A. Raviv, A. Peretz, U. Berkovich, and F. Pracca, "Towards a continuous non-invasive assessment of intra-abdominal pressure based on bioimpedance and microwave reflectometry: A pilot run on a porcine model," *Biomedical Signal Processing and Control*, vol. 44, pp. 96–100, 2018.

[87] M. David, A. Raviv, A. Guttel, V. Reyes, F. Simini, and F. Pracca, "Non-invasive indirect monitoring of intra-abdominal pressure using microwave reflectometry: system design and proof-of-concept clinical trial," *Journal of Clinical Monitoring and Computing*, 2020.

[88] S. Brown, "Mechanically relevant consequences of the composite laminate-like design of the abdominal wall muscles and connective tissues," *Medical Engineering and Physics*, vol. 34, pp. 521–523, 2012.

[89] O. Akkus, A. Oguz, M. Uzunlulu, and M. Kizilgul, "Evaluation of skin and subcutaneous adipose tissue thickness for optimal insulin injection," *Journal of Diabetes and Metabolism*, vol. 3, no. 8, pp. 1–5, 2012.

[90] D. Tran, D. Mitton, D. Voirin, F. Turquier, and P. Beillas, "Contribution of the skin, rectus abdominis and their sheaths to the structural response of the abdominal wall ex vivo," *Journal of Biomechanics*, vol. 47, no. 12, pp. 3056–3063, 2014.

[91] L. Astruc, M. De Meulaere, J. Witz, V. Novacek, F. Turquier, T. Hoc, and M. Brieu, "Characterization of the anisotropic mechanical behavior of human abdominal wall connective tissues," *Journal of the Mechanical Behavior of Biomedical Materials*, vol. 82, pp. 45–50, 2018.

[92] M. Korenkov, A. Beckers, J. Koebke, R. Lefering, T. Tiling, and H. Troidl, "Biomechanical and morphological types of the linea alba and its possible role in the pathogenesis of midline incisional hernia," *European Journal of Surgery*, vol. 167, pp. 909–914, 2001.

[93] M. Cardoso, "Experimental study of the human anterolateral abdominal wall: Biomechanical properties of fascia and muscles," Ph.D. dissertation, Universidade do Porto, 2012, pp. 7–16, 52.

[94] H. Abdelounis, S. Nicolle, M. Ottenio, P. Beillas, and D. Mitton, "Effect of two loading rates on the elasticity of the human anterior rectus sheath," *Journal of the Mechanical Behavior of Biomedical Materials*, vol. 20, pp. 1–5, 2013.

[95] P. Martins, E. Pena, N. Jorge, A. Santos, L. Santos, T. Mascarenhas, and B. Calvo, "Mechanical characterization and constitutive modelling of the damage process in rectus sheath," *Journal of the Mechanical Behavior of Biomedical Materials*, vol. 8, pp. 111–122, 2012.

[96] A. Kureshi, P. Vaiude, S. Nazhat, A. Petrie, and R. Brown, "Matrix mechanical properties of transversalis fascia in inguinal herniation as a model for tissue expansion," *Journal of Biomechanics*, vol. 41, no. 16, pp. 3462–3468, 2008.

[97] T. Wolloscheck, A. Gaumann, A. Terzic, A. Heintz, T. Junginger, and M. Konerding, "Inguinal hernia: Measurement of the biomechanics of the lower abdominal wall and the inguinal canal," *Hernia*, vol. 8, pp. 233–241, 2004.

[98] B. Hernandez-Gascon, A. Mena, E. Pena, G. Pascual, J. Bellon, and B. Calvo, "Understanding the passive mechanical behavior of the human abdominal wall," *Annals of Biomedical Engineering*, vol. 41, no. 2, pp. 433–444, 2012.

[99] E. Pena, B. Hernandez-Gascon, and B. Calvo, "Human abdomen: Mechanical modeling and clinical applications," in *Biomechanics of Living Organs*, 2017, ch. 12, pp. 267–285.

[100] P. Pachera, P. Pavan, S. Todros, C. Cavinato, C. Fontanella, and A. Natali, "A numerical investigation of the healthy abdominal wall structures," *Journal of Biomechanics*, vol. 49, no. 9, pp. 1818–1823, 2016.

[101] L. Tham, H. Lee, and C. Lu, "Cupping: From a biomechanical perspective," *Journal of Biomechanics*, vol. 39, pp. 2183–2193, 2006.

[102] C. Deeken and S. Lake, "Mechanical properties of the abdominal wall and biomaterials utilized for hernia repair," *Journal of the Mechanical Behavior of Biomedical Materials*, vol. 74, pp. 411–427, 2017.

[103] D. Grassel, A. Prescher, S. Fitzek, D. von Keyserlingk, and H. Axer, "Anisotropy of human linea alba: A biomechanical study," *Journal of Surgical Research*, vol. 124, pp. 118–125, 2005.

[104] G. Cooney, S. Lake, D. Thompson, R. Castile, D. Winter, and C. Simms, "Uniaxial and biaxial tensile stress-stretch response of human linea alba," *Journal of the Mechanical Behavior of Biomedical Materials*, vol. 63, pp. 134–140, 2016.

[105] A. Levillain, M. Orhant, F. Turquier, and T. Hoc, "Contribution of collagen and elastin fibers to the mechanical behavior of an abdominal connective tissue," *Journal of the Mechanical Behavior of Biomedical Materials*, vol. 61, pp. 308–317, 2016.

[106] A. Rath, P. Attali, J. Dumas, D. Goldlust, J. Zhang, and J. Chevrel, "The abdominal linea alba: An anatomo-radiologic and biomechanical study," *Journal of Clinical Anatomy*, vol. 18, pp. 281–288, 1996.

[107] A. Rath, J. Zhang, and J. Chevrel, "The sheath of the rectus abdominis muscle: an anatomical and biomechanical study," *Hernia*, vol. 1, pp. 139–142, 1997.

[108] M. Kirilova, S. Stoytchev, D. Pashkouleva, and V. Kavardzhikov, "Experimental study of the mechanical properties of human abdominal fascia," *Medical Engineering and Physics*, vol. 33, pp. 1–6, 2011.

[109] M. Kirilova-Doneva, D. Pashkouleva, and V. Kavardzhikov, "The effects of strain amplitude and localization on viscoelastic mechanical behaviour of human abdominal fascia," *Acta of Bioengineering and Biomechanics*, vol. 18, no. 4, pp. 127–133, 2016.

[110] Y. Yang, L. Wang, F. Yan, X. Xiang, Y. Tang, L. Zhang, J. Liu, and L. Qiu, "Determination of normal skin elasticity by using real-time shear wave elastography," *Journal of Ultrasound in Medicine*, vol. 37, no. 11, pp. 2507–2516, 2018.

[111] D. MacDonald, A. Wan, M. McPhee, K. Tucker, and F. Hug, "Reliability of abdominal muscle stiffness measured using elastography during trunk rehabilitation exercises," *Ultrasound in Medicine and Biology*, vol. 42, no. 4, pp. 1018–1025, 2016.

[112] D. Tran, F. Podwojewski, P. Beillas, M. Ottenio, D. Voirin, F. Turquier, and D. Mitton, "Abdominal wall muscle elasticity and abdomen local stiffness on healthy volunteers during various physiological activities," *Journal of the Mechanical Behavior of Biomedical Materials*, vol. 60, pp. 451–459, 2016.

[113] S. Todros, N. de Cesare, G. Concheri, A. Natali, and P. Pavan, "Numerical modelling of abdominal wall mechanics: The role of muscular contraction and intra-abdominal pressure," *Journal of the Mechanical Behavior of Biomedical Materials*, vol. 103, 2020.

[114] D. Francois, A. Pineau, and A. Zaoui, "Elastic Behaviour," in *Mechanical Behaviour of Materials*, 2nd ed., Springer, 2012, ch. 2, pp. 83–154.

[115] M. Konerding, M. Bohn, T. Wolloscheck, B. Batke, J. Holste, S. Wohlert, J. Trzewik, T. Forstemann, and C. Hartung, "Maximum forces acting on the abdominal wall: Experimental validation of a theoretical modeling in a human cadaver study," *Medical Engineering and Physics*, vol. 33, no. 6, pp. 789–792, 2011.

[116] K. Ramalingam, *Handbook of Mechanical Engineering Terms*. New Age International Ltd., 2009.

[117] A. Choi and Y. Zheng, "Estimation of Young's modulus and Poisson's ratio of soft tissue from indentation using two different-sized indentors: Finite element analysis of the finite deformation effect," *Medical and Biological Engineering and Computing*, vol. 43, no. 2, pp. 258–264, 2005.

[118] M. Lu, R. Mao, Y. Lu, L. Zheng, T. Wang, and S. Chen, "Quantitative imaging of Young's modulus of soft tissues from ultrasound water jet indentation: A finite element study," *Computational and Mathematical Methods in Medicine*, vol. 2012, pp. 1–6, 2012.

[119] W. Hayes, G. Herrmann, L. Mockros, and L. Keer, "Mathematical analysis for indentation tests of articular cartilage," *Journal of Biomechanics*, vol. 5, pp. 541–551, 1972.

[120] H. Woodard and D. White, "The composition of body tissues," *The British Journal of Radiology*, vol. 59, no. 708, pp. 1209–1219, 1986.

[121] D. Francois, A. Pineau, and A. Zaoui, "Viscoelasticity," in *Mechanical Behaviour of Materials*, 2nd ed., Springer, 2012, ch. 5, pp. 445–505.

[122] J. Konstantinova, G. Cotugno, P. Dasgupta, K. Althoefer, and T. Nanayakkara, "Palpation force modulation strategies to identify hard regions in soft tissue organs," *PLOS One*, vol. 12, pp. 1–24, 2017.

[123] M. Zugel, C. Maganaris, J. Wilke, K. Jurkat-Rott, W. Klingler, S. Wearing, T. Findley, M. Barbe, J. Steinacker, A. Vleeming, W. Bloch, R. Schleip, and P. Hodges, "Fascial tissue research in sports medicine: From molecules to tissue adaptation, injury and diagnostics: Consensus statement," *British Journal of Sports Medicine*, vol. 52, pp. 1–9, 2018.

[124] L. Chaitow, P. Coughlin, T. Findley, and T. Myers, "Fascial palpation," in *Fascia: The Tensional Network of the Human Body*, R. Schleip, T. Findley, and P. Huijing, Eds., 1st ed., Elsevier, 2012, ch. 6.2, pp. 269–277.

[125] J. Wilke, L. Vogt, T. Pfarr, and W. Banzer, "Reliability and validity of a semi-electronic tissue compliance meter to assess muscle stiffness," *Journal of Back and Musculoskeletal Rehabilitation*, vol. 31, no. 5, pp. 991–997, 2018.

[126] S. Agyapong-Badu, M. Warner, D. Samuel, and M. Stokes, "Practical considerations for standardized recording of muscle mechanical properties using a myometric device: Recording site, muscle length, state of contraction and prior activity," *Journal of Musculoskeletal Research*, vol. 21, no. 2, pp. 1–13, 2018.

[127] G. Tarsi, R. Gould, J. Chung, A. Xu, A. Bozkurt, and J. Butcher, "Method for non-optical quantification of in situ local soft tissue biomechanics," *Journal of Biomechanics*, vol. 46, no. 11, pp. 1938–1942, 2013.

[128] M. Kutz, "Measurement of Material Characteristics," in *Mechanical engineers handbook: Materials and engineering mechanics*, 4th, New Jersey: John Wiley and Sons, 2015, ch. 6, pp. 852–855.

[129] A. Peipsi, R. Kerpe, H. Jager, S. Soeder, C. Gordon, and R. Schleip, "Myoton Pro: A novel tool for the assessment of mechanical properties of fascial tissues," *Journal of Bodywork and Movement Therapies*, vol. 16, no. 4, p. 527, 2012.

[130] Y. Feng, Y. Li, C. Liu, and Z. Zhang, "Assessing the elastic properties of skeletal muscle and tendon using shearwave ultrasound elastography and MyotonPRO," *Nature: Scientific Reports*, vol. 8, pp. 1–9, 2018.

[131] Y. Zheng and Y. Huang, *Measurement of Soft Tissue Elasticity in Vivo: Techniques and Applications*. Taylor and Francis Group, 2016.

[132] Myoton AS, *MyotonPRO Digital Palpation User Manual*, Revision No. 20, 2020, 2010.

[133] B. Muller, J. Elrod, M. Pensalfini, R. Hopf, O. Distler, C. Schiestl, and E. Mazza, "A novel ultra-light suction device for mechanical characterization of skin," *PLOS ONE1*, vol. 13, no. 8, pp. 1–22, 2018.

[134] G. Wernicke, R. Rosenblatt, M. Rasca, P. Parhar, P. Christos, A. Fischer, B. Parashar, and D. Nori, "Quantitative assessment of radiation-induced fibrosis of the breast with tissue compliance meter, palpation, and radiological imaging: Preliminary results," *Breast Journal*, vol. 15, no. 6, pp. 583–592, 2009.

[135] N. Jacobson and M. Driscoll, "Mechanical deformation-based assessment methods," in *Fascia: The Tensional Network of the Human Body*, 2nd ed., ISBN: 978-070-207-1836-0 In Press, Elsevier, 2021, ch. 6.4, pp. 1–10.

[136] L. Draaijers, Y. Botman, F. Tempelman, R. Kreis, E. Middelkoop, and P. Van Zuijlen, "Skin elasticity meter or subjective evaluation in scars: A reliability assessment," *Burns*, vol. 30, pp. 109–114, 2004.

[137] R. Bayford and A. Tizzard, "Bioimpedance imaging: An overview of potential clinical applications," *Analyst*, vol. 137, pp. 4635–4643, 2012.

[138] R. Simon-Allue, B. Calvo, A. Oberai, and P. Barbone, "Towards the mechanical characterization of abdominal wall by inverse analysis," *Journal of the Mechanical Behavior of Biomedical Materials*, vol. 66, pp. 127–137, 2017.

[139] S. McAuliffe, K. McCreesh, H. Purtill, and K. O'Sullivan, "A systematic review of the reliability of diagnostic ultrasound imaging in measuring tendon size: Is the error clinically acceptable?" *Physical Therapy in Sport*, vol. 26, pp. 52–63, 2017.

[140] R. Sigrist, J. Liau, A. Kaffas, M. Chammas, and J. Willmann, "Ultrasound elastography: Review of techniques and clinical applications," *Theranostics*, vol. 7, no. 5, pp. 1303–1329, 2017.

[141] S. Hirsch, J. Braun, and I. Sack, "Introduction," in *Magnetic Resonance Elastography*, Wiley, 2017, pp. 1–5.

[142] K. Glaser and R. Ehman, "Perspectives on the development of elastography," in *Magnetic Resonance Elastography*, S. Venkeatesh and R. Ehman, Eds., New York: Springer New York, 2014, ch. 2, pp. 3–18.

[143] P. Yen, "Palpation sensitivity analysis of exploring hard objects under soft tissue," in *IEEE/ASME International Conference on Advanced Intelligent Mechatronics*, Kobe, Japan, 2003, pp. 1102–1106.

[144] K. Nichols and A. Okamura, "Methods to segment hard inclusions in soft tissue during autonomous robotic palpation," *IEEE Transactions on Robotics*, vol. 31, no. 2, pp. 344–354, 2015.

[145] H. Oflaz and O. Baran, "A new medical device to measure a stiffness of soft materials," *Acta of Bioengineering and Biomechanics*, vol. 16, no. 1, pp. 125–131, 2014.

[146] R. Williams, W. Ji, J. Howell, and R. Conatser, "Device for measurement of human tissue properties *in vivo*," *Journal of Medical Devices*, vol. 1, pp. 197–205, 2007.

[147] A. Nava, E. Mazza, F. Kleinermann, N. Avis, J. McClure, and M. Bajka, "Evaluation of the mechanical properties of human liver and kidney through aspiration experiments.," *Technology and Health Care*, vol. 12, pp. 269–280, 2004.

[148] S. Elahi, N. Connesson, G. Chagnon, and Y. Payan, "*In vivo* soft tissues mechanical characterization: Volume-based aspiration method validated on silicones," *Experimental Mechanics*, vol. 59, pp. 251–261, 2019.

[149] D. Valtorta and E. Mazza, "Dynamic measurements of soft tissue viscoelastic properties with a torsional resonator device," *Medical Image Analysis*, vol. 9, no. 5, pp. 481–490, 2005.

[150] N. Narayanan, A. Bonakdar, J. Dargahi, M. Packirisamy, and R. Bhat, "Design and analysis of a micromachined piezoelectric sensor for measuring the viscoelastic properties of tissues in minimally invasive surgery," *Smart Materials and Structures*, vol. 15, pp. 1684–1690, 2006.

[151] K. Moerman, C. Holt, S. Evans, and C. Simms, "Digital image correlation and finite element modeling as a method to determine mechanical properties of human soft tissue *in vivo*," *Journal of Biomechanics*, vol. 42, pp. 1150–1153, 2009.

[152] L. Zhang, S. Thakku, M. Beotra, M. Baskaran, T. Aung, J. Goh, N. Strouthidis, and M. Girard, "Verification of a virtual fields method to extract the mechanical properties of human optic nerve head tissues *in vivo*," *Biomechanics and Modeling in Mechanobiology*, vol. 16, no. 3, pp. 871–887, 2017.

[153] S. Bensamoun, L. Robert, G. Leclerc, L. Debernard, and F. Charleux, "Stiffness imaging of the kidney and adjacent abdominal tissues measured simultaneously using magnetic resonance elastography," *Clinical Imaging*, vol. 35, pp. 284–287, 2011.

[154] F. Dittmann, H. Tzschatzch, S. Hirsch, E. Barnhill, J. Braun, I. Sack, and J. Guo, "Tomoelastography of the abdomen: Tissue mechanical properties of the liver, spleen, kidney, and pancreas from single MR elastography scans at different hydration states," *Magnetic Resonance in Medicine*, vol. 78, pp. 976–983, 2017.

[155] T. Courtney, *Mechanical Behavior of Materials: Second Edition*, 2nd ed. Waveland Press, 2005, pp. 44–84.

[156] O. Yoshino, A. Quail, C. Oldmeadow, and Z. Balogh, "The interpretation of intra-abdominal pressures from animal models: The rabbit to human example," *Injury*, vol. 43, pp. 169–173, 2012.

[157] A. Vleeming, M. Schuenke, L. Danneels, and F. Willard, "The functional coupling of the deep abdominal and paraspinal muscles: the effects of simulated paraspinal muscle contraction on force transfer to the middle and posterior layer of the thoracolumbar fascia," *Journal of Anatomy*, vol. 225, pp. 447–462, 2014.

[158] K. El-Monajjed and M. Driscoll, "A finite element analysis of the intra-abdominal pressure and paraspinal muscle compartment pressure interaction through the thoracolumbar fascia," *Computer Methods in Biomechanics and Biomedical Engineering*, vol. 23, no. 10, pp. 585–596, 2020.

[159] I. El Bojairami, K. El-Monajjed, and M. Driscoll, "Development and validation of a timely and representative finite element human spine model for biomechanical simulations," *Scientific Reports*, vol. 10, no. 21519, pp. 1–15, 2020.

[160] E. Newell and M. Driscoll, "Investigation of physiological stress shielding within lumbar spinal tissue as a contributor to unilateral low back pain: A finite element study," *Computer in Biology and Medicine*, vol. 133, pp. 1–8, 2021.

[161] A. Warren, Z. LaCross, J. Volberding, and M. O'Brien, "Acute outcomes of myofascial decompression (cupping therapy) compared to self-myofascial release on hamstring pathology after a single treatment," *International Journal of Sports Physical Therapy*, vol. 15, pp. 579–592, 2020.

[162] A. Al-Shidhani and A. Al-Mahrezi, "The role of cupping therapy in pain management: A literature review," *InTech Open*, 2020.

[163] P. Moortgat, M. Anthonissen, J. Meirte, and K. Maertens, "The physical and physiological effects of vacuum massage on the different skin layers: a current status of the literature," *Burns and Trauma*, vol. 4, pp. 1–12, 2016.

[164] E. Rozenfeld and L. Kalichman, "New is the well-forgotten old: The use of dry cupping in musculoskeletal medicine," *Journal of Bodywork and Movement Therapies*, vol. 20, pp. 173–178, 2016.

[165] Y. Chiu, I. Manousakas, S. Kuo, J. Shiao, and C. Chen, "Influence of quantified dry cupping on soft tissue compliance in athletes with myofascial pain syndrome," *PLOS One*, vol. 15, pp. 1–15, 2020.

[166] W. Worret and B. Jessberger, "Effectiveness of LPG treatment in morphea," *Journal of the European Academy of Dermatology and Venereology*, vol. 18, pp. 527–530, 2004.

[167] C. DaPrato, R. Krug, R. Souza, and D. Motamedi, "The immediate and long-term effects of negative pressure soft tissue mobilization on the iliotibial bands of runners using magnetic resonance imaging," *Journal of Bodywork and Movement Therapies*, vol. 22, no. 4, p. 863, 2018.

[168] R. Stylinski, A. Alzubedi, and S. Rudzki, "Parastomal hernia - current knowledge and treatment," *Videosurgery and Other Miniinvasive Techniques*, vol. 1, pp. 1–8, 2018.

[169] S. Antoniou, F. Agresta, J. Garcia Alamino, D. Berger, F. Berrevoet, H. Brandsma, K. Bury, J. Conze, D. Cuccurullo, U. Dietz, R. Fortelny, C. Frei-Lanter, B. Hansson, F. Helgstrand, A. Hotouras, A. Janes, L. Kroese, J. Lambrecht, I. Kyle-Leinhase, M. Lopez-Cano, L. Maggiori, V. Mandala, M. Miserez, A. Montgomery, S. Morales-Conde, M. Prudhomme, T. Rautio, N. Smart, M. Smietanski, M. Szczepkowski, C. Stabilini, and F. Muysoms, "European Hernia Society guidelines on prevention and treatment of parastomal hernias," *Hernia*, vol. 22, pp. 183–198, 2018.

[170] P. Tenzel, D. Christian, J. Fischer, and W. Hope, "The Use of Prophylactic Mesh in the Prevention of Incisional and Parastomal Hernia Repair," in *Textbook of Hernia*, W. Hope, W. Cobb, and G. Adrales, Eds., Switzerland: Springer International Publishing Switzerland, 2017, ch. 26, pp. 195–199.

[171] F. Primiano, "Theoretical analysis of chest wall mechanics," *Journal of Biomechanics*, vol. 15, no. 12, pp. 919–931, 1982.

[172] I. Breslavsky, M. Amabili, and M. Legrand, "Static and dynamic behavior of circular cylindrical shell made of hyperelastic arterial material," *Journal of Applied Mechanics*, vol. 83, no. 5, pp. 1–12, 2016.

[173] B. Muvdi and J. W. McNabb, "Selected Topics," in *Engineering Mechanics of Materials*, 3rd ed., Springer New York, 1991, ch. 13, pp. 590–646.

[174] A. Flint, K. Rexrode, F. Hu, R. Glynn, H. Caspard, J. Manson, W. Willett, and E. Rimm, "Body mass index, waist circumference, and risk of coronary heart disease: a prospective study among men and women," *Obesity Research and Clinical Practice*, vol. 4, no. 3, pp. 171–181, 2010.

[175] C. Fryar, Q. Gu, and C. Ogden, "Anthropometric Reference Data for Children and Adults: United States, 2007–2010," U.S. Department of Health and Human Services, Tech. Rep., 2012, DHHS Publication No. (PHS) 2013–1602 1–40.

[176] N. Tahan, K. Khademi-Kalantari, M. Mohseni-Bandpei, S. Mikaili, A. Baghban, and S. Jaberzadeh, "Measurement of superficial and deep abdominal muscle thickness: An ultrasonography study," *Journal of Physiological Anthropology*, vol. 35, no. 17, pp. 1–5, 2016.

[177] D. Magee, "Lumbar Spine," in *Orthopedic Physical Assessment*, 6th ed., Saunders, 2014, ch. 9, pp. 550–648.

[178] F. Azadinia, E. Ebrahimi, M. Kamyab, M. Parnianpour, J. Cholewicki, and N. Maroufi, "Can lumbosacral orthoses cause trunk muscle weakness? A systematic review of literature," *The Spine Journal*, vol. 17, no. 4, pp. 589–602, 2016.

[179] J. Mens, G. Hoek van Dijke, A. Pool-Goudzwaard, V. van der Hulst, and H. Stam, "Possible harmful effects of high intra-abdominal pressure on the pelvic girdle," *Journal of Biomechanics*, vol. 39, pp. 627–635, 2006.

[180] D. Theret, M. Levesque, M. Sato, R. Nerem, and L. Wheeler, "The application of a homogeneous half-space model in the analysis of endothelial cell micropipette measurements," *Journal of Biomechanical Engineering*, vol. 110, no. 3, pp. 190–199, 1988.

[181] M. Kuyumcu, M. Halil, O. Kara, B. Cunib, G. Caglayan, S. Guven, Y. Yesil, G. Arik, B. Yavuz, M. Cankurtaran, and L. Ozcakar, "Ultrasonographic evaluation of the calf muscle mass and architecture in elderly patients with and without sarcopenia," *Archives of Gerentology and Geriatrics*, vol. 65, pp. 218–224, 2016.

[182] T. Boudou, J. Ohayon, Y. Arntz, G. Finet, C. Picart, and P. Tracqui, "An extended modeling of the micropipette aspiration experiment for the characterization of the Young's modulus and Poisson's ratio of adherent thin biological samples: Numerical and experimental studies," *Journal of Biomechanical Engineering*, vol. 39, no. 9, pp. 1677–1685, 2006.

[183] R. Drillis and R. Contini, "Body Segment Parameters," Office of Vocational Rehabilitation, New York, Tech. Rep., 1966, Report 1166–03.

[184] D. Adcock, S. Paulsen, K. Jabour, S. Davis, L. Nanney, and R. Shack, "Analysis of the effects of deep mechanical massage in the porcine model," *Plastic Reconstructive Surgery*, vol. 108, no. 1, pp. 233–240, 2001.

[185] M. Zhang, Y. Zheng, and A. Mak, "Estimating the effective Young's modulus of soft tissues from indentation tests—nonlinear finite element analysis of effects of friction and large deformation," *Medical Engineering and Physics*, vol. 19, no. 6, pp. 512–517, 2006.

[186] R. Shedge, K. Krishan, V. Warrier, and T. Kanchan, *Postmortem changes*. StatPearls Publishing, 2021.

[187] K. He, X. Zhou, Y. Zhu, B. Wang, X. Fu, Q. Yao, H. Chen, and X. Wang, "Muscle elasticity is different in individuals with diastasis recti abdominis than healthy volunteers," *Insights into Imaging*, vol. 12, no. 87, pp. 1–11, 2021.

[188] D. Chmielewska, M. Stania, G. Sobota, K. Kwasna, E. Blaszczak, J. Taradaj, and G. Juras, "Impact of different body positions on bioelectrical activity of the pelvic floor muscles in nulliparous continent women," *Biomedical Research International*, vol. 2015, pp. 1–9, 2015.

[189] H. Hencky, "On the stress state in circular plates with vanishing bending stiffness," *Zeitschrift fur Mathematik und Physik*, vol. 63, pp. 311–317, 1915.

[190] J. Sun, Y. Lian, Y. Li, X. He, and Z. Zheng, "Closed-form solution of elastic circular membrane with initial stress under uniformly-distributed loads: Extended Hencky solution," *ZAMM Zeitschrift fur Angewandte Mathematik und Mechanik*, vol. 95, no. 11, pp. 1335–1341, 2015.

[191] W. Fichter, "Some Solutions for the Large Deflections of Uniformly Loaded Circular Membranes," *NASA Technical Paper*, vol. 3658, 1997.

[192] S. Timoshenko and J. Goodier, *Theory of Elasticity*. McGraw-Hill International Editions, 1970.

[193] M. Malbrain, D. Roberts, M. Sugrue, B. De Keulenaer, R. Ivatury, P. Pelosi, F. Verbrugge, R. Wise, and W. Mullens, "The polycompartment syndrome: A concise state-of-the-art review," *Anesthesiology Intensive Therapy*, vol. 46, no. 5, pp. 433–450, 2014.

[194] S. Ben-Haim and G. Saidel, "Mathematical model of chest wall mechanics: A phenomenological approach," *Annals of Biomedical Engineering*, vol. 18, pp. 37–56, 1990.

[195] S. Parker, C. Wood, D. Sanders, and A. Windsor, "Nomenclature in abdominal wall hernias: Is it time for consensus?" *World Journal of Surgery*, vol. 41, pp. 2488–2491, 2017.

[196] D. Bartelink, "Role of abdominal pressure in relieving the pressure on the lumbar intervertebral discs," *Journal of Bone and Joint Surgery*, vol. 39B, no. 4, pp. 718–725, 1957.

[197] S. Strong, "The difficult stoma: Challenges and strategies," *Clinical Colon and Rectal Surgery*, vol. 29, pp. 152–159, 2016.

[198] J. Basford, "The Law of Laplace and its relevance to contemporary medicine and rehabilitation," *Archives of Physical Medicine and Rehabilitation*, vol. 83, no. 8, pp. 1165–1170, 2002.

[199] F. Podwojewski, M. Ottenio, P. Beillas, G. Guerin, F. Turquier, and D. Mitton, "Mechanical response of human abdominal walls *ex vivo*: Effect of an incisional hernia and a mesh repair," *Journal of the Mechanical Behavior of Biomedical Materials*, vol. 38, pp. 126–133, 2014.

[200] M. Panjabi, "Clinical spinal instability and low back pain," *Journal of Electromyography and Kinesiology*, vol. 13, no. 4, pp. 371–379, 2003.

[201] A. White, R. Johnson, M. Panjabi, and W. Southwick, "Biomechanical analysis of clinical instability in the cervical spine," *Clinical Orthopaedics and Related Research*, vol. 109, pp. 85–96, 1975.

[202] M. Lu, W. Yu, Q. Huang, Y. Huang, and Y. Zheng, "A hand-held Indentation system for the assessment of mechanical properties of soft tissues *in vivo*," *IEEE Transactions on Instrumentation and Measurement*, vol. 58, no. 9, pp. 3079–3085, 2009.

[203] C. Lung, Y. Jan, J. Lu, C. Chen, F. Kuo, and B. Liau, "The Evaluation of Mechanical Properties of Soft Tissue on Pressure Ulcers Among Bedridden Elderly Patients," in *Advances in Physical Ergonomics and Human Factors*, R. S. Goonetilleke and W. Karwowski, Eds., Springer International Publishing, 2020, pp. 360–368.

[204] J. Kottner, S. Brorson, A. Donner, and B. Gajewski, "Guidelines for reporting reliability and agreement studies (GRRAS) were proposed," *Journal of Clinical Epidemiology*, vol. 64, pp. 96–106, 2015.

[205] C. Sessler, M. Gosnell, M. Grap, G. Brophy, P. O'Neal, K. Keane, E. Tesoro, and R. Elswick, "The Richmond Agitation–Sedation Scale," *American Journal of Respiratory and Critical Care Medicine*, vol. 166, no. 10, pp. 1338–1344, 2002.

[206] J. Fleiss, "Reliability of Measurement," in *The Design and Analysis of Clinical Experiments*, New York: John Wiley and Sons Inc., 1986, ch. 1, pp. 1–32.

[207] J. Cohen, "The Significance of a Product Moment," in *Statistical Power Analysis for the Behavioral Sciences*, 2nd ed., Lawrence Erlbaum Associates, 1988, ch. 3, pp. 75–105.

[208] S. Walter, M. Eliasziw, and A. Donner, "Sample size and optimal designs for reliability studies," *Statistics in Medicine*, vol. 17, pp. 101–110, 1998.

[209] P. Yock, S. Zenios, J. Makower, T. Brinton, U. Kumar, and F. Watkins, "Part II: Invent," in *Biodesign: the process of innovating medical technologies*, 2nd ed., Cambridge University Press, 2015, ch. 3-4, pp. 249–449.

[210] R. Miller, A. Kolipaka, M. Nash, and A. Young, "Relative identifiability of anisotropic properties from magnetic resonance elastography," *NMR in Biomedicine*, vol. 31, pp. 1–12, 2018.

[211] J. Kuteesa, O. Kituuka, D. Namuguzi, C. Ndikuno, S. Kirunda, D. Mukunya, and M. Galukande, "Intra-abdominal hypertension; prevalence, incidence and outcomes in a low resource setting; a prospective observational study," *World Journal of Emergency Surgery*, vol. 10, no. 57, pp. 1–9, 2015.

[212] M. Driscoll and L. Blyum, "Investigation of the inter-dependence between intra-abdominal pressure and spinal stability," *Clinical Biomechanics*, vol. 69, pp. 164–167, 2019.

[213] A. Handorf, Y. Zhou, M. Halanski, and W. Li, "Tissue stiffness dictates development, homeostasis, and disease progression," *Organogenesis*, vol. 11, pp. 1–15, 2015.

[214] O. Gozubuyuk, S. Devran, and M. Akikol, "The effects of dry cupping therapy on muscle thickness and elasticity of upper back muscles," *Journal of Bodywork and Movement Therapies*, vol. 22, p. 851, 2018.

[215] J. Saeki, M. Nakamura, S. Nakao, K. Fujita, K. Yanase, and N. Ichihashi, "Muscle stiffness of posterior lower leg in runners with a history of medial tibial stress syndrome," *Scandinavian Journal of Medical Science in Sport*, vol. 28, no. 1, pp. 246–251, 2018.

[216] S. Ohya, M. Nakamura, T. Aoki, D. Suzuki, T. Kikumoto, E. Nakamura, W. Ito, R. Hirabayashi, T. Takabayashi, and M. Edama, "The effect of a running task on muscle shear elastic modulus of posterior lower leg," *Journal of Foot and Ankle Research*, vol. 10, no. 56, pp. 246–251, 2017.

[217] K. Chino and H. Takahashi, "Measurement of gastrocnemius muscle elasticity by shear wave elastography: association with passive ankle joint stiffness and sex differences," *European Journal of Physiology*, vol. 116, no. 4, pp. 823–830, 2016.

[218] J. Zhou, J. Yu, C. Liu, C. Tang, and Z. Zhang, "Regional elastic properties of the Achilles tendon is heterogeneously influenced by individual muscle of the gastrocnemius," *Applied Bionics and Biomechanics*, vol. 2019, pp. 1–10, 2019.

[219] J. Zhou, J. Yu, Y. Feng, C. Liu, P. Su, S. Shen, and Z. Zhang, "Modulation in the elastic properties of gastrocnemius muscle heads in individuals with plantar fasciitis and its relationship with pain," *Nature Scientific Reports*, vol. 10, no. 2770, pp. 1–8, 2020.

[220] P. Sahoo, "Tribology Measurements," in *Mechanical Engineers Handbook: Materials and Engineering Mechanics*, M. Kutz, Ed., John Wiley and Sons, 2015, pp. 837–860.

[221] N. Jacobson and M. Driscoll, "Design Synthesis and Preliminary Evaluation of a Novel Tool to Non-Invasively Characterize Pressurized, Physiological Vessels," *Journal of Medical Devices*, vol. 15, no. 2, pp. 1–7, 2020.

[222] J. Kottner, S. Brorson, A. Donner, and B. Gajewski, "Guidelines for reporting reliability and agreement studies (GRRAS) were proposed," *Journal of Clinical Epidemiology*, vol. 64, no. 1, pp. 96–106, 2011.

[223] T. Koo and M. Li, "A guideline of selecting and reporting intraclass correlation coefficients for reliability research," *Journal of Chiropractic Medicine*, vol. 15, no. 2, pp. 155–163, 2016.

[224] P. Lee, C. Liu, C. Fan, C. Lu, W. Lu, and C. Hsieh, "The test-retest reliability and the minimal detectable change of the Purdue pegboard test in schizophrenia," *Journal of the Formosan Medical Association*, vol. 112, no. 6, pp. 332–337, 2013.

[225] M. Mukaka, "Statistics corner: A guide to appropriate use of correlation coefficient in medical research," *Malawi Medical Journal*, vol. 24, no. 3, pp. 69–71, 2012.

[226] F. Angst, M. Verra, S. Lehmann, and A. Aeschlimann, "Responsiveness of five condition-specific and generic outcome assessment instruments for chronic pain," *BMC Medical Research Methodology*, vol. 8, no. 26, pp. 1–8, 2008.

[227] I. Gilbert, N. Gaudreault, and I. Gaboury, "Intra- and inter-evaluator reliability of the MyotonPRO for the assessment of the viscoelastic properties of caesarean section scar and unscarred skin," *Skin Research and Technology*, 2020.

[228] D. Bonett and T. Wright, "Sample size requirements for estimating Pearson, Spearman and Kendall correlations," *Psychometrika*, vol. 65, no. 1, pp. 23–28, 2000.

[229] J. Husted, R. Cook, V. Farewell, and D. Gladman, "Methods for assessing responsiveness: a critical review and recommendations," *Journal of Clinical Epidemiology*, vol. 53, no. 5, pp. 459–468, 2000.

[230] M. David, A. Raviv, U. Berkovich, and F. Pracca, "A numerical analysis towards the continuous non-invasive assessment of intra-abdominal pressure in critical patients based on bioimpedance and microwave reflectometry," in *2017 IEEE Biomedical Circuits and Systems Conference (BioCAS)*, IEEE, 2017.

[231] A. Kett and F. Sichting, "Sedentary behaviour at work increases muscle stiffness of the back: Why roller massage has potential as an active break intervention," *Applied Ergonomics*, vol. 82, pp. 1–6, 2020.

A Appendix

A.1 Hencky Solution Derivation

Section 3 describes the Hencky solution [189] as a means of evaluating underlying pressures. The derivation of said formula is explored in the following. It should be noted that Sun *et al*.'s work was largely extrapolated for its derivation of the extended Hencky problem, in which pre-stress exists in the membrane [190]. Figure A.1.1 illustrates the presented problem.

The Hencky solution assumes: [190], [191]

- Initially flat, circular membrane
- Linear elastic material
- Rotationally symmetric
- Taut membrane
- Transverse uniformly distributed load
- Fixed perimeter (clamped at its bounds)
- Pre-tension exists - this is the expansion of the original Hencky equation of interest in the present work.
- Plane stress: stress vector is 0 along the z-plane
- Large deflections

Variables considered are:

- Young's modulus of membrane material = E
- Poisson's ratio of membrane material = ν
- Thickness of membrane = h
- Radius of membrane = a
- Uniformly distributed load = q
- Stress, radial and tangential = σ_r and σ_t, respectively

- Strain, radial and tangential = ε_{r} and ε_{t}, respectively
- Position along the radial axis = r
- Position along the tangential axis = $w(r)$
- Initial distension, radially, due to pre-tension = u_0
- Radial displacement = u.

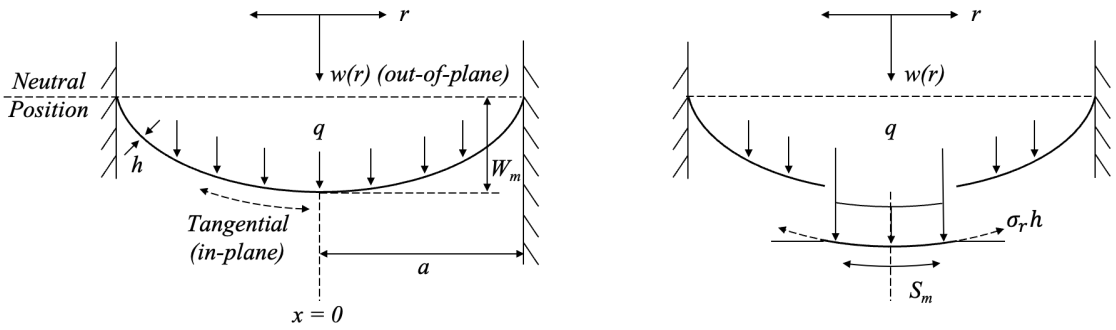

Figure A.1.1: Free body diagram of the extended Hencky problem, largely adapted from Sun et al. [190]. The left presents the general problem geometry, whereas the right image resects the center portion of the curve to elaborate on forces found along the length of the membrane.

From Timoshenko and Goodier's *Theory of Elasticity*, let us consider a unit that undergoes deformation u and v in the radial and tangential directions, respectively, in polar coordinates [192]. Thus, the unit elongation (strain) of a point along the membrane in the radial direction (out-of-plane) is

$$\varepsilon_{\mathrm{r}} = u + \frac{1}{dr}\frac{du}{dr}. \tag{A.1.1}$$

Considering the present problem's geometry and variables, this equation adjusts to

$$\varepsilon_{\mathrm{r}} = \frac{du}{dr} + \frac{1}{2}(\frac{dw}{dr})^2. \tag{A.1.2}$$

The unit elongation of a unit along the membrane in the tangential direction (in-plane), assuming only the effect of deformation u is

$$\varepsilon_{\theta} = \frac{u}{r}. \tag{A.1.3}$$

Again, with the present problem's geometry and variables, this equation adjusts to

$$\varepsilon_{\mathrm{t}} = \frac{u}{r}. \tag{A.1.4}$$

The equilibrium equations of the present problem, according to Timoshenko and Goodier, is [192]

$$\begin{aligned} &\frac{d\sigma_{\mathrm{r}}}{dr} + \frac{1}{r}\frac{d\tau_{\mathrm{r}\theta}}{d\theta} + \frac{(\sigma_{\mathrm{r}} - \sigma_{\theta})}{r} + R = 0 \\ &\frac{1}{r}\frac{d\sigma_{\theta}}{d\theta} + \frac{d\tau_{\mathrm{r}\theta}}{dr} + \frac{2\tau_{\mathrm{r}\theta}}{r} + S = 0. \end{aligned} \tag{A.1.5}$$

In the present problem, there exists no shear (τ), and $R = S = 0$. Thus, simplifying yields the equilibrium equations:

$$\begin{aligned} &\sigma_{\theta} = \frac{dr\sigma_{\mathrm{r}}}{dr} \\ &\frac{1}{r}\frac{d\sigma_{\theta}}{d\theta} = 0 \end{aligned} \tag{A.1.6}$$

Reorganizing for the present geometry and variables gives the in-plane equilibrium equation:

$$0 = \frac{drh\sigma_{\mathrm{r}}}{dr} - h\sigma_{\mathrm{t}}. \tag{A.1.7}$$

If we consider a force balance of problem along the $w(r)$ axis, the equilibrium equation for out-of-plane relations may be written:

$$\sigma_{\mathrm{r}} h\frac{dw}{dr} = \frac{-qr}{2}. \tag{A.1.8}$$

Under plane stress, Hooke's law simplifies to:

$$\begin{aligned} \sigma_{\mathrm{r}} &= \frac{E(\varepsilon_{\mathrm{r}} + \nu\varepsilon_{\mathrm{t}})}{(1-\nu^2)}, \\ \sigma_{\mathrm{t}} &= \frac{E(\nu\varepsilon_{\mathrm{r}} + \varepsilon_{\mathrm{t}})}{(1-\nu^2)}, \textit{and} \\ \tau_{\mathrm{rt}} &= \frac{E(\varepsilon_{\mathrm{rt}})}{(1+\nu)}. \end{aligned} \tag{A.1.9}$$

The final equation needed to evaluate the given problem is the compatibility equation. In

polar coordinates, the general relation is expressed as

$$\frac{1}{r^2}\frac{d^2\varepsilon_{\mathrm{r}}}{d\theta^2}+\frac{d^2\varepsilon_{\theta}}{dr^2}-\frac{2}{r}\frac{d^2\varepsilon_{\mathrm{r}\theta}}{drd\theta}-\frac{1}{r}\frac{d\varepsilon_{\mathrm{r}}}{dr}+\frac{2}{r}\frac{d\varepsilon_{\theta}}{dr}-\frac{2}{r^2}\frac{d\varepsilon_{\mathrm{r}\theta}}{d\theta}=0. \tag{A.1.10}$$

Here, this simplifies to

$$r\frac{d}{dr}\{\frac{1}{r}\frac{d}{dr}(r^2h\sigma_{\mathrm{r}})\}+\frac{Eh}{2}(\frac{dw}{dr})^2=0. \tag{A.1.11}$$

Let the following non-dimensional variables be introduced:

$$\begin{aligned} Q &= \frac{a^4q}{Eh^4},\\ W &= \frac{w}{h},\\ S_{\mathrm{r}} &= \frac{a^2\sigma_{\mathrm{r}}}{Eh^2},\\ S_{\mathrm{t}} &= \frac{a^2\sigma_{\mathrm{t}}}{Eh^2}, and\\ x &= \frac{r^2}{a^2}. \end{aligned} \tag{A.1.12}$$

Using Eq. A.1.8 and A.1.7, and combining with Eq. A.1.11 and A.1.12, the following transformation can be made:

$$S_{\mathrm{r}}\frac{dW}{dx}=-\frac{Q}{4}, \tag{A.1.13}$$

$$\frac{d^2}{dx^2}(xS_{\mathrm{r}})+\frac{1}{2}(\frac{dW}{dx})^2=0, \tag{A.1.14}$$

and

$$S_{\mathrm{t}}=S_{\mathrm{r}}+2x\frac{dS_{\mathrm{r}}}{dx} \tag{A.1.15}$$

Also of note are the boundary conditions of the problem, such that at $r = a$, $w(a)$ and $u(a)$ = 0. Further, at $r = 0$, $dw/dr = 0$, and $u(0) = u_0$. Evaluating Eq. A.1.2 and A.1.4 at $r = 0$ gives

$$\begin{aligned} \varepsilon_{\mathrm{r}} &= \frac{du}{dr}\\ \varepsilon_{\mathrm{t}} &= \frac{u}{r}. \end{aligned} \tag{A.1.16}$$

Adding Eq. A.1.16 to Eq. A.1.9 results in

$$\begin{aligned}\sigma_r &= \frac{E}{1-\nu^2}(\frac{du}{dr}+\nu\frac{u}{r})\\ \sigma_t &= \frac{E}{1-\nu^2}(\nu\frac{du}{dr}+\frac{u}{r}).\end{aligned} \tag{A.1.17}$$

Inserting into Eq. A.1.7 gives

$$r^2\frac{d^2u}{dr^2}+r\frac{du}{dr}-u=0. \tag{A.1.18}$$

To solve Eq. A.1.18, the boundary conditions, $u(0) = 0$ and $u(a) = u_0$ must be considered. This results in

$$\frac{u(r)}{r}=\frac{u_0}{a}. \tag{A.1.19}$$

Inserting into Eq. A.1.16 and A.1.17 gives the initial conditions of the problem (that is, ε_0 and σ_0):

$$\begin{aligned}\varepsilon_0 &= \varepsilon_r = \varepsilon_t = \frac{u_0}{a}\\ \sigma_0 &= \sigma_r = \sigma_t = \frac{E}{1-\nu}\frac{u_0}{a}\end{aligned} \tag{A.1.20}$$

Sun *et al*. now introduce a proportional coefficient, γ: [190]

$$\frac{\sigma_0}{E}=\gamma\frac{1}{2}(\frac{q\pi a^2}{2\pi ahE})^{2/3} \tag{A.1.21}$$

This allows Eq. A.1.20 to be rewritten

$$\varepsilon_0=(1-\nu)\gamma\frac{h^2}{2a^2}(\frac{Q}{2})^{2/3}, \tag{A.1.22}$$

which equates to u/r, when $W = 0$ at $x = 1$.

Now, let $xS_r = (Q/2)^{2/3}Z/2$ to create

$$\frac{d^2Z}{dx^2}+\frac{x^2}{Z^2}=0. \tag{A.1.23}$$

From Sun *et al*., the power series expansion for Eq. A.1.23 is [190]

$$Z(x) = c^{-4/3}(cx)f(cx) \tag{A.1.24}$$

where c in an unknown constant, and $f(x)$ expands to

$$\begin{aligned} f(x) = 1 &- \frac{1}{2}x - \frac{1}{6}x^2 - \frac{13}{144}x^3 - \frac{17}{288}x^4 \\ &- \frac{37}{864}x^5 - \frac{1205}{36288}x^6 - \frac{219241}{8128512}x^7 - \frac{6634069}{292626432}x^8 \\ &- \frac{51523763}{2633637888}x^9 - \frac{998796305}{57940033536}x^{10} - \frac{118156790413}{7648084426752}x^{11} + ... \end{aligned} \tag{A.1.25}$$

Combining Eq. A.1.24 and A.1.15 gives

$$\begin{aligned} S_\mathrm{r} &= (\frac{Q}{2})^{2/3}\frac{1}{2c^{1/3}}f(cx) \\ S_\mathrm{t} &= (\frac{Q}{2})^{2/3}\{\frac{1}{2c^{1/3}}f(cx) + c^{2/3}xf'(cx)\} \end{aligned} \tag{A.1.26}$$

Returning to Eq. A.1.22,

$$\frac{u}{r} = \frac{h^2}{2a^2c}(\frac{Qc}{2})^{2/3}(2cxf'(cx) + (1-\nu)f(cx)). \tag{A.1.27}$$

Using Eq. A.1.13, the following equation can also be obtained:

$$W = -(\frac{Qc}{2})^{1/3}g(cx)x + A \tag{A.1.28}$$

where A, similarly to c, is an unknown constant, and $g(x)$ is

$$\begin{aligned} g(x) = 1 &+ \frac{1}{4}x + \frac{5}{36}x^2 + \frac{55}{576}x^3 + \frac{7}{96}x^4 \\ &+ \frac{205}{3456}x^5 + \frac{17051}{338688}x^6 - \frac{2864485}{65028096}x^7 + \frac{103863265}{2633637888}x^8 \\ &+ \frac{27047983}{752467968}x^9 + \frac{42367613873}{1274680737792}x^{10} + \frac{14561952041}{468250066944}x^{11} + ... \end{aligned} \tag{A.1.29}$$

Combining Eq. A.1.27, A.1.28, and A.1.22 results in

$$v(f(c) - \gamma c^{1/3}) = 2cf'(c) + f(c) - \gamma c^{1/3}, \tag{A.1.30}$$

as well as,

$$A = (\frac{Qc}{2})^{1/3} g(c). \tag{A.1.31}$$

What may be of most value when evaluating a given problem are the stress and deformation maxima at $x = 0$ (S_{m} and W_{m}, respectively):

$$S_{\mathrm{m}} = (\frac{Q}{2})^{2/3} \frac{1}{2c^{1/3}} \tag{A.1.32}$$

and

$$W_{\mathrm{m}} = (\frac{Q}{2})^{1/3} c^{1/3} g(c). \tag{A.1.33}$$

The values needed at the onset of a problem to be able to solve it completely are: ν, σ_0, and q.

A.2 International Review Board Approvals

Ethical approval was sought for the clinical studies completed in Sections 4 and 5. As such, the official approvals for each study and their associated amendments are appended. To note, A12-M63-19A refers to the study of Section 4 which included 3 approved amendments prior to completing the study. A09-M59-20B refers to the approval for the study in Section 5, for which no amendments were required.

McGill

Faculty of Medicine
3655 Promenade Sir William Osler #633
Montreal, QC, H3G 1Y6

Faculté de médecine
3655, promenade Sir William Osler #633
Montréal, QC H3G 1Y6

Fax/Télécopieur:
(514) 398-3870
Tél/Tel: (514) 398-3124

December 18, 2019

Dr. Mark Driscoll
Department of Mechanical Engineering
Macdonald Engineering Bulding - Room 153
Montreal, Quebec H3A 0C3

RE: IRB Review Number: A12-M63-19A (19-12-043)

Novel device for the non-invasive measurement of abdominal wall elasticity

Dear Dr. Driscoll,

Thank you for submitting on behalf of your PhD candidates Natasha Jacobson and Trevor Cotter, the above-referenced study for an ethics review.

As this study involves no more than minimal risk, and in accordance with Articles 2.9 and 6.12 of the 2nd Edition of the Canadian Tri-Council Policy Statement of Ethical Conduct for Research Involving Humans (TCPS 2 2018) and U.S. Title 45 CFR 46, Section 110 (b), paragraph (1), we are pleased to inform you that approval for the study and consent form (version 1.0 dated 19/11/2019) was provided by an expedited/delegated review on 18-Dec-2019, valid until **17-Dec-2020**. The study proposal will be presented for corroborative approval at the next meeting of the Committee.

Prior to initiating the study, please revise the contact information in the consent form from Lynda McNeil to: **McGill Ethics Officer, Ilde Lepore at 514-398-8302 or ilde.lepore@mcgill.ca.**

The Faculty of Medicine Institutional Review Board (IRB) is a registered University IRB working under the published guidelines of the Tri-Council Policy Statement 2, in compliance with the Plan d'action ministériel en éthique de la recherche et en intégrité scientifique (MSSS, 1998), and the Food and Drugs Act (17 June 2001); and acts in accordance with the U.S. Code of Federal Regulations that govern research on human subjects (**FWA 00004545**). The IRB working procedures are consistent with internationally accepted principles of good clinical practice.

The Principal Investigator is required to immediately notify the Institutional Review Board Office, via amendment or progress report, of:

- Any significant changes to the research project and the reason for that change, including an indication of ethical implications (if any);
- Serious Adverse Effects experienced by participants and the action taken to address those effects;
- Any other unforeseen events or unanticipated developments that merit notification;
- The inability of the Principal Investigator to continue in her/his role, or any other change in research personnel involved in the project;
- A delay of more than 12 months in the commencement of the research project, and;
- Termination or closure of the research project.

The Principal Investigator is required to submit an annual progress report (continuing review application) on the anniversary of the date of the initial approval (or see the date of expiration).

The Faculty of Medicine IRB may conduct an audit of the research project at any time.

If the research project involves multiple study sites, the Principal Investigator is required to report all IRB approvals and approved study documents to the appropriate Research Ethics Office (REO) or delegated authority for the participating study sites. Appropriate authorization from each study site must be obtained before the study recruitment and/or testing can begin at that site. Research funds linked to this research project may be withheld and/or the study data may be revoked if the Principal Investigator fails to comply with this requirement. A copy of the study site authorization should be submitted the IRB Office.

It is the Principal Investigator's responsibility to ensure that all researchers associated with this project are aware of the conditions of approval and which documents have been approved.

The McGill IRB wishes you and your colleagues every success in your research.

Sincerely,

Roberta Palmour, PhD
Chair
Institutional Review Board

cc: Natasha Jacobson, Trevor Cotter
Sylvain Baillet, Associate Dean, Research
A12-M63-19A (19-12-043)

McGill

Faculty of Medicine
3655 Promenade Sir William Osler #633
Montreal, QC, H3G 1Y6

Faculté de médecine
3655, promenade Sir William Osler #633
Montréal, QC H3G 1Y6

Fax/Télécopieur:
(514) 398-3870
Tél/Tel: (514) 398-3124

March 10, 2020

Dr. Mark Driscoll
Department of Mechanical Engineering
Macdonald Engineering Bulding - Room 153
Montreal, Quebec H3A 0C3

RE: IRB Review Number: A12-M63-19A (19-12-043)

Novel device for the non-invasive measurement of abdominal wall elasticity

Dear Dr. Driscoll,

Thank you for submitting on behalf of your PhD candidates Natasha Jacobson and Trevor Cotter, an amendment to the above-referenced study.

At a meeting on March 9, 2020, the following amendment and documents received full Board review and approval:

- Addition of measurements at standing and sitting positions, in addition to the existing supine and 30 degree raised head positions (25/2/2020);
- Inclusion of positive pressure as a test mechanism (25/2/2020);
- Revised consent form (version 2.0, dated 21/2/2020);
- Data form (version 2.0, date 21/2/2020)

It is the Principal Investigator's responsibility to ensure that all researchers associated with this project are aware of the conditions of approval and which documents have been approved.

Sincerely,

Carolyn Ells, PhD
Co-Chair
Institutional Review Board

cc: Natasha Jacobson, Trevor Cotter
A12-M63-19A (19-12-043)

McGill Faculty of Medicine

Institutional Review Board
- Amendment Submission Form -

NOTE TO RESEARCHERS: Researchers proposing any changes to an approved study must obtain the approval of the IRB before proceeding with these changes, except when necessary to eliminate an immediate hazard to the participant (in this latter situation, the IRB must then be immediately notified and the modification submitted for consideration.) Amendments may include, but are not limited to, changes to the research design, participant population, or consent procedures.

At the discretion of the IRB Chair or Co-Chair, amendments may be reviewed via an expedited process. However, significant revisions will require that the proposal be reviewed by the IRB Committee at a scheduled meeting.

RECEIVED McGill University MAR - 3 2020 FACULTY OF MEDICINE IRB

Principal Investigator	Dr. Mark Driscoll
Study Title	Novel device for the non-invasive measurement of abdominal wall elasticity
IRB Study Number	A12-M63-19A
Please describe the proposed study amendment or modification and the rationale. Is it **Minor** (e.g., administrative changes, change in sponsorship/study funding) or **Major** (e.g., adding an intervention such as additional blood tests, or changes to the study design, changes to the study population)?	Major Modification (1): Include measurements at standing and sitting positions, in addition to the existing supine and 30 degree raised head positions. Major Modification (2): Include positive pressure as a test mechanism. The protocol follows the same steps, though a second series of data is taken for positive pressure.

What follow-up action do you recommend for study participants *who are already enrolled in the study*?

- ☐ Inform study participants ASAP
- ☐ Revise the consent/assent forms (please enclose)
- ☐ No action required
- ☑ Other (please describe): N/A No participants enrolled at this time.

Documentation: The following documentation is required for an ethics review of the amendment:

- Signed and dated amendment submission form;
- Revised study documents,where applicable.

Please submit **one (1)** copy of the revised documents and the completed submission form to the Institutional Review Board, Faculty of Medicine, McIntyre Medical Building, Room 633. Minor amendments may be submitted by e-mail to: submit2irb.med@mcgill.ca. Amendments requiring a full Board review should be submitted to the IRB at least **one (1) week prior** to the designated committee's scheduled meeting (the last digit of the IRB study number indicates the designated committee.)

For additional information, please contact the IRB office.

DATE OF I.R.B. APPROVAL MAR - 9 2020 Faculty of Medicine McGill University

SIGNATURE

Principal Investigator 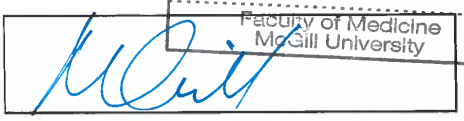 Date 25-02-20

McGill

PARTICIPANT CONSENT FORM

Research study title: Novel device for the non-invasive measurement of abdominal wall elasticity.

Researcher(s): Ms. Natasha Jacobson, Ph. D. Candidate
Mechanical Engineering, McGill University
T: (204)232-4931
E: natasha.jacobson@mail.mcgill.ca

Mr. Trevor Cotter, Ph. D. Candidate
Mechanical Engineering, McGill University
E: trevor.cotter@mail.mcgill.ca

Supervisor(s): Dr. Mark Driscoll, Ph. D., Assistant Professor
Mechanical Engineering, McGill University
T: 514-398-6299
E: mark.driscoll@mcgill.ca

Sponsor(s): NSERC 245375

Introduction: You are invited to participate in the following research project: A Novel device for the non-invasive measurement of abdominal wall elasticity. This form exists to provide informed consent. The study purpose, procedure, risks and benefits are outlined, here. Should you, at any time, have a question or concern, feel free to ask. Participation in this research is entirely voluntary. Should you wish to withdraw at any time, feel free to do so. There are no negative consequences for withdrawn participants now or in the future. Please take the time to read and fully understand this form prior to consenting.

Purpose of the Study: Objective

PART 1: Demonstrate the novel tool's efficacy as a stiffness measurement tool by determining inter-, intra-rater reliability, and concurrent validity against existing popularized measurement methods (here, myometry with the MyotonPro, and indentation). onstrate the novel tool's efficacy as a stiffness measurement tool.

PART 2: Exploit the novel tool to evaluate the effect of applied positive versus negative pressures at different body positions.

Hypothesis

PART 1: Isotropic Young's modulus measurements taken with a novel device have an intra-rater reliability in excess of an intraclass correlation coefficient (ICC) of 0.75 when compared with stiffness measurements taken with existing popularized measurement methods.

McGill

DATA FORM

Research study title: Novel device for the non-invasive measurement of abdominal wall elasticity.

Patient ID _____

Researcher(s): 1 _____

2 _____

Initialization:

1 Participant informed of procedure? ☐
2 Participant signed consent form? ☐
3 Have you been previously pregnant? ☐
4 Do you have:
a. any history of abdominal surgery? ☐
b. acute peritonitis? ☐
c. an abdominal mass? ☐
d. acute cystitis? ☐
e. neurogenic bladder? ☐
f. pelvic hematoma? ☐
g. a pelvic fracture? ☐
h. an acute injury to the urinary bladder? ☐
5 Have you consumed muscle relaxants in the last 48 hours? ☐
6 Mark the following locations on participant's abdomen:
A 5 cm subxiphoid (linea alba) ☐
B 5 cm cranial to umbilicus (linea alba) ☐
C 5 cm left of B (rectus abdominis above arcuate) ☐

DATE OF I.R.B. APPROVAL
MAR - 9 2020
Faculty of Medicine
McGill University

McGill

Faculty of Medicine and Health Sciences
3655 Promenade Sir William Osler #633
Montreal, QC H3G 1Y6

Faculté de médecine et des sciences de la santé
3655, Promenade Sir William Osler #633
Montréal, QC H3G 1Y6

Tel: 514 398-3124

2 September 2020

Dr. Mark Driscoll
Department of Mechanical Engineering
Macdonald Engineering Building
817 Sherbrooke Street West, Room 153
Montreal QC H3A 0C3

RE: IRB Study Number A12-M63-19A / 19-12-043
Novel device for the non-invasive measurement of abdominal wall elasticity

Dear Dr./Prof. Driscoll,

On 2 September 2020, the following amendment received an expedited/delegated review and approval:

- Amended Study Protocol version August 2020
- Participant Consent Form, version September 2, 2020.

The Investigators are reminded of the requirement to report all McGill IRB approved study documents to the Research Ethics Offices (REOs) of participating study sites, if applicable. Please contact the individual REOs for instructions on how to proceed. Research funds may be withheld and/or the study's data may be revoked if there is a failure to comply with this requirement.

Sincerely,

Roberta Palmour, PhD
Chair
Institutional Review Board

Cc: A12-M63-19A / 19-12-043

McGill | Faculty of Medicine and Health Sciences | Faculté de médecine et des sciences de la santé

3655 Sir William Osler #633
Montreal, Quebec H3G 1Y6

3655, Promenade Sir William Osler #633
Montréal (Québec) H3G 1Y6

Tél/Tel: (514) 398-3124

10 November 2020

Dr. Mark Driscoll
Department of Mechanical Engineering
Macdonald Engineering Building
817 Sherbrooke Street West, Room 153
Montreal QC H3A 0C3

RE: IRB Study Number A12-M63-19A / 19-12-043
Novel device for the non-invasive measurement of abdominal wall elasticity

Dear Dr. Driscoll,

On 09 November 2020, at a meeting of the Institutional Review Board, the following amendment received a full Board review and approval:

- Amendment Notification dated 03-10-2020
- Participant Consent Form, version November 3, 2020.

The Investigators are reminded of the requirement to report all McGill IRB approved study documents to the Research Ethics Offices (REOs) of participating study sites, if applicable. Please contact the individual REOs for instructions on how to proceed. Research funds may be withheld and/or the study's data may be revoked if there is a failure to comply with this requirement.

Sincerely,

Roberta Palmour, PhD
Chair
Institutional Review Board

Cc: A12-M63-19A / 19-12-043

Faculty of Medicine and Health Sciences
3655 Promenade Sir William Osler #633
Montreal, QC H3G 1Y6

Faculté de médecine et des sciences de la santé
3655, Promenade Sir William Osler #633
Montréal, QC H3G 1Y6

Tel: 514 398-3124

10 September 2020

Dr. Mark Driscoll
Department of Mechanical Engineering
Macdonald Engineering Building
817 Sherbrooke Street West, Room 153
Montreal QC H3A 0C3

Info-Ed File Number: **20-09-018** **(IRB Internal Study Number:** A09-M59-20B**)**

Study/Protocol Title: *Novel device for the non-invasive measurement of intra-abdominal pressure*

Principal Investigator: Mark Driscoll

Sponsor Name (if applicable): Natural Sciences and Engineering Research Council (NSERC)

Dear Dr./Professor Driscoll,

Thank you for submitting the above-referenced study for an ethics review.

As this study involves no more than minimal risk, and in accordance with Articles 2.9 and 6.12 of the 2nd Edition of the Canadian Tri-Council Policy Statement of Ethical Conduct for Research Involving Humans (TCPS 2) and U.S. Title 45 CFR 46, Section 110 (b), paragraph (1), we are pleased to inform you that a delegated review was conducted and ethics approval for the study was provided by the IRB Chair on 10 September 2020. **The ethics certificate is valid until 09 September 2021**. The study proposal will be presented for corroborative approval at the next meeting of the Institutional Review Board.

The following documents were reviewed and approved:

- Study Protocol (IRB dated August 2020).

The Faculty of Medicine Institutional Review Board (IRB) is a registered University IRB working under the published guidelines of the Tri-Council Policy Statement 2, in compliance with the Plan d'action ministériel en éthique de la recherche et en intégrité scientifique (MSSS, 1998), and the Food and Drugs Act (17 June 2001); and acts in accordance with the U.S. Code of Federal Regulations that govern research on human subjects (**FWA 00004545**). The IRB working procedures are consistent with internationally accepted principles of good clinical practice.

The Principal Investigator is required to immediately notify the Institutional Review Board Office, via amendment or progress report, of:

- Any significant changes to the research project and the reason for that change, including an indication of ethical implications (if any);

- Serious Adverse Effects experienced by participants and the action taken to address those effects;
- Any other unforeseen events or unanticipated developments that merit notification;
- The inability of the Principal Investigator to continue in her/his role, or any other change in research personnel involved in the project;
- A delay of more than 12 months in the commencement of the research project, and;
- Termination or closure of the research project.

The Principal Investigator is required to submit an annual progress report (continuing review application) on the anniversary of the date of the initial approval (or see the date of expiration).

The Faculty of Medicine IRB may conduct an audit of the research project at any time.

If the research project involves multiple study sites, the Principal Investigator is required to report all IRB approvals and approved study documents to the appropriate Research Ethics Office (REO) or delegated authority for the participating study sites. Appropriate authorization from each study site must be obtained before the study recruitment and/or testing can begin at that site. Research funds linked to this research project may be withheld and/or the study data may be revoked if the Principal Investigator fails to comply with this requirement. A copy of the study site authorization should be submitted the IRB Office.

It is the Principal Investigator's responsibility to ensure that all researchers associated with this project are aware of the conditions of approval and which documents have been approved.

The McGill IRB wishes you and your colleagues every success in your research.

Kind regards,

Roberta Palmour, PhD
Chair
Institutional Review Board

cc: Associate Dean, Research (Medicine)
A09-M59-20B / 20-09-018

A.3 Device Drawings

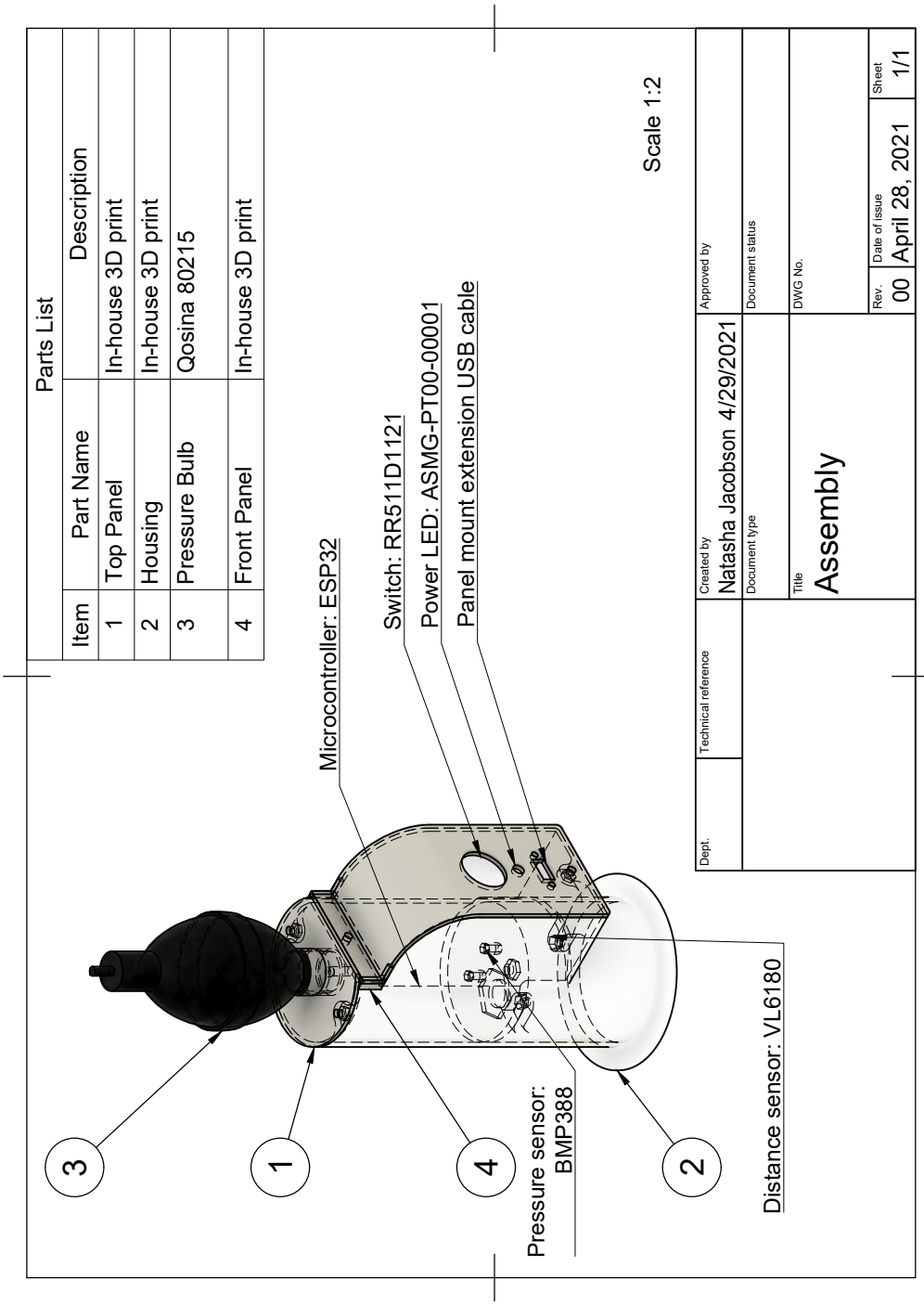

Figure A.3.1: Device assembly.

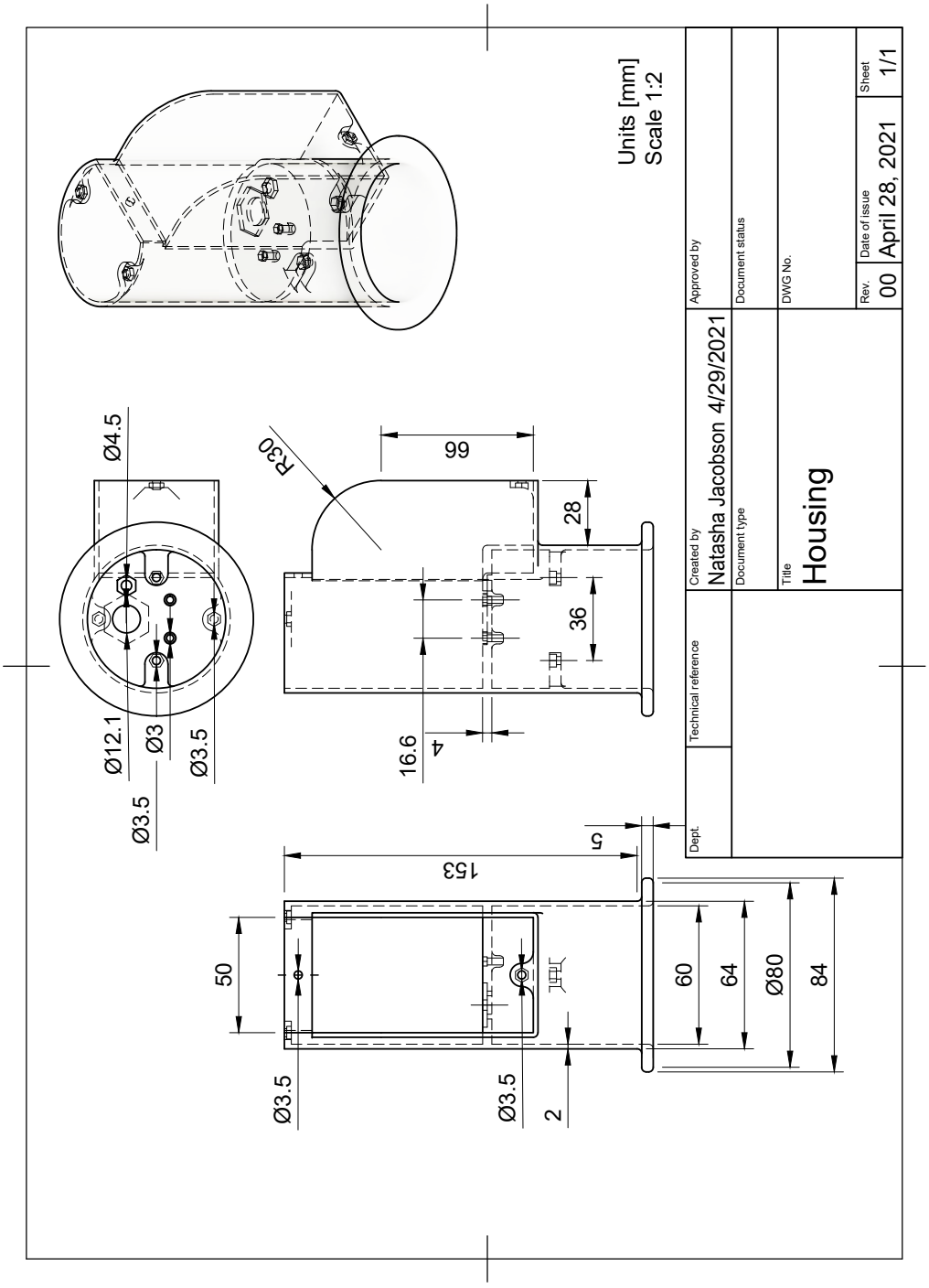

Figure A.3.2: Device housing.

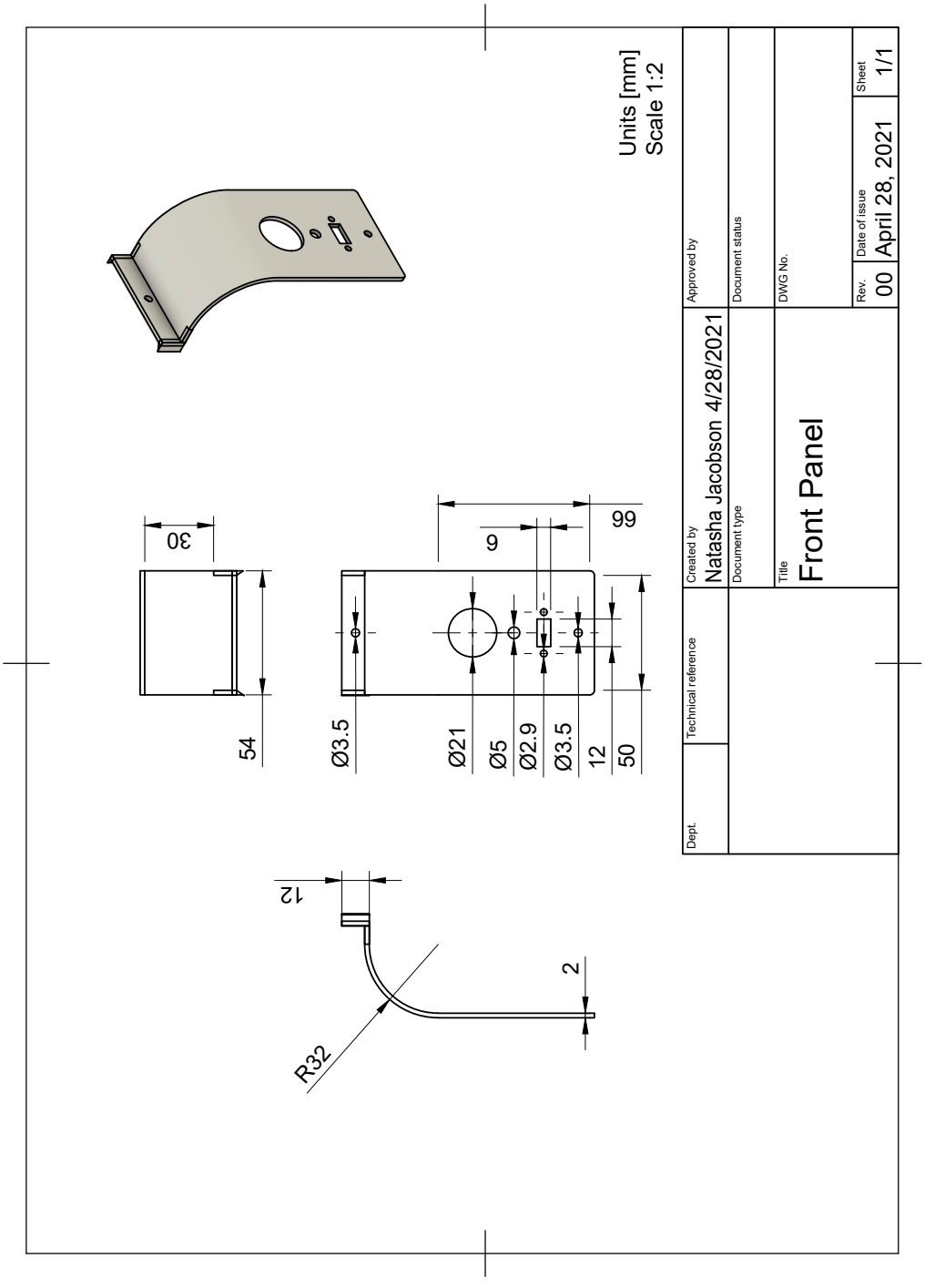

Figure A.3.3: Device front panel.

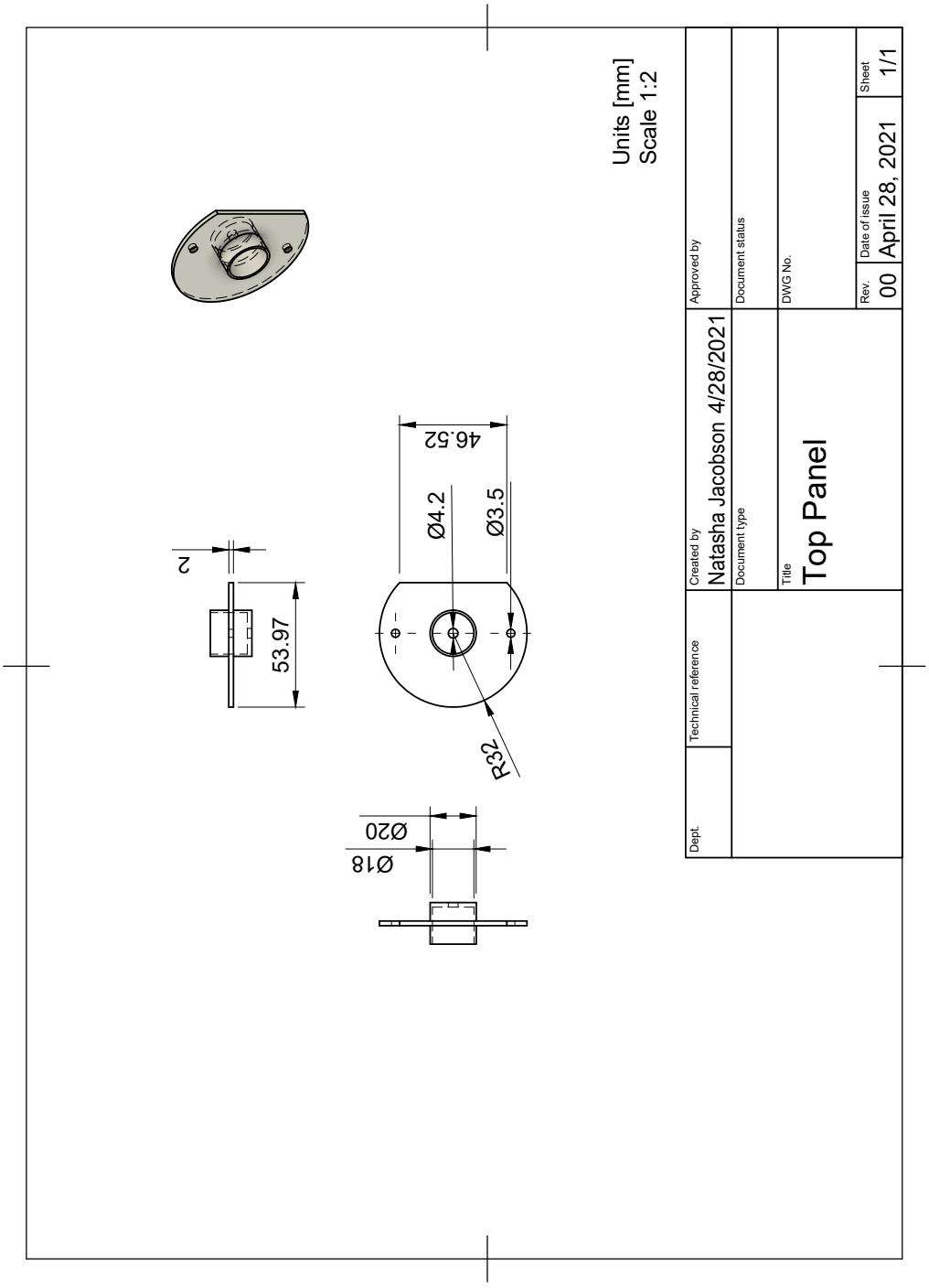

Figure A.3.4: Device top panel.

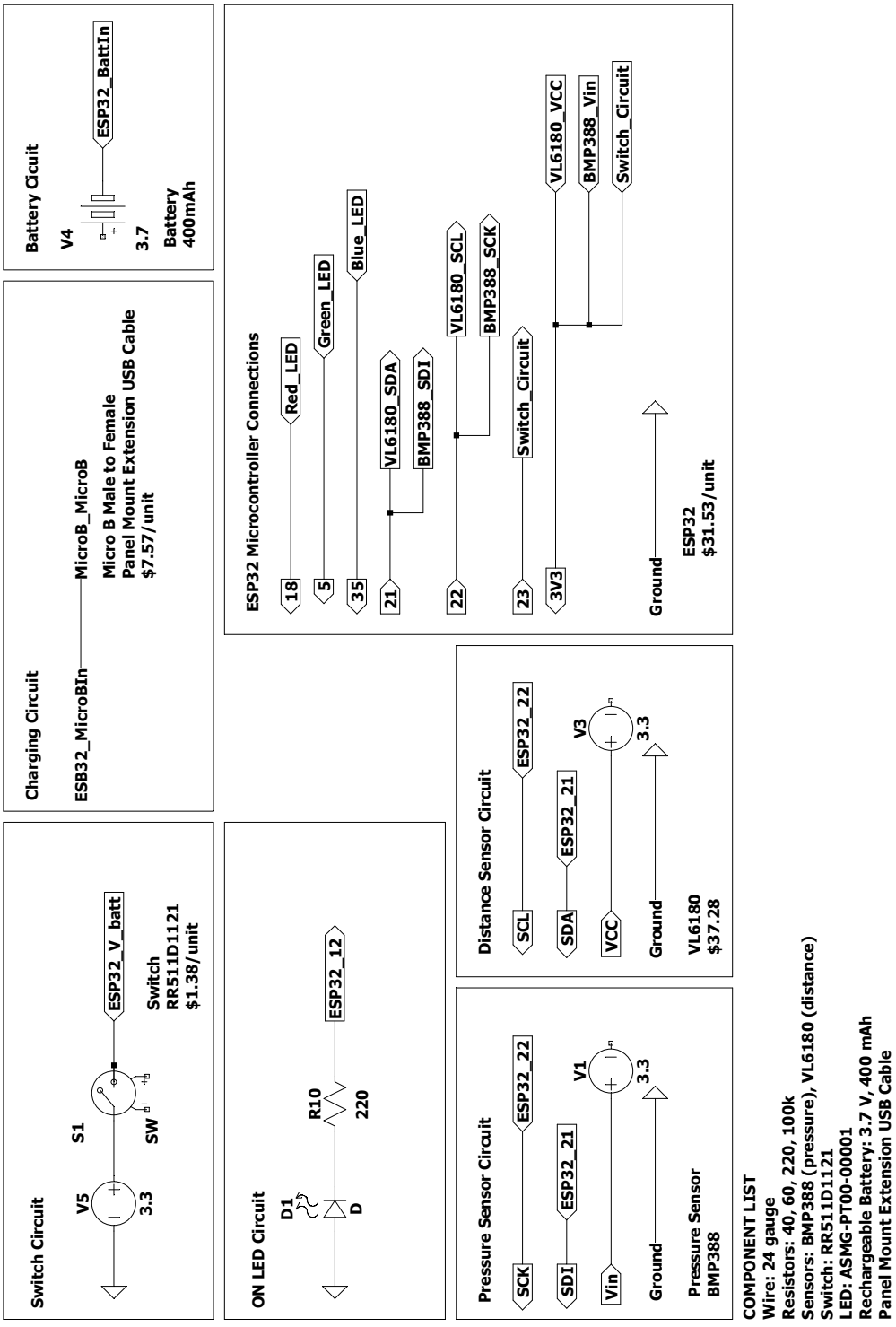

Figure A.3.5: Device circuitry.

A.4 Device Bill of Materials

The following table provides a brief overview of the bill of materials used in the tested prototype used throughout the present work. By providing transparency in product development, it is the hope of the authors that future researchers may either develop their own, similar device for research purposes, or consider the limitations of the present design in provided studies. The following categories are provided for component purchase:

- **Description:** The Component referred to the research group's naming convention, whereas the Description allowed for improved understanding of the Component's importance to the overall design.
- **Unit Cost:** This was the unit cost as per June 2021 from the associated distributor.
- **Bulk Unit Cost:** Should bulk purchasing have been available, this was the bulk unit cost as per June 2021 from the associated distributor.
- **Distributor and Distributor P/N:** Product distributors and part numbers as of June 2021.
- **Manufacturer and Manufacturer P/N:** Product manufacturers and part numbers as of June 2021. This is the main contact point for data sheets and part retrieval should a product become discontinued.

Table A.4.1: Bill of Materials (all costs in CAD)

	Component	Qty	Description	Unit Cost	Bulk Unit Cost	Total	Total (bulk)	Distributor	Distributor P/N	Manufacturer	Manufacturer P/N
Electronics	Red LED	1	LED RED DIFFUSED T-1 3/4 T/H	0.83	0.30	0.83	0.30	Digikey	511-1264-ND	Rohm Semiconductor	SLR-56VR3F
	Microcontroller	1	SPARKFUN ESP32 THING	31.53	31.53	31.53	31.53	Digikey	1568-1444-ND	SparkFun Electronics	DEV-13907
	Switch	1	SWITCH ROCKER SPST 20A 125V	1.38	1.10	1.38	1.10	Digikey	EG4777-ND	E-Switch	RR511D1121
	Rechargeable Battery	1	3.7V 400mAh	31.99	31.99	31.99	31.99	Amazon	IYWQ-UOZYDS	XD1PY	303442
	220 Ohm Resistor	1	RES 220 OHM 0.4W 5% AXIAL	0.20	0.07	0.20	0.07	Digikey	BC4361CT-ND	Vishay BC Components	SFR2500002200JA500
	Board hook-up wire	1	HOOK-UP SOLID 24AWG VIOLET 5’	1.35	0.86	1.35	0.86	Digikey	C2003V-5-ND	General Cable/-Carol Brand	C2003A.12.19
	Jumper Wires	5	JUMPER WIRE M/F 6” 10PCS	0.54	0.54	2.70	2.70	Digikey	1568-1792-ND	SparkFun Electronics	PRT-09140
	Header Pins	2	CONN SIL HDR MALE PIN 32POS TIN	7.62	6.09	15.24	12.18	Digikey	952-2521-ND	Harwin Inc.	D01-9923246
	Breadboard	1	BREADBOARD GENERAL PURPOSE PTH	4.03	4.03	4.03	4.03	Digikey	1568-1083-ND	SparkFun Electronics	PRT-12702
	MicroB Male-Female	1	PANEL MOUNT EXTENSION USB CABLE	7.57	7.57	7.57	7.57	Digikey	1528-1786-ND	Adafruit Industries	3258
Sensors	Distance Sensor	1	BOARD RANGE SENSOR TOF VL6180	37.28	37.28	37.28	37.28	Digikey	1568-1073-ND	SparkFun Electronics	SEN-12785
	Pressure Sensor	1	Board Mount Pressure Sensor 0psi to 5psi Differential 4-Pin	37.27	37.27	37.27	37.27	Arrow Electronics	5 PSI-D-HGRADE-MINI	All Sensors Corporation	5 PSI-D-HGRADE-MINI
	Pressure Bulb	1	Hand pump	4.00	4.00	4.00	4.00	Qosina	80215	Qosina	80215

Continued on next page

Table A.4.1: Continued from previous page

	Component	Qty	Description	Unit Cost	Bulk Unit Cost	Total	Total (bulk)	Distributor	Distributor P/N	Manufacturer	Manufacturer P/N
Tubing	Straight barb	2	Straight barb	0.32	0.36	0.64	0.72	Qosina	11822	Qosina	11822
	Quad-Y connector (soft	1	Quad-Y connector (soft)	0.83	0.92	0.83	0.92	Qosina	81481	Qosina	81481
	Tubing (≈30 mm)	1	70A Durometer; 0.17 inch ID x 0.25 inch OD (4.3 mm x 6.4 mm), 250 ft coil (76.2 m)	167.00	167.00	167.00	167.00	Qosina	T4309	Qosina	T4309
	10-32 thread to barb	1	10-32 thread to barb	0.14	0.14	0.14	0.14	Qosina	MS430	Qosina	MS430
Fasteners	3.5 mm hole fasteners - M3x20mm screw	4	500 Pieces Stainless Steel M3 Bolts Nut Washers Kit Hex Socket Head Screws	N/A	N/A	N/A	20.01	Amazon	M3BOLT-KIT	Reegoo	M3BOLT-KIT
	M3 nuts	6	500 Pieces Stainless Steel M3 Bolts Nut Washers Kit Hex Socket Head Screws	N/A	N/A	N/A	Part of kit	Amazon	M3BOLT-KIT	Reegoo	M3BOLT-KIT
	3.5 mm hole fasteners for distance sensor - M3x16mm screw	2	500 Pieces Stainless Steel M3 Bolts Nut Washers Kit Hex Socket Head Screws	N/A	N/A	N/A	Part of kit	Amazon	M3BOLT-KIT	Reegoo	M3BOLT-KIT
	O-ring	1	O-Ring, Black, AS-006	0.13	0.13	0.13	0.13	Qosina	13031	Qosina	13031
Body	Housing	1	Custom 3D print SLA Acrylic resin, transparent, 100 micron resolution	N/A	N/A	N/A	N/A	N/A	N/A	In-house	N/A

Continued on next page

Table A.4.1: Continued from previous page

	Component	Qty	Description	Unit Cost	Bulk Unit Cost	Total	Total (bulk)	Distributor	Distributor P/N	Manufacturer	Manufacturer P/N
	Front panel	1	Custom 3D print SLA Acrylic resin, transparent, 100 micron resolution	N/A	N/A	N/A	N/A	N/A	N/A	In-house	N/A
	Top panel	1	Custom 3D print SLA Acrylic resin, transparent, 100 micron resolution	N/A	N/A	N/A	N/A	N/A	N/A	In-house	N/A

A.5 Device Codes

During a sample measurement, suction is applied using the novel device. Measurements are taken via sensors, whose outputs are reported using code in Arduino, as shown in the following. With raw data, a comma-separated values file is made and inputted into a corresponding MATLAB code (immediately proceeding Arduino code, here). Resulting IAP and elasticity may then be related to the user. Code is commented for improved understanding.

```
////////////////////// INITIALIZE //////////////////////
const int ledPin = 12;

////////////////////// Distance Sensor //////////////////////
#include <Arduino.h>
#include <Wire.h>
#include <SparkFun_VL6180X.h>
#define VL6180X_ADDRESS 0x29

VL6180xIdentification identification;
VL6180x sensor(VL6180X_ADDRESS);

int(distanceValue) = 0.0;

////////////////////// Pressure Sensor //////////////////////
#include <Adafruit_BMP3XX.h>
#include <bmp3.h>
#include <bmp3_defs.h>

#include <SPI.h>
#include <Adafruit_Sensor.h>
#include "Adafruit_BMP3XX.h"

#define SEALEVELPRESSURE_HPA (1013.25)

Adafruit_BMP3XX bmp; // I2C

void setup() {
 Serial.begin(115200);

 // setup pin 12 as a digital output pin
 pinMode (ledPin, OUTPUT);

////////////////////// Distance Sensor //////////////////////
 Wire.begin(); // Start I2C library
 delay(1000); //Take some time to open up the Serial Monitor

 sensor.getIdentification(&identification); // Retrieve manufacture info from device memory

  if(sensor.VL6180xInit() != 0){
  Serial.println("FAILED TO INITALIZE"); //Initialize device and check for errors
 };

 sensor.VL6180xDefautSettings(); //Load default settings to get started.
```

```
   delay(1000); // delay 1s

////////////////////// Pressure Sensor //////////////////////

  while (!Serial);
  Serial.println("BMP388 test");

  if (!bmp.begin()) {
    Serial.println("Could not find a valid BMP3 sensor, check wiring!");
    while (1);
  }

  // Set up oversampling and filter initialization
  bmp.setTemperatureOversampling(BMP3_OVERSAMPLING_8X);
  bmp.setPressureOversampling(BMP3_OVERSAMPLING_4X);
  bmp.setIIRFilterCoeff(BMP3_IIR_FILTER_COEFF_3);
  //bmp.setOutputDataRate(BMP3_ODR_50_HZ);
}

void loop() {

////////////////////// LED //////////////////////////
  digitalWrite (ledPin, HIGH);  // turn on the LED

////////////////////// Distance Sensor //////////////////////
  Serial.print("Distance(mm)= ");
  distanceValue = sensor.getDistance(); // add for calibration here (if off by 2 mm, ex.)
  Serial.println( distanceValue );

////////////////////// Pressure Sensor //////////////////////
  if (! bmp.performReading()) {
    Serial.println("Failed to perform reading :(");
    return;
  }

  Serial.print("Pressure(kPa)= ");
  Serial.println(bmp.pressure / 1000.0);

  delay(1000);

}
```

```
clear all
clc

%%%%%%%%%%%%%%%%%%%%%%%%%%%% INITIALIZE
%%%%%%%%%%%%%%%%%%%%%%%%%%%%

a = 0.03; % cup radius in m
t = 0.03; %t = 0.03; % wall thickness in m
phi = 2.1; % Phi(eta) function
nu = 0.499;
SampRate = 1000; % Sampling rate used 1000 ms = 1
sec.

T =
readtable('Study3\Participant_15\091120_01_03b.csv'
); % Call on .csv data file
waist = 0.715/(2*pi);
rows = height(T); % number of rows in the imported
plot

T2 = table2array(T(2:rows, 3));

x = [0]; % Time matrix

Press = [0.0]; % Pressure matrix

Dist = [0]; % Distance matrix


%%%%%%%%%%%%%%%%%%% CREATE MATRIX OF VALUES
%%%%%%%%%%%%%%%%%%%%%%

i_ = 1;
j = 1;
k = 1;

zero_P = [];
zero_D = [];

%%%% Find the zeroed P and d %%%%%
```

```
while k <= 5 % averaging the first 2 seconds (5
rows)
    j = 2*i_;
    k = 2*i_-1;
    next_0Press = T2(k,1); % Pressure needs to be
first in table. Change 101.0 depending on zeroed
pressure.
    zero_P = [zero_P;next_0Press];
    next_0Dist = T2(j,1); % change this value
depending on the zeroed measure of distance
    zero_D = [zero_D;next_0Dist];
    i_ = i_+1;
end

zero_Press = mean(zero_P);
zero_Dist = mean(zero_D);

i_ = 1;
j = 1;
k = 1;

%%%% Create table of data

while i_ <= (rows/2-1)
    disp(i_);
    x = [x;i_];
    j = 2*i_;
    k = 2*i_-1;
    next_Press = T2(k,1) - zero_Press; % Pressure
needs to be first in table. Change 101.0 depending
on zeroed pressure.
    Press = [Press;next_Press];
    next_Dist = T2(j,1)- zero_Dist; % this value
changes depending on the zeroed measure of distance

    if (255-zero_Dist) == abs(next_Dist)
        next_Dist = 0;
    else
```

```
        next_Dist = abs(next_Dist);
    end
    Dist = [Dist;next_Dist];

    i_ = i_+1;
end
%%%%%%%%%%%%%%%%%%%% PLOTTING
%%%%%%%%%%%%%%%%%%%%%%%%%%%%%
figure(1)
yyaxis left
plot(x,Press, '--')
title('Pressure and Distance Measurements over
Time')
xlabel('Time')
ylabel('Pressure Applied (kPa)')
yyaxis right
plot(x,Dist)
ylabel('Tissue Deformation (mm)')
legend('Applied Pressure (kPa)', 'Resulting
Deformation (mm)')
legend('Location', 'northwest')

%%%%%%%%%%%%%%%%%% Testing at the peaks of pressure
%%%%%%%%%%%%%%%%

[pks1,locs1] = findpeaks(-
Press,'MinPeakHeight',1.0);
n = 0;
x2 = [0];
count = length(locs1)-1;
pressApplied = [0];
distPeak = [0];
EPeak = [0];
IAPPeak = [0];
waist_in = waist-t;


while n <= count
    pressApplied_next = Press(locs1(n+1));
```

```
    pressApplied = [pressApplied;
pressApplied_next];
    distPeak_next = Dist(locs1(n+1)-3);
    distPeak = [distPeak; distPeak_next];
    E_next = 0.117*1.098*(zero_Press-
pressApplied_next)*a/(distPeak_next/1000); %use
0.117 for tests as this used the average
    % thick. from tests to solve for alpha
    % use 0.8426 for the stiff pad tests
    % use 0.047 for quads/calf
    EPeak = [EPeak;E_next];
    r2 = (a^2 +
(distPeak_next/1000)^2)/(2*(distPeak_next/1000));
    r1 = r2-t;
    IAP_next = (-
pressApplied_next)*(2*r1^3+r2^3)*(waist^2-
waist_in^2)/((2*(r2^3-
r1^3))*x0*(waist^2+waist_in^2)-
(2*r1^3+r2^3)*(waist^2-waist_in^2));
    IAPPeak = [IAPPeak;IAP_next];
    n = n + 1;
    x2 = [x2;n];
end

distPeak(1,:) = []
pressApplied(1,:) = []
EPeak(1,:) = []
IAPPeak(1,:) = []
x2(1,:) = [];

pressApplied = -pressApplied;
distPeak = distPeak;
count = length(distPeak); %;-1;
pressFinal = pressApplied;
distFinal = distPeak;
n = 1;
check = 0;
while n <= count
```

```
    if distPeak(n+check) == 0
        distFinal(n) = [];
        pressFinal(n) = [];
        count = count - 1;
        check = check + 1;
    elseif pressFinal(n) < 1
        distFinal(n) = [];
        pressFinal(n) = [];
        count = count - 1;
        check = check + 1;
    else
        n = n+1;
    end
end

distFinal = distFinal;
pressFinal = pressFinal;
pAvg = mean(pressFinal); % this is in kilopascals
dAvg = mean(distFinal)/1000; % put in m
pSD = std(pressFinal);
dSD = std(distFinal)/1000; % put in m

%%%%%%%%%%%%%%%%%% Plotting each set of peaks
%%%%%%%%%%%%%%%%

[pks1,locs1] = findpeaks(-
Press,'MinPeakHeight',1.0);

% now let's break apart the data sets at the
locations where peaks were identified.

n = 0;
crit_times = [0];

while n <= (length(locs1)-1) % this outputs an
array of the peak times (x)
    crit_times_next = x(locs1(n+1));
    crit_times = [crit_times; crit_times_next];
    n = n + 1;
```

```
end

crit_times(1,:) = []; % empty out the first point
in the array
Dist_set = []; % this is one set of data from a
suction episode
Press_set = [];
Dist_final = [];
Press_final = [];
prev_Dist_set = [];
prev_Press_set = [];
n = 1;
i_ = 1;

while n <= (length(crit_times)) % so for each x
(time) that a peak occurred, we will create an
array of dist
                                % and press
measurements up to that time.
    while i_ < crit_times(n)
        if i_ > 2
            Dist_set = [Dist_set; (Dist(i_-2))];
            Press_set = [Press_set; -
1*(Press(i_))];
        else
            Dist_set = [Dist_set; (Dist(i_))];
            Press_set = [Press_set; -
1*(Press(i_))];
        end
        i_ = i_ + 1;
    end

    n = n + 1;
    i_ = crit_times(n-1);
    Dist_set(1,:) = []; % empty out the first point
in the array
    Press_set(1,:) = []; % empty out the first
point in the array
```

```
    Dist_final{n-1} = [Dist_set];
    Press_final{n-1} = [Press_set];

    Dist_set = [];
    Press_set = [];
end

figure(2)
n = 1;
colour =
{'k','b','r','g','k','b','r','g','k','b','r','g',
'b', 'k'};
shape = {'+', '*', 'o', 'x', '*', '+', 'o', 'x',
'*', '+', 'o', 'x', 'o', '*'};
slope_all = [];
while n <= (length(Dist_final))
    scatter(Dist_final{n},Press_final{n},
colour{n}, shape{n});
    hold on
    fit = polyfit(Dist_final{n},Press_final{n}, 1);
    plot(Dist_final{n}, polyval(fit,
Dist_final{n}), colour{n})
    slope = fit(1);
    slope_all = [slope_all; slope];
    n = n + 1;
end

hold off

title('Pressure versus Distance across different
tests')
xlabel('Tissue Deformation (mm)')
ylabel('Pressure Applied (kPa)')
n = 1;
str_legend = {};
while n <= (length(Dist_final))
    str = {strcat('Test:' , num2str(n))};
    str_legend = [str_legend, str];
```

```
    str = {strcat('Best fit of Test:' ,
num2str(n))};
    str_legend = [str_legend, str];
    n = n + 1;
end
legend(str_legend{:})
legend('Location', 'northwest')


figure(3)
scatter(crit_times, slope_all);
hold on
title('Stiffness over time')
xlabel('Time (s)')
ylabel('Slope')
fit = polyfit(crit_times, slope_all, 3);
plot(crit_times, polyval(fit, crit_times))
hold off

figure(4)
scatter(crit_times, EPeak);
hold on
title('E over time')
xlabel('Time (s)')
ylabel('E [kPa]')
fit = polyfit(crit_times, EPeak, 2);
plot(crit_times, polyval(fit, crit_times))
hold off

%%%%%%%%%%%%%%%%%% Calculating E and IAP
%%%%%%%%%%%%%%%%

waist_in = waist-t;
r2 = (a^2 + dAvg^2)/(2*dAvg);
r1 = r2-t;
theta = asin(a/r2);
```

```
E_5 = 1.098*(zero_Press-pAvg)*a/dAvg;  % from book
on stiffness testing
E_6 = 0.117*E_5; % alpha = 1.16e-4 for ball, alpha
= 0.47 abdomen (3 cm thick), alpha = 0.047 for
quads/calves,
% alpha = 0.366 for 1" thick piece, alpha = 0.0854
for 1/2" thick
% alpha = 0.185 abdomen 1.78 cm thick

% now consider the resected tissue to be a thick
walled sphere (works better)
IAP_2 = (pAvg)*(2*r1^3+r2^3)*(waist^2-
waist_in^2)/((2*(r2^3-
r1^3))*x0*(waist^2+waist_in^2)-
(2*r1^3+r2^3)*(waist^2-waist_in^2));
IAP_2mmHg = IAP_2*7.50062;

pAvg = pAvg
dAvg = dAvg

Results = [E_6 IAP_2 IAP_2mmHg]
% These results were found to have better values
statistically. They take the average pressure and
distance measurements to calculate IAP and E

Results2 = [mean(EPeak) mean(IAPPeak)
mean(IAPPeak)*7.50062]

% These results are still good to consider. They
take the pairs of pressure/distance data points to
calculate IAP and E, then average these results to
determine the final IAP and E.
```

A.6 Device Pipeline

1. Plug in device and ensure red LED turns on to signify correct power up.
2. Apply ultrasound jelly or comparable lubricant along the rim of the device to improve seal against subject's skin.
3. Open Arduino program and relevant code, as described in Section A.5.
4. Upload Arduino code to device board. Ensure Arduino program is set to the correct device (ESP32).
5. Upon upload, open the Serial Monitor. Place the device on the subject's anatomy of interest. Once flat against the body, select "Show Timestamp" in the Serial Monitor. This identifies test commencement.
6. Take note of the pressure on the Serial Monitor prior to suction. This will be referred to as P_0.
7. Begin suction: Hold device down on subject's skin with enough force to maintain seal. Apply one pump using the handheld pressure bulb. Watch the Serial Monitor for a corresponding drop in pressure. Wait until the pressure returns to P_0. Do not move the device during the test.
8. Complete the previous step two more times for a data set of 3 suction pumps; results for IAP and elasticity (E) will be averaged from this data.
9. Select "Show Timestamp" again on the Serial Monitor to identify test completion. Do not remove the device from the body until this step has been completed as it will cause a spike in deformation results unrelated to applied suction.
10. Testing with the device is now complete: the device may be set aside while compiling data. Select the data outputted in the Serial Monitor that contains timestamps. Copy and paste this data into a .CSV file.
11. Separate data into appropriate columns (in Excel, this is done using Data - Text to Columns). Three columns should result: (1) Timestamp, (2) Identifier, either Distance or Pressure, and (3) Value.
12. Ensure the first data point is a distance measure. The MATLAB code assumes it is calling on distance, first, in its order of operations. Save the .CSV file.

13. Open MATLAB and relevant code, as described in Section A.5.

14. Ensure code is calling on the correct .CSV file for interpretation.

15. Run the program. The outputted array denoted "Results" with 3 values is the most useful piece of information in the code. This array describes (1) E, (2) IAP in kPa, and (3) IAP in mmHg.

To note: the MATLAB program will output a number of tables, as well. One of particular interest is the raw data showing spikes in pressure and their corresponding spikes in deformation. There is a delay between deformation and pressure data. In the code, this delay was offset by 3 seconds in all studies, but it may vary in reality, test-to-test. A filter of 1 kPa was also used in all studies to find the peak applied pressures (*i.e.* suction pulses) during testing. Finally, the first three data points are used to average P_0 and the initial deformation from which all other data points are compared. Thus, all values are relative to the initial data points.

A.7 Material stress-strain curves

Stress-strain curves for each material (as described in Section 3.3) were compiled and summarized in the following. It should be noted that only data at the 150 mm/min strain rate is recorded, here. For the CDRM material, both strains up to 50 and 60% are shown to demonstrate its early-onset hyperelasticity.

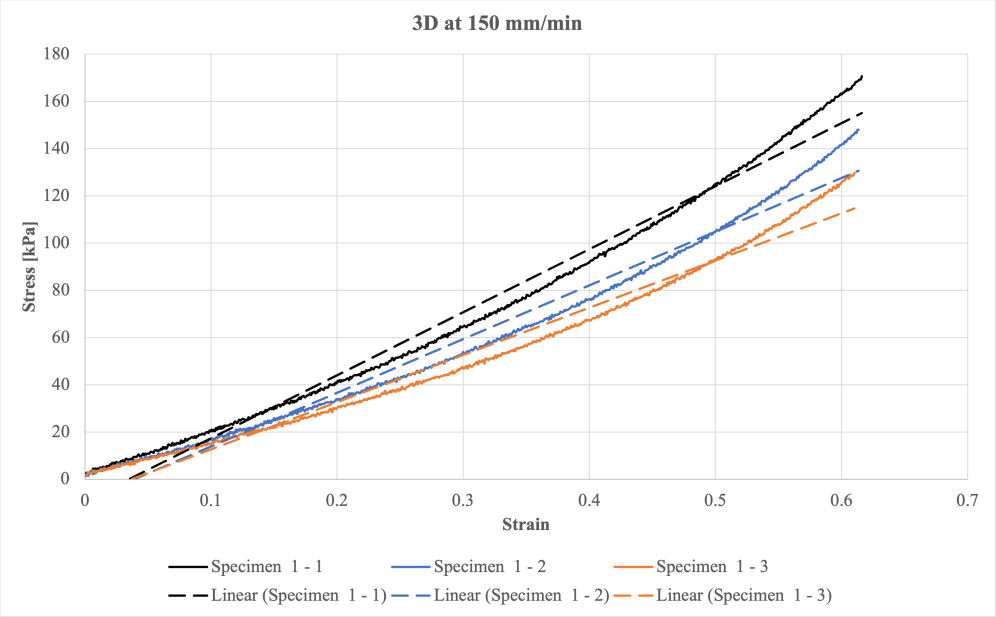

Figure A.7.1: Stress-strain curve for 3D at 150 mm/min strain rate.

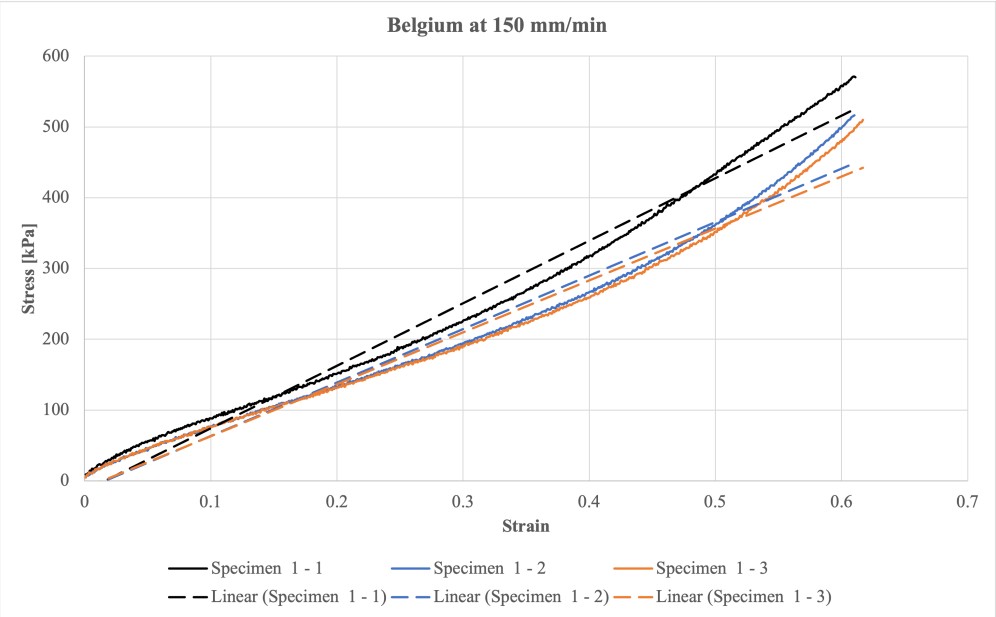

Figure A.7.2: Stress-strain curve for Belgium at 150 mm/min strain rate.

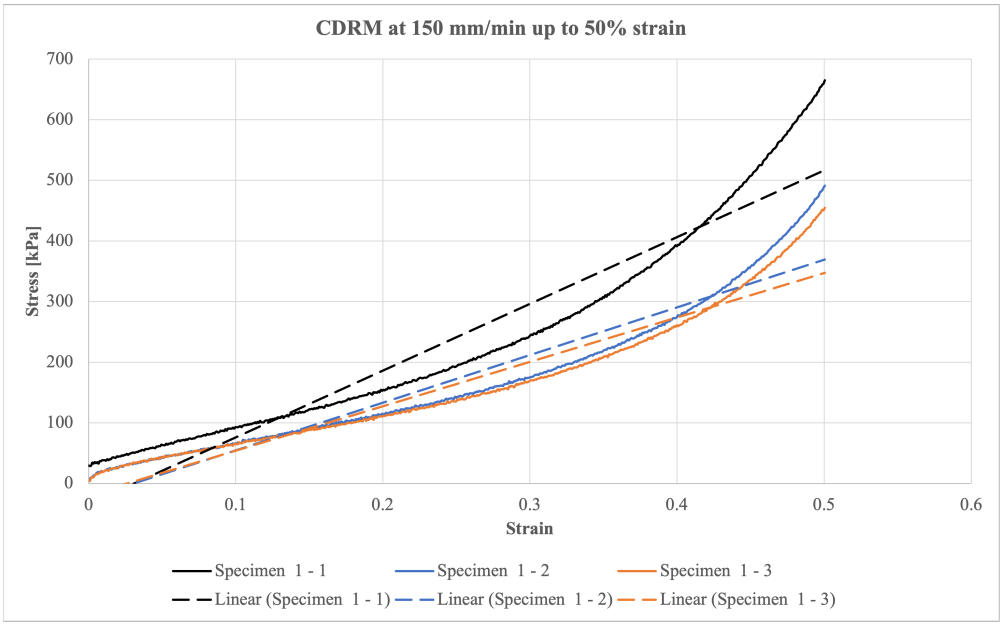

Figure A.7.3: Stress-strain curve for CDRM at 150 mm/min strain rate up to 50% strain.

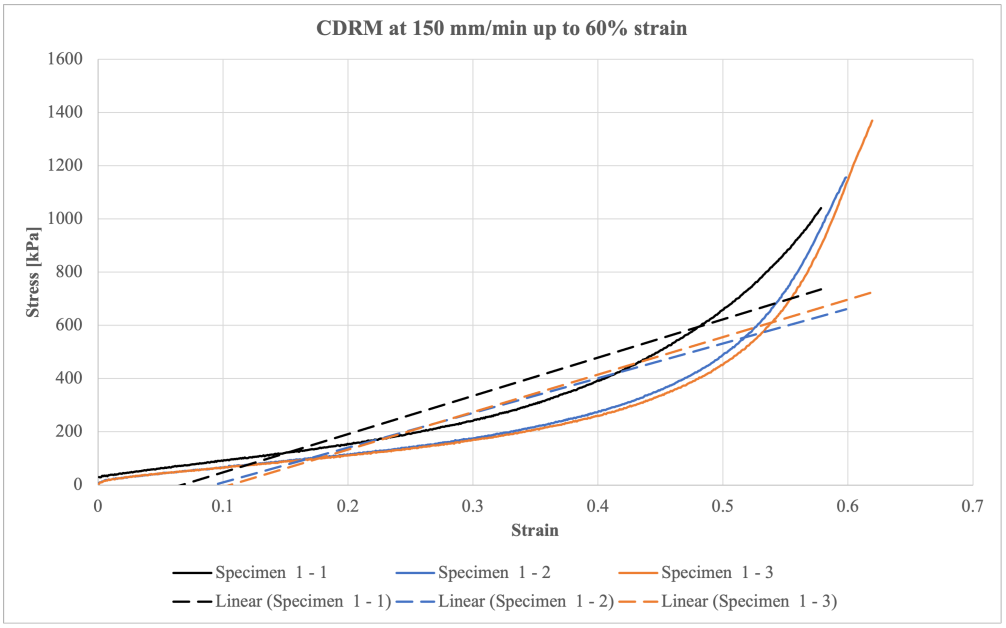

Figure A.7.4: Stress-strain curve for CDRM at 150 mm/min strain rate up to 60% strain.

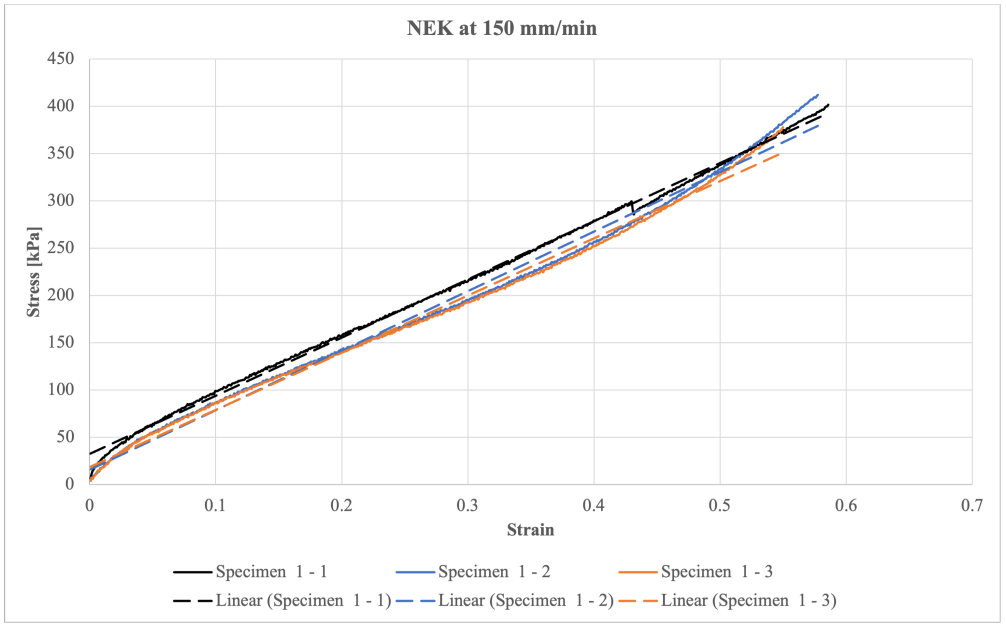

Figure A.7.5: Stress-strain curve for NEK at 150 mm/min strain rate.

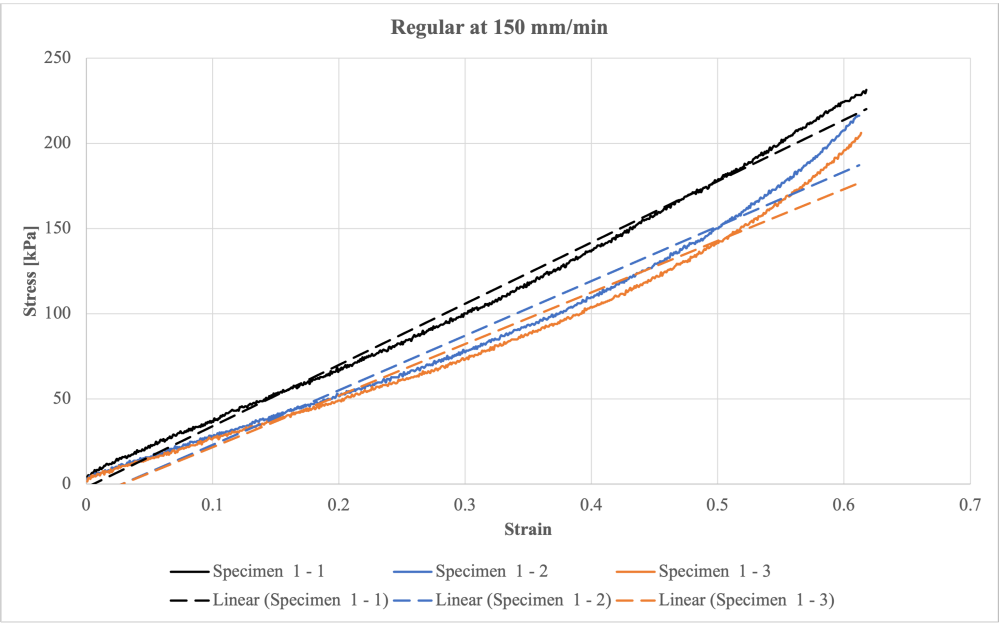

Figure A.7.6: Stress-strain curve for Regular at 150 mm/min strain rate.

A.8 Reference Summaries

A brief summary of each reference is supplied for future research. **Bolded items** are those of particular significance to this thesis. Table A.9.1 follows, summarizing the key content of referenced literature.

[1] Strandring (2016): An anatomy text that further detailed anatomical features. This textbook was more in depth and designed for clinical use rather than for general anatomy understanding (as was the case in [12] or [11]).

[2] Malbrain *et al*. (2014): This is a critical set of articles by Malbrain *et al*. in terms of defining and establishing a framework in which to study IAP and the IAV. Part-1 focused largely on defining the anatomy of the thorax, and what happens to the geometry of the IAV during insufflation. A key point made was the change in abdominal geometry given a volumetric change of the IAV. The cross-section of the abdomen changed from a cylindrical area to a spherical one with increasing IAV.

[3] Stokes *et al*. (2011): Using a biomechanical model, Stokes *et al*. evaluated lumbar stability with changes in AW muscle activation.

[4] Malbrain *et al*. (2014): Part-2 of Malbrain *et al*.'s 2014 articles considered measurement devices for compliance. Of particular interest was the discussion on human versus animal studies for IAP evaluation. Animal studies were deemed urreliable for IAV evaluation because the pressure-volume curve is entirely non-linear whereas humans are linear until a critical IAV, where the graph changes to an exponential function. This suggested the inefficacy of animal studies in compliance research, as well. An evaluation of existing means of measuring IAV, IAP and C_{ab} was also tabulated, including the advantages and disadvantages of each.

[5] Hodges *et al*. (2005): Hodges *et al*. determined the connection between IAP and spinal stability (*i.e*. stiffness in the spine).

[6] Malbrain *et al*. (2006): In a team of 16 experts, a set of definitions for IAP were proposed as a means of standardizing language, as well as measurement techniques. It should be noted that "normal" IAP was defined as the average IAP taken at a supine position with a bladder catheter. Given this definition, a range of values for normal IAP was concluded to be between 5 and 7 mmHg.

[7] Roberts *et al*. (2016): Updated definitions for WSACS including a finalized definition of clinical C_{ab}.

[8] Tayashiki *et al*. (2016): Experimental study of a training regimen on abdominal bracing (co-contraction of abdominal muscles). Muscle thicknesses and IAP were recorded pre- and post-test with the training group and control group.

[9] Malbrain (2004): This article critically evaluated all current methods of measuring IAP. It was stated that there exists no "gold-standard" and all methods are invasive. That said, there is value in each of existing measurement method, depending on the state of the patient (*i.e*. If the bladder is compromised, measure IAP via the uterus, stomach).

[10] Ott (2019): Ott described the need for measuring C_{ab} in order to determine the limits of laparoscopy in patients. Equipment was required to validate numerical analyses completed to estimate the maximum volume induced during surgery. This overview of C_{ab} was thorough and clear. The need for continuous monitoring of C_{ab} was made evident, while the mechanics of the property were well explained.

[11] Drake *et al*. (2018): A chapter of the classic Gray's Anatomy textbook describing the AW. This was a full description of the entire AW, both anterior and posterior, as well as across the thorax. This provided an excellent overview of the anatomy of interest.

[12] Gosling *et al*. (2017): Another anatomy text reviewing the AW. This book section provided another opinion on how to describe the AW, specifically considering the differences in naming conventions of various components.

[13] Tuktamyshev *et al*. (2016): This article provided evidence that the IAV contained an incompressible fluid, thus allowing for IAP measurements taken anywhere in the IAV to be equivalent.

[14] Forstemann *et al*. (2011): An *ex vivo* experiment to quantify the mechanical properties of the linea alba was completed. This article is well-cited among researchers, and also contains a simulation that could be validated by the in-house measurements.

[15] Blaser *et al*. **(2015):** Literature review covering papers studies from 1994 to 2011 that measured IAV and IAP *in vivo*. Calculated compliance among acute and chronic IAH patients were compared among studies to determine if a "normal" range of C_{ab} could be determined.

[16] Stedman (2006): Medical dictionary with pertinent terms including myometer, peritoneum, and pneumo-. Excellent reference text for those without a medical background.

[17] Accarino *et al*. (2009): This experimental study on patients with and without bloating evaluated approximate measures for IAV. Further measurements included gaseous volumes separated by the stomach and colon. Results were taken from helical multi-slice CT scans.

[18] Agnew *et al*. (2010): Pre- and post-op evaluation of IAV in hernia patients indicated an increase in IAV; a conclusion intuitively unexpected. Reasons for IAV increase were attributed to weakness in AW caused by the detachment of oblique muscle tissue from fascia (*i.e*. decreasing stiffness).

[19] Villoria *et al*. (2008): In both a supine and standing position, patients were insufflated, while AW muscle activation and diaphragm position were studied. It was noted that, at higher IAP, the responses of the AW muscles and diaphragm change if the patient is standing or sitting, in order to best protect visceral components.

[20] Malbrain *et al*. **(2016):** This essential article is an updated take on [2], [4], [193]. This is a literature review expanding on the effect of C_{ab} in organ-organ interactions.

[21] Papavramidis *et al*. (2011): Fifteen patients with abdominal fluid build-up were evaluated pre- and post-fluid removal. UBP and the volume of fluid removed (change in IAV) were measured and C_{ab} was evaluated. This article proved the linear relationship between IAP and IAV removing volume rather than adding it, conversely to some other research groups.

[22] Mulier *et al*. (2008): This well-researched article evaluated the IAP/IAV relationship up to 12 mmHg *in vivo*. A linear relationship, determined with 3 check points, was determined in all subjects. IAP greater than 12 mmHg was not explored given its association with abdominal compartment syndrome.

[23] Abu-Rafea *et al*. (2006): The intra-peritoneal cavity was insufflated with carbon dioxide up to 30 mmHg, and the intra-peritoneal pressure, as well as intra-peritoneal volume were measured. This article showed interesting parallels to IAP/IAV studies, though went beyond the traditional 12 mmHg insufflation pressure.

[24] Song *et al*. **(2006):** Eighteen patients (male and female) were insufflated with carbon dioxide prior to laparoscopic surgery up to 12 mmHg. Prior to experimentaiton, average muscle and skin/fat thicknesses in the abdomen were measured at 6 standard points. Test results included measurement of volume change, a visualization of volumetric shape change, and AW elasticity.

[25] Mulier *et al*. (2008): Mulier *et al*. followed up on their research in the same year with a poster presentation on the shape change present in the abdominal compartment given increases in IAP beyond 12 mmHg (up to 25 mmHg).

[26] Pracca *et al*. (2011): This work described a preliminary study for a new treatment method for IAP reduction termed ABDOPRE. With a vacuum chamber against the AW, IAV was increased with the expectation of a corresponding IAP decrease. One case of note in this study was the effect of subcutaneous fat in an obese patient. In this case, IAP increased with increasing IAV, a concern for future developments.

[27] David *et al*. (2011): A complementary article to [26], David *et al*. further describe the ABDOPRE system, particularly in terms of its design and preliminary findings.

[28] Severgnini *et al*. (2007): This review article considered imaging techniques in the assessment of abdominal pathologies. Of particular interest to the authors was the non-invasive diagnosis of abdominal fluid build-up following trauma.

[29] Sugerman *et al*. (1997): Sugerman's research group evaluated the correlation between IAP and obesity indicators such as weight, body mass index (BMI), sagittal abdominal diameter, and waist to hip ratio. The greatest correlation was seen between IAP and sagittal abdominal diameter.

[30] Malbrain *et al*. (2009): Malbrain's research group discussed the efficacy of using abdominal perimeter as a means of estimating IAP. Conclusions were that little to no correlation could be confirmed between these two values, thus, it was not of interest to pursue this avenue.

[31] Guerrero-Romero *et al*. (2003): Abdominal volume index was defined and reviewed as a means of abdominal volume measurement. It should be noted that the anatomic reference points have the abdominal volume calculated for the entire trunk, including the spinal column, skin, fatty tissues and back muscles.

[32] Valdez *et al*. (1993): Valdez *et al*. considered the conicity index (C-index) as a means of geometric gauge for abdominal adiposity. The C-index is of interest, here, for its use in IAV measurement.

[33] Cohen *et al*. (1994): Cohen *et al*. described their design and development of respiratory inductance plethysmography for measurement of air capacity or obstruction. Of note is the anatomical location that the RIP coils are placed on the rib cage and abdomen.

[34] Tayebi *et al*. **(2020):** A literature review was conducted on existing non-invasive methods of IAP measurement. Tayebi *et al*. were thorough in their research and suggested theoretical approaches, as well as tested ones.

[35] Cobb *et al*. (2005): An experimental study conducted on men and women of varying BMI. The sample size, here, was quite small (only 20 subjects enrolled), but results tended to agree with literature published at later times. Two items of note were the positive correlation between IAP and BMI, as well as the apparent lack of connection between IAP and sex.

[36] De Keulenaer *et al*. **(2012):** A literature review that examined articles in three areas as they apply to IAP: BMI, body position, and respiratory cycle (*i.e*. end-expiratory, end-inspiratory, etc.). This article was very useful in comparing IAP against everyday movements.

[37] Chionh *et al*. (2006): This study provided further evidence for "normal" IAP values at changing anatomical positions. Units for pressure were [cmH_2O].

[38] Sanchez *et al*. (2001): Additional data were added to "normal" IAP with randomly selected hospitalized patients. One conflicting conclusion this research group found with other works was a correlation between BMI and IAP.

[39] Vasquez *et al*. (2007): UBP in overweight populations ($n = 45$) was evaluated across a series of head of bed positions (supine, 15, 30 and 45°). Part of [36] review.

[40] Lambert *et al*. (2005): Lambert's research group focussed on determining "normal" IAP in overweight populations. Units for pressure were [cmH_2O].

[41] Arfvidsson *et al*. (2005): This study confirmed a combination of theories previously presented: iliofemoral venous pressure was correlated to IAP in obese patients, and obese patients saw greater baseline IAP over their normal counterparts.

[42] Davis *et al*. (2005): A comparison study between intra-gastric pressure, UBP, and intra-peritoneal pressure was conducted on paediatric patients. With intra-peritoneal pressure as a baseline, UBP saw better correlations than intra-gastric pressure, just as shown in adult studies.

[43] Ejike *et al*. (2008): A paediatric study on "normal" IAP was conducted and was found to be 7 mmHg in critically ill children. Contrary to the recommended instillation volume for UBP in adults (25 mL), Ejike's research team recommended 3 mL to be instilled for IAP measurement.

[44] Thabet and Ejike (2017): This review article provided benchmarks for IAP diagnostics in children. To note, there was no age bracket provided to define "paediatric" patients.

[45] Papavramidis *et al*. (2011): A standardization article that looked to clarify definitions, diagnostic techniques, and treatment of ACS and IAH. This was written after [2], so many definitions were taken from the WSACS conference.

[46] Blaser *et al*. (2019): A multi-center analysis of IAH in 15 ICUs worldwide, accumulating nearly 500 patient results, was completed. Rates of IAH were said to be almost 50% (48.9% during observation) in intensive care unit patients.

[47] Milanesi *et al*. (2016): A literature review examining articles that measured IAP in patients using a variety of techniques. The interest, here, was identifying IAH and ACS instances, and to determine if one measurement technique was more reliable. Essentially, this article corroborated WSACS paper: "Intra-abdominal pressure should be expressed in mmHg and measured in the supine position, at end-expiration and in the absence of abdominal muscle contraction."

[48] Sugerman *et al*. (1997): Nine female patients with pseudotumor cerebri (pressure around the brain causing headaches and vision blurring) were measured for IAP (with UBP) and intracranial pressure. Both pressure sets were higher in obese/ill patients than control group from previous study. Part of [36] review.

[49] Sugerman *et al*. (1998): UBP in patients with drastic weight loss (n = 15) was measured pre- and post-gastric bypass (1 year later). BMI, sagittal abdominal diameter, UBP all decreased. Part of [36] review.

[50] Dejardin *et al*. (2007): This paper provided a set of paired data for intra-peritoneal volume and intra-peritoneal pressure, or, IAP and IAV. This data allowed C_{ab} to be extrapolated, though this mechanical property was not discussed in the paper. Dejardin *et al*. simply wanted to consider the intra-peritoneal pressure/intra-peritoneal volume relationship, and concluded that pressure and volume were highly correlated in a linear fashion.

[51] Smit *et al*. (2016): This observational study looked at patients pre- and post-op in the cardiovascular wing of a hospital. Correlations of IAP in the study group were considered against BMI, waist circumference, waist/hip ratio and obesity indicators (*i.e*. C-reactive protein and serum creatinine). The only correlation was found between IAP and BMI.

[52] Cheatham *et al*. (2009): Nearly 160 patients participated in this study. IAP was taken at supine, 15°, and 30° supine to determine the effect of head of bed or body position on IAP. Measurements were taken via UBP on intensive care unit patients.

[53] Morris *et al*. (1961): This is the anchor of the present research, that is, an undeniable connection between spinal stability and IAP was elucidated by Morris *et al*..

[54] Montgomery (2017): A comprehensive overview of parastomal hernias: causes, symptoms, treatments, and physiological presentation.

[55] Talasz *et al*. (2011): The brief letter to the editor considered the misconceptions surrounding the "Valsalva Maneuver". Conclusions were that the Valsalva maneuver was the forced pushing with closed nose and mouth, but open glottis (*i.e*. throat). This allowed air to enter ear cavities and equate pressure. Alternatively, abdominal straining was the forced pushing with closed glottis, such as during defecation.

[56] Al-Khan *et al*. (2011): IAP in 100 pregnant women was recorded pre- and post-delivery. All women underwent cesarean-sections and displayed a significant decrease in IAP post-operatively. The median IAP recorded immediately prior to delivery was 22 mmHg; a value of dangerous proportions in the average population.

[57] Beer *et al*. (2012): This was a classic mechanics of materials textbook, for which chapter 10 (columns) was of particular interest. A potential avenue for research was to consider buckling of the spine simulated as a column.

[58] Davis (1985): This article summarized research done on IAP until 1985. The greatest contributors, at this time, to IAP were defined as (1) hydrostatics, (2) respiration, (3) defecation, (4) active contraction and (5) physical activity. IAP was measured using indwelling catheters, implanted balloons and radiosonde (the preferred method by the author) developed by Watson *et al*.

[59] van Ramshorst *et al*. **(2011):** Following up on their 2008 article, this research group tested their device on 42 healthy students and 14 corpses. Correlation coefficients found for the corpses were then used to estimate IAP in the healthy students, but were not validated with UBP. IAP was measured in the corpses upon insufflation using a laparoscope and Veress needle.

[60] Chen *et al*. (2015): Chen *et al*. paralleled the study completed by van Ramshorst *et al*. and found an alternative correlation curve. Explana-

tions for this discrepancy were reasoned by sample differences; *i.e.* van Ramshorst *et al.* worked with a younger population. That said, Chen *et al.* compared results to UBP, values which were not provided by van Ramshorst *et al.*

[61] Malbrain *et al.* (2010): Malbrain *et al.* completed a case study of four patients whose intra-gastric pressures and intra-bladder pressures (UBP) were measured, simultaneously. The ratio of intra-gastric pressure to intra-bladder pressure did not consistently measure 1, indicating the presence of local compartment syndromes (*i.e.* pressure peaks in the stomach, but not in the IAV, as a whole). This finding disputes the theory that the IAV contains an incompressible fluid, and should be considered in future studies.

[62] Freitag *et al.* (2003): "Normal" blood pressure was defined as a result of a literature review. A recommended 115/75 mmHg blood pressure was determined as the new "norm".

[63] Hackett *et al.* (2013): A literature review of studies conducted on Valsava maneuvers is conducted. Peak IAP during Valsalva maneuvers and during AW activation are listed from a number of research groups. The effect of peak IAP on blood pressure is discussed.

[64] Addington *et al.* (2008): Measurements (in cmH_2O) were taken for voluntary coughs and laryngeal cough reflex in 11 females aged 18 to 75. Peak pressures reached 139.5 cmH_2O and 164.9 cmH_2O for for voluntary coughs and laryngeal cough reflex, respectively.

[65] Aquina *et al.* (2014): This literature review on parastomal herniation and prevention techniques discussed discrepancies in definitions and helped to clarify for a clinical project. It is important to note that the authors described the Valsalva maneuver as the testing method for hernia diagnosis.

[66] Cheatham *et al.* (2007): Part-2 of the 2006 review on ACS/IAH terminology. In Part-2, the current IAP knowledge base is critiqued, and recommendations for areas of future research are given.

[67] Otto *et al.* (2009): IAP was measured directly by implanting a piezoresistive pressure measurement probe in the peritoneal cavity. Results were in agreement with simultaneous intra-vesical values, but fragility of the device posed the greatest concern.

[68] Pracca *et al.* (2007): A cannula connected to a Codman microsensor was tapped into the AW at the junction of the anterior rectus abdominis and line connecting iliac anterosuperior spines. This transducer directly measured the pressure of the peritoneal cavity and compared it to "Kron's technique" (*i.e.* the basic UBP measurement system).

[69] Al-Hwiesh *et al.* (2011): This study concretely defines IAP and IPP to be the same at erect and supine positions. In testing of 25 patients, there were no statistically significant differences between IAP and IPP, indicating the ability of readers to use them interchangeably in future research.

[70] Al-Abassi *et al.* (2018): A comparative study between urinary bladder pressure (or, intra-bladder pressure) and IAP (found laporascopically, thus intra-peritoneal pressure) measurement was conducted to evaluate IAP measurement techniques. UBP was in agreement with IAP, but this research group was not able to measure pressures above 12 mmHg reliably.

[71] Aguilera *et al.* **(2018):** The esophageal, gastric, central venous (superior vena cava, not inferior vena cava), rectal, and bladder pressures were measured simultaneously *in vivo* during a series of coughs. Results were mapped and compared to evaluate if cough pressure could be evaluated at differing compartments. That said, the article also provided evidence of the efficacy of each method in IAP evaluation.

[72] De Waele *et al.* **(2009):** An important article that outlined the recommended research practices for novel measurement techniques in IAP. Statistical analyses, patient state, etc. were all discussed.

[73] Homma *et al.* (2002): This chapter presents a broad summation of urodynamics with an emphasis on testing and diagnostics. Of greatest interest is the recommended protocol for detrusor pressure measurement, accompanied with relevant medical terminology.

[74] Leitner *et al.* (2016): This paper performs an evaluation of urodynamics to determine whether healthy urinary tract function can be divulged during testing. Figure 3 in Leitner *et al.*'s paper is of value in its visual interpretation of healthy bladder function. Detrusor pressure, intra-vesical pressure, and IAP are shown during saline injection and forced bladder evacuation.

[75] National Kidney and Urologic Diseases Information Clearinghouse (NKUDIC) (2012): Urological testing was explored and defined. Parallels between cystometric testing and IAP measurement were apparent, indicating the need for language consistencies.

[76] Lee (2012): This summary article in *Critical Care Nurse* is of value in its description of measurement techniques, as suggested by the WSACS, of IAP.

[77] Wauters *et al*. (2012): This "novel" device study seemed to follow the same procedure as the standard intra-gastric measurement device. The study was presented on a porcine model and results were compared to intra-peritoneal pressure, intra-gastric pressure, and UBP.

[78] Sugrue *et al*. (1994): Evaluation of intra-gastric pressure measurement, with variation of +4 mmHg or -3 mmHg against UBP. Conclusions, here, were that this made intra-gastric pressure a reasonable alternative, but would not be appropriate today given the WSACS requirements for IAP measurement tools.

[79] Shafik *et al*. (1997): Intra-rectal pressure was compared to IAP. IAP was measured directly with a Veress needle, while intra-rectal pressure was found with a fluid-filled balloon catheter.

[80] Dowdle (1997): An intra-uterine pressure measurement device was compared to the present (1997) "gold standard" in intra-uterine pressure measurement. The function of both devices was the same: introduce a fluid-filled catheter into the uterus. With an attached strain gauge, the applied pressure was determined. The novel device offered changes in size/material/transducer to improve use and comfort.

[81] Lacey *et al*. (1987): In a rabbit study, a number of pressure measurement systems were evaluated simultaneously to determine agreement. IAP was measured with a bladder catheter, and the bladder filled with 3 mL of saline (much lower than today's standards). A cannula was put through the inferior vena cava, superior vena cava, femoral artery and brachial artery. Correlation was only found for the inferior vena cava and bladder, a statement in disagreement with accepted gastric, and rectal measurement systems.

[82] Johnson *et al*. (2009): The development of a novel intra-vaginal transducer as a means of IAP measurement was explained. Results were compared both *in simulacra* (benchtop testing) and *in vivo* experiments, but transducer placement was not specified. The device was only mentioned to be situated in the "upper vagina".

[83] Coleman *et al*. (2012): Coleman *et al*. built on the results of [82] by enabling wireless access to an intra-vaginal transducer. Measured values (*in vivo*) were compared to those measured by a rectus balloon at the same time in the same subject. High accuracy supports the further development of such a device.

[84] Bloch *et al*. (2018): Ultrasound guided tonometry was used to correlate with IAP as a means of discriminating between low, normal, and high IAP levels. Initial testing was completed on porcine models whose IAP was increased by the injection of saline. This is very similar to AWT monitoring, with the added benefit of flow management.

[85] van Ramshorst *et al*. (2008): A preliminary study of indentometry to evaluate IAP on 2 corpses was conducted. Correlation was evident, supporting further work in the area.

[86] David *et al*. (2018): Animal testing on a novel non-invasive IAP measurement device using bioimpedance and microwave reflectometry was completed. IAP was monitored and adjusted using a trocar directly placed in the abdominal compartment. Just as with [59], [60], results were correlated to measured IAP, rather than directly measuring the pressure.

[87] David *et al*. (2020): Building on the theory presented in [86], the given work tested microwave reflectometry as an indirect method of IAP measurement in a proof-of-concept clinical trial ($n = 5$).

[88] Brown (2012): Brown presented a mathematical evaluation of the AW to support the generally accepted hypothesis that the AW acts as a composite-laminar material. The stress distribution and stiffness of the soft tissue were described, as well as the mechanical response to loading.

[89] Akkus *et al*. (2012): The *in vivo* measurement of skin and subcutaneous tissue (adipose tissues, specifically) thickness was conducted. Thickness values were taken at different anatomic regions. Here, of interest was the anterior abdomen thickness.

[90] Tran *et al*. (2014): An excised AW was subjected to 3 kPa of pressure to evaluate the resulting strain. After each pressurization, a layer was dissected to determine how each layer contributed to the overall effect of the abdominal strength. The dissected layers were (1) skin and subcutaneous tissue, (2) anterior rectus sheath, and (3) rectus abdominis.

[91] Astruc *et al*. (2018): This was an important article that considered the mechanical properties of AW fascia. The linea alba and posterior/anterior rectus sheaths were measured and discussed in transverse and longitudinal loading. Further, hyperelastic properties were evaluated in all three tissues.

[92] Korenkov *et al*. (2001): The fibers of the linea alba were evaluated for thickness orientation and tensile strength. Irregular fiber orientation was found and supports further studies showing the anisotropy of the linea alba.

[93] Cardoso (2012): Cardoso's M.Sc. thesis determined the mechanical properties of all the major layers of the AW, including fascia and muscle tissues. The values found by Cardoso have been used in a number of simulations, since.

[94] Abdelounis *et al*. (2013): Viscoelasticity in the rectus sheath was confirmed by testing *ex vivo* samples at different strain rates. Whether the right or left rectus sheath was tested was not confirmed.

[95] Martins *et al*. (2012): The anterior rectus sheath was evaluated *ex vivo* to determine the longitudinal and transverse properties.

[96] Kureshi *et al*. (2008): Herniated and non-herniated transversalis fascia were evaluated to determine the *ex vivo* mechanical properties. Both break strength and modulus were determined.

[97] Wolloscheck *et al*. (2004): The transversalis fascia, peritoneum, aponeuroses of the internal obliques and external obliques were tested *ex vivo* to determine the tensile strength of each layer. Punch tests and suction tests (using the Cutometer) were completed and resulted in the conclusion that the transversalis fascia is the weakest tissue, and the external oblique aponeuroses the strongest. These results were then compared to hernia mesh materials.

[98] Hernandez-Gascon *et al*. (2012): Another mechanical model of the abdomen was developed to evaluate where abdominal stability could be traced to. Following a similar set of steps as [99], [100], this research group developed a model without skin or fat under passive loading conditions, to determine that the linea alba was the apex of mechanical stability in the AW.

[99] Pena *et al*. (2017): This book chapter reveals a step-by-step evaluation in developing a computational model for the human abdomen. To note, the authors neglected skin and subcutaneous tissues in their geometry due to their negligible stiffnesses when compared to muscle or aponeurosis (linea alba).

[100] Pachera *et al*. (2016): A well-described model using ABAQUS for the AW is reviewed. Mechanical properties were taken from articles including [14], [93], [94]. The skin and subcutaneous tissue were not considered, and their neglect was not explained. Model validation was completed by increasing IAP and comparing deformation to [115]. It should be noted that IAP due to jumping was said to be 171 mmHg taken from [93].

[101] Tham *et al*. **(2006):** This article provided an extremely relevant mathematical and experimental model of traditional Chinese cupping therapy. The skin, fat, and muscle layers were considered under a localized negative pressure using ABAQUS. The math behind the simulation was clarified and, finally, experimental validation corroborated results.

[102] Deeken *et al*. **(2017):** This literature review evaluated existing data on the properties of the AW found through *in vivo*, *ex vivo*, computational, and analytical means. Assumptions were described and the detriments/advances of each study were included. The "future work" section of this article was of value given its wide range of tangible studies that have yet to be completed on the AW. Emphasis was placed on biomaterials for hernia mesh repairs and how these materials conflict/coincide with natural, healthy tissues.

[103] Grassel *et al*. (2005): Grassel *et al*. evaluated the anisotropy of the linea alba *ex vivo*. The main fiber directions were appreciated and results demonstrated a greater stiffness in the transverse direction than the longitudinal fibers. Stiffness further increased in the infraumbilical linea alba of females (as opposed to supraumbilical). Another interesting result was the decrease in linea alba stiffness in men than women.

[104] Cooney *et al*. (2016): *Ex vivo* uniaxial and equiload biaxial tests were completed on the linea alba. Average thicknesses were determined, as well as transverse/longitudinal Young's moduli of the linea alba.

[105] Levillain *et al*. (2016): The reorientation of elastin and collagen in AW fascia under loading is explored. Both porcine and human linea alba are evaluated, with collagen reorientation only evident in the longitudinal orientation.

[106] Rath *et al*. (1996): Dynamometer tests were completed on dissected human linea alba at the umbilical, supra-, and infra-umbilical.

[107] Rath *et al*. (1997): Similarly to Rath *et al*.'s 1996 paper [106], dynamometer tests were completed on the anterior and posterior rectus sheath. Supra and infra-arcuate sheaths were analyzed.

[108] Kirilova *et al*. (2011): Transversalis fascia was explored *ex vivo* to find the constitutive parameters of the fascia.

[109] Kirilova-Doneva *et al*. (2016): Transversalis and umbilical fasciae continued to be studied by the Kirilova group. This time, the viscoelastic properties were demonstrated *ex vivo*, such that, at higher strain rates, the fascia stiffened.

[110] Yang *et al*. (2018): Yang *et al*. used ultransonography to measure the thickness and Young's modulus of skin. In the introduction, the existing means of stiffness measurement were well-detailed (both advantages, and disadvantages). This was an *in vivo* evaluation.

[111] MacDonald *et al*. (2016): MacDonald *et al*. confirmed inter-rater reliability of muscle stiffness evaluation. Both abdominal bracing and hollowing were evaluated and compared to muscle Young's modulus at rest. The internal obliques, external obliques, transversus abdominis, and rectus abdomins were all considered. Elastography, electromyography and ultrasound were used to evaluate muscle activation and stiffness.

[112] Tran *et al*. (2016): In supine, sitting and weighted positions, the AW stiffness was determined. Composite properties were evaluated at the rectus abdominis, linea alba and oblique muscles.

[113] Todros *et al*. (2020): A comprehensive computational model of the human thorax is explored with respect to the function of abdominal muscles under varying IAPs. Function of the model matched well with experimental studies on a single participant; though this is a limitation of the model, it demonstrates the ability of the system to deduce abdominal movement and activation correctly.

[114] Francois *et al*. (2012): Chapter 2 of Francois *et al*.'s textbook discusses elastic behaviour of materials. This chapter reviewed the basic equations for elastic matrices of isotropic through anisotropic materials. Effective modulus was discussed, here.

[115] Konerding *et al*. (2011): Konerding *et al*.'s study provided a useful benchmark for analytical comparison. Of particular interest was the research group's findings on AW force required to maintain closure of an incision along the linea alba, despite high applied IAP (around 150 mmHg).

[116] Ramalingam (2009): Ramalinam's reference text defined a number of engineering terms, including symbols and simple equations.

[117] Choi and Zheng (2005): This research duo explored Poisson's ratio and Young's modulus using two different indenters.

[118] Lu *et al*. (2012): Lu's research group explored methods of soft tissue stiffness measurement. In this article, ultrasound water jet indentation was described.

[119] Hayes (1972): The mathematical theory behind indentation was described, using articular cartilage as a fascia example.

[120] Woodard and White (1986): This research duo evaluated the composition of a number of tissues across the body (muscle, digestive systems, brain, bone, etc.), particularly noting water, lipid, and protein contents in each. This was of use in identifying simplification opportunities when evaluating the density of the human body, however, the authors did not comment on an approximation for average water density in the entire body.

[121] Francois (2012): Chapter 5 of Francois *et al*.'s textbook discussed material viscoelasticity.

[122] Konstantinova *et al*. (2017): Palpation strategies and the ability of human subjects (n = 12) to correctly detect stiffer regions were assessed. The results were then analyzed and applied to a robotic palpation system to determine whether automated systems could respond as well as, or better than, human testers.

[123] Zugel *et al*. (2018): This is an important review article that provided a list of existing fascial measurement methods. This article also considered the landscape of fascia research and future areas of work.

[124] Chaitow *et al*. (2012): This brief article provided a description of fascial palpation and how it is used to diagnose, treat and evaluate patients.

[125] Wilke *et al*. **(2018):** This was an important article with respect to the present research, as the methods described in this paper helped to model the present clinical studies. Wilke *et al*. studied the reliability and validity of a novel soft tissue semi-electronic compliance meter. In a study of n = 34 healthy participants, the medial gastrocnemius was evaluated for stiffness with a semi-electronic compliance meter versus the MyotonPro. Good correlation between the two methods was found.

[126] Agyapong-Badu *et al*. (2018): Proposed standards for myometry use. Probe location, muscle length, level of contraction, prior physical activity all significantly affected stiffness, tone, and elasticity results with the MyotonPro. This article did not outline rules, but provided recommendations to improve future studies that intended to use MyotonPro.

[127] Tarsi *et al*. **(2013):** Tarsi *et al*. considered a suction device for soft tissue stiffness measurement. To measure the deformation height of the tissue, electrodes were placed along the wall of the aspiration tube to drop the voltage each time an adjacent electrode was in contact. This device assumed the tissue would climb the tubing walls, though did not consider the volume of the domed top created by the inflated tissue. This article described the design process and components that may be helpful in future prototypes.

[128] Kutz *et al*. (2015): This fundamental text provided basic equations and information on materials and engineering mechanics.

[129] Peipsi *et al*. (2012): A brief overview of the MyotonPro, a novel (2012) tool built on pre-existing successful devices (Myoton-2, Myoton-3). The MyotonPro measures tissue tone, stiffness, elasticity, viscoelasticity (creep-ability, mechanical stress relaxation time) in myofascial tissues.

[130] Feng *et al*. (2018): This study compared the MyotonPro against shear wave ultrasound elastography at the gastrocnemius and Achilles tendon. Only moderate correlation (0.463 - 0.544) was found between the two measurement sets, but the MyotonPro did exhibit intra-operator reliability.

[131] Zheng and Huang (2016): This extensive literature review explores all forms of soft tissue elasticity measurement until around 2009. This book is the baseline for further exploration of soft tissue measurement.

[132] Myoton AS (2010, revised 2020): The user manual for the MyotonPro provides specific information on device geometry and loading rates.

[133] Müller *et al*. (2018): A comparison of novel aspiration device, “Nimble”, and industry standard, “Cutometer” was completed. The Nimble used a set deformation height of 1 mm. The full product design was laid out, and the deformation was reached when the vertical pump tube was closed (via touching skin).

[134] Wernicke *et al*. (2009): In a group of 300 patients (n = 300), palpation was compared to a tissue compliance meter (analog handheld device) to evaluate for preference in evaluation of radiation-induced fibrosis in breast cancer survivors. The tissue compliance meter was shown to best quantify radiation-induced fibrosis. A radiologist also evaluated patient US and MRI images, though, imaging proved to also be inferior to the tissue compliance meter in quantifying the condition.

[135] Jacobson and Driscoll (2021): A brief summary is provided on elasticity measurement methods for soft tissue (particularly fascia). Only non-invasive systems are evaluated, with an emphasis on deformation-based methods including indentometry, myometry, and aspiration.

[136] Draaijers *et al*. (2004): A reliability study of the Cutometer was conducted. This article was referenced in [133] as a manuscript that well established the Cutometer as a tissue measurement system.

[137] Bayford *et al*. (2012): This review of bioimpedance (or, electrical impedance tomography) offered opportunities for future research.

[138] Simon-Allue *et al*. (2017): Using virtual imaging, that is, external cameras in combination with numerical analysis, the passive mechanical behaviour of New Zealand rabbits was evaluated *in vivo*. Rabbits were insufflated to 12 mmHg, wherein shear modulus was calculated by inverse analysis using external trackers on the rabbits' abdomens.

[139] McAuliffe *et al*. (2017): Utrasound was considered at tendons across the body for relative and absolute reliability in thickness measurement. Intra- and inter-rater reliability ranged from moderate to excellent.

[140] Sigrist *et al*. (2017): A step-by-step mathematical breakdown of ultrasounds, both shear wave, strain imaging and b-mode. This is a great article to clarify differences in mechanical properties analyzed.

[141] Hirsch *et al*. (2017): The fundamentals of elastography were explained in this introductory chapter. For further information on magnetic resonance elastography, Hirsch has an extended textbook on the topic.

[142] Glaser and Ehman (2014): Book section on the theory behind elastography (mathematical and hardware-related). Anatomic landscapes can be provided with MRI, US, X-ray or other related technologies.

[143] Yen (2003): Comparison of palpation techniques when constant force was applied versus constant deformation. It was determined that considering a constant depth of palpation offered greater ability to distinguish between stiff tissues.

[144] Nichols and Okamura (2015): This proof-of-concept study evaluated a robotic palpation device that used machine learning technology to improve tumour identification. Qualitative evaluation from machine learning allowed for stiff and flexible tissues to be distinguished, though had not yet been tested in humans.

[145] Oflaz *et al*. (2014): Proof-of-concept indentation technique compared to durometer. Denoted the soft tissue stiffness meter.

[146] Williams *et al*. (2007): Measurements of stiffness using a "softcometer" for use in haptic simulations systems was evaluated. This device essentially used the same system as any other indentometer, that is, measured the resultant deformation given a point load.

[147] Nava *et al*. (2004): A preliminary study for an aspiration device for *in vivo* mechanical evaluation of the soft tissue of internal organs was conducted. Cameras and optics were used to map motion.

[148] Elahi *et al*. (2019): A novel method of measuring volumetric tissue deformation using pistons was explored. Suction was applied and the resulting pressure changes were measured. The calibration technique for this device was well laid-out for future works.

[149] Valtorta *et al*. (2005): A proof-of-concept study on a torsional rotation device for soft tissue measurement *in vivo* was completed. No axial force was applied, only the shear torque applied on the superficial tissue was examined. Vibrations applied and responses were measured with electromagnetic transducers to evaluate the "complex shear modulus".

[150] Narayanan *et al*. (2006): Evaluation of a piezoelectric sensor for mechanical evaluation of soft tissue. Young's modulus and viscoelastic properties were measured. The sensor applied a small voltage across two piezoelectric slides, and measured the resulting impedance.

[151] Moerman *et al*. (2009): Moerman's research group considered a benchtop model to evaluate material parameters of a hyperelastic system. Digital image correlation was used in conjunction with finite element modeling to evaluate said parameters of a silicone gel pad of known properties.

[152] Zhang *et al*. (2017): Zhang *et al*. validated a finite element model of the eye given experimental results for applied pressure, resulting deformation and intra-ocular pressure. The model was validated and solved for the constitutive mechanical properties of the eye layers, but was only accurate for the given geometry and specimen (*i.e*. not patient specific).

[153] Bensamoun *et al*. (2011): This explorative study evaluated the stiffness of the liver, kidney, psoas, and spleen using MRI elastography. The various layers of the kidney were also evaluated.

[154] Dittmann *et al*. (2017): An analysis of how visceral stiffness changes depending on hydration state. Measurements were taken using tomoelastography (using MRI elastography).

[155] Courtney *et al*. (2005): A fundamentals textbook for mechanical behaviour of materials. This textbook goes more into constitutive equations than [57].

[156] Yoshino *et al*. (2012): This comparison of AW elastance (inverse of C_{ab}) between animal and human studies suggested the invalidity of animals as an indication of human properties. The pressure-volume curve between species followed a non-linear shape for animals, versus a linear to exponential curve in humans.

[157] Vleeming *et al*. (2014): Vleeming's research team considered paraspinal or abdominal muscles, and the thoracolumbar fascia as they relate to low back pain. This test was conducted on a benchtop model to evaluate the proportion of stress distributed to each muscular or fascial tissue.

[158] El-Monajjed and Driscoll (2020): Expanding on [157], El-Monajjed developed a computational model to evaluate how stresses are distributed through the thoracolumbar fascia given changing IAP and muscular compartment pressures.

[159] El Bojairami *et al*. (2020): A comprehensive computational model of the human torso was developed comprising muscles, skeletal structures, IAP and fascia for the evaluation of factors that contribute to low back pain. Possible avenues for future research with this model include the evaluation of C_{ab} and effect of AW elasticity on IAP.

[160] Newell and Driscoll (2021): A computational model of the lumbar spine was developed comprising muscles, skeletal structures, and fascia for the evaluation of factors that contribute to low back pain. Stress distribution towards the thoracolumbar fascia was noted in model adjustments to simulate an unhealthy system.

[161] Warren *et al*. (2020): Cupping therapy was compared to self-myofascial release (heat and foam rolling) as means of increasing range of motion in the hamstring. Participant (n = 17) preferences were for cupping therapy, though, results suggested both therapies were equivalent in success rates.

[162] Al-Shidhani and Al-Mahrezi (2020): A second literature review was conducted on the benefits and history of cupping therapy. Of note were the definitions of different types of cupping therapies. This was one of the clearest synopses on cupping therapy techniques.

[163] Moortgat *et al*. (2016): A literature review was conducted on the benefits of cupping therapy. One noted conclusion from this review was the need for more objective research tools, though most compiled data was subjective. This is a much more rigorous review than [162].

[164] Rozenfeld and Kalichman (2016): The history of cupping therapy was described and its use in modern medicine was proposed. This is a general source of information on the background of the therapy and expert opinion on its instatement as a staple in musculoskeletal medicine.

[165] Chiu *et al*. (2020): The effect of negative pressure (long-term cupping therapy) on 40 ($n = 40$) baseball players' myofascial pain was investigated. Tissue "compliance" was evaluated by measuring tissue resection distance [mm] compared to applied pressure [mmHg]. Tissue compliance decreased in each group of normal and myofascial pain patients between the first and final cupping therapy session.

[166] Worret *et al*. (2004): Treatment for morphea using the "LPG" technique (Endermology) was evaluated. Following treatment, clinical appearance of morphea lesions improved, induration reduced and pain reduced. Elasticity of the tissue was also increased. Endermology may be described as a dynamic cupping therapy, in which a portion of skin is resected between two rollers via suction, and mobilized.

[167] DaPrato *et al*. (2018): DaPrato *et al*. considered cupping therapy biomechanically, asking the question: what happens to deep tissues and fascia when negative pressure is applied locally? MRI evidence suggested the movement of multiple tissue layers under negative pressure, indicating the possibility of volumetric measurement.

[168] Stylinski *et al*. (2018): Stylinski *et al*. provided a literature review of disputing statistics and perspectives from research groups regarding parastomal herniation rates and locations. Two points of contention recorded in disputing articles as facts were: (1) colostomies have higher rates of parastomal hernia occurrence than ileostomies, (2) there is a lower risk of parastomal hernia if the stoma is made through the rectus abdominis, as opposed to lateral to the muscle group.

[169] Antoniou *et al*. (2018): This article summarized European guidelines outlining "best practices" regarding parastomal hernia prevention and treatment. The article noted that, to date, there are no agreed upon guidelines, as experts choose various methods to treat and prevent the disease.

[170] Tenzel *et al*. (2017): Tenzel *et al*. considered a common treatment mechanism for incisional and parastomal hernias (among others): prophylactic mesh augmentation, or the insertion of a physical mesh in a weakened area of the abdomen to prevent future damage.

[171] Primiano *et al*. (1982): The mathematical model for the human thorax introduced in Primiano's article simplified the torso into a series of stacked pressurized cylinders. Of interest is a proof supplied in the appendix illustrating the efficacy of the Laplace equation on this model. The only stiffness of concern, thus, becomes the tangential stiffness in the AW.

[172] Breslavsky *et al*. (2016): A numerical analysis of thick-walled, pressurized, hyperelastic cylinders was completed. Mathematical proofs and step-by-step calculations explained how to correctly interpret biological materials (inherently hyperelastic) under radial loading, point loading, and distributed loading due to internal and external pressures. This article was useful as a means of expanding on the Lamé and Laplace equations to more accurately predict movement in biological cavities.

[173] Muvdi (1991): Mathematical proofs and explanations on thin- and thick-walled cylinder evaluation. This was a great resource to understand how to calculate wall stress in a pressurized cylinder or sphere.

[174] Flint *et al*. (2010): Table 1 and 2 of this article reviewed around 60 000 study participants' BMI and waist circumference, respectively. This article, thus, provided anthropometric basics for future study analytics.

[175] Fryar *et al*. (2012): Vital Statistics at the USA Center for Disease Control collected a huge amount of data on anthropometrics divided into gender and age group. This is a great reference text for theoretical and simulation experiments.

[176] Tahan *et al*. (2016):Given 156 healthy subjects, the average AWT was measured with ultrasound for each of the major abdominal muscle groups. The thickest muscle was the rectus abdominis (17 mm), however, due to layering of other muscle groups, total wall thickness was summed in other areas.

[177] Magee (2014): The text by Magee put anatomy into a physical therapy context. Of particular interest, here, were notes on the range of motion of the lumbar spine, as it pertained to general health.

[178] Azadinia *et al*. (2016): A literature review evaluated current research on lumbosacral orthoses (hernia belts) and their impact on core muscle strength. The authors suggested abdominal weakening may be a side effect of prolonged hernia belt use.

[179] Mens *et al*. **(2006):** This is a great summary article on the clinical impact of IAP until 2006. Studied in this experiment was the force on the pelvic girdle due to IAP, as well as reduced by pelvic bracing. This is a theoretical analysis and a great comparison to the present study on hernia belts in Section 3.3. Pain thresholds were introduced and may lend insight into clinically significant differences required in IAP measurement.

[180] Theret *et al*. (1988): As described in [131], Theret *et al*. worked to improve the evaluation of Young's modulus using suction in soft tissues by considering the pipette geometry, namely the ratio of pipette wall thickness to pipette radius (η). Thus, the coefficient $\phi(\eta)$ was suggested.

[181] Kuyumcu *et al*. (2016): An excellent summary of anatomical measurements (thickness of varying tissues) at the calf. Both healthy (without sarcopenia) and unhealthy (with sarcopenia) patient findings were reported. However, given that this is a geriatric journal, the mean age of participants was 70 and 77 for healthy and unhealthy, respectively.

[182] Boudou *et al*. (2006): As described in [131], Boudou *et al*. worked to improve the evaluation of Young's modulus using suction in soft tissues by considering the underlying tissue geometry, namely Poisson's ratio (ν) and a ratio of tissue thickness to pipette radius (ζ). Thus, the coefficient $\alpha(\zeta, \nu)$ was suggested. To note, the coefficient suggested by Boudou *et al*. is a complement to the work by [180].

[183] Drillis and Contini (1966): This is a significant piece of reference work in anthropometric relations. Average dimensions of the human body with respect to height were given for limbs and other segments (neck, torso, waist, etc.). These reference ratios were used in some calculations

throughout the thesis.

[184] Adcock *et al*. (2001): Twelve (n = 12) pigs were divided into 3 groups to undergo deep mechanical massage (Endermologie) to evaluate the effect of treatment on dissected tissue sections. Important conclusions included: (1) the resulting alignment of collagen fibres in the subcutaneous tissue layer and (2) differences in force profiles were evident depending on the massage movement used.

[185] Zhang *et al*. (1997): Mathematical proofs were given for the evaluation of effective Young's modulus in soft tissue using indentation as a deformation mechanism. The difference between this work and previous studies was largely in its consideration of large deformations and presence of friction.

[186] Shedge *et al*. (2021): Shedge *et al*. briefly summarized post-mortem changes, particularly in the interest of identifying time of death. Of interest in this book chapter is livor mortis, or, the settling of fluids due to gravitational effects and the lack of blood flow across the body.

[187] He *et al*. (2021): Diastasis rectus abdomini was used to evaluate "healthy" and "unhealthy" AW elasticities. AW elasticity in participants was evaluated by shear wave ultrasound elastography. Results were only provided at the rectus abdominis and oblique muscles, though, for the composite tissue. The equation to highlight, here, is $G = {C_s}^2\rho$ where G is shear modulus, C_s is shear wave speed, and ρ is tissue density (assumed to be 1000 kg/m^3). This equation allows for the conversion of C_s into the more familiar form of elasticity.

[188] Chmielewska *et al*. (2015): Chmielewska *et al*. considered the activation of pelvic floor muscle, rectus abdominis, and transversus abdominis when nulliparous women moved from lying, sitting, and standing positions. Pelvic floor muscle activation was evaluated with a vaginal surface electromyography probe, while external electrodes were placed on the rectus abdominis and transversus abdominis for monitoring.

[189] Hencky (1915): The original work of Hencky and his derivation of stress and deformation calculations in circular plates with negligible bending stiffnesses.

[190] Sun *et al*. **(2015):** The extended Hencky solution was explored and detailed [189]; that is, a thin membrane under a pre-tension was subjected to a uniform loading and responds with large deflections. This concept is fundamental to the overall function of the novel device.

[191] Fichter (1997): A NASA technical paper outlining the basics of the classic Hencky problem and solution was described. This article considered the application of the Hencky solution in space, thus, considered a uniform pressure across a thin membrane undergoing large deflections [189].

[192] Timoshenko and Goodier (1970): This foundational text provided the basis for proofs described in [190]. Of particular interest were 2D problems in polar coordinates, and plane stress.

[193] Malbrain *et al*. (2014): Part-3 of Malbrain *et al*.'s 2014 articles discussed a polycompartmental model for evaluation of compartment pressures across the human body. Four major compartments in the body were defined: (1) head, (2) chest, (3) abdomen and (4) extremities. Pathologies in each were evaluated, while the possible effect of compartment syndromes on neighbouring compartments was proposed.

[194] Ben-Haim *et al*. (1990): The paper by Ben-Haim *et al*. introduced a more in-depth model of the human thorax than Primiano in 1982 [171]. The significant difference in these two systems was the implication of rib cage dynamics. As such, the newly proposed model by Ben-Haim's group advanced on Primiano's work, still considering the pressure balance across the thorax, but with the addition of a major skeletal system in the area.

[195] Parker *et al*. (2017): Similar to [65], this article looked to demystify some of the terms used in the hernia community to reach some sort of consensus on definitions. A good diagram on the different layers of the AW and where meshes can sit was provided.

[196] Bartelink *et al*. (1957): Bartelink was one of the first researchers to consider the effect of IAP on relieving pressure on intravertebral discs. This study was spurred given research in 1945 that indicated impossibly high pressures that proved to fail intravertebral discs *ex vivo*. IAP was measured using a balloon inserted in the bladder of a test subject. IAPs nearing 150 mmHg were measured when masses around 90 kg were raised.

[197] Strong (2016): Strong provided a complete overview of stomas, sites for operation, and procedural complications. Of note in this article was the description of ideal stoma location depending on the given patient's needs and body type.

[198] Basford (2002): Basford evaluated whether or not using the Laplace equation was a valuable simplification in analyzing anatomical systems. It was determined that, though the equation provided mathematical reasoning behind medical phenomenon (*i.e* easier to urinate when bladder volume is small), it was not useful in more complicated scenarios. Biological tissue is often elastic or viscoelastic and, therefore, does not adhere to Laplace's assumption that pressurized containers are perfectly rigid.

[199] Podwojewski *et al*. (2014): This *ex vivo* experiment took a pressurized container and put a dissected AW at one end. As the container was pressurized, the deformation in the AW was measured. Concerns with this experiment included the fact that, *in vivo*, muscular contraction typically occurs, thereby reducing the amount of inflation that occurs. That said, it gave a reasonable idea as to the reaction of the AW under pressure.

[200] Panjabi (2003): Another article that detailed the connection between spinal instability and low back pain.

[201] White *et al*. (1975): This paper looked to define clinical instability in the cervical spine. That said, the overarching definition of clinical stability may be extrapolated to the lumbar spine, as well.

[202] Lu *et al*. (2009): Evaluation of an electrical handheld indentometer. Resolution was high but still required users to hold the device perpendicular to the skin, reducing inter-rater reliability.

[203] Lung *et al*. (2020): An evaluation of pressure ulcer healing using ultrasound indentation to measure soft tissue stiffness/thickness.

[204] Kottner *et al*. (2015): This work provided a framework from which reliability and agreement studies in medical research should be reported. It was recommended to use these guidelines for future reporting to improve standardization in research.

[205] Sessler *et al*. (2002): Sessler *et al*. described the RASS reporting system (Richmond agitation-sedation scale). The importance of this article was in defining patient alertness in designing future clinical studies. For example, for invasive surgical operations involving the abdomen, it was recommended to have patients rating a -5 ("unarousable") on RASS.

[206] Fleiss *et al*. (1986): This paper defined three sets of intraclass correlation coefficient values as: ¡0.4 (poor); 0.4-0.75 (fair); ¿ 0.75 (excellent).

[207] Cohen *et al*. (1988): Statistics textbook that highlighted how to use Pearson correlation coefficient as a means of evaluating the statistical strength of two data sets' relationship.

[208] Walter *et al*. (1998): A clear and concise means of calculating the required sample size for reliability studies was described. Equation 12 was most important, especially in conjunction with tables suggesting sample sizes given study statistical powers.

[209] Yock *et al*. (2015): A biodesign textbook on problem statements, concept selection/scoring, and market evaluation with a focus on biomedical product design.

[210] Miller *et al*. **(2018):** This study evaluated the effect of changing damping coefficients and Poisson's ratio on measured Young's modulus in elastography. The conclusion was significant: quantifiable evidence supported the use of a Poisson's ratio of 0.5 for soft biological tissues.

[211] Kuteesa *et al*. (2015): An evaluation of IAH prevalence was completed on 192 patients, in which distinguishing remarks were made between paediatric and adult subjects. IAH rates were 25% and 17.4% for children and adults, respectively.

[212] Driscoll and Blyum (2016): A preliminary analysis of spinal stability in cerebral palsy patients as a function of IAP was conducted. IAP was measured with a custom indentometer and compressive force was correlated to a pressure.

[213] Handorf *et al*. (2015): This article focused on the extracellular matrix in tissue engineering, though, from a mechanical perspective. The stiffness of this matrix was evaluated, and the clinical/chemical consequences of weakness were elucidated.

[214] Gozubuyuk *et al*. (2018): In a cohort of 20 healthy volunteers, trapezius and spinal muscles were evaluated for stiffness before and after (immediately and in 30 minutes) cupping therapies. At the trapezius, stiffness decreased and muscle thickness increased following treatment, while limited change was seen in the paraspinals, perhaps due to the depth of muscle tissue.

[215] Saeki *et al*. (2018): Posterior lower leg stiffnesses were evaluated in healthy (n = 14) and unhealthy (n = 10) (presenting with medial tibial stress syndrome) patients to determine which muscles may contribute to the tested condition. The following muscles were evaluated using shear wave elastography: lateral/medial gastrocnemius, soleus, peroneus longus, peroneus brevis, flexor hallucis longus, flexor digitorum longus, and tibialis posterior.

[216] Ohya *et al*. (2017): Similarly to the research of [215], Ohya *et al*. evaluated posterior lower leg stiffnesses in healthy males (n = 20) before and after a 30-minute run. The following muscles were evaluated using shear wave elastography: lateral/medial gastrocnemius, peroneus longus, peroneus brevis, tibialis posterior, flexor digitorum longus, and flexor digitorum tibialis. The objective of this study was to determine whether a change in specific muscles' elastic modulus following a run suggested which muscles contribute to medial tibial stress syndrome.

[217] Chino *et al*. (2016): Using shear wave elastography, 26 men and 26 women were tested for medial gastrocnemius elasticity given varying ankle positions: 30° plantar flexion, neutral position, and 20° dorsiflexion. These results were then used to extrapolate conclusions on passive joint stiffness.

[218] Zhou *et al*. (2019): Twenty healthy participants (n = 20) were tested using shear wave elastography for achilles tendon and medial/lateral gastrocnemius elasticities. Correlation between tendon and individual muscle elasticities were then evaluated to determine if targeted therapies on a particular muscle is of greater benefit given achilles tendon conditions.

[219] Zhou *et al*. (2020): Following up on their 2019 article, Zhou *et al*. considered medial/lateral gastroncemius elasticities via shear wave elastography in relation to plantar fasciitis.

[220] Sahoo *et al*. (2015): This textbook chapter described existing methods of measuring mechanical friction and viscosity typically used in structural materials. That said, the item of greatest interest in this chapter to the present research was the discussion on durometry: a device for measuring tissue/material hardness.

[221] Jacobson and Driscoll (2020): As presented in Section 3.

[222] Kottner *et al*. (2011): In a cohort of 8 experts, a series of guidelines to improve reliability and agreement reporting in studies was proposed.

[223] Koo ***et al*****. (2016):** This statistical guideline described intraclass correlation coefficient, namely how to select the correct version and report it appropriately.

[224] Lee *et al*. (2013): Though topically not relevant to the present work, the statistical evaluation of reliability and minimum detectable change in this study are of value. This article is listed as a sample for analysis in the present research.

[225] Mukaka (2012): This is an excellent summary of Pearson and Spearman correlation for research statistics. This article reviewed how to correctly select and report said correlations.

[226] Angst *et al*. (2008): Like [224], Angst *et al*.'s work may not be topically relevant to the present work, however, the statistical evaluation of effect size and standardized response mean are of value.

[227] Gilbert *et al*. (2020): This article is of interest for its reporting of abdominal elasticities using the MyotonPro. In 19 women (n = 19), Cesarean section scars and healthy abdominal skin were evaluated with the MyotonPro and compared for viscoelastic response. The purpose of [227] for the present work is to compare findings at the abdomen with the authors' findings as a means of comparison and validation for elasticity at the AW.

[228] Bonett and Wright (2000): This is an important reference for evaluating sample sizes in Pearson, Kendall, and Spearman correlations. Tables and equations provided suggestions for determining said minimum sample sizes.

[229] Husted ***et al*****. (2000):** This is an excellent summary of evaluating responsiveness in studies. Statistics were defined, and recommendations were made for selecting and reporting results.

[230] David *et al*. (2017): Building on their previous work [27], David's research group considers IAP measurement with bioimpedance considering radiofrequency signal changes given a change in abdominal compression as a direct result of IAP.

[231] Kett and Fichter (2020): Though focussed on low back pain alleviation methods, Kett and Fichter quantitatively evaluated treatment methods with an IndentoPro. The authors reference [125] as a means of reliability and validity evaluation of standard indentometers, rather than perform a unique study to the IndentoPro, itself.

A.9 Literature Classification

The following table provides a brief overview of the available literature referenced, presently, and of use in future studies. Each reference is allocated a mark if it applies to a certain area of interest. As such, the following sections assist in efficient retrieval of information:

- **Anatomy and Mechanics:** This is a general category that identifies whether a paper referenced a particular anatomical feature (General or Abdominal Wall), or if it highlighted physiological properties associated with human biology (IAP, IAV, C_{ab}, or Soft Tissue Stiffness).
- **Existing Devices:** This is the most pertinent category for the present work, given the emphasis on device development. Subcategories in Existing Devices include IAV, IAP, C_{ab}, and the generic "Other" category. When a reference is highlighted for this category, it either refers to a manuscript describing a novel system, or building on validity/reliability studies of an older technology.
- **Novel Experimentation:** To quickly determine whether a study considered *in vivo* or other experimentation methods, this category identifies these critical areas of study for immediate retrieval.
- **Pathophysiology:** Many manuscript objectives are tied to a pathophysiology to emphasize the importance of the given work in a clinical setting. As such, a few recurring conditions are identified, including Spinal Stability, ACS/IAH, Herniation, and the generic "Other" category.
- **Other:** This broad category is important for identifying major works, such as Literature Reviews, clarifications on Terminology, fundamental Mathematics pertinent to the present work, or "Other", should a manuscript fall in no other subsection.

Table A.9.1: Reference Summary (IAV: intra-abdominal volume; IAP: intra-abdominal pressure; ACS: abdominal compartment syndrome; IAH: intra-abdominal hypertension; C_{ab}: abdominal compliance

Ref.	First Author	Year	Anatomy and Mechanics					Existing Devices					Novel Experimentation								Pathophysiology				Other			
			General	Abdominal Wall	IAV	IAP	C_{ab}	Soft Tissue Stiffness	IAV	IAP	C_{ab}	Other	*in silico* (numerical)	*in silico* (computational)	*in simulacra* (benchtop)	*ex vivo* (animal)	*ex vivo* (human)	*in vivo* (animal)	*ex vivo* (cadaver)	*in vivo* (human)	Spinal Stability	ACS/IAH	Herniation	Other	Literature Review	Terminology	Mathematics	Other
[1]	Strandring	2016	X	X		X																				X		
[2]	Malbrain	2014		X	X	X	X						X									X			X	X	X	
[3]	Stokes	2011		X										X							X							
[4]	Malbrain	2014							X	X	X											X	X	X	X	X	X	
[5]	Hodges	2005	X	X		X														X	X							
[6]	Malbrain	2006				X				X												X			X	X		
[7]	Roberts	2016				X	X														X				X	X		
[8]	Tayashiki	2016		X		X														X								
[9]	Malbrain	2004				X				X															X	X		
[10]	Ott	2019		X	X	X	X				X														X	X		
[11]	Drake	2018	X	X		X																				X		
[12]	Gosling	2017	X	X		X																				X		
[13]	Tuktamyshev	2016		X	X	X	X																					
[14]	Forstemann	2011		X		X								X			X											
[15]	Blaser	2015			X	X	X				X														X			
[16]	Stedman	2006	X																							X		
[17]	Accarino	2009			X	X			X											X				X				
[18]	Agnew	2010		X	X	X			X											X			X					
[19]	Villoria	2008		X	X	X	X	X												X								
[20]	Malbrain	2016		X	X	X	X	X		X												X			X	X	X	
[21]	Papavramidis	2011			X	X	X													X				X				
[22]	Mulier	2008			X	X														X								
[23]	Abu-Rafea	2006	X	X								X								X								
[24]	Song	2006		X	X	X														X								

Continued on next page

Table A.9.1: Continued from previous page

Ref.	First Author	Year	Anatomy and Mechanics					Existing Devices					Novel Experimentation								Pathophysiology				Other			
			General	Abdominal Wall	IAV	IAP	C_{ab}	Soft Tissue Stiffness	IAV	IAP	C_{ab}	Other	*in silico* (numerical)	*in silico* (computational)	*in simulacra* (benchtop)	*ex vivo* (animal)	*ex vivo* (human)	*in vivo* (animal)	*ex vivo* (cadaver)	*in vivo* (human)	Spinal Stability	ACS/IAH	Hernation	Other	Literature Review	Terminology	Mathematics	Other
[25]	Mulier	2008			X	X														X								
[26]	Pracca	2011		X	X	X	X					X								X		X						
[27]	David	2011		X	X	X	X					X								X		X						
[28]	Severgnini	2007			X	X																X			X			
[29]	Sugerman	1997			X	X														X				X				
[30]	Malbrain	2009		X		X				X										X								
[31]	Guerrero-Romero	2003	X		X	X			X											X						X	X	
[32]	Valdez	1993			X				X															X				
[33]	Cohen	1994	X	X								X									X			X				
[34]	Tayebi	2020			X	X	X		X	X	X														X			
[35]	Cobb	2005				X														X								
[36]	De Keulenaer	2012				X																X			X			
[37]	Chionh	2006				X														X								
[38]	Sanchez	2001				X														X								
[39]	Vasquez	2007				X														X								
[40]	Lambert	2005				X														X								
[41]	Arfvidsson	2005				X														X								
[42]	Davis	2005				X														X					X			
[43]	Ejike	2008				X	X													X								
[44]	Thabet	2017				X				X												X			X	X		
[45]	Papavramidis	2011				X																X			X	X		
[46]	Blaser	2019				X																X						
[47]	Milanesi	2016				X				X												X			X			
[48]	Sugerman	1997				X														X				X				
[49]	Sugerman	1998				X														X								

Continued on next page

Table A.9.1: Continued from previous page

Ref.	First Author	Year	Anatomy and Mechanics					Existing Devices					Novel Experimentation								Pathophysiology				Other			
			General	Abdominal Wall	IAV	IAP	C_{ab}	Soft Tissue Stiffness	IAV	IAP	C_{ab}	Other	*in silico* (numerical)	*in silico* (computational)	*in simulacra* (benchtop)	*ex vivo* (animal)	*ex vivo* (human)	*in vivo* (animal)	*ex vivo* (cadaver)	*in vivo* (human)	Spinal Stability	ACS/IAH	Hernia	Other	Literature Review	Terminology	Mathematics	Other
[50]	Dejardin	2007			X	X														X		X						
[51]	Smit	2016	X			X														X				X				
[52]	Cheatham	2009				X														X								
[53]	Morris	1961	X	X		X														X	X							
[54]	Montgomery	2017																					X		X	X		
[55]	Talasz	2011		X		X																				X		
[56]	Al-Khan	2011				X														X				X				
[57]	Beer	2012																								X	X	
[58]	Davis	1985				X				X												X			X	X		
[59]	Van Ramshorst	2011		X		X				X									X	X								
[60]	Chen	2015		X		X				X										X								
[61]	Malbrain	2010				X				X										X		X			X			
[62]	Freitag	2003	X																						X	X		
[63]	Hackett	2013	X	X		X														X	X				X			
[64]	Addington	2008				X														X								
[65]	Aquina	2014										X											X					
[66]	Cheatham	2007				X				X												X			X	X		
[67]	Otto	2009				X				X										X								
[68]	Pracca	2007				X				X										X								
[69]	Al-Hwiesh	2011				X				X										X								
[70]	Al-Abassi	2018				X				X										X		X						
[71]	Aguilera	2018				X				X		X								X				X				
[72]	De Waele	2009				X																X			X	X		
[73]	Homma	2002	X							X		X												X	X	X		
[74]	Leitner	2016	X							X		X								X				X				

Continued on next page

Table A.9.1: Continued from previous page

Ref.	First Author	Year	Anatomy and Mechanics					Existing Devices					Novel Experimentation								Pathophysiology				Other			
			General	Abdominal Wall	IAV	IAP	C_{ab}	Soft Tissue Stiffness	IAV	IAP	C_{ab}	Other	*in silico* (numerical)	*in silico* (computational)	*in simulacra* (benchtop)	*ex vivo* (animal)	*ex vivo* (human)	*in vivo* (animal)	*ex vivo* (cadaver)	*in vivo* (human)	Spinal Stability	ACS/IAH	Hernia	Other	Literature Review	Terminology	Mathematics	Other
[75]	NKUDIC	2012	X			X						X												X	X			
[76]	Lee	2012				X				X												X			X	X		
[77]	Wauters	2012				X				X								X										
[78]	Sugrue	1994				X				X										X								
[79]	Shafik	1997				X				X										X								
[80]	Dowdle	1997				X				X										X								
[81]	Lacey	1987				X				X										X								
[82]	Johnson	2009				X				X					X					X								
[83]	Coleman	2012				X				X					X					X								
[84]	Bloch	2018		X		X		X		X								X										
[85]	Van Ramshorst	2008		X		X				X									X									
[86]	David	2018		X		X				X								X										
[87]	David	2020				X				X										X								
[88]	Brown	2012		X																						X	X	
[89]	Akkus	2012		X																X								
[90]	Tran	2014		X													X											
[91]	Astruc	2018		X													X											
[92]	Korenkov	2001		X													X											
[93]	Cardoso	2012		X		X											X								X	X	X	
[94]	Abdelounis	2013		X													X											
[95]	Martins	2012		X													X											
[96]	Kureshi	2008		X													X						X					
[97]	Wolloscheck	2004		X													X						X					
[98]	Hernandez -Gascon	2012		X		X								X														

Continued on next page

Table A.9.1: Continued from previous page

Ref.	First Author	Year	Anatomy and Mechanics					Existing Devices					Novel Experimentation								Pathophysiology				Other			
			General	Abdominal Wall	IAV	IAP	C_{ab}	Soft Tissue Stiffness	IAV	IAP	C_{ab}	Other	*in silico* (numerical)	*in silico* (computational)	*in simulacra* (benchtop)	*ex vivo* (animal)	*ex vivo* (human)	*in vivo* (animal)	*ex vivo* (cadaver)	*in vivo* (human)	Spinal Stability	ACS/IAH	Hernia	Other	Literature Review	Terminology	Mathematics	Other
[99]	Pena	2017	X	X		X								X											X	X		
[100]	Pachera	2016		X		X								X									X					
[101]	Tham	2006		X				X						X						X								
[102]	Deeken	2017		X																					X			
[103]	Grassel	2005		X													X											
[104]	Cooney	2016		X													X											
[105]	Levillain	2016		X												X	X											
[106]	Rath	1996		X													X											
[107]	Rath	1997		X													X											
[108]	Kirilova	2011		X													X											
[109]	Kirilova-Doneva	2016		X													X											
[110]	Yang	2018		X																X					X			
[111]	MacDonald	2016		X				X												X								
[112]	Tran	2016		X				X												X								
[113]	Todros	2020		X		X								X												X	X	
[114]	Francois	2012																								X	X	
[115]	Konerding	2011		X		X											X						X					
[116]	Ramalingam	2009																								X	X	
[117]	Choi	2005						X																				
[118]	Lu	2012						X																				
[119]	Hayes	1972						X																		X	X	
[120]	Woodard	1986	X														X											
[121]	Francois	2012																									X	
[122]	Konstantinova	2017	X					X							X					X								
[123]	Zugel	2018	X					X																X	X			

Continued on next page

Table A.9.1: Continued from previous page

Ref.	First Author	Year	Anatomy and Mechanics					Existing Devices					Novel Experimentation								Pathophysiology				Other			
			General	Abdominal Wall	IAV	IAP	C_{ab}	Soft Tissue Stiffness	IAV	IAP	C_{ab}	Other	*in silico* (numerical)	*in silico* (computational)	*in simulacra* (benchtop)	*ex vivo* (animal)	*ex vivo* (human)	*in vivo* (animal)	*ex vivo* (cadaver)	*in vivo* (human)	Spinal Stability	ACS/IAH	Hernia	Other	Literature Review	Terminology	Mathematics	Other
[124]	Chaitow	2012	X					X																	X	X		
[125]	Wilke	2018						X												X				X				
[126]	Agyapong-Badu	2018						X																				
[127]	Tarsi	2013						X							X									X				
[128]	Kutz	2015						X																				
[129]	Peipsi	2012	X					X																				
[130]	Feng	2018	X					X												X								
[131]	Zheng	2016						X																	X	X	X	
[132]	Myoton AS	2010	X					X																	X	X		
[133]	Müller	2018						X																				
[134]	Wernicke	2009	X					X												X				X				
[135]	Jacobson	2021	X					X																X	X	X		
[136]	Draaijers	2004						X				X								X								
[137]	Bayford	2012	X					X																	X			
[138]	Simon-Allue	2017		X		X		X										X										
[139]	McAuliffe	2017	X									X								X				X				
[140]	Sigrist	2017						X																				
[141]	Hirsch	2017						X																		X		
[142]	Glaser	2014	X					X																	X	X	X	
[143]	Yen	2003						X												X								
[144]	Nichols	2015						X							X													
[145]	Oflaz	2014						X							X												X	
[146]	Williams	2007						X																				
[147]	Nava	2004						X																				
[148]	Elahi	2019						X																				

Continued on next page

Table A.9.1: Continued from previous page

Ref.	First Author	Year	Anatomy and Mechanics					Existing Devices					Novel Experimentation								Pathophysiology				Other			
			General	Abdominal Wall	IAV	IAP	C_{ab}	Soft Tissue Stiffness	IAV	IAP	C_{ab}	Other	*in silico* (numerical)	*in silico* (computational)	*in simulacra* (benchtop)	*ex vivo* (animal)	*ex vivo* (human)	*in vivo* (animal)	*ex vivo* (cadaver)	*in vivo* (human)	Spinal Stability	ACS/IAH	Hernia	Other	Literature Review	Terminology	Mathematics	Other
[149]	Valtorta	2005						X																				
[150]	Narayanan	2006						X																				
[151]	Moerman	2009							X							X												
[152]	Zhang	2017						X																				
[153]	Bensamoun	2011	X					X												X								
[154]	Dittmann	2017						X																				
[155]	Courtney	2005																								X	X	
[156]	Yoshino	2012		X		X												X										
[157]	Vleeming	2014		X		X									X						X			X				
[158]	El-Monajjed	2020		X		X								X										X				
[159]	El Bojairami	2020	X	X	X	X								X							X			X				
[160]	Newell	2021	X											X							X			X				
[161]	Warren	2020	X																	X				X				
[162]	Al-Shidhani	2020	X									X													X			
[163]	Moortgat	2016	X									X													X			
[164]	Rozenfeld	2016	X																							X		X
[165]	Chiu	2020	X																	X				X				
[166]	Worret	2004	X																	X				X				
[167]	DaPrato	2018	X									X								X				X				
[168]	Stylinski	2018										X											X		X			
[169]	Antoniou	2018		X		X						X											X			X		
[170]	Tenzel	2017																					X		X	X		
[171]	Primiano	1982				X		X					X														X	
[172]	Breslavsky	2016																									X	
[173]	Muvdi	1991																									X	
[174]	Flint	2010	X																	X				X				

Continued on next page

Table A.9.1: Continued from previous page

Ref.	First Author	Year	Anatomy and Mechanics					Existing Devices					Novel Experimentation								Pathophysiology				Other			
			General	Abdominal Wall	IAV	IAP	C_{ab}	Soft Tissue Stiffness	IAV	IAP	C_{ab}	Other	*in silico* (numerical)	*in silico* (computational)	*in simulacra* (benchtop)	*ex vivo* (animal)	*ex vivo* (human)	*in vivo* (animal)	*ex vivo* (cadaver)	*in vivo* (human)	Spinal Stability	ACS/IAH	Hernation	Other	Literature Review	Terminology	Mathematics	Other
[175]	Fryar	2012	X																									X
[176]	Tahan	2016	X	X				X												X								
[177]	Magee	2014																							X	X		
[178]	Azadinia	2016																			X				X			
[179]	Mens	2006			X	X	X		X				X											X			X	
[180]	Theret	1988						X							X												X	
[181]	Kuyumcu	2016	X							X										X				X				
[182]	Boudou	2006						X							X												X	
[183]	Drillis	1966	X																								X	X
[184]	Adcock	2001	X					X										X						X				
[185]	Zhang	1997																									X	
[186]	Shedge	2021	X																					X		X		
[187]	He	2021		X				X												X				X				
[188]	Chmielewska	2015	X	X								X								X								
[189]	Hencky	1915																									X	
[190]	Sun	2015																								X	X	
[191]	Fichter	1997																								X	X	
[192]	Timoshenko	1970																								X	X	
[193]	Malbrain	2014		X	X	X																			X	X		
[194]	Ben-Haim	1990				X		X					X														X	
[195]	Parker	2017		X								X											X			X		
[196]	Bartelink	1957		X		X				X									X	X	X							
[197]	Strong	2016		X								X											X		X			
[198]	Basford	2002	X	X		X																			X	X	X	
[199]	Podwojewski	2014		X		X	X										X											
[200]	Panjabi	2003	X														X				X							

Continued on next page

Table A.9.1: Continued from previous page

Ref.	First Author	Year	Anatomy and Mechanics					Existing Devices					Novel Experimentation								Pathophysiology				Other			
			General	Abdominal Wall	IAV	IAP	C_{ab}	Soft Tissue Stiffness	IAV	IAP	C_{ab}	Other	*in silico* (numerical)	*in silico* (computational)	*in simulacra* (benchtop)	*ex vivo* (animal)	*ex vivo* (human)	*in vivo* (animal)	*ex vivo* (cadaver)	*in vivo* (human)	Spinal Stability	ACS/IAH	Hernation	Other	Literature Review	Terminology	Mathematics	Other
[201]	White	1975	X			X	X										X				X					X		
[202]	Lu	2009	X					X												X								
[203]	Lung	2020						X												X				X				
[204]	Kottner	2015																								X		
[205]	Sessler	2002																		X						X		
[206]	Fleiss	1986																									X	
[207]	Cohen	1988																									X	
[208]	Walter	1998																									X	
[209]	Yock	2015																										
[210]	Miller	2018	X					X																			X	
[211]	Kuteesa	2015				X																X						
[212]	Driscoll	2019		X		X														X	X			X				
[213]	Handorf	2015	X																						X			
[214]	Gozubuyuk	2018						X												X				X				
[215]	Saeki	2018	X					X												X				X				
[216]	Ohya	2017	X					X												X				X				
[217]	Chino	2016	X					X												X								
[218]	Zhou	2019	X					X												X				X				
[219]	Zhou	2020	X					X												X				X				
[220]	Sahoo	2015										X														X		
[221]	Jacobson	2020		X				X		X										X	X	X					X	
[222]	Kottner	2011																							X	X	X	X
[223]	Koo	2016																							X	X	X	X
[224]	Lee	2013																	X					X			X	X
[225]	Mukaka	2012																							X	X	X	X
[226]	Angst	2008		X				X												X				X				

Continued on next page

Table A.9.1: Continued from previous page

Ref.	First Author	Year	Anatomy and Mechanics					Existing Devices					Novel Experimentation								Pathophysiology				Other			
			General	Abdominal Wall	IAV	IAP	C_{ab}	Soft Tissue Stiffness	IAV	IAP	C_{ab}	Other	*in silico* (numerical)	*in silico* (computational)	*in simulacra* (benchtop)	*ex vivo* (animal)	*ex vivo* (human)	*in vivo* (animal)	*ex vivo* (cadaver)	*in vivo* (human)	Spinal Stability	ACS/IAH	Hernia	Other	Literature Review	Terminology	Mathematics	Other
[227]	Gilbert	2020		X					X											X								
[228]	Bonett	2000																							X	X	X	X
[229]	Husted	2000																							X	X	X	X
[230]	David	2017		X		X				X								X										
[231]	Kett	2020	X					X												X	X			X				